VU VRIJE UNIVERSITEIT AMSTERDAM

VU Research Portal

Cooperative 1,3-P,N-ligands and non-innocent NHCs

Rong, Mark Karsten

2021

document version
Publisher's PDF, also known as Version of record

Link to publication in VU Research Portal

citation for published version (APA)
Rong, M. K. (2021). *Cooperative 1,3-P,N-ligands and non-innocent NHCs*. s.n.

General rights
Copyright and moral rights for the publications made accessible in the public portal are retained by the authors and/or other copyright owners and it is a condition of accessing publications that users recognise and abide by the legal requirements associated with these rights.

- Users may download and print one copy of any publication from the public portal for the purpose of private study or research.
- You may not further distribute the material or use it for any profit-making activity or commercial gain
- You may freely distribute the URL identifying the publication in the public portal ?

Take down policy
If you believe that this document breaches copyright please contact us providing details, and we will remove access to the work immediately and investigate your claim.

E-mail address:
vuresearchportal.ub@vu.nl

Download date: 05. Nov. 2022

Cooperative 1,3-P,N-ligands and non-innocent NHCs

M.K. Rong

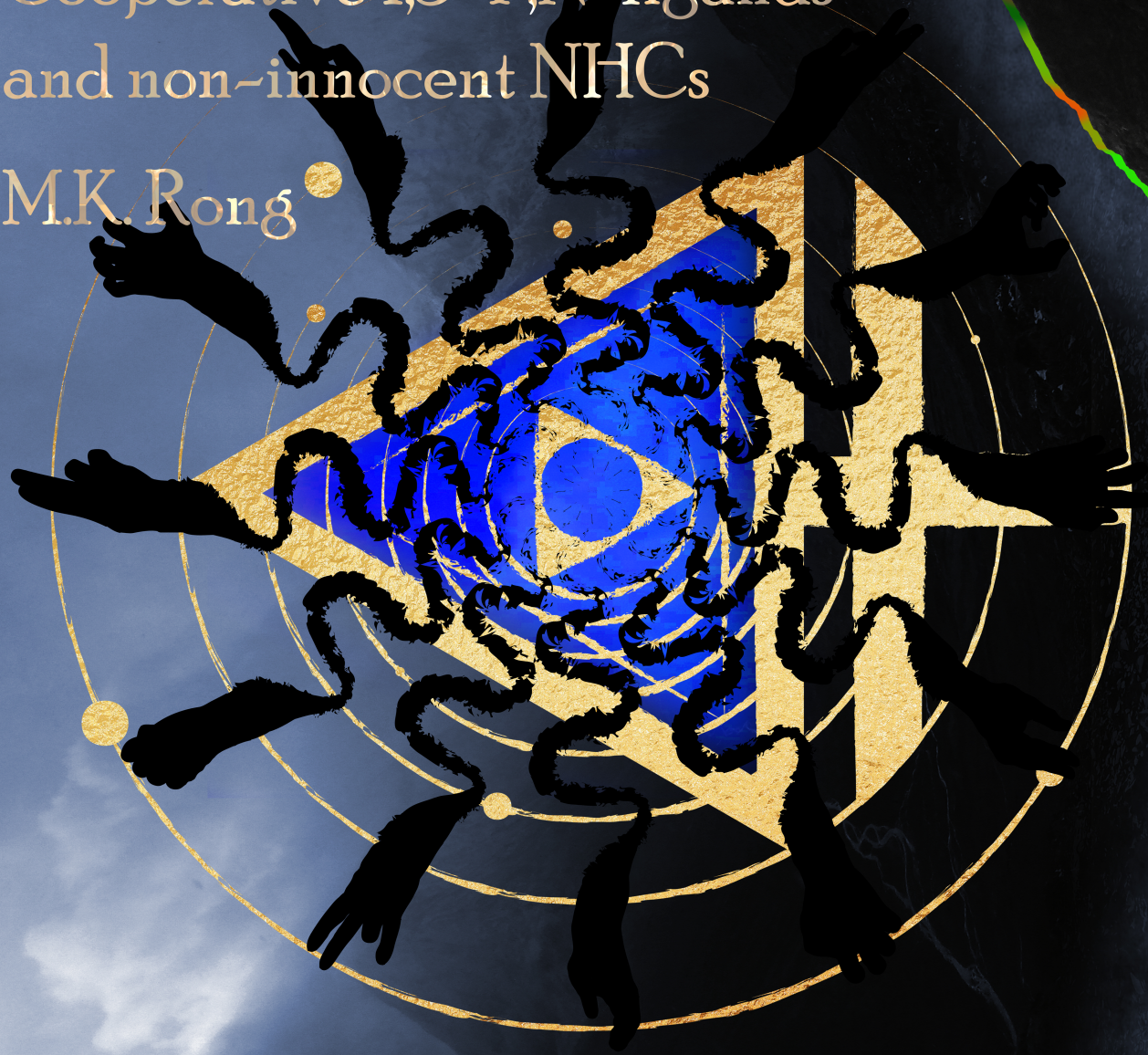

Cooperative 1,3-P,N-ligands and non-innocent NHCs

Mark K. Rong

2021

© 2021, M.K. Rong

Printed by: ProefschriftMaken

ISBN: 978-94-6423-545-6

VRIJE UNIVERSITEIT

Cooperative 1,3-P,N-ligands and non-innocent NHCs

ACADEMISCH PROEFSCHRIFT

ter verkrijging van de graad Doctor aan
de Vrije Universiteit Amsterdam,
op gezag van de rector magnificus
prof.dr. C.M. van Praag,
in het openbaar te verdedigen
ten overstaan van de promotiecommissie
van de Faculteit der Bètawetenschappen
op donderdag 2 december 2021 om 11.45 uur
in een bijeenkomst van de universiteit,
De Boelelaan 1105

door

Mark Karsten Rong

geboren te Hoorn

promotor:	prof.dr. K. Lammertsma
copromotoren:	dr. J.C. Slootweg
	dr. A.W. Ehlers
promotiecommissie:	prof.dr. F.M. Bickelhaupt
	prof.dr. I.J.P. de Esch
	dr. M.A. Fernández Ibáñez
	prof.dr. C. Müller
	dr. E. Otten
	dr. S. Pullen
	prof.dr. J.I. van der Vlugt

"Time's not what matters – it's you that does."

Porfiry Petrovich in Crime and Punishment, Fyodor Dostoyevsky

Table of Contents

Preface

In 1902, Emil Fischer speculated that man would resort to 'synthetic enzymes' in the future.[1] Presently, achieving enzyme-like reactivity for homogeneous catalysts is still a major goal and cooperative interactions between metals and ligands are indispensable to accomplish this.[2,3]

Traditionally, homogeneous catalysis relies heavily on complexes consisting of a transition metal-core that determines the overall activity and its stabilization by one or more non-reactive 'innocent' organic ligands.[3] Second and third row metals are preferred due to their high reactivity, but they also have become increasingly rare, inaccessible, and costly.[2] Especially the high demands of advanced technology has led to a rapid depletion of readily available rare earth metal reserves.[4] The use of first row base-metal-based alternatives is hampered by their inherent different reactivity, but the desired/required overall activity may still be achieved by the inclusion of secondary reactive centers to synergistically assist the activation of substrates.[2,3] Cooperative activations are best demonstrated by metalloenzymes in nature,[2,5] which in turn inspired synthetic cooperative strategies.[3]

Cooperative metal-reactivity can be realized by the presence of a second metal center (multinuclear catalysis)[6] or reactive ligands can be used to actively assist in the catalytic transformations (cooperative catalysis).[2,3,5] Several types of ligand-reactivity can support transformations on the metal center and ligands are classified accordingly.[2,3,5] Non-innocent ligands are actively involved in redox processes, by transferring electrons to or from the metal, for instance via

π-system reorganizations. Hemilabile ligands can stabilize the reactive free coordination site at the metal and dissociate in favor of a substrate when required. Cooperative ligands may also assist the metal center in bifunctional activations, for instance, by acting as Lewis or Brønsted base outside of the inner coordination sphere and facilitate substrate activation through hydrogen bonding or protonation/deprotonation ('proton shuttling').

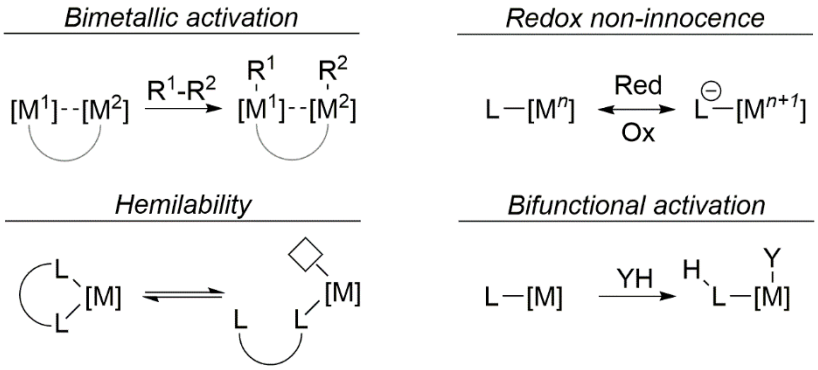

Hybrid ligands are composed of donor-atoms with contrasting preferences and can therefore be used cooperatively:[7] one donor is tightly anchored to the metal, while the other is available for cooperative interactions. For instance, the anchor may be phosphorus while the reactive group can be nitrogen-based. Such P,N-ligands can have different topologies and, when in a 1,3-relationship, their favorable positioning allows for varied coordination chemistry including complexes with a mononuclear (**Chapter 1**) or multinuclear (**Chapter 2**) metallic core, which have mainly found application in catalysis and photoluminescence, respectively. **Chapter 3** explores the applicability of novel imidoyl-phosphanes — historically: iminophosphanes; IUPAC: *C*-phosphanyl imines — as highly tunable 1,3-P,N-ligands by demonstrating their coordination to Rh^{III} and their performance in cooperative Ru^{II} catalysis.

C,N-Cyclised iminophosphanes with flexible, highly basic tetrahydroazepine rings were obtained by capturing the Beckmann rearrangement's nitrilium intermediate in **Chapter 4**. Their distinctive properties were apparent from their W^0(carbonyl) and hemilabile Rh^{III} complexes, while their Ru^{II} and Ir^{I} complexes were active cooperative catalysts. Furthermore, asymmetric ligands were prepared from L-menthone. Finally, **Chapter 5** investigates the interactions of protic N-heterocyclic carbenes coordinated to iridium, which allows the capture of acetonitrile. Under reductive conditions, the *β*-NH-metal interactions become more prominent, to give a highly unusual diiridium complex.

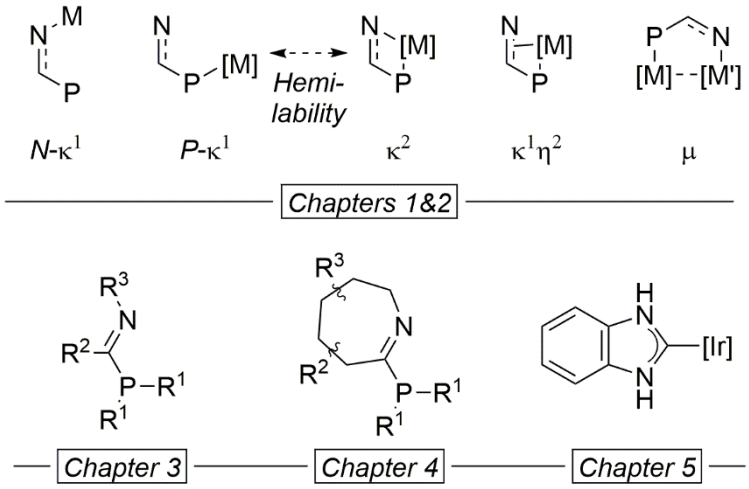

References

[1] Fischer, E.; *Nobel Lecture*, **1902**.

[2] Van der Vlugt, J. I. *Eur. J. Inorg. Chem.* **2012**, *2012*, 363–375.

[3] Khusnutdinova, J. R.; Milstein, D. *Angew. Chem., Int. Ed.* **2015**, *54*, 12236–12273.

[4] (a) de Boer, M.A.; Lammertsma, K. *ChemSusChem* **2013**, *6*, 2045-2055. (b) Rhodes, C.J. *Sci. Prog.* **2019**, 1-47. (c) Henckens, M.L.C.M.; Driessen, P.P.J.; Worrell, E. *Resour. Conserv. Recy.* **2014**, *93*, 1-8.

[5] Trincado, M.; Grützmacher, H. in *Cooperative Catalysis: Designing Efficient Catalysts for Synthesis*, Wiley-VCH Verlag GmbH & Co. KGaA , **2015**, 67-110.

[6] Weiss, M.; Peters, R. in *Cooperative Catalysis: Designing Efficient Catalysts for Synthesis*, Wiley-VCH Verlag GmbH & Co. KGaA , **2015**, 227-262.

[7] Zhang, W.-H.; Chien, S. W.; Hor, T. S. A. *Coord. Chem. Rev.* **2011**, *255*, 1991–2024.

Chapter I

1,3-P,N hybrid ligands in mononuclear coordination chemistry and homogeneous catalysis

Mark K. Rong, Flip Holtrop, J. Chris Slootweg, and Koop Lammertsma

1,3-P,N-ligands are prominent hybrid ligands which provide valuable mononuclear transition metal complexes, due to their varied bonding modes with an inherent usefulness in cooperative processes such as ligand-assisted substrate activation and both homogeneous and heterogeneous catalysis. Reviewed are recent developments in an expanding number of applications, including coordination chemistry, catalysis, and bio-inorganic applications.

Coord. Chem. Rev. **2019**, *380*, 1-16.

1 Introduction

The translation of the activity and reactivity of the less abundant second and third row transition metal systems to cheaper, more available, but generally less reactive first row metals, requires successfully combining metal- with ligand-based reactivity.[1] This approach of 'ligand cooperativity', or 'non innocence' for redox active ligands, can be pursued with hybrid ligands, which combine the distinctive bonding preferences of different donor atoms to provide cooperative metal-ligand interactions such as hemilability, ligand assisted substrate recognition, substrate activation and proton shuttling (Figure 1),[2,3] and have found prominent applications in homogeneous catalysis.[4]

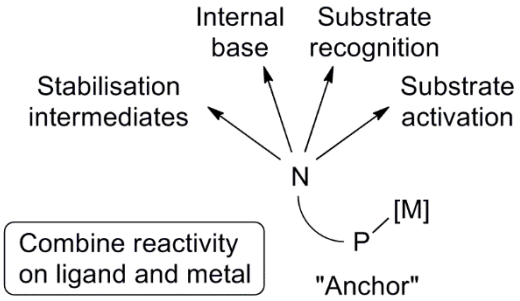

Figure 1. Cooperative P,N-ligands.

Since their introduction in 1972,[5] the hybrid 1,3-P,N-ligands (Figure 2) have provided rich coordination chemistry, due to the fruitful combination of a soft phosphorus donor with a hard nitrogen.[6,7] Besides rich multinuclear chemistry in which the ligands coordinate in a bridging mode between (hetero)metals to facilitate the formation of metal-metal bonds,[8,9] they also form *N*-monodentate,[10] *P*-monodentate,[11,12] and bidentate mononuclear complexes[12] (Figure 3), which are active in catalytic reactions including the Ru^{II}-catalyzed hydration of nitriles,[12f] the Ru^{II}-catalyzed hydrogenation of alkynes and transfer hydrogenation of ketones,[12e] the Ru^{II}-catalyzed hydrogenation of alkenes,[12d] the Rh^{I}-

and Ir^{I}-catalyzed hydroformylation of alkenes,[8e,12a] the Pd^{II}-catalyzed carbonylation of alkynes,[11b, 12b,c] and the Pd^{II}-catalyzed Buchwald-Hartwig and Suzuki-Miyaura cross-coupling reactions.[13] The number of catalytic applications is still growing.

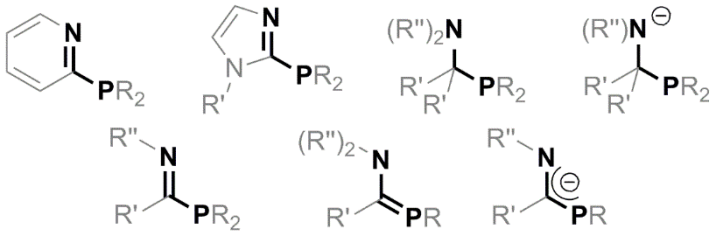

Figure 2. 1,3-P,N-ligands in recent mononuclear complexes.

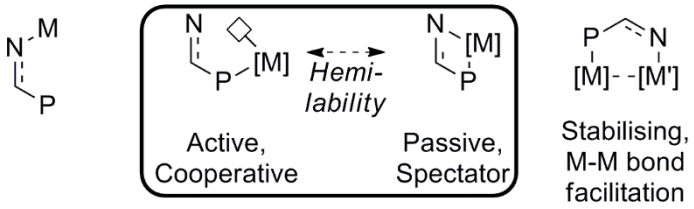

Figure 3. 1,3-P,N-ligands as hemilabile cooperative ligands.

To provide insight into why these ligands are so valuable, we review recent developments in mononuclear 1,3-*P,N* chemistry from 2009[6,7] to mid-2017 with a focus on catalysis and coordination chemistry. Excluded are systems in which one of the donors is unavailable (e.g., *P*-oxidized systems, 2-pyrrolyl-phosphanes, *P*- or *N*-cationic *P,N*-systems),[14,15] those that contain an additional donor atom that can actively participate (e.g., bis-/tris-(pyridyl)phosphanes, ClickPHOS, *N,N'*-coordinating phosphaguanidinates, 1,3,5-P,N,X-ligands)[16,17] or ligands that are conformationally restricted in such a fashion that their chemistry is not comparable to the titular compounds (e.g., benzaphospholes, 1,3,5-triaza-7-phosphaadamantate (PTA) ligands).[18] After an overview of synthetic

developments, recent 1,3-P,N-containing mononuclear complexes will be discussed in ascending Group number.

2 Synthesis

Recent synthetic developments are discussed first to provide background for the ligands discussed in sections 2-7.

2.1 2-Pyridyl- and 2-imidazolylphosphanes

Most reports improve on the syntheses and expand on the substituent scope of known ligand systems. To overcome the limited access to substituted 2-pyridylphosphanes ($PyPPh_2$),[7a,12c] cross-coupling reactions have been developed to selectively access their 6-substituted precursors **1.2** by using Cu^{I}-catalysis for *t*-alkyl groups (Scheme 1; five examples, 74-92%, cat. loading 3.5-10 mol%) or a Ni^{II}-catalysis/$POCl_3$ sequence for others (eight examples; step 1: 53-98%, cat. loading 0.3-3 mol%; step 2: 60-94%).[19] Subsequent couplings provide **1.3** (10 examples, 58-86%). Nickel was also used to cross couple 2-pyridyl nitrile with $HPPh_2$ to $PyPPh_2$ (40%; 10 mol% $Ni(COD)_2$ + 8-hydroxyquinoline, 90°C, 16 h).[20] A primary 2-pyridylphosphane has been cyclo-condensed to phospholane **2.1** (Scheme 2).[21]

Intriguing derivatives of 2-imidazolylphosphanes with the intrinsically chiral paracyclophane group **3.5** have been reported (Scheme 3).[22] Imidazolylphosphanes **4.3a,b** for heterogeneous applications were obtained by binding the *N*-site of imidazole **4.1** to a polystyrene residue (Merrifield-resin) via two linkertypes (giving **4.2**), followed by phosphination (Scheme 4).[23] P,N-borate **5.2** was obtained from bromide-lithium exchanged **5.1** and BPh_3 (Scheme 5); despite its anionicity, **5.2** coordinates with neutral donors (see section 4.2.7).[24]

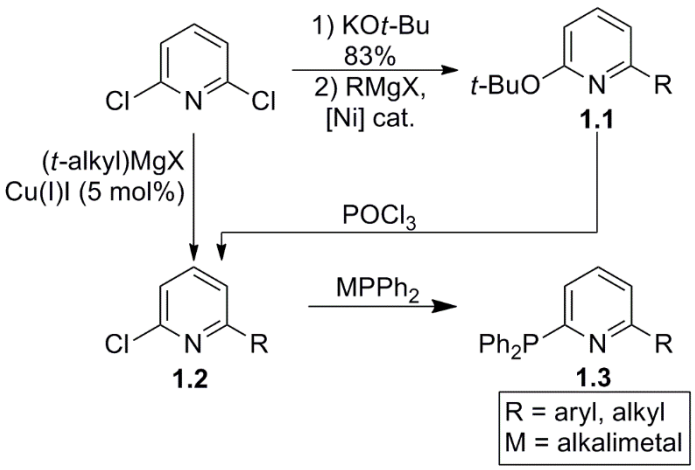

Scheme 1. 6-Functionalisation of $PyPPh_2$.

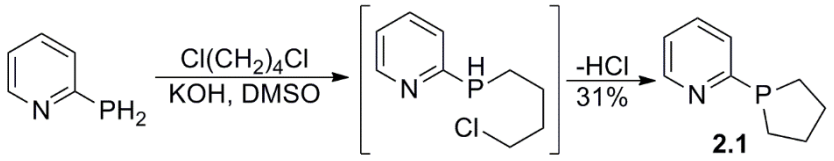

Scheme 2. Cyclocondensation to 2-pyridyl-phospholane.

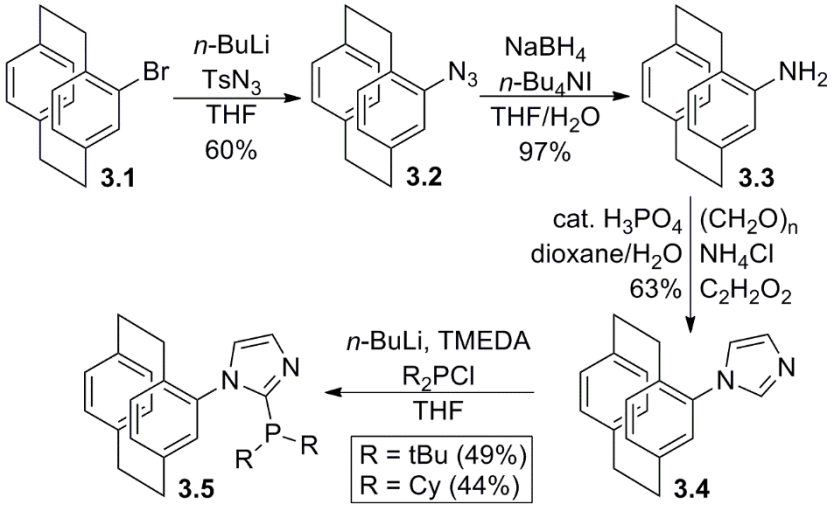

Scheme 3. Cyclophane-based 2-imidazolyl-phosphanes.

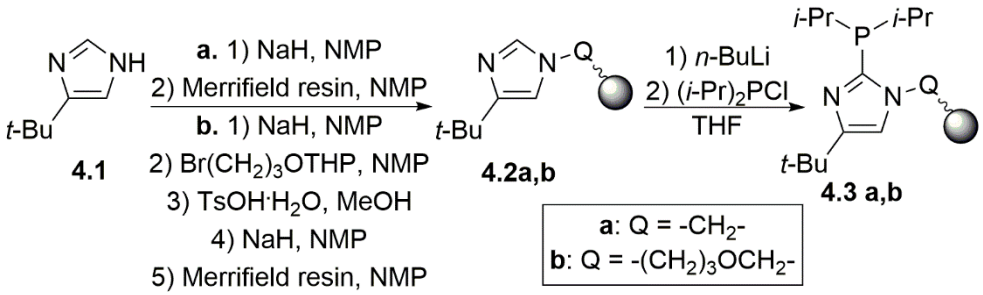

Scheme 4. Solid-supported 2-imidazolyl-phosphanes.

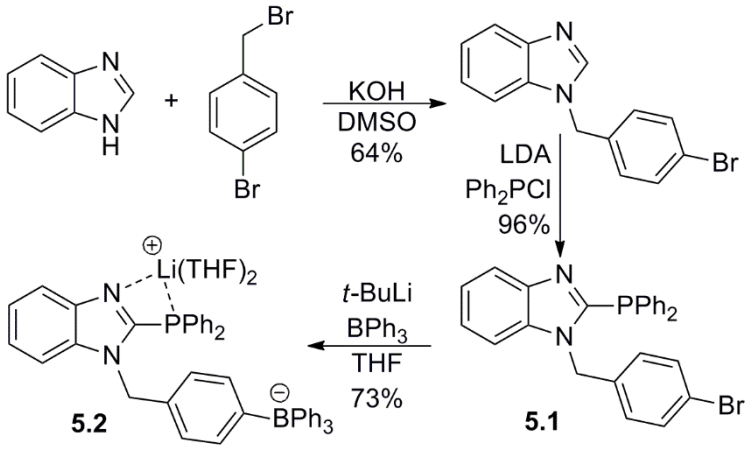

Scheme 5. Backbone anionicity in borane-tethered 2-benzimidazolyl-phosphanes.

The 1-substituted 4-imidazolylphosphanes **6.2** have been generated by treating 2-alkyl imidazoles **6.1** with I_2/KI and a base, followed by *N*-methylation, two consecutive iodide-magnesium exchanges and quenching with diphenylchlorophosphane (Scheme 6; R = *i*-Pr: 23% over 4 steps; R = *t*-Bu: 16% over 4 steps, purification unsuccessful).[25]

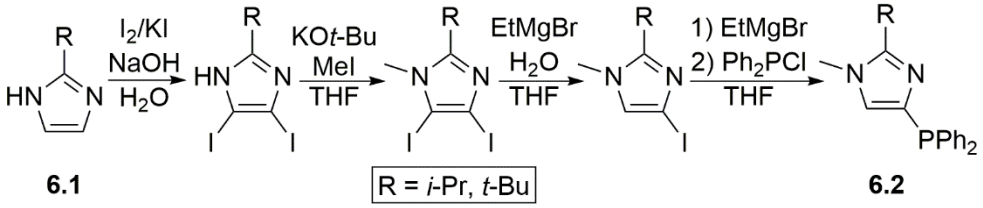

Scheme 6. 2-functionalized 4-imidazolylphosphanes.

2.2 Amino- and iminophosphanes

Nitrilium triflate **7.2**, generated from imidoyl chloride **7.1** and $SiMe_3OTf$, has been reacted with primary phosphanes and a base to yield iminophosphanes **7.3** (Scheme 7; three examples, 79-88%) and, after a subsequent 1,3-H-shift, the sterically congested tautomer **7.4** (R = Mes*, 88%); treatment of either with *n*-BuLi was shown to afford lithium phosphaamidinates **7.5** (R = Ph: 86%, R = Mes*: 66%).[26] Using secondary phosphanes instead gave non-tautomerisable water-stable iminophosphanes **8.2** (Scheme 8; **A**: 13 examples, 46-95%),[27,28] which could also be obtained from air and thermally stable imidoyl-pyridinium salts **8.3** (Scheme 8; **B**: seven examples, 71-94%).[29] Structural variations affect the ligand parameters, as evidenced by X-ray diffraction studies.[27,28] The milder approach allowed more substituent variations than the classic approach from imidoyl chlorides and silylphosphanes (8 examples, 40-87%).[30,31] Whereas, air-sensitive phosphanes can be protected by P-BR_3 substituents,[32] P-BR_2 bonds remain reactive, as illustrated by the coupling of diphenylphosphinopinacolborane to an aldimine, which yielded the pinacolboronate of an iminophosphane akin to **8.2** (95%).[33]

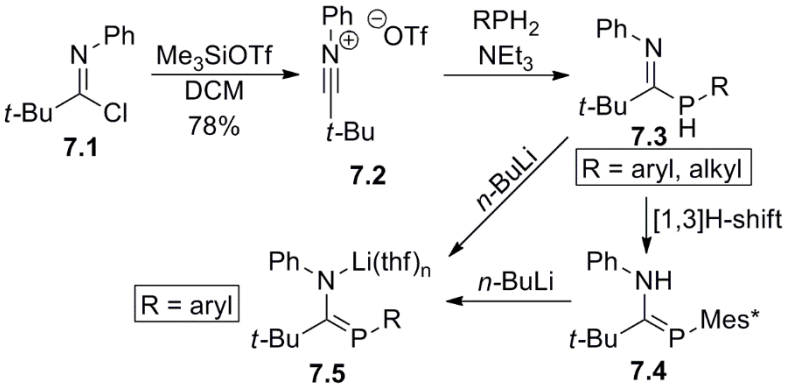

Scheme 7. Synthesis of secondary iminophosphanes/phosphaamidines and their derived aminates.

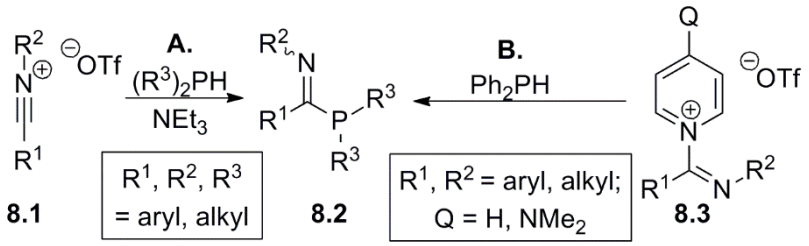

Scheme 8. Synthesis of tertiary iminophosphanes.

Amines have been shown to condense with (hydroxylmethyl)phosphanes to phosphane-amine ligands **9.1** (Scheme 9, four examples, 93-98%),[34] using substituent-dependent procedures. Deprotonation provided the *N*-anionic **9.2** (R^1 = Cy, 96%).

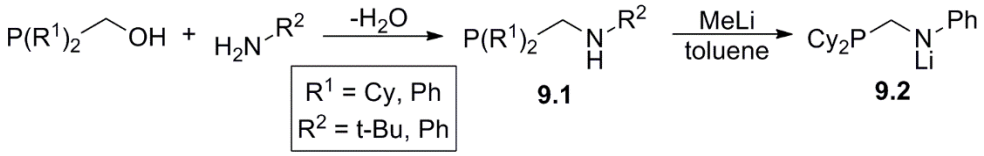

Scheme 9. Phosphane-amine and amido-phosphane preparation.

3 Groups IV-VII

1,2-Insertion of benzonitrile into the zirconium-phosphide bond of **10.1** provided Zr-complex **10.2** which features a rare *N*-coordinated iminatophosphane with a near linear Zr-N=C angle and a short Zr-N distance that suggest double bonding (Scheme 10; R = Cy, 86%; R = Ph, 72%).[35,36]

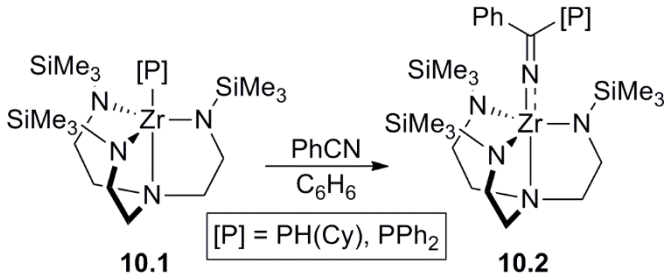

Scheme 10. Template-approach to iminatophosphanes.

Iminophosphanes provided bidentate complexes with Cr^0 (2 examples, 81-90%) and Cr^{III} (2 examples, 25-27%) (Scheme 11).[31] The Cr^{III} complexes are of interest for ethylene oligomerization, in which especially the bulky ligands provided very high selectivity for 1-hexene in the liquid fractions (up to 97.3 wt. %; 8 examples, 1 eq. Cr(2-ethylhexanoate)$_3$, 1 eq ligand, 500 eq. MMAO-3A, 100 eq. $ZnEt_2$, $P(C_2H_4)$ = 40 bar, methylcyclohexane, 60 °C, 60-200 min.). Bulky 2-imidazolylphosphanes were shown to react with $[W(CO)_5(THF)]$ to yield $(\kappa^1\text{-P,N})W(CO)_5$ and after reflux $(\kappa^2\text{-P,N})W(CO)_4$.[37] As no IR data was obtained for the unstable κ^1-complex, its ligand donor strength cannot be compared to $PyPPh_2$.[38] Reaction of $[Re(CO)_3Br(THF)]_2$ with $PyPPh_2$ provided the poorly photoluminescent κ^2-$(PyPPh_2)Re(CO)_3Br$ complex (61%, λ_{em} = 550 nm, φ = 0.001).[39]

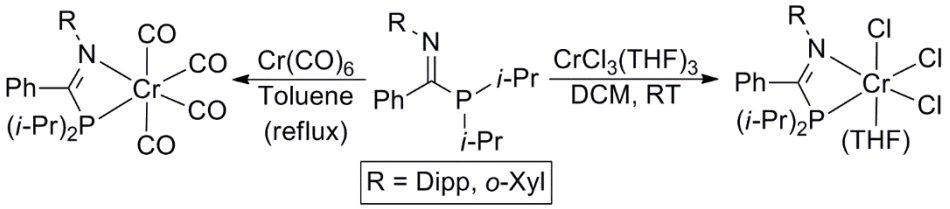

Scheme 11. Iminophosphane chromium coordination.

4 Group VIII

The focus of this section is nearly exclusively on 1,3-*P,N*-Ru-complexes, which were very prominent in catalysis. We are aware of only a single new report on Fe-complexes.

4.1 Iron

The first $PyPPh_2$ Fe^{III} complex was obtained from $FeCl_3$ and $PyPPh_2$ (**12.1**; Scheme 12).[40] It has a rare low-spin state (RT, −200 °C), which makes it suited to model the active site of non-heme metalloenzymes, but

no comments were made which factors contribute to this rare electronic state.

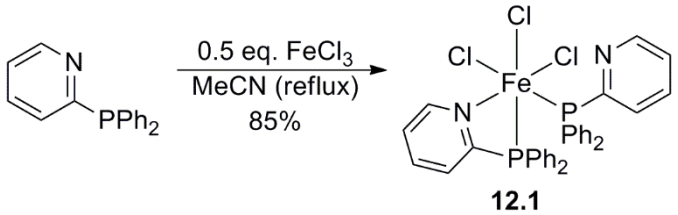

12.1

Scheme 12. A rare example of a low-spin Fe^{III} complex.

4.2 Ruthenium

Ruthenium is, along with palladium, the most common partner for *1,3-P,N*-ligands in catalysts. Reviewed here are nitrile hydration, alkyne hydration, transfer hydrogenation, hydroformylation, alkene-isomerization, [2+2] cycloadditions and coordination chemistry.

4.2.1 Catalysis – Nitrile hydration

Because the nitrile hydration catalyst **13.1** is only active at temperatures over 180 °C, presumably due to its high acac dissociation energy,[12f] the catalytic properties of **13.2** were explored (Scheme 13).[41] Whereas the methylallyl ligands seemed to give no improvement over acac, the increased *N*-basicity of the P,N-ligand showed enhanced interactions with the water substrate. Using three equivalents of the ligand further enhanced the catalytic activity to enable even conversion of less reactive aliphatic nitriles (11 examples, 38-99%). The observed behavior concurs with reported aqueous Ru-catalysis, as a study on the κ^1- and κ^2-(P,N)$Ru^{II/IV}$ catalysts shown in Scheme 14 found that additional P,N-ligand boosted the catalytic performance, while free arene decreased it, which suggests *in situ* dissociation of the arene.[42] Reacting $(PyPPh_2)Ru^{II}(p\text{-cym})Cl_2$ with 2.2 eq. P,N-ligand formed the highly active catalyst **15.1** (Scheme 14 and 15),[43] which displayed hemilability in the presence of benzonitrile. Combined, these reports suggest the incipient

formation of $[Ru^{II}(P,N)_3]$ to be relevant in the catalytic process. The hydration of benzonitrile in DME or H_2O was shown to be enhanced by changing the 1,3-P,N-ligand of the $(\kappa^1\text{-}PyPPh_2)Ru^{II}(p\text{-}cym)Cl_2$ catalyst to an iminophosphane (Scheme 16; **A**: 3 → 87%; **B**: 57 → 94%); the ligand substitution-pattern affected the catalyst performance in a solvent-less protocol (**C**: five examples, 70-82%).[28]

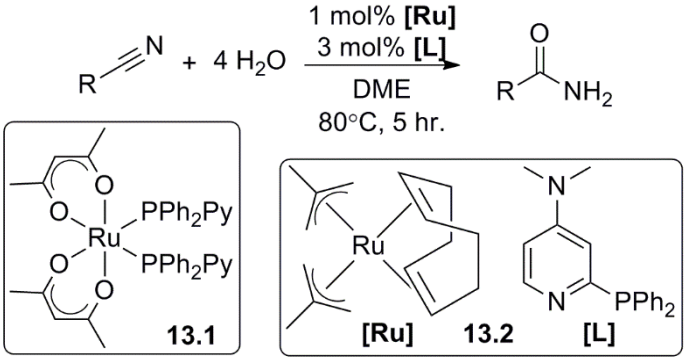

Scheme 13. Ru-catalyzed nitrile hydration.

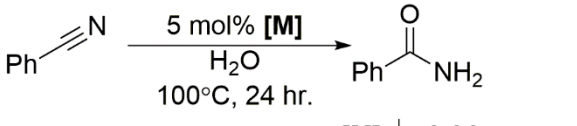

[M]	yields
$Ru(II)(\kappa1\text{-}L)(arene)Cl_2$	45-69%
$Ru(II)(PPh_3)(arene)Cl_2$	21-48%
$[Ru(II)(\kappa2\text{-}L)(arene)Cl]SbF_6$	7-37%
$Ru(IV)(\eta3\text{–}\eta3\text{–}C_{10}H_{16})(\kappa1\text{-}\mathbf{L3})Cl_2$	62%
$Ru(IV)(\eta3\text{–}\eta3\text{–}C_{10}H_{16})(PPh_3)Cl_2$	56%
$[Ru(IV)(\eta3\text{–}\eta3\text{–}C_{10}H_{16})(\kappa2\text{-}L)Cl]SbF_6$	7-34%
15.1	>99%

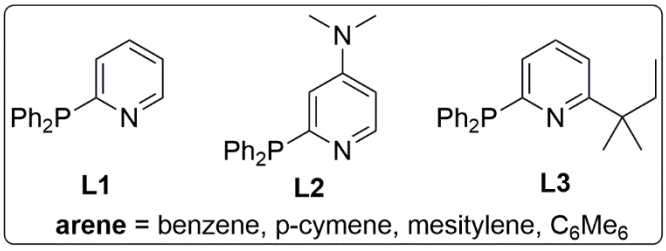

Scheme 14. Aqueous nitrile hydration.

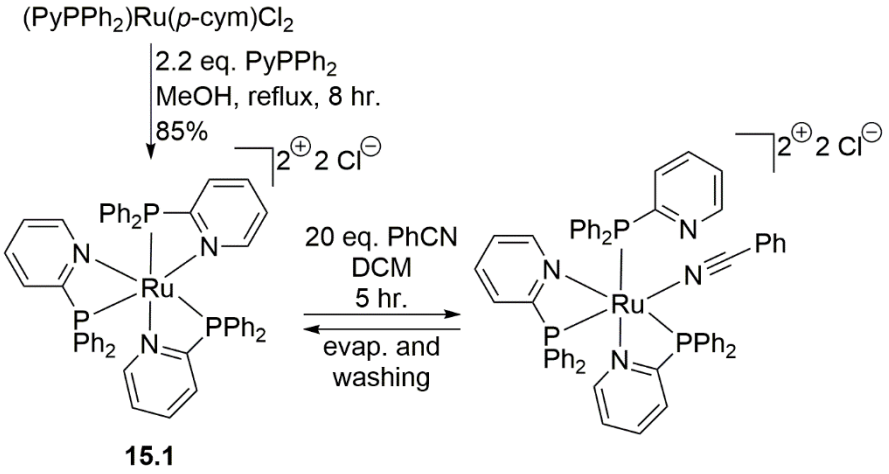

Scheme 15. Formation of the highly active $[(P,N)_3Ru^{II}]Cl_2$.

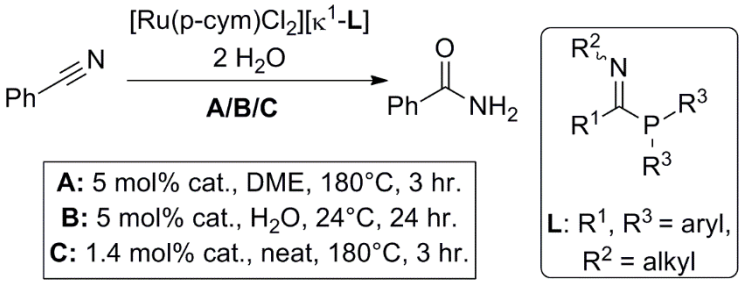

Scheme 16. Iminophosphane-Ru^{II} catalyzed nitrile hydration.

4.2.2 Catalysis – Anti-Markovnikov alkyne hydration

Ru^{II}-bis(P,N)-complexes were shown to catalyze the anti-Markovnikov hydration of terminal alkynes to aldehydes, in which the P,N-ligand first accelerates an alkyne/vinylidene isomerisation and then assists the hydration step by acting as proton shuttle (Scheme 17).[44] Since bulky substituents enhance catalytic activity,[45] a series of (6-substituted-Py)PPh_2 ligands was assessed in a model reaction with 1-octyne (Scheme 18; 16 examples, relative rates 0.02-4.2 with respect to R = *t*-Bu).[19] Increased steric bulk boosted catalytic activity, as did increased P,N-ligand basicity. Investigations with 2- and

4-imidazolylphosphanes disappointed in the same model reaction (up to 9% after 22 hr.; conditions from Scheme 18),[25] which is surprising, considering the activity of other imidazolylphosphane derived Ru^{II} catalysts.[46] These catalysts were all prepared *in situ*, but isolated homoleptic and heteroleptic species have been reported as well.[47] Heteroleptic complexes also led to the discovery that the second P,N-ligand does not contribute to the catalytic process.[48] Using one 1,3-P,N ligand and a 'place holder' ligand provides superior catalysts, which are easily accessible *in situ* from $RuCp(PPh_3)_2Cl$ and two equivalents of P,N-ligand (Scheme 19, **19.2**), and show high activity in the hydration of aliphatic, aromatic, acid- and base-sensitive alkynes, with excellent functional group tolerance (Scheme 20; 11 examples, 61-99%).

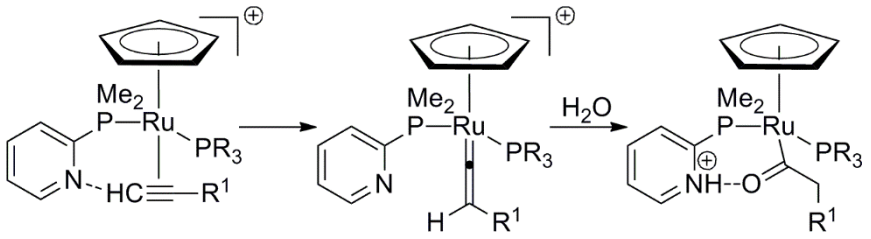

Scheme 17. P,N-assisted alkyne/vinylidene isomerisation and hydration.

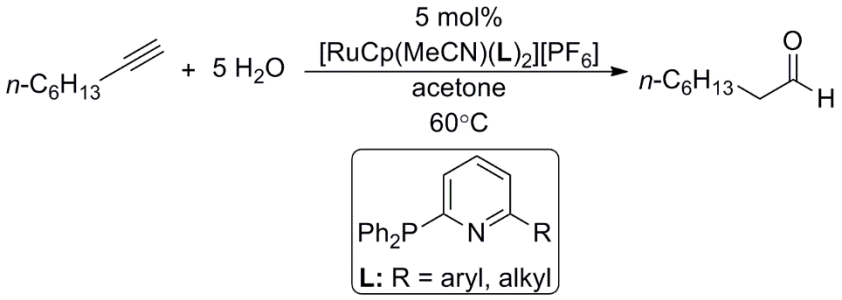

Scheme 18. Ru^{II} catalyzed alkyne hydration with 6-substituted $PyPPh_2$.

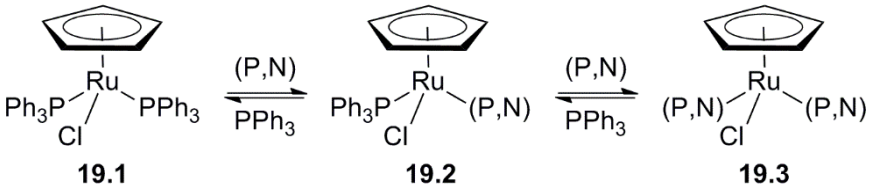

Scheme 19. In situ generation of heteroleptic catalyst **19.2**.

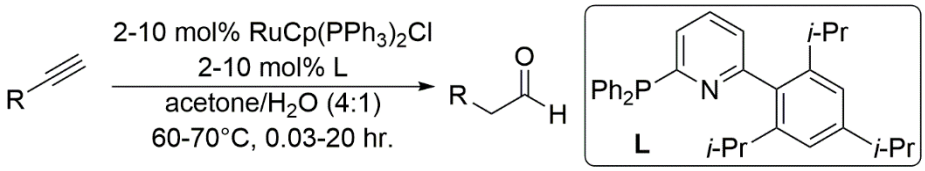

Scheme 20. Ru-catalyzed alkyne hydration.

An anti-Markovnikov hydration/transfer hydrogenation tandem process to convert alkynes to terminal alcohols with excellent functional group tolerance has been realized by combining hydration-catalyst **21.1** with hydrogenation-catalyst **21.2** (Scheme 21; **A**: alkynes, 12 examples, 80-96%; **B**: enynes, 5 examples, 85-90%).[49] Considering the activity of $Ru^{II}Cp(P,N)$ complexes in transfer hydrogenation (vide infra), a single catalyst for this tandem transformation may be interesting to pursue.

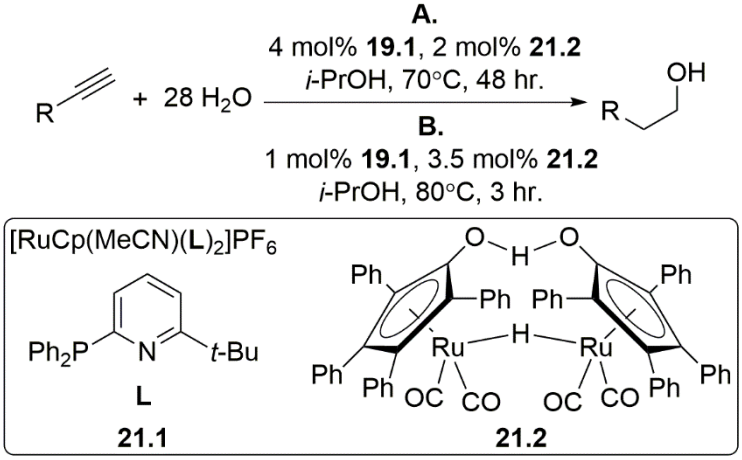

Scheme 21. Ru-catalyzed alkyne hydration/transfer hydrogenation.

4.2.3 Catalysis – Transfer hydrogenation

$(PyPPh_2)Ru^{II}Cp(PPh_3)Cl$ has been used to catalyze the transfer hydrogenation of benzaldehydes, with good conversions for electron-poor substrates (Scheme 22; 5 examples, 35-95%).[50] PPh_3 dissociation was proposed to provide the $16e^-$ active species, but it seems likely that *N*-coordination of $PyPPh_2$ might stabilize this species. The transfer hydrogenation of ketones was achieved with **23.1** (scheme 23; five examples, 16-96%).[51]

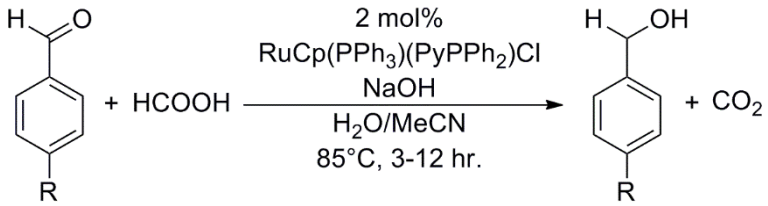

Scheme 22. Ru-catalyzed transfer hydrogenation of benzaldehydes.

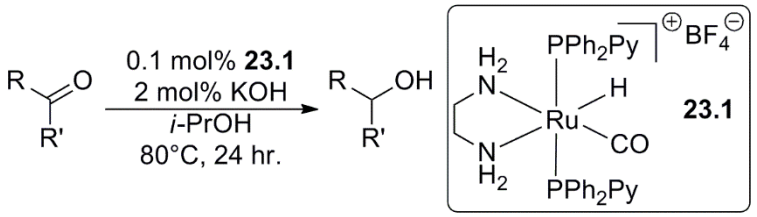

Scheme 23. Ru-catalyzed transfer hydrogenation of ketones.

4.2.4 Catalysis – Hydroformylation

A domino hydroformylation/hydrogenation sequence was reported to transform alkenes to linear alcohols, using highly active Ru^0-catalysts with excellent tolerance, good yields, and high selectivity (Scheme 24; 13 examples, 28-99%).[52] The 1,3-P,N-motive was essential to obtain good regioselectivity. Complex **25.2** was proposed to be the active species, which equilibrates with isolated **25.1** (Scheme 25). Its catalytic performance depends strongly on its preformation conditions and seems

specific for this ligand structure.[53] The domino hydrogenation activity could also be diminished to favor only hydroformylation, as shown in the *n*-selective conversion of 1-octene (Scheme 26).[54] Again complex **25.2** was the active species.

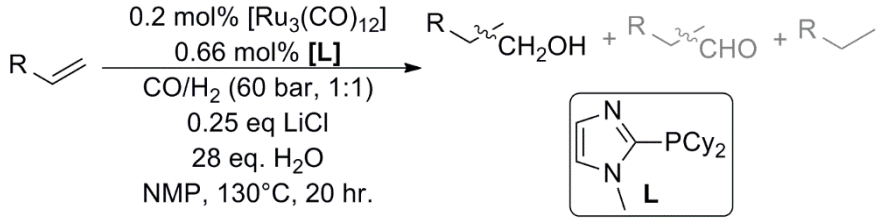

Scheme 24. Ru-catalyzed tandem hydroformylation/hydrogenation.

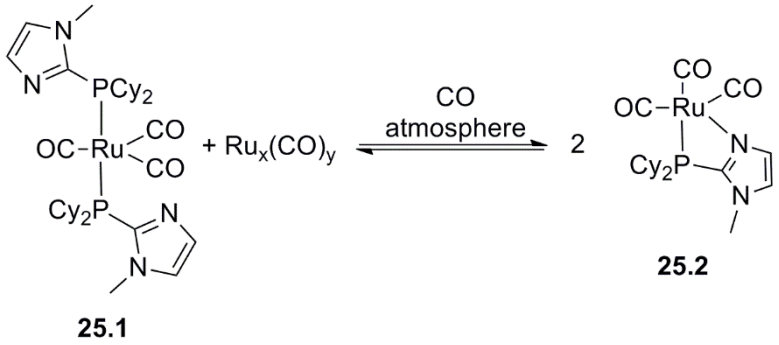

Scheme 25. CO-driven equilibrium between isolated **25.1** to catalyst **25.2**.

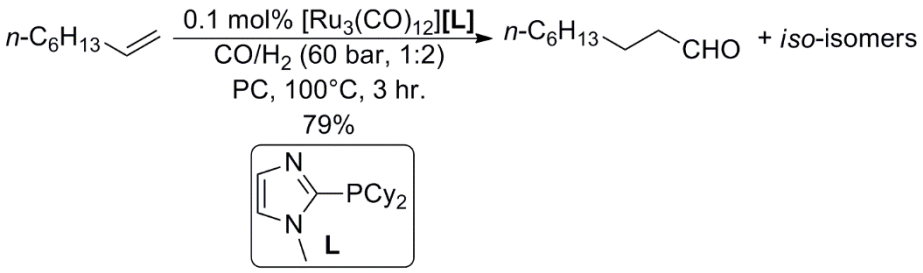

Scheme 26. Ru-catalyzed hydroformylation of 1-octene.

4.2.5 Catalysis – Alkene isomerisation

In 2007 (κ^2-2-imidazolylphosphane) $Ru^{II}Cp$ was found to catalytically isomerize alkenes.[11a] A DFT study showed that the P,N-ligand

deprotonates the alkene's α-CH_2, after which a P-Ru rotation and allyl-protonation at the terminal carbon provides the isomerized alkene (Scheme 27).[55] Unprecedented selectivity for trans-2-alkene products was achieved experimentally by replacing the Cp for a Cp* ligand (Scheme 28; 11 examples, 81.7-97.7%).[56] However, increased steric bulk in such catalysts decreases their rates.[57] The Cp-based catalyst was also explored in combination with a W-catalyst for a tandem isomerisation/metathesis coupling (Scheme 29, top).[58] The dual catalyst selectively transformed mixtures of trans olefins, but the W-complex decomposed in the presence of the Ru^{II} catalyst. Changing to the less decomposition-sensitive Hoveyda metathesis catalyst **H-II** allowed for the conversion of allylbenzenes to cinnamates and ferulates (Scheme 29, bottom; six examples, quant. yields).[59]

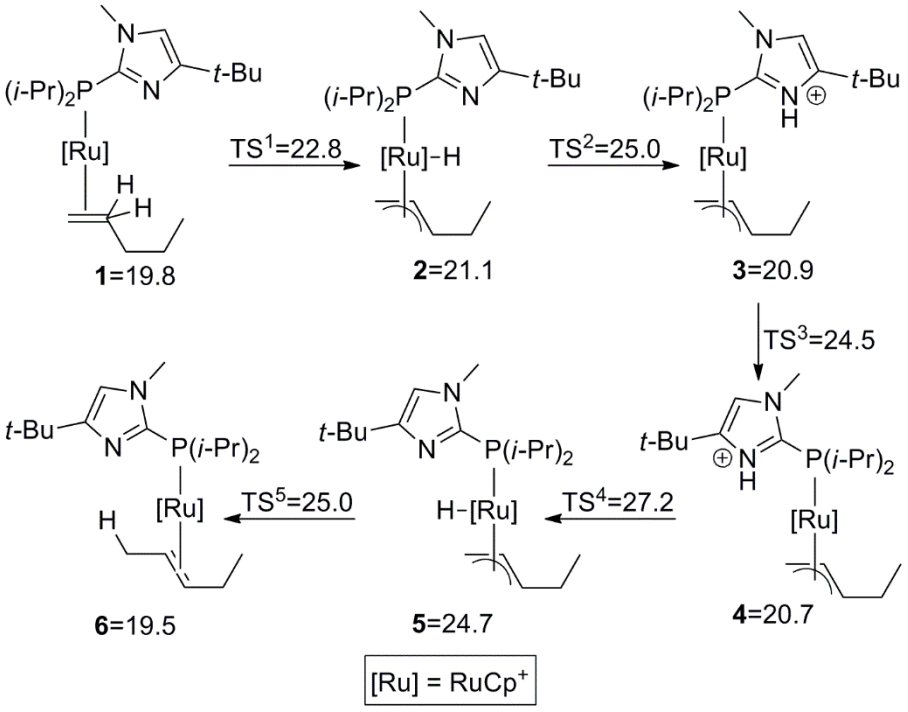

Scheme 27. DFT-modeled Ru-catalyzed isomerization 1-pentene. ΔG in kcal/mol.

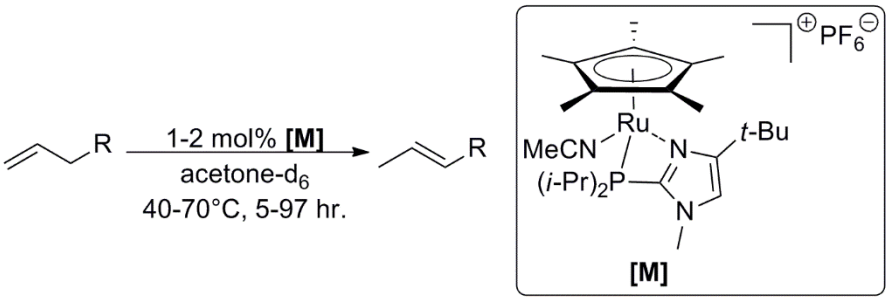

Scheme 28. Selective Ru-catalyzed isomerization 1-alkenes to 2-alkenes.

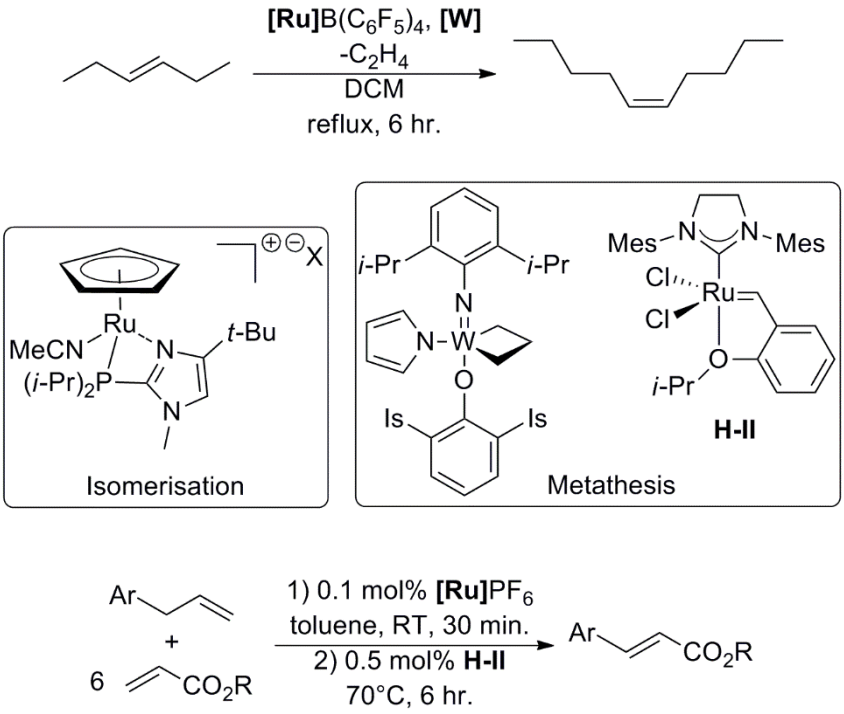

Scheme 29. Tandem alkene isomerization and metathesis.

4.2.6 Catalysis – Other

Based on the accelerated alkyne/vinylidene isomerization observed for 6-substituted 2-pyridylphosphane Ru^{II} systems in alkyne hydrations (section 4.2.2), such catalysts were explored for the oxidation of terminal alkynes, via vinylidene intermediates, to ketenes in the presence of

intramolecular sulfoxide oxidants.[60] The *in situ* generated ketenes were shown to undergo [2+2] cycloadditions intramolecularly with alkenes (Scheme 30; seven examples, 62-91%) and intermolecularly with imines (Scheme 31; six examples, 34-95%). Using the same strategy propargyl sulfoxides could be rearranged to α,ß-unsaturated thioesters (Scheme 32; seven examples, 71-89%).[61]

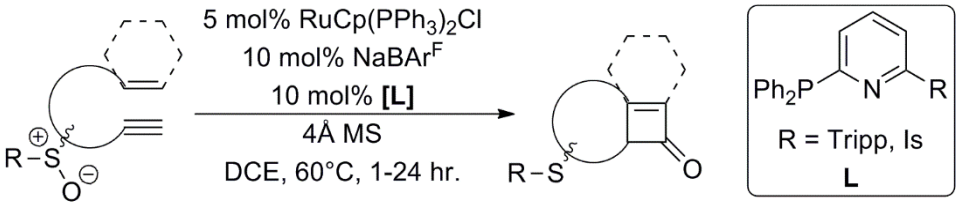

Scheme 30. Ru-catalyzed [2+2] cycloaddition of in situ generated ketenes and alkenes.

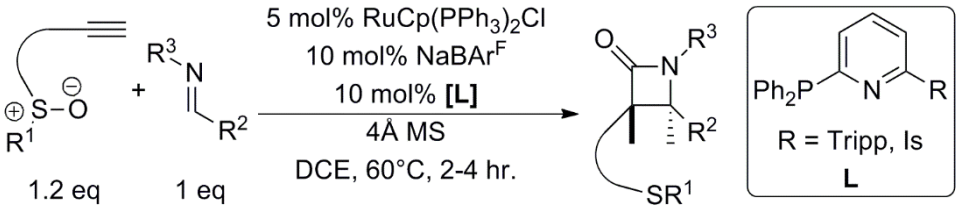

Scheme 31. Ru-catalyzed [2+2] cycloaddition of in situ generated ketenes and imines.

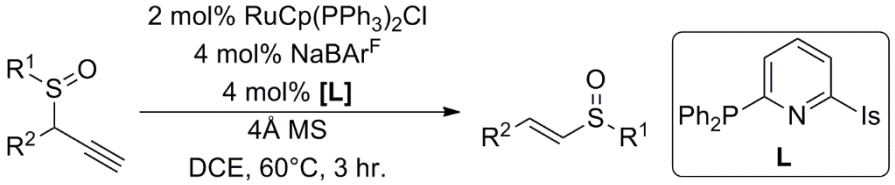

Scheme 32. Ru-catalyzed propargyl sulfoxide rearrangement.

$PyPPh_2$ was also tested in the Ru^0-catalyzed amination of cyclohexanol with ammonia (1 mol% [Ru_3CO_{12}], 6 mol% $PyPPh_2$, cyclohexane, 140 °C, 21 hr., 29%),[62] but was outperformed by 2-pyrrolylphosphanes. This result is notable in light of the scarcity of homogeneous catalysts for this transformation. A $PyPPh_2$ containing Ru-catalyst converted

benzaldoximes into benzamides via a Beckmann rearrangement (1 mol% $[Ru^{II}(Terpy)(PyPPh_2)_2]Cl_2$, toluene, reflux, 10 hr.; three examples, 80-82%);[63] a hydration mechanism via nitriles (section 4.2.1) was experimentally ruled out. The complex $[Ru(p\text{-}cym)(PhO)(CO)\text{-}(PyPPh_2)]BF_4$ has been shown to catalyze the hydrothiolation of phenyl acetylene with benzyl thiol (2 mol%, H_2O/THF, RT, 2h; 90% (E:Z = 74:26)).[64] $PyPPh_2$ did not perform well in the $[PR_3\text{-}RuCp^*Cl_2]$-catalyzed atom transfer radical polymerization of methylmethacrylate.[65]

4.2.7 Coordination chemistry

The electronic and conformational effects of $PyPPh_2$ in $Ru^{II}(CO)$ complexes have been studied with X-ray crystallography and NMR- and IR-spectroscopy.[66] Ru^{II} and Ru^{IV} systems were used to transmetallate bulky 6-substituted $PyPPh_2$ ligands to coinage metals (vide infra, section 7.1).[67] Borate-tethered ligand **5.2** has been reacted with $Ru^{II}Cp^*(CO)_2Cl$ and $Ru^{II}Cl(C_5R_5)(PPh_3)_2$ to provide bidentate complexes **33.1** and **33.2** (Scheme 33).[24] Hemilability in **33.1** allowed heat-driven CO displacement and re-coordination under CO pressure. Like other $Ru^{II}(P,N)$ systems (sections 4.2.2, 4.2.6), complex **33.2** readily isomerized terminal alkynes to vinylidenes (**33.3**), which then were attacked by nitrogen atom of the P,N-ligand (**33.4**; four examples, 56-84%).

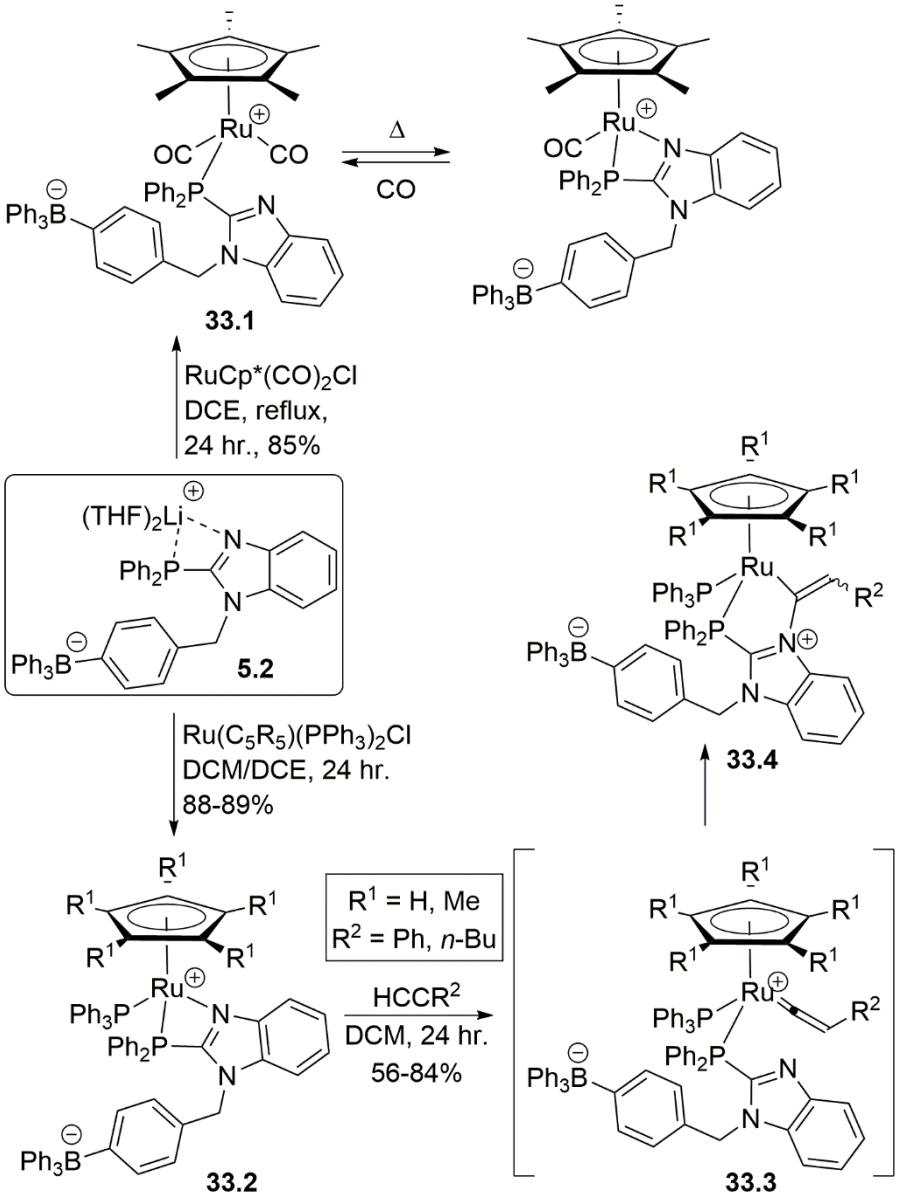

Scheme 33. Coordination chemistry and reactivity of P,N-borates.

4.2.8 Bio-inorganic

A series of $[Ru^{II}(Terpy)(PyPPh_2)_2]Cl_2$ complexes showed antimalarial activity, but PPh_3-based analogues outperformed them.[63] A κ^1-2-imidazolylphosphane Ru^{II} arene complex was found to be cytotoxic

for colon- and ovarian-cancer cells in μM concentrations (IC_{50} = 58 μM, 38 μM) due to its relatively high lipophilicity.[68] Tests on 2-imidazolylphosphane and 2-pyridylphosphane complexes demonstrated that both interact with DNA and are efficient inhibitors of breast- and pancreatic-cancer cells, rivalling cis-platin (IC_{50} = 3.3-3.77 μM, 6.6-6.94 μM).[69]

5 Group IX

1,3-P,N-Group IX developments have mainly focused on coordination chemistry.

5.1 Cobalt

The pyridyl 3-position of $PyPPh_2$ is activated by $Co^I(CH_3)(PMe_3)_4$ to form a four-membered metallacycle that readily underwent ring-expansion by CO insertion into the Co-C bond but showed slow oxidative addition activity with iodomethane (Scheme 34).[70]

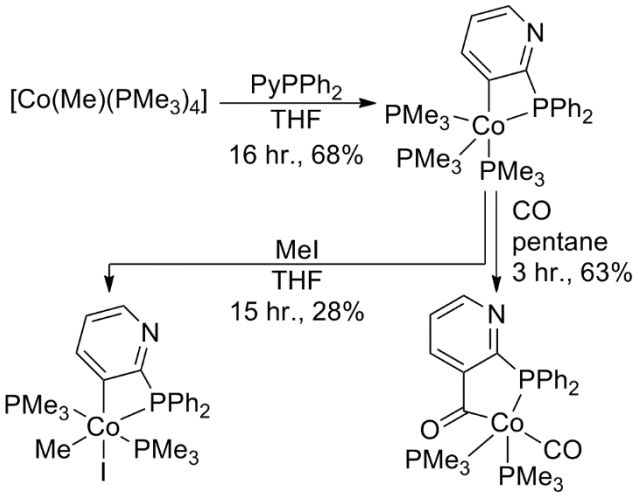

Scheme 34. Pyridyl 3-activation by Co^I.

5.2 Rhodium

The coordination behavior of $PyPPh_2$ in Rh-complexes has been compared with that of the PPh_3 ligand.[71,72] Enhanced electron donation of the $PyPPh_2$ ligand was concluded based on IR characteristics and was confirmed by the increased reaction rates of oxidative addition of MeI for $Rh^I(PR_3)(CO)$(acac/cupferrate) complexes. P,N-bidentate coordination in a pentacoordinate pyramidal transition state was proposed to cause the fluxional behavior of dienes in (κ^1-P,N)Rh^I(diene)Cl (Scheme 35).[73]

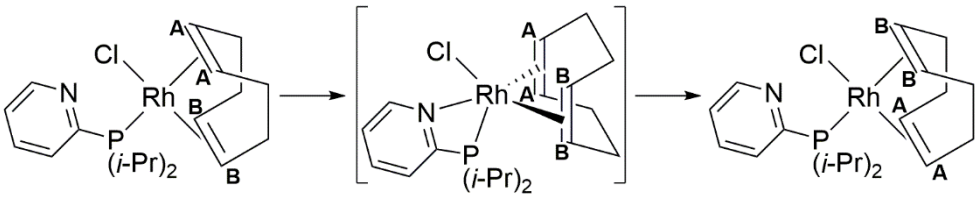

Scheme 35. Fluxional behavior of dienes (labeled **A** and **B**) in P,N-Rh^I complexes.

The neutral phosphane-amines were found to coordinate to Rh^I(COD)Cl (Scheme 36).[34] Whereas it is surprising that κ^2-coordination does not occur with the anionic ligands, as they proposedly capture LiCl instead (**36.1**), subsequent quenching with H_2O followed by ion exchange gave the Rh-complex with the neutral bidentate ligand. Phosphaamidinates with a delocalized anionic charge were shown to give P,N-bidentate Rh^I-coordination in which the ligand retains its anionicity (Scheme 37).[26] Rh^{III}-coordination of iminophosphanes **38.1** with varying *N*-donor strengths provided either the κ^1-complex (**38.2**) or a mixture of both the κ^1- and κ^2-complexes (**38.2** and **38.3**; Scheme 36).[26,28] Chloride abstractions yielded κ^2-complexes **38.4/5**.

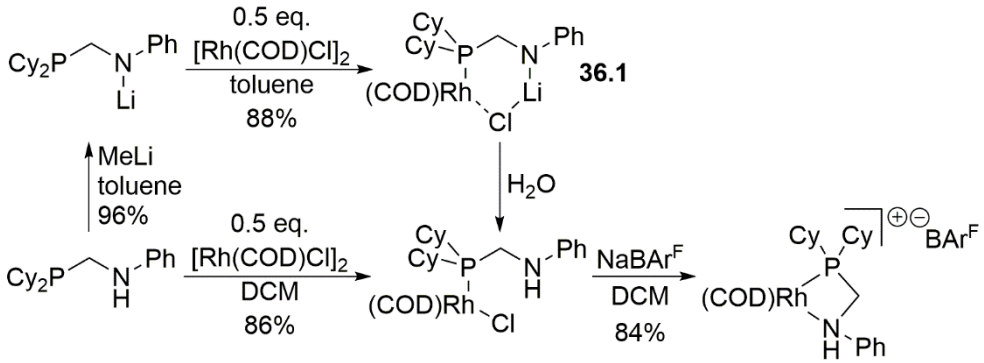

Scheme 36. Rh^{I} coordination of phosphane-amines and amidophosphanes.

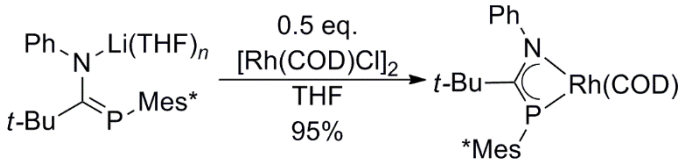

Scheme 37. Rh^{I} coordination of phosphamidinates.

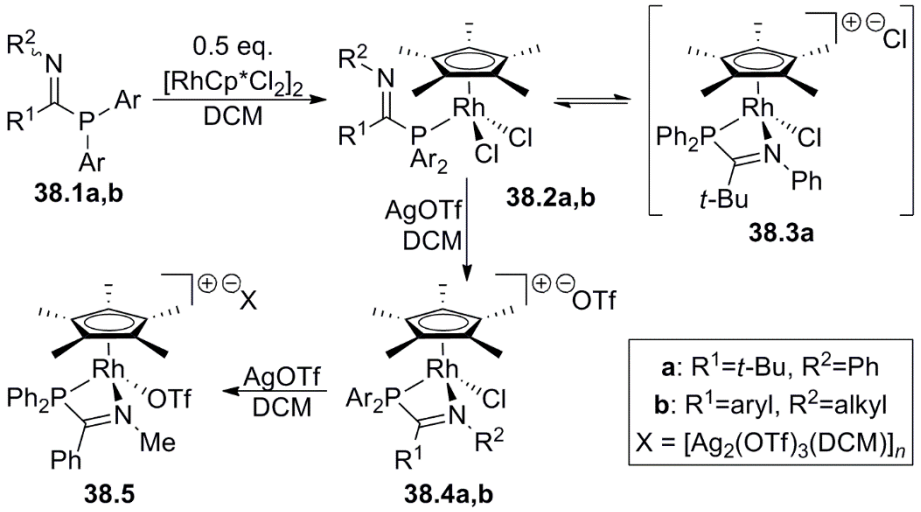

Scheme 38. Iminophosphane coordination to Rh^{III}.

5.2.1 Catalysis – Nitrile hydration and transfer hydrogenation

Complex **38.2b** (Scheme 38; R^1 = Ph, R^2 = Me) is the first Rh^{III} complex to catalyze the hydration of benzonitrile (22%; 5 mol%, DME, 180 °C,

3 hr.).[28] For aqueous $Rh^{I}(COD)Cl$ catalyzed nitrile hydration three 2-pyridylphosphanes were explored, but the yields were low (3-21%), reportedly due to the formation of the corresponding bidentate complexes.[74] However, the bidentate $[Rh^{I}(coe)(\kappa^2\text{-}PyPPh_2)Cl]$ complex did successfully catalyze the transfer hydrogenation of ketones in high yield (three examples, 91-97%; cat. loading 1 mol%, 0.5 eq. KOH, *i*-PrOH, 83 °C, 30 min.).[75]

5.3 Iridium

Coordination of iminophosphanes to Ir^{III} contrasts with the analogous Rh^{III} as exclusively bidentate complex **39.2a** was obtained, as confirmed by chloride abstraction with AgOTf to **39.3a**, which provided nearly identical NMR data. (Scheme 39).[27] Nevertheless, there are reports on κ^1-species such as the studies on $(\kappa^1\text{-}PyPPh_2)IrCp^*(N_3)_2$ and the hemilabile $[(\kappa^2\text{-}PyPPh_2)IrCp^*(N_3)]OTf$.[76] Both the κ^1- and $\kappa^2\text{-}Ir^{III}Cp^*$ complexes have been used to study the H-bonding interactions of protic 2-imidazolylphosphanes by X-ray diffraction, NMR spectroscopy (^1H, ^{13}C, ^{15}N, ^{31}P) and IR spectroscopy ($\nu_{N\text{-}H}$), (Scheme 40).[77] Complex **40.2b** has shown activity in the transfer hydrogenation of acetophenone (Scheme 41; conditions unoptimized),[77] but its activity does not rival Ru^{II} (section 4.2.3) or other Ir^{III} catalysts.[78]

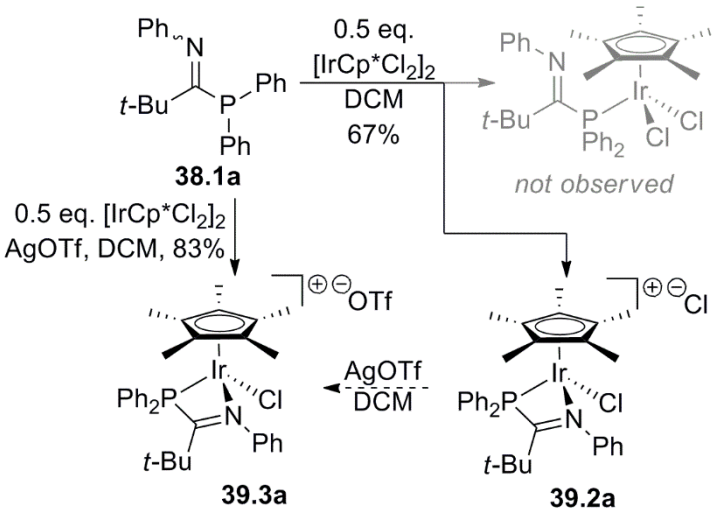

Scheme 39. Iminophosphane coordination to Ir^{III}.

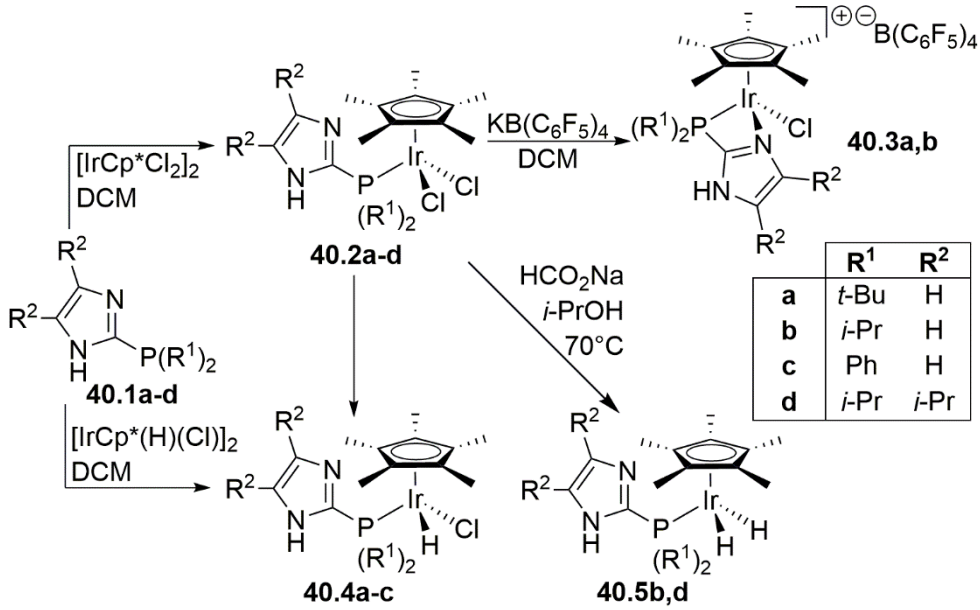

Scheme 40. Hydrogen bonding in protic P,N-ligands.

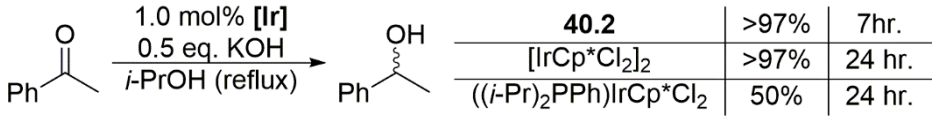

Scheme 41. Ir^{III} catalyzed transfer hydrogenation.

6 Group X

Nickel was explored in only a single report, whereas palladium is a far more popular choice for P,N-chemistry, with many reports on carbonylation and cross coupling catalysis. The focus of the P,N-platinum complexes has been mostly on coordination chemistry.

6.1 Nickel

$PyPPh_2$ was compared to PPh_3, Py_2PPh and Py_3P in a series of tetrahedral *in situ* prepared $(PR_3)_2Ni(CO)_2$, $(PR_3)_2Ni$(bisphosphane) and $(PR_3)_4Ni$ κ^1-complexes to assess their potential for aqueous catalysis, but their rapid decomposition only allowed for a study of their ^{31}P NMR spectroscopic characteristics.[79]

6.2 Palladium

Beside mechanistic DFT studies on Pd-catalyzed carbonylation, the emphasis of the P,N-ligated Pd-complexes has been on coordination chemistry and cross-coupling reactivity, including Suzuki-Miyaura coupling, Heck reaction, *β*-arylation and other aryl halide functionalizations, which are reviewed below.

6.2.1 Coordination chemistry

Coordination studies on P,N-ligated Pd-complexes have focused on the effect of cooperative reactivity of the *N*-site. NMR-analyses of (methyl-allyl)$Pd^{II}X$ complexes with κ^1-$PyPPh_2$ ligands revealed that pyridyl protonation reduced their σ-donation and increased their π-acceptance without affecting the stability of the complexes.[15,80] Pyridyl protonation of [(1,2-dicyanoethene)Pd^{II} $(PyPPh_2)_2]^{2+}$ effected the release of the alkene ligand from the electron deficient metal center. Ligand hemilability (*N*-release, $\kappa^2 \rightarrow \kappa^1$) in $[(\kappa^2\text{-}PyPPh_2)(\kappa^1\text{-}PyPPh_2)Pd^{II}Cl]^+$, could be induced

by strong donors, like PPh_3 and Cl^-, but not by weaker donors, like CO or alkynes,[81] which seems to contradict the proposed Pd-catalyzed methoxycarbonylation mechanism (vide infra).

P,N-ligand assisted heterolytic cleavage of H_2 by $(PyPPh_2)Pd^{II}(dppf)$ complexes **42.1** to **42.2** was shown to be enhanced by substituting the pyridyl group at the 6-position (Scheme 42).[82] Rapid rearrangement to **42.3** could only be prevented for Pt^{II} analogues (section 6.3).

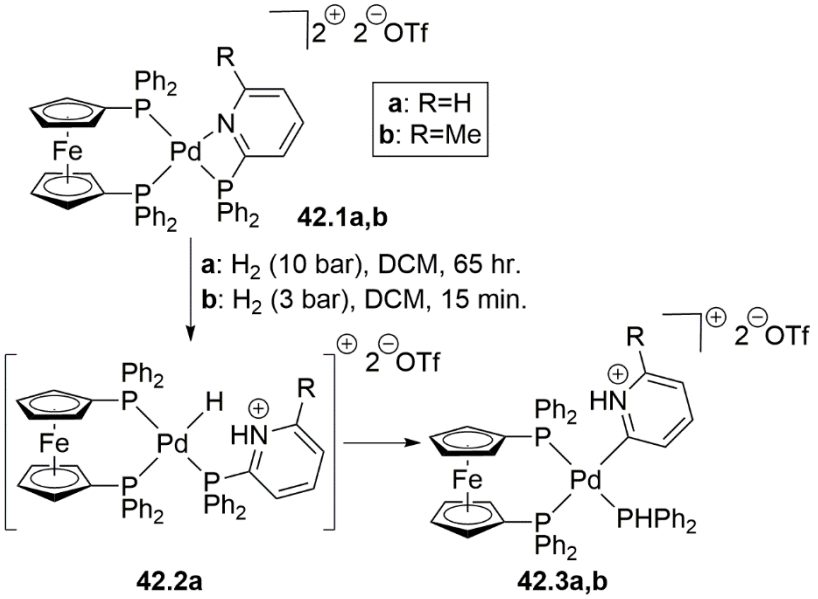

Scheme 42. PN-assisted heterolytic H_2 cleavage and rearrangement.

6.2.2 Catalysis – Alkoxycarbonylation

A combined DFT and experimental study addressed the mechanism of the Pd-catalyzed methoxycarbonylation of propyne to methylmethacrylate (Scheme 43).[83] After propyne coordination (step **I**), the ligand's N-H and the alkyne's methyl group were calculated to sterically determine the regioselectivity (**II**), which could be enhanced by methyl substitution at the 6-position of the pyridine. After CO insertion

(**III**, **IV**), MeOH coordinates to Pd and shows H-bonding interactions with the pyridyl group (**V**). The final and rate-determining heterolytic alcoholysis step (**VI**) are predicted to be accelerated by increasing the ligand basicity or hydrogen bonding interactions, while protonation of the second $PyPPh_2$ ligand would enhance solvolysis and regioselectivity.

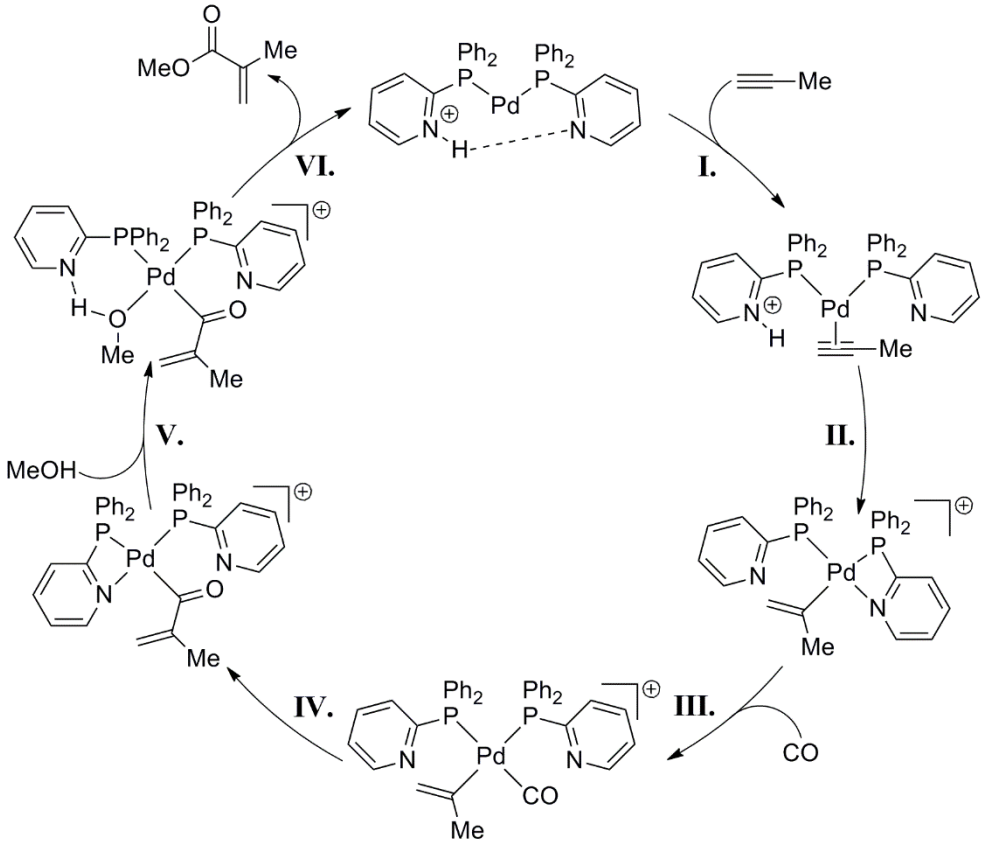

Scheme 43. Proposed mechanism for methoxycarbonylation of propyne.

When polymerized vinyl-functionalized $PyPPh_2$ **44.1** was treated with $Pd(OAc)_2$, it provided a heterogeneous catalyst for ethylene methoxycarbonylation with higher TOFs than the homogeneous $PyPPh_2/Pd(OAc)_2$ catalyst under the employed conditions (Scheme 44; 4.6×10^{-3} mmol $Pd(OAc)_2$, 0.115 mmol p-toluenesulfonic acid, acetone, 5 mL

CH_3OH, $P(C_2H_2)$ = 0.12 MPa, P(CO) = 4.8 MPa, 50 °C, 1 hr.).[84] Copolymerization of the ligand with *p*-styrene sulfonic acid (**44.2**) gave an enhancement, which was attributed to the porous nature of the catalyst (3.5×10^{-3} mmol $Pd(OAc)_2$, 5 mmol alkyne or $P(C_2H_2)$ = 0.12 MPa, P(CO) = 4.8 MPa, ROH, 50 °C, 1-4 hr.; 7 examples, TON = 145-949).[85] The catalyst could be reused, with only slight Pd-leaching (up to 0.114 ppm/run).

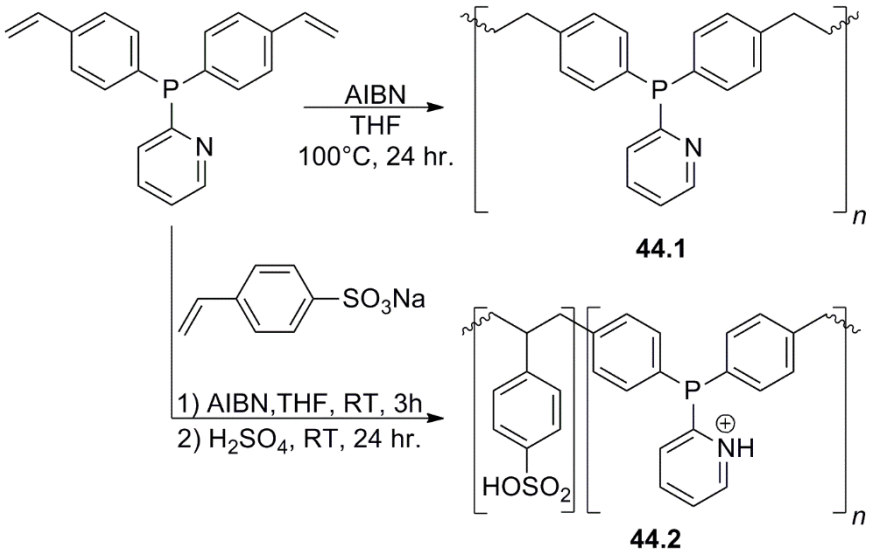

Scheme 44. Polymeric ligands for Pd^{II}-catalyzed alkoxycarbonylation of alkynes.

6.2.3 Catalysis – Suzuki-Miyaura cross-coupling reaction

When $[(\kappa^2\text{-}PyPPh_2)Pd^{II}](ClO_4)_2$ was immobilized by silica-bound pyridine ligands it was shown to be an effective Suzuki-Miyaura catalyst to couple aryl bromides and iodides with phenyl boronic acids (Scheme 45; 9 examples, 82-98%; reusable, <2% leached Pd/six runs).[86]

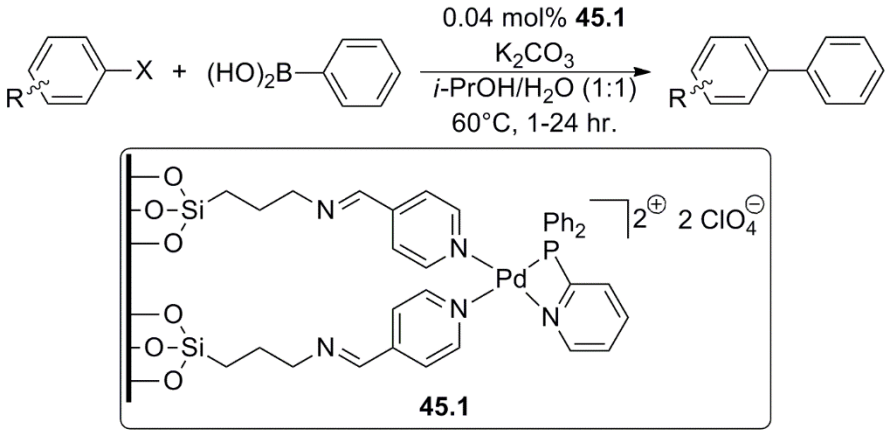

Scheme 45. Heterogeneous Suzuki-Miyaura cross-coupling.

Catalysts generated from 2-imidazolyl-phosphanes and $Pd^{II}Cl_2$ enabled the coupling of phenyl boronic acid with alkyl- and arylhalides and showed good functional group tolerance (Scheme 46; 17 examples, 40-99%; for X = Cl: double cat. loading, 24 hr.; 30-85%).[87] The coupling of (4-methyl)phenyl halides and phenylboronic acid with catalysts obtained from cyclophane-based 2-imidazolylphosphane ligands and $Pd(OAc)_2$ performed less favorably and an atroposelective process seems more worthwhile to pursue.[22] Whereas two (κ^2-$PyPPh_2$) Pd^{II}(imidazole) complexes have been associated with the coupling of 4-bromonitrobenzene and phenylboronic acid, the actual catalytic process has been attributed to Pd nanoparticles formed during the reaction.[88]

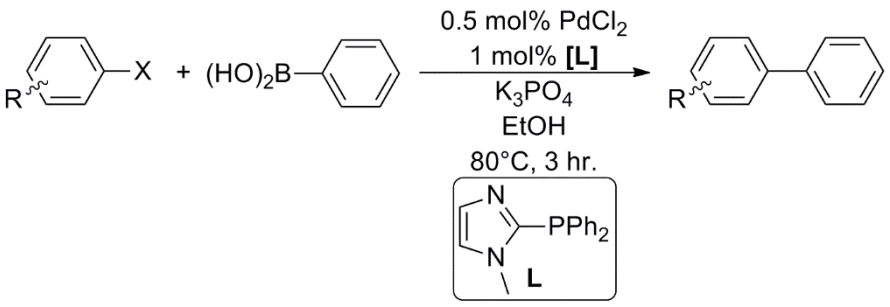

Scheme 46. Suzuki-Miyaura cross-coupling.

6.2.4 Catalysis – Heck cross-coupling reaction

Pd^{II}(cinnamyl)chloride and a bulky 2-imidazolylphosphane have been used for a carbonylative Heck reaction in which styrene was coupled to aryl iodides and bromides with excellent tolerance (Scheme 47; 22 examples, 41-90%). Also functionalized olefins could be used, of which three reacted with >99% trans-selectivity (10 examples, 51-88%).[89]

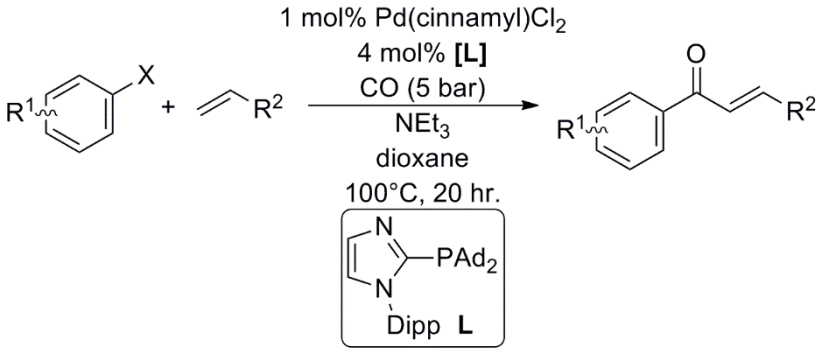

Scheme 47. Carbonylative Heck coupling.

6.2.5 Catalysis – Cross-coupling of aryl halides

$Pd_2(dba_3)_3$ and a bulky 2-imidazolylphosphane selectively hydroxylated aryl chlorides/ bromides, with reasonable functional group tolerance, while suppressing coupling to diaryl ethers (Scheme 48; 15 examples, 50-99%).[90] Changing the Pd-precursor to $[Pd(COD)(CH_2SiMe_3)_2]$ significantly enhanced the activity and substrate tolerance (Scheme 49; 17 examples, 67-99%),[91] which was attributed to the fast generation of the (κ^2-P,N)Pd^0 complex, as well as the ligand's hemilabile nitrogen donor and bulky steric properties.

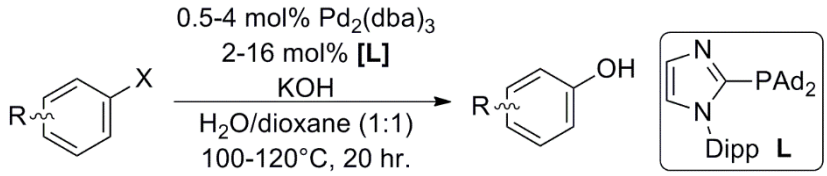

Scheme 48. Aryl halide hydroxylation.

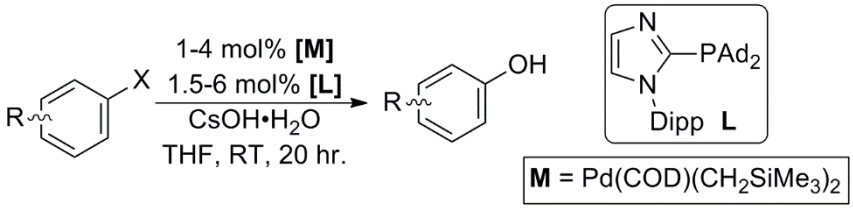

Scheme 49. Ambient aryl halide hydroxylation.

Bulky imidazolylphosphane ligands were also shown to perform well for the [$Pd^{II}(TFA)_2$] catalyzed arylnitrile formation from aryl chlorides and $K_4[Fe(CN)_6]$ (Scheme 50; 10 examples, 18-75%).[92]

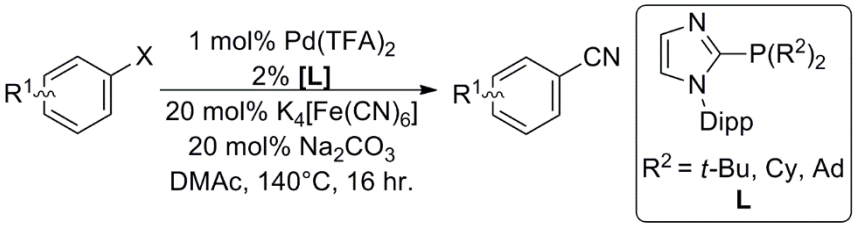

Scheme 50. Aryl halide cyanation.

6.2.6 Catalysis – Buchwald-Hartwig cross-coupling reaction

The size and charge of the borate-tethered P,N-ligand **51.1** was studied in the Buchwald-Hartwig coupling of aryl bromides with primary amines (Scheme 51; 10 examples 36-97%).[93] Loss of charge as in ligand **51.2** had no effect on the yield but reduction in the steric bulk as in ligand **51.3** proved to be detrimental. Possibly the large substituents prevent catalyst poisoning, as was reported for the bulky P,N-ligand **52.1** in the Pd-catalyzed formation of monoarylamines from ammonia and aryl

chlorides and bromides (Scheme 52; 20 examples, 28-99%);[94] electronically and sterically varied substrates were tolerated.

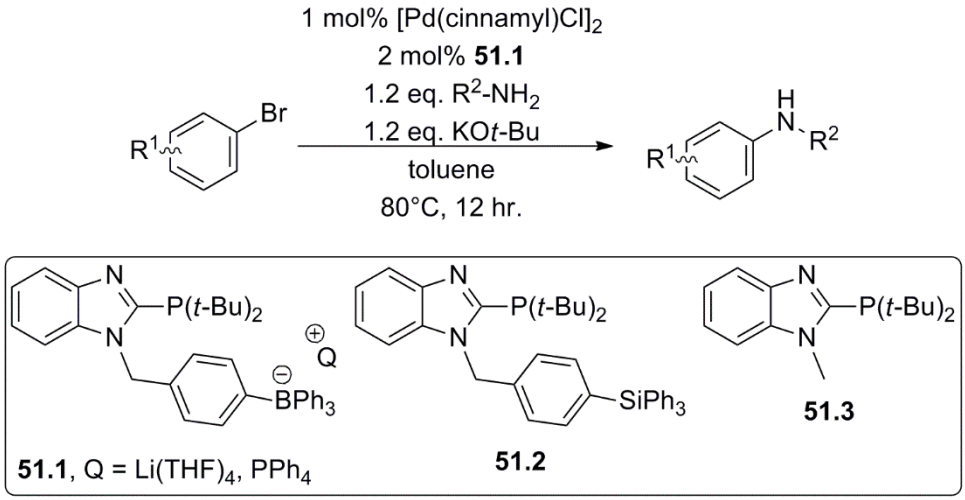

Scheme 51. Aryl halide amination.

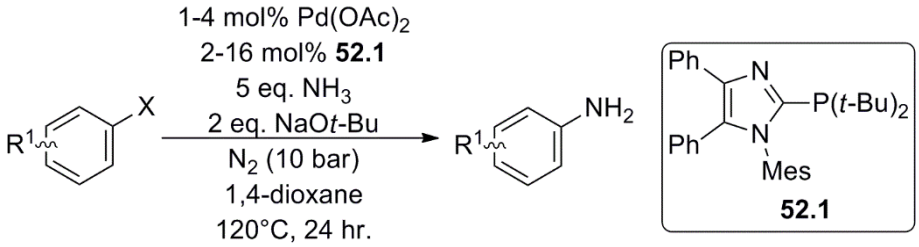

Scheme 52. Aryl halide amination.

6.2.7 Catalysis – β-Arylation by migrative Negishi coupling

The *α*/*β*-selectivity for the Pd-catalyzed *β*-arylation of *N*-Boc protected acyclic amines with aryl halides was shown to be sterically controlled by the bulky P,N-ligand **53.1** (Scheme 53; 8 examples, 39-63%).[95]

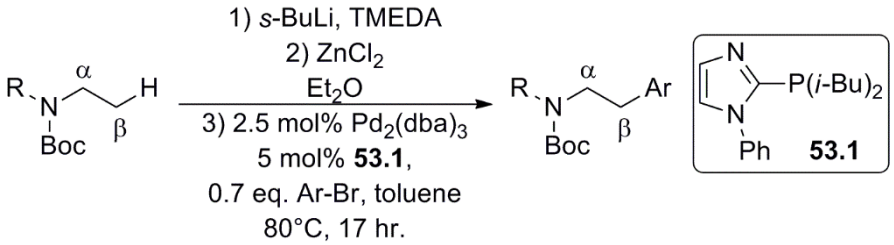

Scheme 53. The ß-arylation of N-Boc protected acyclic amines.

6.2.8 Bio-inorganic

Complex [(κ^1-PyPPh$_2$)Pd^{II}(dithiocarbamate)Cl] was cytotoxic for cis-platin-resistant prostate cancer cells (IC_{50} of 1.55 μM) due to hydrogen bonding of the PyPPh$_2$ ligand to the cell's DNA; H-bonding with bacterial cell constituents gave an antibacterial effect against three Gram positive and two Gram negative strains.[96] Non-toxic complex (κ^1-PyPPh$_2$)$_2$Pd^{II}Cl$_2$ showed low inhibition of HIV-1 protease (10-25% inhibition at 10-100 μM).[97]

6.3 Platinum

Platinum complexes [Pt(diphosphane)(PyPPh$_2$)](OTf)$_2$ **54.1** were shown to cleave dihydrogen heterolytically (Scheme 54), without subsequently cleaving the P-Py bond as was observed for the analogous Pd-complexes **42.1** that were discussed in section 6.2.1.[82] Increasing the steric bulk of the diphosphane enhanced the P,N-hemilability and thereby the rate of reaction.

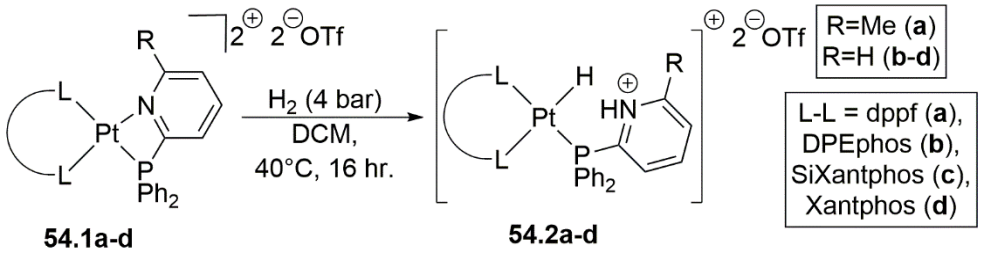

Scheme 54. P,N-assisted heterolytic H_2 cleavage.

Platinum complex $(\kappa^1\text{-PyPPh}_2)_2\text{Pt}^{II}\text{Cl}_2$ was found to give up to 30% inhibition of HIV-1 protease at 10-100 µM.[97] Complex (κ^2-2,2'-bipyridine-N-oxide)$\text{Pt}^{II}(\kappa^1\text{-PyPPh}_2)$(Me) complex showed cytotoxicity against human lung, ovarian, and breast cancer cells (IC_{50} = 9.72-35.08),[98] as did the related and more effective (2-phenylpyridynate)$\text{Pt}^{II}(\kappa^1\text{-PyPPh}_2)$(S-R) complexes (R = 2-pyridyl: IC_{50} = 11.66-15.11; R = 2-pyrimidyl: IC_{50} = 4.58-16.33).[99]

7 Groups XI-XII

Mononuclear P,N-coinage metal complexes have been used mainly as precursor for multinuclear species and a few reports explored their applications in catalysis too. One report focused on zinc.

7.1 Group XI

Mononuclear P,N-coinage chemistry has mainly focused on photoluminescence. Of the reported $\text{Cu}^{I}(\kappa^1\text{-PyPPh}_2)$(thiocyanate) complexes, $[\text{Cu}^{I}(\text{NCS})(\text{PyPPh}_2)_3]$ displayed weak photoluminescent emission at λ = 562 nm.[100] AgOTf with two equivalents of PyPPh_2 provided a mixture of photoluminescent isomers (λ = 491 nm, τ = 51.8 µs), whereas three equivalents provided the proposed trigonal planar $[\text{Ag}(\kappa^1\text{-PyPPh}_2)_3]$OTf complex ($\lambda$ = 494 nm, τ = 25.7 µs).[101]

Most 1,3-P,N-Au^{I} complexes have been used as precursors for photoluminescent multinuclear complexes with straightforward linear κ^1-P-Au-X coordinations [102]. Iminophosphane ligands **55.1** with varied substitution patterns coordinated to Au(tht)Cl/(SMe_2)AuCl to give **55.2** show comparable coordination parameters (90%-quant, Scheme 55).[27] Me_2S-Ru coordination drives Ru^{II} and Ru^{IV} complexes to transmetallate their 6-substituted PyPPh_2 ligands to Au^{I} (Scheme 56). [67] Two

equivalents $PyPPh_2$ with $(Me_2S)Au^ICl$ provided a rare bis(phosphino)Au^I complex, the trigonal planar $(\kappa^1\text{-}PyPPh_2)_2AuCl$.[103]

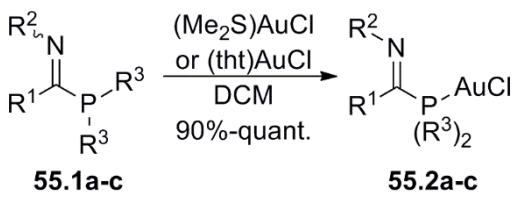

	R1	R2	R3
a	*t*-Bu	Ph	Ph
b	Ph	*i*-Pr	Ph
c	*t*-Bu	Ph	*t*-Bu

Scheme 55. Iminophosphane coordination to Au^I.

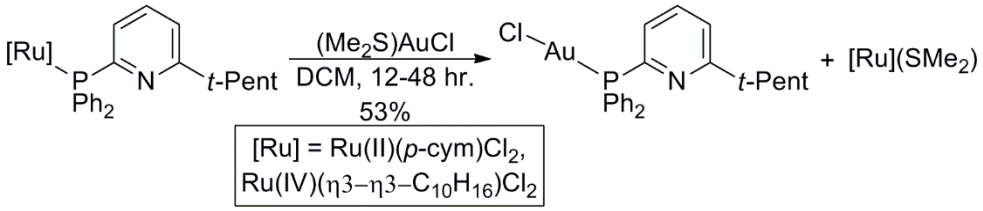

Scheme 56. P,N-transmetallation.

The $[Au(PyPPh_2]X$ complex catalyzed the Markovnikov hydration of 1-pentyne to 2-pentanone (5 mol%, MeCN, 50 °C (X = NTf, BF_4) or 70 °C (X = OTf), 100%).[103] The catalyst deactivated as the trinuclear $Au(PyPPh_2)_3X_3$ complex. Aggregation to catalytically inactive multinuclear structures was also observed for the complexes with imidazolylphosphane ligands.[104]

κ^1-2-imidazolyl- and κ^1-4-imidazolylphosphane Au^I complexes were found to be cytotoxic with the former showing generally a higher activity than cis-platin on ovarian cancer and leukemia cell lines, including cis-platin resistant strains (0.93-4.21 μM).[105] Using the $PyPPh_2$ ligand in the antitumor $[(PR_3)Au^I(\text{amino acid})]OTf$ complexes increased the cytotoxicity with respect to PPh_3. For human lung, liver, ovarian and breast cancer, as well as mouse tumor cell lines, the activity was comparable to cis-platin (IC_{50} = 0.65-25.35 μM).[106] Additionally,

(PyPPh$_2$)AuCl was found to have an ideal lipophilicity/hydrophilicity balance for increased selectivity in cytotoxic applications, for instance anti-HIV (IC_{50} = 12.5 ± 2.5 μM).[107]

7.2 Group XII

(*N*-κ^1-PyPPh$_2$)$_2$-ZnCl$_2$ presents a rare example of an *N*-monodentate P,N-ligand that reacts with CO_2 via the free P-atom (Scheme 57), which lowers the reduction potential of CO_2 by 0.6V, to catalytically produce CO and H_2O in the presence of acetic acid.[108]

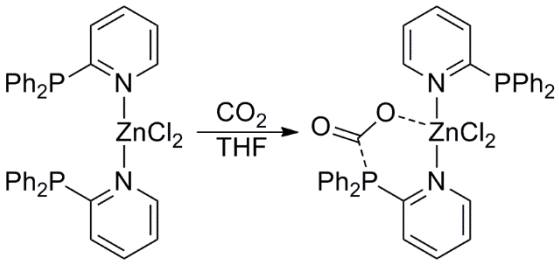

Scheme 57. P,N-Zinc facilitated CO_2 reduction.

8 Conclusions

The favorable parameters and presence of two heterodonor atoms in 1,3-P,N-ligands remains a fruitful combination with transition metal complexes in the exploration of (cooperative) metal-ligand reactivity. Especially homogeneous catalysis still flourishes with mainly ruthenium and palladium mediated processes benefitting from the ligands' hemilabile coordination, enhanced electron-donation and proton-shuttling abilities. P,N-Complexes for novel transformations are still being identified, including less typical applications, such as heterogeneous catalysis and antibacterial/anticancer bio-inorganic chemistry. Overall, a shift to first-row transition metals would be desirable because they benefit most from cooperative ligands. These systems are currently underrepresented in the literature. Nevertheless,

based on the understanding and control of the reactivity in reviewed studies, this will be only a matter of time.

9 References

[1] J. I. van der Vlugt, Eur. J. Inorg. Chem., (2012), 363-375.

[2] For a review on hybrid ligands, see: W.-H. Zhang, S.W. Chien, T.S.A. Hor, Coord. Chem. Rev., 255 (2011), 1991-2014.

[3] H. Grützmacher, Angew. Chem. Int. Ed., 47 (2008), 1814-1818.

[4] The potential of hybrid ligands is best demonstrated by the success of the SHOP process, one of the world's most prominent applications of homogeneous catalysis. A. Bader, E. Lindner, Coord. Chem. Rev., 108 (1991), 27-110.

[5] H.G. Ang, W.E. Kow, K.F. Mok, Inorg. Nucl. Chem. Lett., 8 (1972), 829-832.

[6] For a review on P,N-ligands, see: S. Maggini, Coord. Chem. Rev., 253 (2009), 1793-1832.

[7] For reviews on 2-pyridylphosphanes, see: a) G.R. Newkome, Chem. Rev., 93 (1993), 2067-2089. b) Z.-Z. Zhang, H. Cheng, Coord. Chem. Rev., 147 (1996), 1-39. c) P. Espinet, K. Soulantica, Coord. Chem. Rev., 193-195 (1999), 499-556.

[8] a) F. Shafiq, R. Eisenberg, Inorg. Chem., 32 (1993), 3287-3294. b) H. Ishii, M. Goyal, M. Ueda, K. Takeuchi, M. Asai, J. Mol. Catal. A Chem., 148 (1999), 289-293. c) H. Ishii, M. Goyal, M. Ueda, K. Takeuchi, M. Asai, Macromol. Rapid Commun., 22 (2001), 376-381.

[9] a) V.J. Catalano, S.J. Horner, Inorg. Chem., 42 (2003), 8430-8438. b) D. Drommi, F. Nicolò, C.G. Arena, G. Bruno, F. Faraone, R. Gobetto, Inorg. Chim. Acta, 221 (1994), 109-116. c) Q.-M. Wang, Y.-A. Lee, O. Crespo, J. Deaton, C. Tang, H.J. Gysling, M.C. Gimeno, C. Larraz, M.D. Villacampa, A. Laguna, R. Eisenberg, J. Am. Chem. Soc., 126 (2004), 9488-9489. d) Z.-Z. Zhang, H.-P. Xi, W.-J. Zhao, K.-Y. Jiang, R.-J. Wang, H.-G. Wang, Y. Wu, J. Organomet. Chem., 454 (1993), 221-228. e) G. Franciò, R. Scopelliti, C.G. Arena, G. Bruno, D. Drommi, F. Faraone, Organometallics, 17 (1998), 338-347.

[10] a) P. Braunstein, D.G. Kelly, A. Tiripicchio, F. Ugozzoli, Bull. Soc. Chim. Fr., 132 (1995), 1083-1086. b) E.C. Carson, S.J. Lippard, J. Am. Chem. Soc., 126 (2004), 3412-3413.

[11] a) D.B. Grotjahn, C.R. Larsen, J.L. Gustafson, R. Nair, A. Sharma, J. Am. Chem. Soc., 129 (2007), 9592-9593. b) J.J.M. de Pater, C.E.P. Maljaars, E. de Wolf, M. Lutz, A.L. Spek, B.-J. Deelman, C.J. Elsevier, G. van Koten, Organometallics, 24 (2005), 5299-5310.

[12] a) K. Kurtev, D. Ribola, R.A. Jones, D.J. Cole-Hamilton, G. Wilkinson, J. Chem. Soc., Dalton Trans., (1980), 55-58. b) E. Drent, P. Arnoldy, P.H.M. Budzelaar, J. Organomet. Chem., 455 (1993), 247-253. c) E. Drent, P. Arnoldy, P.H.M. Budzelaar, J. Organomet. Chem., 475 (1994), 57-63. d) I. Moldes, E. de la Encarnación, J. Ros, Á. Alvarez-Larena, J.F. Piniella, J. Organomet. Chem., 566 (1998), 165-174. e) A. Caballero, F.A. Jalón, B.R. Manzano, G. Espino, M. Pérez-Manrique, A. Mucientes, F.J. Poblete, M. Maestro, Organometallics, 23 (2004), 5694-5706. f) T. Oshiki, H. Yamashita, K. Sawada, M. Utsunomiya, K. Takahashi, K. Takai, Organometallics, 24 (2005), 6287-6290.

[13] a) S. Harkal, F. Rataboul, A. Zapf, C. Fuhrmann, T. Riermeier, A. Monsees, M. Beller, Adv. Synth. Catal., 346 (2004), 1742-1748. b) R.A. Singer, N.J. Tom, H.N. Frost, W.M. Simon, Tetrahedron Letters, 45 (2004), 4715-4718.

[14] See for instance: a) T.M. Shaikh, F.-E. Hong, Beilstein J. Org. Chem., 9 (2013), 1578-1588. b) X. Fang, R. Jackstell, M. Beller, Angew. Chem. Int. Ed., 52 (2013), 14089-14093. c) X. Fang, M. Zhang, R. Jackstell, M. Beller, Angew. Chem. Int. Ed., 52 (2013), 4645-4649. d) J. Schranck, X.-F. Wu, A. Tlili, H. Neumann, M. Beller, Chem. Eur. J., 19 (2013), 12959-12964. e) Y.-Y. Kuo, M.F. Haddow, A. Pérez-Redondo, G.R. Owen, Dalton Trans., 39 (2010), 6239-6248. f) T. Mino, S. Komatsu, K. Wakui, H. Yamada, H. Saotome, M. Sakamoto, T. Fujita, Tetrahedron Asymm., 21 (2010), 711-718.

[15] For more information on the use of N-cationic π-accepting 1,3-P,N-ligands, see for instance: a) M. Alcarazo, Chem. Eur. J., 20 (2014), 7868-7877. b) H. Tinnermann, C. Wille, M. Alcarazo, Angew. Chem. Int. Ed., 53 (2014), 8732-8736. c) J. Zhang, Y. Wang, X. Zhao, Y. Liu, Eur. J. Inorg. Chem., (2014), 975-985. d) X. Wang, Y. Wang, J. Zhang, X. Zhao, Y. Liu, J. Organomet. Chem., 762 (2014), 40-47. e) H. You, Y. Wang, X. Zhao, S. Chen, Y. Liu, Organometallics, 32 (2013), 2698-2704.

[16] See for instance: a) T. van Dijk, M.K. Rong, J.E. Borger, M. Nieger, J.C. Slootweg, K. Lammertsma, Organometallics, 35 (2016), 827-835. b) M. Płotek, R. Starosta, U.K. Komarnicka, A. Skórska-Stania, G. Stochel, A. Kyzioł, M. Jeżowska-Bojczuk, RSC Adv., 5 (2015), 2952-2955. c) D.M. Zink, T. Baumann, M. Nieger, S. Bräse, Eur. J. Org. Chem., (2011), 1432-1437. d) R. Veillard, E. Bernoud, I. Abdellah, J.-F. Lohier, C. Alayrac, A.-C. Gaumont, Org. Biomol. Chem., 12 (2014), 3635-3640. e) A. Nemati Kharat, B. Tamaddoni Jahromi, A. Bakhoda, A. Abbasi, J. Coord. Chem., 63 (2010), 3783-3791. f) M.M. Bittner, J.S. Baus, S.V. Lindeman, A.T. Fiedler, Eur. J. Inorg. Chem., (2012), 1848-1856. g) P.C. Kunz, M. Börgardts, F. Mohr, Inorg. Chim. Acta, 380 (2012), 392-398. h) C.G.J. Tazelaar, E. Nicolas, T. van Dijk, D.L.J. Broere, M. Cardol, M. Lutz, D. Gudat, J.C. Slootweg, K. Lammertsma, Dalton

Trans., 45 (2016), 2237-2249. i) T.A.Shuttleworth, A.M. Miles-Hobbs, P.G. Pringle, H.A. Sparkes, Dalton Trans., 46 (2017), 125-137.

[17] See for instance: a) A.C. Behrle, J.A.R. Schmidt, Organometallics, 32 (2013), 1141-1149. b) A.G.M. Barrett, M.R. Crimmin, M.S. Hill, P.B. Hitchcock, S.L. Lomas, M.F. Mahona, P.A. Procopioud, Dalton Trans., 39 (2010), 7393-7400. c) N.E. Mansfield, J. Grundy, M.P. Coles, P.B. Hitchcock, Polyhedron, 29 (2010), 2481-2488. d) A. Antiñolo, S. García-Yuste, A. Otero, R. Reguillo-Carmona, Eur. J. Inorg. Chem., (2009), 539-544. e) I.A. Shuklov, N.V. Dubrovina, E. Barsch, R. Ludwig, D. Michalik, A. Börner, Chem. Commun., (2009), 1535-1537. f) U. Gellrich, J. Huang, W. Seiche, M. Keller, M. Meuwly, B. Breit, J. Am. Chem. Soc., 133 (2011), 964-975.

[18] See for instance: a) A.D. Worthy, C.L. Joe, T.E. Lightburn, K.L. Tan, J. Am. Chem. Soc., 132 (2010), 14757-14759. b) M. Ghalib, P.G. Jones, S. Lysenko, J.W. Heinicke, Organometallics, 33 (2014), 804-816. c) V. Cadierno, J. Francos, J. Gimeno, Chem. Eur. J., 14 (2008), 6601-6605. d) W.-C. Lee, B.J. Frost, Green Chem., 14 (2012), 62-66.

[19] L. Hintermann, T.T. Dang, A. Labonne, T. Kribber, L. Xiao, P. Naumov, Chem. Eur. J., 15 (2009), 7167-7179.

[20] J.-S. Zhang, T. Chen, J. Yang, L.-B. Han, Chem. Commun., 51 (2015), 7540-7542.

[21] T.I. Fesenko, A.V. Shamsieva, E.I. Musina, I.D. Strelnik, A.A. Karasik, O.G. Sinyashin, Phosphorus Sulfur Silicon Relat. Elem., 188 (2013), 63-65.

[22] R.J. Seacome, M.P. Coles, J.E. Glover, P.B. Hitchcock, G.J. Rowlands, Dalton Trans., 39 (2010), 3687-3694.

[23] G. Erdogan, D.B. Grotjahn, Org. Lett., 16 (2014), 2818-2821.

[24] J.M. Walker, J.P. Tassone, H.A. Jenkins, G.J. Spivak, J. Organomet. Chem., 761 (2014), 56-63.

[25] P.C. Kunz, I. Thiel, A.L. Noffke, G.J. Reiß, F. Mohr, B. Spingler, J. Organomet. Chem., 697 (2012), 33-40.

[26] T. van Dijk, S. Burck, M.K. Rong, A.J. Rosenthal, M. Nieger, J.C. Slootweg, K. Lammertsma, Angew. Chem. Int. Ed., 53 (2014), 9068-9071.

[27] T. van Dijk, S. Burck, A.J. Rosenthal, M. Nieger, A.W. Ehlers, J.C. Slootweg, K. Lammertsma, Chem. Eur. J., 21 (2015), 9328-9331.

[28] M.K. Rong, K. van Duin, T. van Dijk, J.J.M. de Pater, B.-J. Deelman, M. Nieger, A.W. Ehlers, J.C. Slootweg, K. Lammertsma, Organometallics, 36 (2017), 1079-1090. See also Chapter III.

[29] T. van Dijk, M.S. Bakker, F. Holtrop, M. Nieger, J.C. Slootweg, K. Lammertsma, Org. Lett., 17 (2015), 1461-1464.

[30] K. Issleib, H. Schmidt, H. Meyer, J. Organomet. Chem., 160 (1978), 47-57.

[31] J.E. Radcliffe, A.S. Batsanov, D.M. Smith, J.A. Scott, P.W. Dyer, M.J. Hanton, ACS Catal., 5 (2015), 7095-7098.

[32] EtOH efficiently deprotected BH_3-$PPyPh_2$ (4h, 97%). M. Van Overschelde, E. Vervecken, S.G. Modha, S. Cogen, E. Van Der Eycken, J. Van Der Eycken, Tetrahedron, 65 (2009), 6410-6415.

[33] E.N. Daley, C.M. Vogels, S.J. Geier, A. Decken, S. Doherty, S.A. Westcott, Angew. Chem. Int. Ed., 54 (2015), 2121-2125.

[34] E. Payet, A. Auffrant, X.F. Le Goff, P. Le Floch, J. Organomet. Chem., 695 (2010), 1499-1506.

[35] A.J. Roering, S.E. Leshinski, S.M. Chan, T. Shalumova, S.N. MacMillan, J.M. Tanski, R. Waterman, Organometallics, 29 (2010), 2557-2565.

[36] U. Segerer, S. Blaurock, J. Sieler, E. Hey-Hawkins, Organometallics, 18 (1999), 2838-2842.

[37] S. Sauerbrey, P.K. Majhi, J. Daniels, G. Schnakenburg, G.M. Brändle, K. Scherer, R. Streubel, Inorg. Chem., 50 (2011), 793-799. Additionally, the coordination of 1-(t-Bu)-2-diphenylphosphanyl-imidazole was studied with $[Pt^{II}(PhCN)_2Cl_2]$.

[38] For an analysis of the $[(\kappa1\text{-}PyPPh_2)W(CO)_5]$ and $[(\kappa2\text{-}PyPPh_2)W(CO)_4]$ species, see: K. Nishide, S. Ito, M. Yoshifuji, J. Organomet. Chem., 682 (2003), 79-84.

[39] a) N. Pizarro, M. Duque, E. Chamorro, S. Nonell, J. Manzur, J.R. de la Fuente, G. Günther, M. Cepeda-Plaza, A. Vega, J. Phys. Chem. A, 119 (2015), 3929-3935. b) F. Venegas, N. Pizarro, A. Vega, J. Chil. Chem. Soc., 56 (2011), 823-826.

[40] P. Das, P.P. Sarmah, M. Borah, A.K. Phukan, Inorg. Chim. Acta, 362 (2009), 5001-5011.

[41] M. Muranaka, I. Hyodo, W. Okumura, T. Oshiki, Catal. Today, 164 (2011), 552-555.

[42] R. García-Álvarez, S.E. García-Garrido, J. Díez, P. Crochet, V. Cadierno, Eur. J. Inorg. Chem., (2012), 4218-4230.

[43] The crystal structure of the PF_6-salt of **15.1**, obtained from [diruthenium(II,III) $(\mu\text{-acetate})_4(H_2O)_2]PF_6$, was reported in: E. Essoun, R. Wang, M.A.S. Aquino, Inorg. Chim. Acta, 454 (2017), 97-106.

[44] a) D.B. Grotjahn, V. Miranda-Soto, E.J. Kragulj, D.A. Lev, G. Erdogan, X. Zeng, A.L. Cooksy, J. Am. Chem. Soc., 130 (2008), 20-21. b) D.B. Grotjahn, E.J. Kragulj, C.D. Zeinalipour-Yazdi, V. Miranda-Soto, D.A. Lev, A.L. Cooksy, J. Am. Chem. Soc., 130 (2008), 10860-10861.

[45] A. Labonne, T. Kribber, L. Hintermann, Org. Lett., 8 (2006), 5853-5856.

[46] D.B. Grotjahn, C.D. Incarvito, A.L. Rheingold, Angew. Chem. Int. Ed., 40 (2001), 3884-3887.

[47] L. Hintermann, L. Xiao, A. Labonne, U. Englert, Organometallics, 28 (2009), 5739-5748.

[48] F. Boeck, T. Kribber, L. Xiao, L. Hintermann, J. Am. Chem. Soc., 133 (2011), 8138-8141.

[49] L. Li, S.B. Herzon, J. Am. Chem. Soc., 134 (2012), 17376-17379.

[50] P. Kumar, A.K. Singh, S. Sharma, D.S. Pandey, J. Organomet. Chem., 694 (2009), 3643-3652.

[51] P. Kumar, A.K. Singh, M. Yadav, P.-Z. Li, S.K. Singh, Q. Xi, D.S. Pandey, Inorg. Chim. Acta, 368 (2011), 124-131.

[52] I. Fleischer, K.M. Dyballa, R. Jennerjahn, R. Jackstell, R. Franke, A. Spannenberg, M. Beller, Angew. Chem. Int. Ed., 52 (2013), 2949-2953.

[53] C. Kubis, I. Profir, I. Fleischer, W. Baumann, D. Selent, C. Fischer, A. Spannenberg, R. Ludwig, D. Hess, R. Franke, A. Börner, Chem. Eur. J., 22 (2016), 2746-2757.

[54] I. Fleischer, L. Wu, I. Profir, R. Jackstell, R. Franke, M. Beller, Chem. Eur. J., 19 (2013), 10589-10594.

[55] Method: B3LYP/ECP(Ru, P)/LANL2DZ(Ru), 6-311++G(P, N, pentene), 6-31G/ PCM (acetone). J. Tao, F. Sun, T. Fang, J. Organomet. Chem., 698 (2012), 1-6.

[56] C.R. Larsen, G. Erdogan, D.B. Grotjahn, J. Am. Chem. Soc., 136 (2014), 1226-1229.

[57] A.V. Smarun, W. Shahreel, S. Pramono, S.Y. Koo, L.Y. Tan, R. Ganguly, D. Vidović, J. Organomet. Chem., 834 (2017), 1-9.

[58] G.E. Dobereiner, G. Erdogan, C.R. Larsen, D.B. Grotjahn, R.R. Schrock, ACS Catal., 4 (2014), 3069-3076.

[59] C.S. Higman, M.P. de Araujo, D.E. Fogg, Catal. Sci. Technol., 6 (2016), 2077-2084.

[60] Y. Wang, Z. Zheng, L. Zhang, Angew. Chem. Int. Ed., 53 (2014), 9572-9576.

[61] R. Zheng, Y. Wang, L. Zhang, Tetrahedron Lett., 56 (2015), 3144-3146.

[62] D. Pingen, C. Müller, D. Vogt, Angew. Chem. Int. Ed., 49 (2010), 8130-8133.

[63] P. Kumar, A.K. Singh, R. Pandey, D.S. Pandey, J. Organomet. Chem., 696 (2011), 3454-3464.

[64] S. Modem, S. Kankala, R. Balaboina, N.S. Thirukovela, S.B. Jonnalagadda, R. Vadde, C.S. Vasam, Eur. J. Org. Chem., (2016), 4635-4642.

[65] X. Chen, T.T.D. Nguyen, M.Y. Khan, L. Xia, D. He, S.W. Lee, S.K. Noh, J. Polym. Sc. A - Polym. Chem., 53 (2015), 1961-1965.

[66] F.D. Fagundes, J.P. da Silva, C.L. Veber, A. Barison, C.B. Pinheiro, D.F. Back, J.R. de Sousa, M.P. de Araujo, Polyhedron, 42 (2012), 207-215.

[67] E. Tomás-Mendivil, R. García-Álvarez, S.E. García-Garrido, J. Díez, P. Crochet, V. Cadierno, J. Organomet. Chem., 727 (2013), 1-9.

[68] W. Huber, P. Bröhler, W. Wätjen, W. Frank, B. Spingler, P.C. Kunz, J. Organomet. Chem., 717 (2012), 187-194.

[69] C. Aliende, M. Pérez-Manrique, F.A. Jalón, B.R. Manzano, A.m. Rodríguez, J.V. Cuevas, G. Espino, M.Á. Martínez, A. Massaguer, M. González-Bártulos, R. de Llorens, V. Moreno, J. Inorg. Biochem., 117 (2012), 171-188.

[70] R. Beck, H. Sun, X. Li, H.-F. Klein, Z. Anorg. Allg. Chem., 635 (2009), 99-105.

[71] W. Purcell, J. Conradie, T.T. Chiweshe, J.A. Venter, H.G. Visser, M.P. Coetzee, J. Mol. Struct., 1038 (2013), 220-229.

[72] W. Purcell, J. Conradie, T.T. Chiweshe, J.A. Venter, L. Twigge, M.P. Coetzee J. Organomet. Chem., 745-746 (2013), 439-453.

[73] A. Brück, K. Ruhland, Organometallics, 28 (2009), 6383-6401.

[74] E. Tomás-Mendivil, R. García-Álvarez, C. Vidal, P. Crochet, V. Cadierno, ACS Catal., 4 (2014), 1901-1910.

[75] G. Borah, P.P. Sarmah, D. Boruah, Bull. Korean Chem. Soc., 36 (2015), 1226-1230.

[76] T. Suzuki, M. Kotera, A. Takayama, M. Kojima, Polyhedron, 28 (2009), 2287-2293.

[77] D.B. Grotjahn, J.E. Kraus, H. Amouri, M.-N. Rager, A.L. Cooksy, A.J. Arita, S.A. Cortes-Llamas, A.A. Mallari, A.G. DiPasquale, C.E. Moore, L.M. Liable-Sands, J.D. Golen, L.N. Zakharov, A.L. Rheingold, J. Am. Chem. Soc., 132 (2010), 7919-7934.

[78] O. Saidi, J.M.J. Williams, Top. Organomet. Chem., 34 (2011), 77-106.

[79] M.D. Le Page, B.O. Patrick, S.J. Rettig, B.R. James, Inorg. Chim. Acta, 431 (2015), 276-288.

[80] A. Scrivanti, M. Bertoldini, V. Beghetto, U. Matteoli, A. Venzo, J. Organomet. Chem., 694 (2009), 131-136.

[81] J. Liu, C. Jacob, K.J. Sheridan, F. Al-Mosule, B.T. Heaton, J.A. Iggo, M. Matthews, J. Pelletier, R. Whyman, J.F. Bickley, A. Steiner, Dalton Trans., 39 (2010), 7921-7935.

[82] K.Q. Almeida Leñero, Y. Guari, P.C.J. Kamer, P.W.N.M. van Leeuwen, B. Donnadieu, S. Sabo-Etienne, B. Chaudret, M. Lutz, A.L. Spek, Dalton Trans., 42 (2013), 6495-6512.

[83] Method: (B3PW91-D3BJ/SDD(Pd)/6 311+G**/PCM (MeOH)). a) L. Crawford, D.J. Cole-Hamilton, M. Bühl, Organometallics, 34 (2015), 438-449. b) L. Crawford, D.J. Cole-Hamilton, E. Drent, M. Bühl, Chem. Eur. J., 20 (2014), 13923-13926.

[84] X. Chen, H. Zhu, T. Wang, C. Li, L. Yan, M. Jiang, J. Liu, X. Sun, Z. Jiang, Y. Ding, J. Mol. Catal. A - Chem., 414 (2016), 37-46.

[85] X. Chen, H. Zhu, W. Wang, H. Du, T. Wang, L. Yan, X. Hu, Y. Ding, ChemSusChem, 9 (2016), 2451-2459.

[86] C. Sarmah, D. Sahu, P. Das, Catal. Comm., 41 (2013), 75-78.

[87] J.T. Guan, X.M. Song, Z.Y. Zhang, B.M. Wei, Z.Q. Dai, Appl. Organometal. Chem., 29 (2015), 87-89.

[88] G. Borah, D. Boruah, G. Sarmah, S.K. Bharadwaj, U. Bora, Appl. Organometal. Chem., 27 (2013), 688-694.

[89] X.-F. Wu, H. Neumann, A. Spannenberg, T. Schulz, H. Jiao, M. Beller, J. Am. Chem. Soc., 132 (2010), 14596-14602.

[90] T. Schulz, C. Torborg, B. Schäffner, J. Huang, A. Zapf, R. Kadyrov, A. Börner, M. Beller, Angew. Chem. Int. Ed., 48 (2009), 918-921.

[91] A.G. Sergeev, T. Schulz, C. Torborg, A. Spannenberg, H. Neumann, M. Beller, Angew. Chem. Int. Ed., 48 (2009), 7595-7599.

[92] T. Schareina, R. Jackstell, T. Schulz, A. Zapf, A. Cotté, M. Gotta, M. Beller, Adv. Synth. Catal., 351 (2009), 643-648.

[93] J.P. Tassone, G.J. Spivak, J. Organomet. Chem., 841 (2017), 57-61.

[94] T. Schulz, C. Torborg, S. Enthaler, B. Schäffner, A. Dumrath, A. Spannenberg, H. Neumann, A. Börner, M. Beller, Chem. Eur. J., 15 (2009), 4528-4533.

[95] A. Millet, D. Dailler, P. Larini, O. Baudoin, Angew. Chem. Int. Ed., 53 (2014), 2678-2682.

[96] H. Khan, A. Badshah, G. Murtaz, M. Said, Z. Rehman, C. Neuhausen, M. Todorova, B.J. Jean-Claude, I.S. Butler, Eur. J. Med. Chem., 46 (2011), 4071-4077.

[97] N.H. Gama, A.Y.F. Elkhadir, B.G. Gordhan, B.D. Kana, J. Darkwa, D. Meyer, Biometals, 29 (2016), 637-650.

[98] M. Fereidoonnezhad, M. Niazi, M. Shahmohammadi Beni, S. Mohammadi, Z. Faghih, Z. Faghih, H.R. Shahsavari, ChemMedChem, 12 (2017), 456-465.

[99] M. Fereidoonnezhad, M. Niazi, Z. Ahmadipour, T. Mirzaee, Z. Faghih, Z. Faghih, H.R. Shahsavari, Eur. J. Inorg. Chem., (2017), 2247-2254.

[100] G.A. Bowmaker, J.V. Hanna, S.P. King, F. Marchetti, C. Pettinari, A. Pizzabiocca, B.W. Skelton, A.N. Sobolev, A. Tăbăcaru, A.H. White, Eur. J. Inorg. Chem., (2014), 6104-6116.

[101] O. Crespo, M.C. Gimeno, A. Laguna, C. Larraz, Z. Naturforsch., 64b (2009), 1525-1534.

[102] a) M.J. Calhorda, C. Ceamanos, O. Crespo, M.C. Gimeno, A. Laguna, C. Larraz, P.D. Vaz, M.D. Villacampa, Inorg. Chem., 49 (2010), 8255-8269. b) O. Crespo, M.C. Gimeno, A. Laguna, F.J. Lahoz, C. Larraz, Inorg. Chem., 50 (2011), 9533-9544. c) V.J. Catalano, J.M. López-de-Luzuriaga, M. Monge, M.E. Olmos, D. Pascual,

Dalton Trans., 43 (2014), 16486-16497. d) U. Monkowius, M. Zabel, M. Fleck, H. Yersin, Z. Naturforsch., 64b (2009), 1513-1524.

[103] C. Khin, A.S.K. Hashmi, F. Rominger, Eur. J. Inorg. Chem., (2010), 1063-1069.

[104] (Imidazoylphosphane)AuOTf complexes showed low activity in alkyne hydration due to the formation of inactive clusters. This did not hinder the (imidazoylphosphane)AuCl catalysed three-component coupling of benzaldehyde, piperidine and phenylacetylene. C. Wetzel, P.C. Kunz, I. Thiel, B. Spingler, Inorg. Chem., 50 (2011), 7863-7870.

[105] P.C. Kunz, M.U. Kassack, A. Hamacher, B. Spingler, Eur. J. Inorg. Chem., (2009), 7741-7747.

[106] L. Ortego, M. Meireles, C. Kasper, A. Laguna, M.D. Villacampa, M.C. Gimeno, J. Inorg. Biochem., 156 (2016), 133-144.

[107] P. Fonteh, A. Elkhadir, B. Omondi, I. Guzei, J. Darkwa, D. Meyer, Biometals, 28 (2015), 653-667.

[108] E.S. Donovan, B.M. Barry, C.A. Larsen, M.N. Wirtz, W.E. Geiger, R.A. Kemp, Chem. Commun., 52 (2016), 1685-1688.

Chapter II

Enlightening developments in 1,3-P,N-ligand-stabilized multinuclear complexes: a shift from catalysis to photoluminescence

Mark K. Rong, Flip Holtrop, J. Chris Slootweg, and Koop Lammertsma

1,3-P,N-ligands provide the ideal spatial separation to facilitate homo and hetero metal-metal interactions to access multinuclear complexes. The rich chemistry of such complexes includes applications in coordination chemistry, metal-activation and (cooperative) catalysis. However, it has been especially the fruitful combination in photoluminescent P,N-coinage metal complexes which has renewed interest in these ligands. While the field classically focused on dinuclear species, now also coinage metal clusters have been studied for use in catalysis and photophysical applications.

Coord. Chem. Rev. **2019**, *382*, 57-68.

1 Introduction

Multinuclear transition metal complexes are of high interest because they hold significant promise of enhanced catalytic activity, increased chemical reactivity, and extensive tunability of photophysical properties.[1] Especially the direct metal-metal interactions can render favorable physical properties, activate less reactive metals or enable the nuclei to cooperatively perform chemical transformations. An important gateway to such complexes are the hybrid 1,3-P,N-ligands (Figure 1).[2,3]

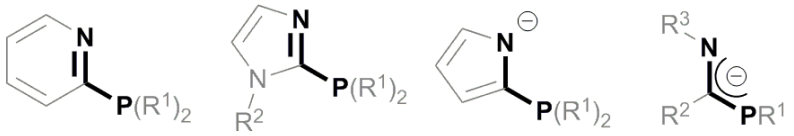

Figure 1. 1,3-P,N-ligands in recent multinuclear transition metal chemistry.

Hybrid ligands combine the distinctive bonding preferences of different donor atoms to enable secondary interactions, such as ligand-based reactivity (cooperativity, non-innocence) and coordination to secondary metals to provide multinuclear complexes.[4,5] Since 1972,[6] 1,3-P,N-structures have been prominent hybrid ligands[2,3] whose combined soft donor character of phosphorus and hard donor character of nitrogen has led to diverse coordination chemistry (Figure 2). Mononuclear complexes display *N*-monodentate,[7] *P*-monodentate,[8,9] or bidentate[9] *P,N*-coordination and support various applications.[8b,9,10,12e] The 1,3-P,N-ligands distinguish themselves from other P,N-ligands in multinuclear complexes. They can coordinate in a bridging mode between metals to provide homo-[11] and heterobimetallic[12] complexes in which the one-carbon spacer provides the ideal spatial separation to facilitate the formation of metal-metal bonds. Such multinuclear complexes may benefit from their well-defined geometry, metal-metal interactions and novel reactivity.[2] For instance, metals may activate each other to provide

more active catalysts, or cooperate in tandem catalysis. So far, multinuclear 1,3-P,N-complexes have been applied in the Rh^{I}_{2}-catalysed hydrogenation of alkenes,[11a] the [Ru^{II}-Rh^{I}]-catalyzed hydroformylation of alkenes,[12b] and the Pd^{I}_{2}- and [Fe^{0}-Rh^{I}]-catalyzed carbonylation of alcohols;[11b,c,12d] while dinuclear Au^{I} and [Au^{I}-Ag^{I}] complexes display interesting photoluminescence.[12a,c]

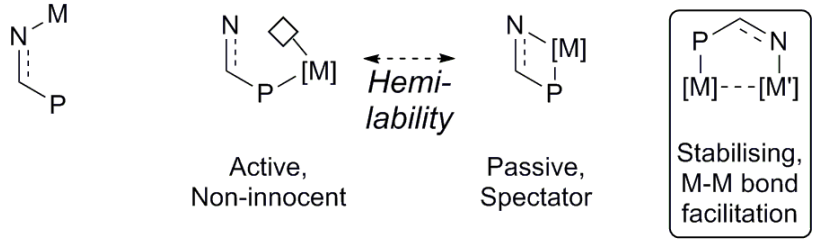

Figure 2. Bridging 1,3-P,N-ligands as metal-metal bond facilitator.

P,N-facilitated multinuclear complexes have attracted renewed interest with additional focus on photoluminescence. To provide insight in what makes these ligands unique and how their properties have been exploited, we review the developments in multinuclear 1,3-P,N chemistry in the areas of organic/organometallic substrate-activations, enzyme mimicry, homogeneous catalysis, and photoluminescence for the period of 2009 to mid-2017. Excluded are systems in which one of the donors is unavailable (e.g., *P*-oxidized systems, 2-pyrrolyl-phosphanes, *N*-alkylated cationic P,N-systems);[13] those with an additional donor atom that can participate in coordination or reactions (e.g. bis-/tris-(pyridyl)phosphanes, 1,3,5-P,N,X ligands);[14,15] and conformationally restricted ligands that are not comparable to the titular compounds (e.g., benzaphospholes, 1,3,5-triaza-7-phosphaadamantate (PTA) ligands).[16] Complexes will be discussed in ascending Group number. Hetero-metallic complexes are discussed by comparing their application with

homo-metallic structural analogues, or, alternatively, by focusing on the determining metal of the study; for an overview, see Table 1.

Table 1. Overview of the discussed multinuclear species.

	M^1	M^2	Ref.
IV	Ti	Fe	[17]
		Ni	[17]
	Zr	Ni	[17]
	Hf	Ni	[17]
VIII	Fe	Fe	[18-20]
		Ti	[17]
	Ru	Ru	[21]
		Rh	[22]
		Ir	[23]
IX	Rh	Ru	[22]
		Ir	[23]
		Au	[56]
	Ir	Ru	[23]
		Rh	[23]
		Ir	[23]
		Au	[56]
X	Ni	Ti	[17]
		Zr	[17]
		Hf	[17]
		Sn	[26]
	Pd	Pd	[24]
		Pt	[25]
		Sn	[26-28]
	Pt	Pd	[25]
		Ag	[30,31]
X	Pt	Au	[56]
		Tl	[31]
		Sn	[26,28]
XI	Cu	Cu	[32-45]
		Ag	[52]
		Au	[46], [52], [54-57], [62-64], [70]
	Ag	Pt	[30,31]
		Cu	[52]
		Ag	[47-52]
		Au	[52], [54], [61], [66-69]
	Au	Rh	[56]
		Ir	[56]
		Pt	[56]
		Cu	[46], [52], [54-57], [62-64], [70]
		Au	[47], [52-54], [58-71]
XIII	Tl	Pt	[31]
XIV	Sn	Ni	[26]
		Pd	[26-28]
		Pt	[26-28]

2 Group IV, VIII, IX: Coordination chemistry

Direct interactions between metal centers can provide access to species with complex or enhanced reactivity.[2,3] It is therefore important in exploring new applications to understand the mutual effects the metals have on each other and to control their reactivity. Recent reports on group IV, VIII and IX metals mainly studied these interactions. Their focus on fundamental coordination chemistry contrasts with the application-aimed reports on group X-XII complexes.

2.1 Group IV

Enhancing the bonding interaction between Lewis acidic group IV metals and late transition metals of the first row was examined using *N*-anionic pyrrole phosphanes (Scheme 1).[17] For the Ni-complexes **1.1a-c**, Ti had the most impact as it has the largest metal-metal orbital overlap, resulting in strong π-interactions. Upon exposure to CO the Ni→Ti donation is lost in favor of CO (**1.2**), but this process is reversible. The Ni-Ti bond could also be broken by reducing the complex (Ti^{IV}→Ti^{III} (**1.3**)). Using iron instead of nickel provided pseudo-C_4-symmetric complex **1.4**, which has a strong Ti-Fe interaction. Reduction of this complex resulted in partial ligand dissociation to a pseudo-trigonal geometry (**1.5**) with a shortened Fe-Ti triple bond due to increased orbital overlap. These electronic effects could be useful to enhance the reactivity of first row metals.

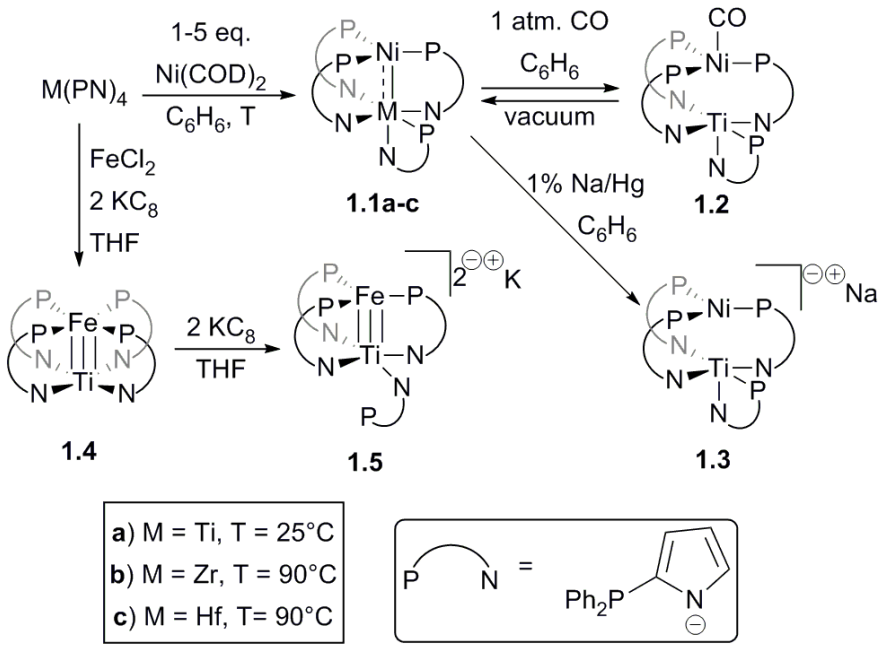

Scheme 1. Lewis acidic effects of Group IV metals.

2.2 Group VIII

Metal-metal bonds can have unexpected effects on reactivity, as has been illustrated for Group VIII complexes. The ($PyPPh_2$)-ligated complex **2.1** was used as a mimic for enzymatic H_2-oxidation/H^+-reduction, because Fe^{II}_2 (dithiolato) complexes bear resemblance to [FeFe]-hydrogenase active sites (Scheme 2).[18,19] Since the P,N-ligand is not coordinated in a bridging fashion, the basic N-site of the pyridyl-phosphane is free to react, as is often observed for mononuclear P,N-complexes.[3] Surprisingly, stepwise treatment with HOTf showed that protonation occurs first at the electron rich Fe-Fe bond and second at the ligand. This emphasizes the potential importance of metal-metal effects for Fe_2 catalysts and also demonstrates the different reactivity multinuclear complexes can have with respect to mononuclear ones.

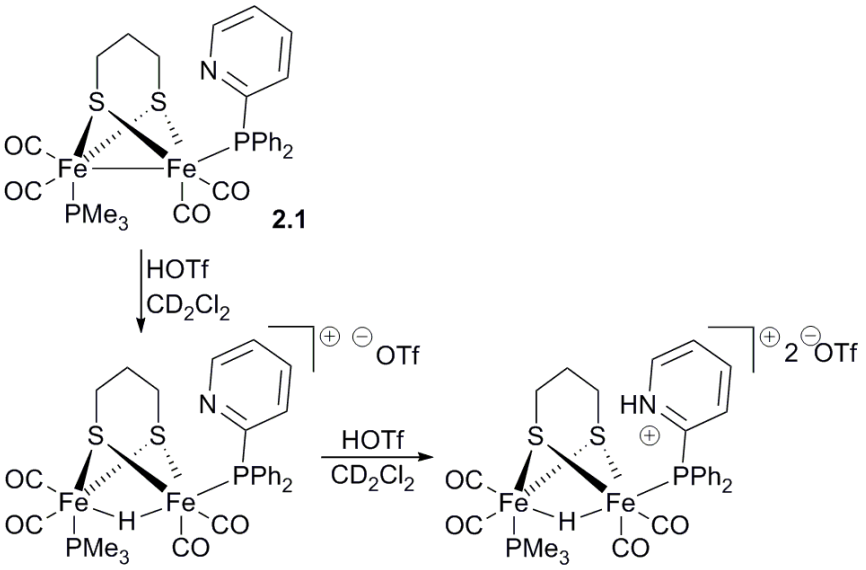

Scheme 2. Dihydrogen reactivity of a P,N-[FeFe]-hydrogenase model.

Reacting $[Fe^0_3(CO)_{12}]$ with $PyPPh_2$ to induce P,N-coordination quite surprisingly generated complex **3.1** (Scheme 3).[20] So far, such a cluster promoted oxidative scission of a P-Py bond was only known for the analogous $[Ru^0_3(CO)]_{12}$ [21]. No mechanistic speculations were made, but a P,N-bridged intermediate seems likely in which the ligand is oxidatively split into two by the iron centers.

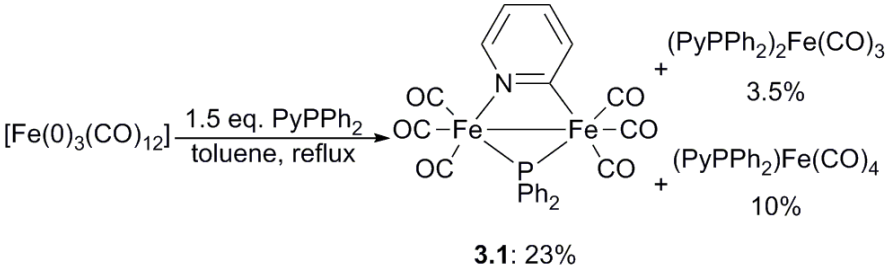

Scheme 3. Fe^0-cluster promoted P-C bond scission.

2.3 Group IX

Since the combination of two metallic cores holds promise for tandem catalysis, for instance in tandem hydroformylation/hydrogenation, the catalytic properties of [Rh^{I}(acac)(μ-$PyPPh_2$)$_2$$Ru^{II}$Cp*]OTf **4.1** were examined in the hydroformylation of 1-octene (Scheme 4).[22] Although activity was observed, the reaction showed poor linear to branched selectivity (99%, l/b = 3.2/1), with alkene-isomerisation (9%) and hydrogenation (4%) as side reactions, which contrasts with the branched-selectivity of related [Rh^{I}-Ru^{II}]- alkene-hydroformylation catalysts (l/b = 1/18).[12b] This was caused by instability of the Rh^{I},Ru^{II}-complex under syngas pressure: it falls apart in several Rh- and Ru-mononuclear complexes that are responsible for, respectively, the hydrogenation and alkene isomerisation, in which mononuclear 1,3-P,N-complexes are known to be proficient.[3d]

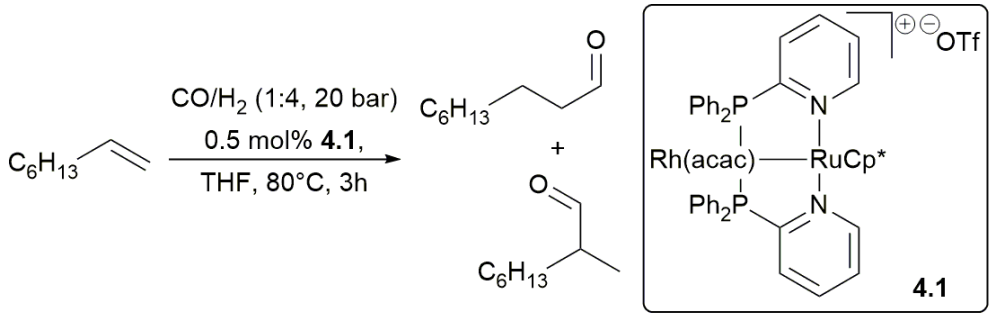

Scheme 4. Rh^{I}-Ru^{II} catalyzed hydroformylation of 1-octene.

[(μ-$PyPPh_2$)(μ-H)Ir-M] complexes **5.2** have been studied to assess the effect of different secondary metals on regioselective alkyne insertions (Scheme 5).[23] The complexes, formed from ($PyPPh_2$)IrH_2Cp* (**5.1**) and Ru^{II}, Rh^{III} or Ir^{III} complexes, reacted stoichiometrically with terminal alkynes to give branched (**5.3**, **5.4**) and linear (**5.5**) vinyl insertion products. Typically, iridium provides the binding site after which the

second metal induces hydrometallation. The product depends on the secondary metals used and the steric bulk of the alkyne.

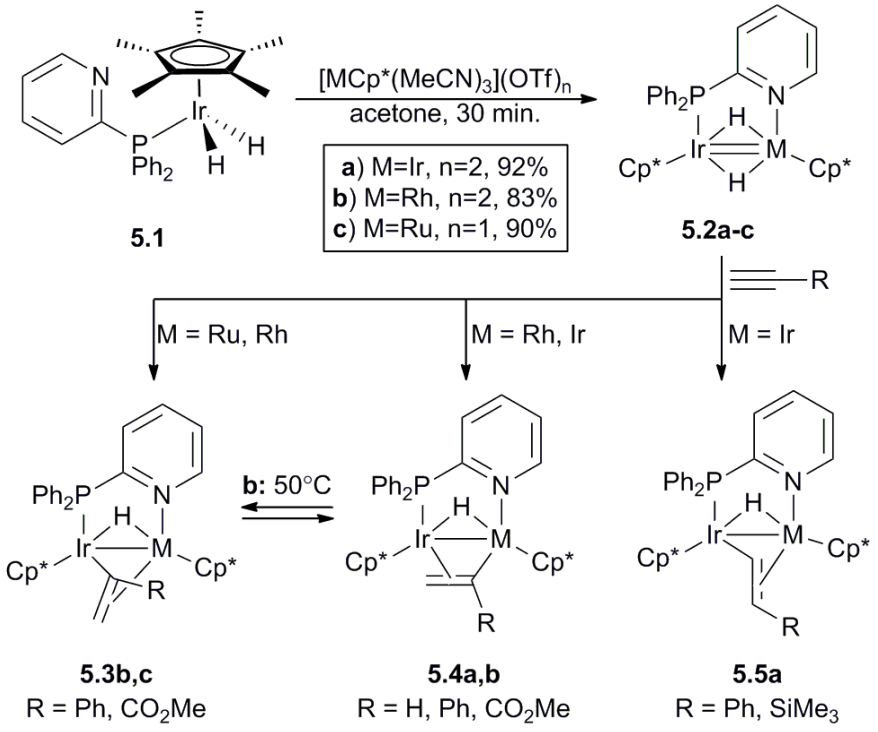

Scheme 5. Synergistic alkyne insertion.

3 Group X: Catalysis and metal activation

Coordinating one metal core to another provides several options to pursue in catalysis. For instance, the second nucleus can cooperate with the first to boost the (catalytic) activity of the entire complex or provide new reactivity in (tandem) catalysis. Both could be achieved using palladium. 1,3-P,N-ligands were also used to stabilize Pd/Pt-Sn interactions.

3.1 β-Borylation/Suzuki-Miyaura

N-anionic 2-indolyl-phosphanes have been used to access novel Pd_2 complexes and explore their catalytic activity (Scheme 6).[24] Catalytic

ß-borylation of α,ß-carbonyl compounds, including esters, ketones, aldehydes and amides, was accomplished with heterogeneous complexes **6.2-6.5** to give modest to high conversion under mild conditions (Scheme 7; 14 examples, 27-99% yield). A tandem ß-borylation / Suzuki-Miyaura cross coupling was also reported (Scheme 8; 6 examples, 14-99% yield). There were no comments made on a possible mechanism, the ligand-choice or the added value of the second Pd nucleus; the latter of which may be due to the absence of direct Pd-Pd interactions in the catalysts (X-ray diffraction: 2.6884(8)-2.7521(4) Å).

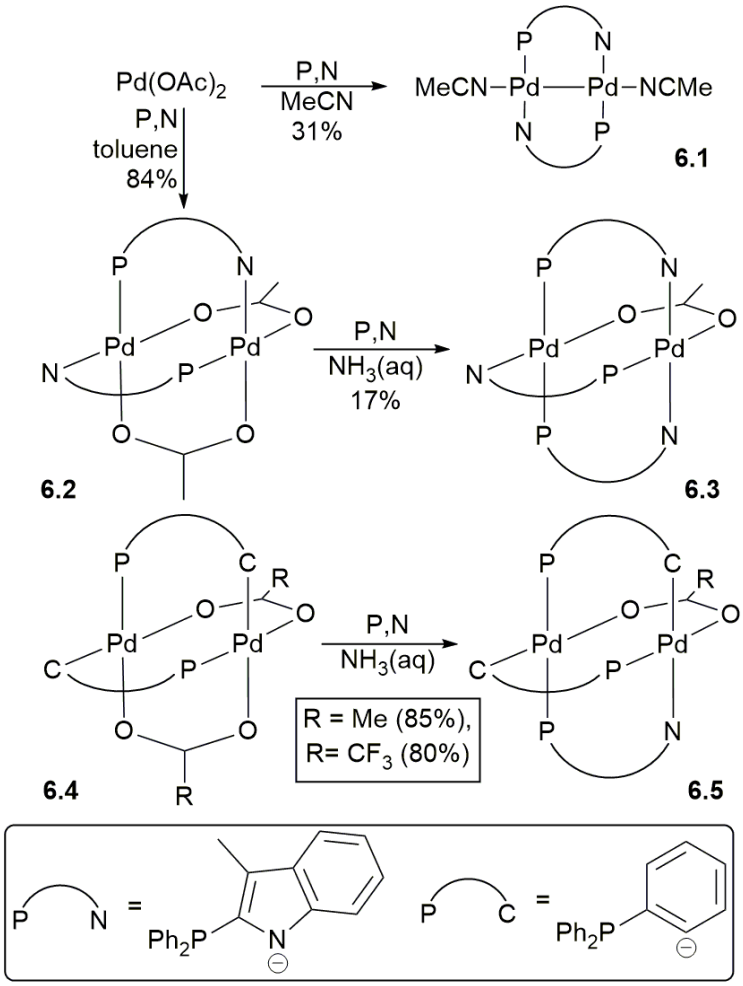

Scheme 6. *N*-anionic indolylphosphane Pd_2 coordination.

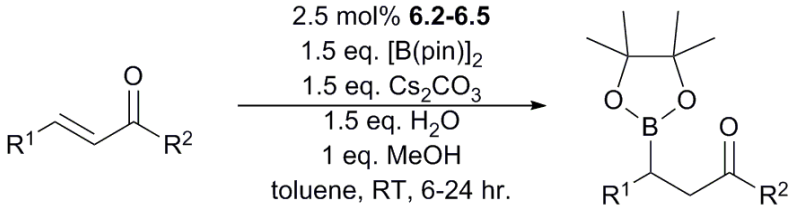

Scheme 7. Catalytic ß-borylation of α,ß-unsaturated carbonyl compounds.

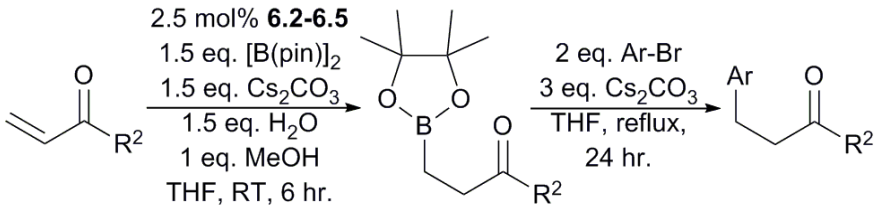

Scheme 8. Tandem ß-borylation/Suzuki-Miyaura coupling of α,ß-unsaturated carbonyls.

Although Pt is generally not active in coupling reactions, binding it to Pd provided a synergistic effect: mixed Pd,Pt-bimetallic complex **9.1** (Scheme 9) with two $PyPPh_2$ ligands was shown to be a highly active heterogeneous Suzuki-Miyaura catalyst useable in water under mild conditions.[25] High yields were observed for aryliodides and bromides, but less so for chlorides (24 examples, 47-99% yield). The bimetallic catalyst was significantly more effective than mononuclear $Pd(PyPPh_2)_2Cl_2$ and $Pt(PyPPh_2)_2Cl_2$ species at 0.8 mol%, which was carefully speculated to be due to electronic interactions between the metal cores.

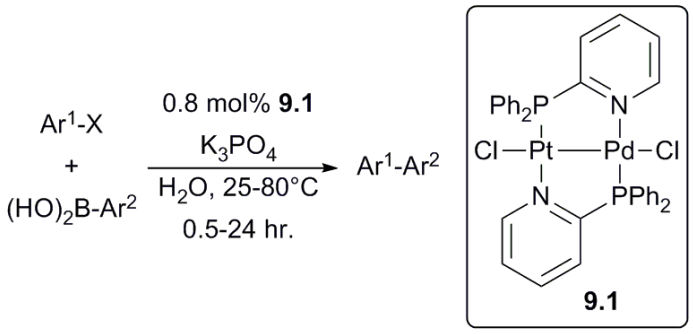

Scheme 9. Pt-Pd catalysed Suzuki-Miyaura coupling.

3.2 Tin activation

$SnCl_2$ is a common but not well-understood co-catalyst for group X metals and was therefore studied using bimetallic complexes containing these metals and 1,3-P,N-ligands.[26] The Sn,Pt-, Sn,Pd-, and Sn,Ni-complexes **10.1** were obtained by reacting $M^{II}Cl_2(PyPPh_2)_2$ (M = Ni, Pd, Pt) with $SnCl_2$ (Scheme 10). The nitrogen atoms of the two bridging P,N-ligands are coordinated to the Sn atom in all three bimetallic complexes. An alkyl/chloride ligand exchange occurs between Pd/Pt and Sn in the analogous reaction of $M^{II}Cl(PyPPh_2)$(alkyl) with $SnCl_2$ to provide the corresponding bimetallic complexes **11.2** (Scheme 11).[27,28] The isomerization is fast for the palladium complex but slow for the platinum complex, which enabled the isolation of the intermediate **11.1**.[28] The bimetallic complexes **11.2** could also be obtained directly by reacting $[M^0(PyPPh_2)_2]$ with Sn^{IV}(alkyl)Cl_3.[27,28] The bridging P,N-ligands in these complexes stabilize the metal-Sn interactions and prevent the side reactions that are observed for analogous PPh_3 complexes that cannot chelate tin, such as Sn dissociation, ß-H elimination of the alkyl groups and the formation of cis/trans coordination isomers.[27]

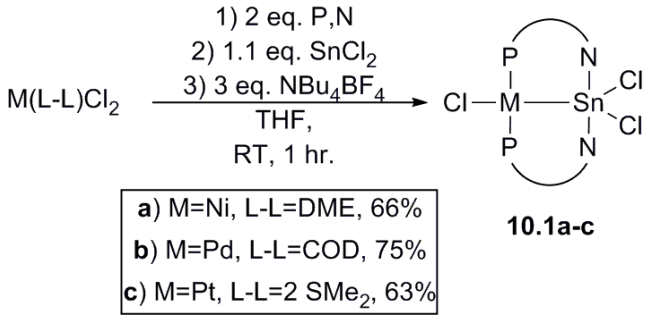

Scheme 10. P,N-stabilized group X-Sn interactions.

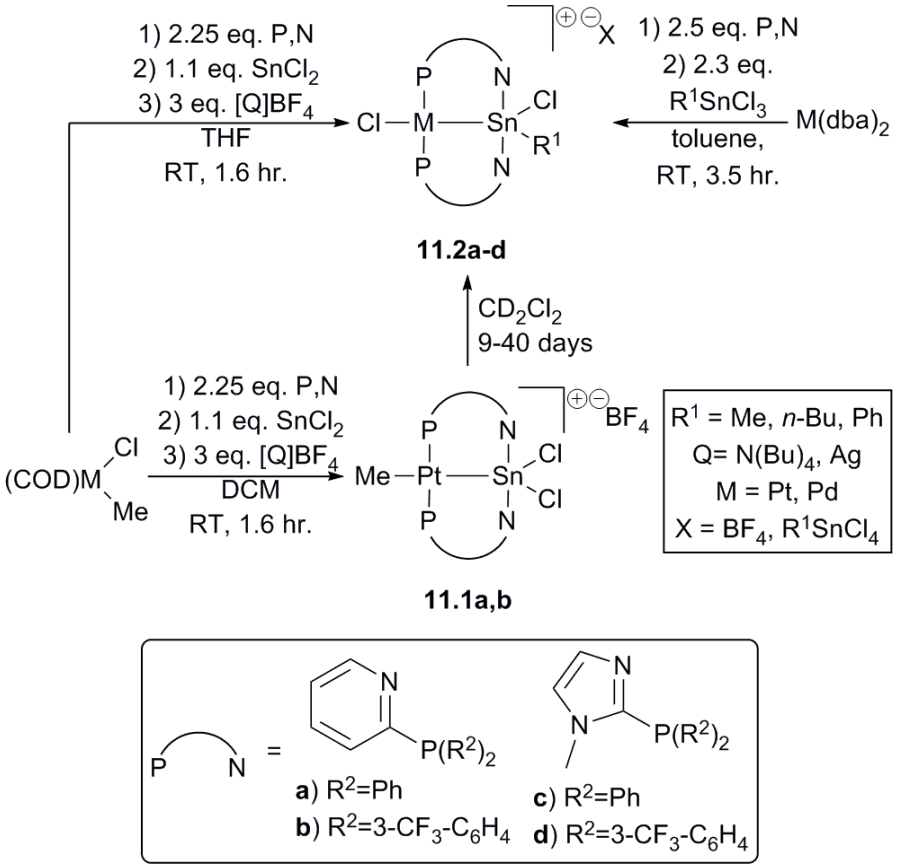

Scheme 11. P,N-stabilized group X-(alkyl)Sn interactions.

4 Group X and XI multinuclear complexes: Photoluminescence

In contrast to the rarely luminescent mononuclear complexes,[3d] 1,3-P,N-bridged multinuclear complexes have shown tremendous advances in photophysical applications over the last years, especially when coinage metals are involved. Their filled d^{10} shells and the absence of low-lying ligand-field states makes such systems attractive for photoluminescence studies.[29] Group XI complexes with more than 4 metal-nuclei are discussed in section 5.

4.1 Group X

The influence of Ag and Tl on the photophysical properties of Pt^{II} containing bimetallic complexes with bridging $PyPPh_2$ ligands has been studied. The reaction of Pt complex **12.1** with $[Ag(MeCN)BF_4]$ resulted in unique tetranuclear Pt_2Ag_2 butterfly complex **12.2**[30] and treatment with $TlPF_6$ afforded both **12.3** and **12.4** (Scheme 12).[31] Photoluminescence with bright emission was observed for **12.2-12.4**. The Ag-Ag bonds participate in the HOMO of **12.2**, contrasting the behavior of other Pt-Ag complexes, and is reflected in an atypical and distinctive red-shift (λ = 590 nm, τ = 8.3 µs, 77K). The Pt-Tl bonds in **12.3** and **12.4** seemingly reduce the non-radiative relaxations, as compared to the non-emissive **12.1**, and cause unstructured bright red emissions (**12.3**: λ = 675 nm, τ = 8.7 µs; **12.4**: λ = 665 nm, τ = 9.3 µs).

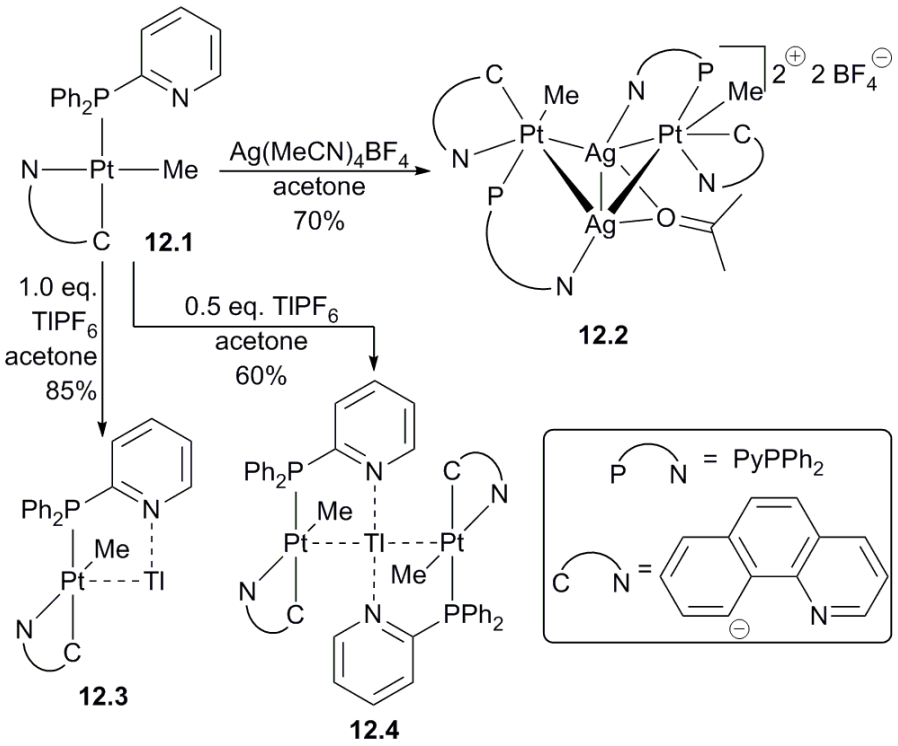

Scheme 12. Pt-heterometal interactions.

4.2 Group XI – Copper

1,3-P,N-bridged dinuclear Cu_2X_2 butterfly complexes **13.2**, obtained on treating P,N-ligands **13.1** with Cu^IX and PR^2_3 (Scheme 13), have received considerable attention as OLED candidates due to their favorable photochemistry, tuneability, and accessibility.[32] The effect of its bridging and terminal ligands on the solubility, stability, and luminescence has been addressed.[33-37] Terminal ligands were found to mainly influence the solubility of the complexes, while changes in the μ-P,N-ligand showed a pronounced effect on the emission wavelengths (12 examples, λ = 500−555 nm, φ = 0.28-0.99). *In silico* studies elucidated these effects by revealing that the HOMO is localized mainly on the Cu_2I_2-core and the LUMO on the μ-P,N-ligand (DFT: BP86, def2-SV(P); TD-DFT: B3LYP, def2-SV(P), SF-TDA). The effect of the 1,3-P,N ligands on these MOs was further verified experimentally.[34] The emission maxima were mostly influenced by electronic variations in the P,N-ligand and little by steric effects (18 examples, λ = 451-558 nm, τ = 1.09-4.22 μs, φ = 0.28-0.99). Also homoleptic 2-$PyPPh_2$ complexes were studied (19 examples, λ = 481-713 nm, φ = 0.03-0.96).[35] These studies were followed by experiments to assess and optimize the complexes for processing methods for practical application.[36] In addition, incorporating a styrene substituent on the 4-position of the pyridyl ring of the bridging $PyPPh_2$ ligand enabled the synthesis of photoluminescent metallopolymers with quantum efficiencies up to 46%.[37] Overall, this bodes well for practical applicability as OLED material.

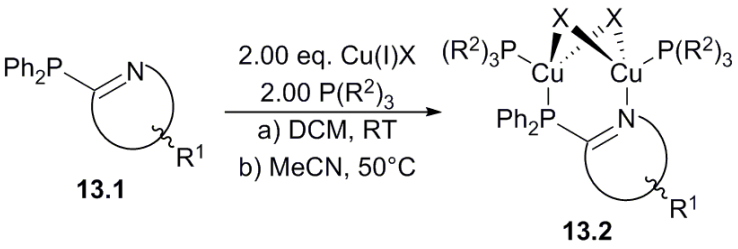

Scheme 13. Highly luminescent P,N-bridged Cu_2I_2 complexes.

Rather different Cu_2I_2 and Cu_4I_4 complexes reportedly result on treating pyridylphospholanes with different ratios of $Cu^{I}I$. An excess of the P,N-ligand resulted in complex **14.1**, an excess of $Cu^{I}I$ gave tetrametallic complex **14.2**, and complex **14.3** was obtained on using equimolar amounts (Scheme 14).[38] All of them displayed photoluminescence (λ = 471-615 nm, φ = 0.01-0.28). A study on the emission decay times of complexes akin to **14.3c**, with general formula $[((6\text{-Me-Py})PPh_2)Cu^{I}(X)]_2$ (X = Cl, Br, I), showed that their emission stems from a combination of fluorescence (80%, excited singlet state) and phosphorescence (20%, triplet state), which shortens the overall decay time.[39]

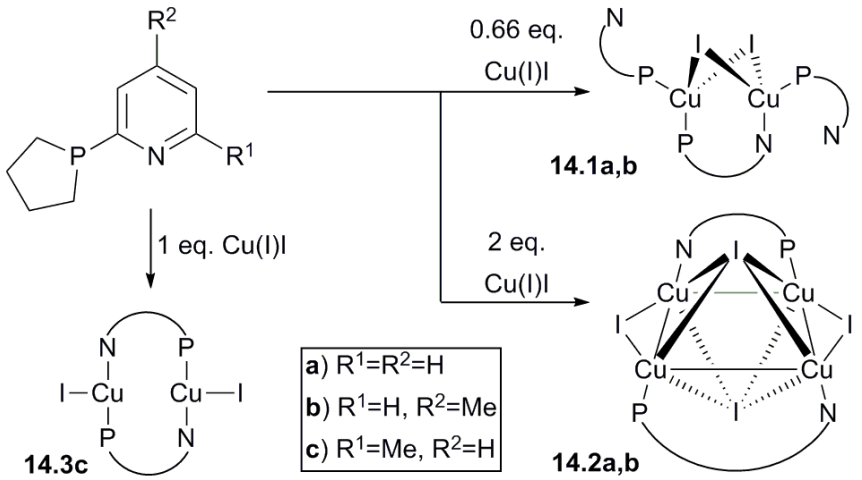

Scheme 14. Various Cu:PN ratios provide photoluminescent complexes.

Several Cu_4X_4 tetrametallic complexes akin to **14.2a,b** have been generated by treating 1,3-P,N-ligands **15.1a-c** with two equivalents of Cu^{I}-halide (Scheme 15).[40] Depending on the halide used, different $(\mu\text{-PyPPh}_2)_2(\mu\text{-X})_4Cu_4$ geometries were obtained. Also the solvent used in the (co)-crystallization had an effect on the resulting geometries, which affected the photoluminescent properties. Complexes could be obtained with rectangular Cu_4 cores (**15.2a**: λ = 548 nm, **15.2b**·2 CH_2Cl_2: λ = 542 nm; **15.2b**: λ = 521 nm) as parallelograms (**15.3a**; polymeric **15.4b**·2

$CHCl_3$: λ = 519 nm), or as structurally nearly identical butterfly complexes (**15.5c** and **15.5c·CHCl₃**). The inclusion of $CHCl_3$ in the crystal lattice of the latter caused a red-shift of the emission from 527 to 576 nm which illustrates the high impact lattice solvates can have. Highly luminescent parallelogrammatical **15.6d** has a high quantum yield and a short decay time (λ = 488 nm, τ = 9.9 μs, φ = 0.90), with an emission that consists almost equally of phosphorescence (52%) and thermally activated delayed fluorescence (48%) due to the low activation energy and strong spin-orbit coupling.[41] Also tetranuclear iminophosphane complexes were obtained (Scheme 16);[42] one equivalent $Cu^{I}Br$ yielded cubic κ^1-complex **16.1**, whereas two gave 'step'-shaped κ^2-complexes **16.2a-c**. No photoluminescence was pursued.

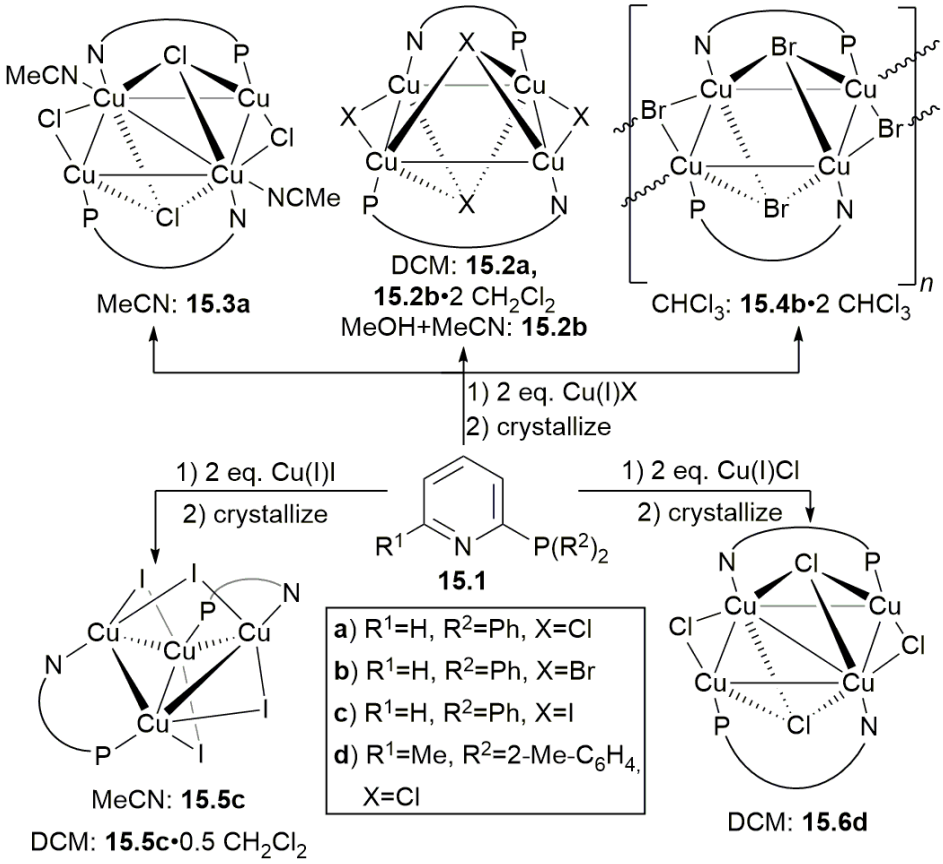

Scheme 15. Structural modulation of Cu_4 cores affects photoluminescence.

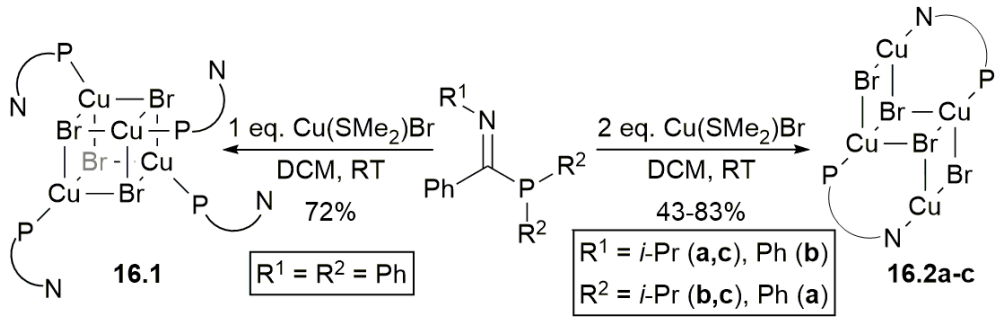

Scheme 16. Iminophosphanes can provide cubic or step-shaped Cu_4 cores.

Cu_2 complexes with non-coordinating anions have also been examined for their photophysical properties. Exemplary is $[(\mu\text{-}PyPPh_2)_3Cu_2(MeCN)](BF_4)_2$ of which the head-to-tail, blue light emitting isomer **17.1** converges under the influence of methanol to the core C_{3v}-symmetric, head-to-head isomer **17.2** that emits green light in the solid state (Scheme 17).[43] The two isomers, which interconvert depending on the crystallizing solvent used, show distinctive triplet emission (**17.1**: λ = 489 nm, τ = 63.7 µs; **17.2**: λ = 520 nm, τ = 39.9 µs) that was attributed to different Py-Ph π-π interactions (TD-DFT). The isomerization can be sterically inhibited by Me-substitution at the 6-position of the pyridine rings of the $PyPPh_2$ ligands. In this case, the exclusive product is the head-to-head complex,[44] which displays triplet emission (λ = 590 nm, τ = 28 and 7 µs, φ = 0.49). It has a chiral helical core, which could be demonstrated by NMR spectroscopy, as replacing the MeCN ligand for $BrCH_2CN$ revealed diastereotopic CH_2 protons. The head-to-tail isomer was obtained when Me groups occupy the 3-Py positions, but no luminescence data was reported.[45] Instead, it was shown that treatment with bipyridine ligands resulted in novel staircase-like metallo-polymers, while a similar reaction with **17.2**-analogue $[(\mu\text{-}PyPPh_2)_3Cu^I_2(H_2O)](BF_4)_2$ provided an inter-penetrating two-dimensional polycyclohexane framework.

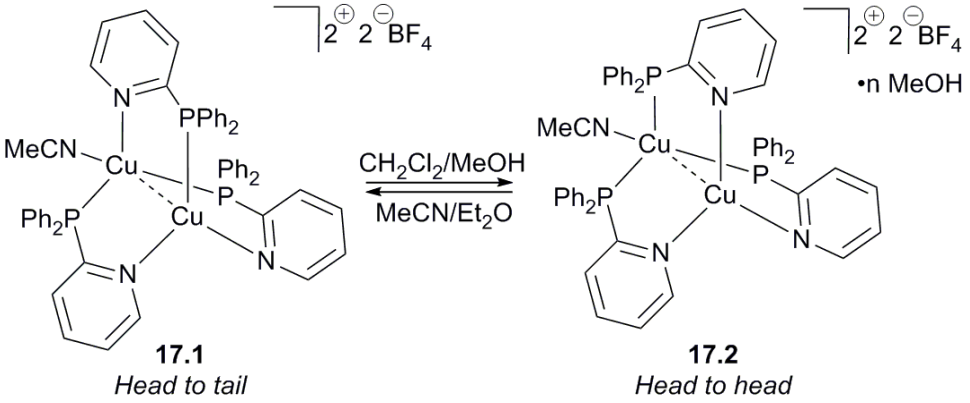

Scheme 17. MeOH-driven rearrangement of $Cu_2(PyPPh_2)_3$ species.

Trigonally coordinated, head-to-head Cu-Au complex **18.1** (Scheme 18) reportedly shows more dynamic behavior than its analogous Cu_2 complex **17.2**.[46] Crystallization afforded two polymorphs and a pseudopolymorph, which luminesce with colors ranging from blue to yellow, and a multimetallic cluster $[Au_3Cu_2(PPh_2py)_5](BF_4)_5$. TD-DFT calculations indicate that anion-cation, anion-π and π-π interactions underlie the different emissions of the three polymorphs of **18.1** (λ = 415, 483, 557 nm).

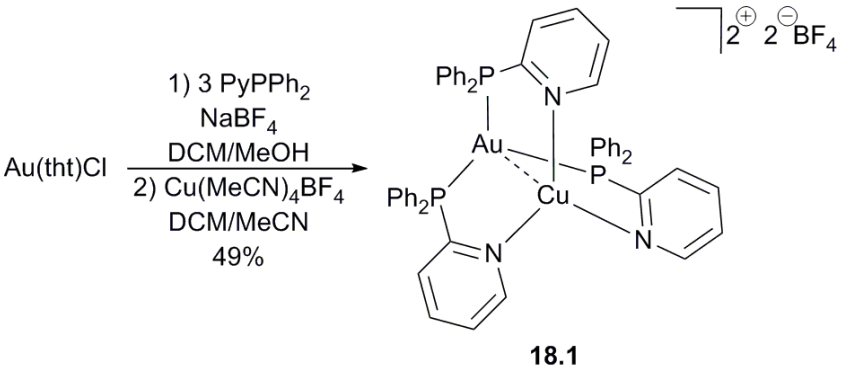

Scheme 18. The reaction to **18.1** provides five complexes with different emission spectra.

4.3 Group XI – Silver

Ag_2 complexes are less well explored than those with Cu_2 (vide supra) and Au_2 cores (vide infra), because they are often more flexible in coordination, which causes their properties to be less predictable. Illustrative are the head-to-tail complexes [(1-methyl-benzimidazolyl-PPh_2)$_2$$M_2$]$(BF_4)_2$ (M = Ag^I, Au^I), of which the Ag_2 is far less tightly coordinated than the Au_2 analogue.[47]

The C_3-symm. head-to-head [(R-CN)(6-MePy)PPh_2)$_3$$Ag^I_2$]$(BF_4)_2$ complexes, akin to Cu_2 complex **17.2**, were shown to readily lose the nitrile ligand to give the Ag-Ag analogue of Au-Cu complex **18.1** п.[48] However, the Ag_2 complex showed highly temperature dependent luminescence behavior, which was attributed to the sensitivity of argentophilic interactions (Ag-Ag) in the solid state and in solution. A broad emission was observed (λ_{max} = 488 nm).

Reacting $PyPPh_2$ with AgOTf in an equimolar ratio provided luminescent head-to-tail Ag_2-complex **19.2a** (Scheme 19).[49,50] When additional ligand was added, it is proposed to coordinate at a terminal position of the complex to generate (**19.3a**), which surprisingly contrasts with the previously discussed $Ag_2(PN)_3$ analogue, Au-Cu complex **18.1** and $Cu_2(PN)_3$ complexes **17.1-2** and unfortunately could not be confirmed by X-ray diffraction. Both complexes showed luminescence (**19.2a**: λ = 497 nm, τ = 53.7 μs; **19.3a**: λ = 496 nm, τ = 10.2), which was attributed to charge transfer from the ligand to the silver. Also, **19.2b**, with the bulkier 2-(6-*t*-pentyl-Py)PPh_2 ligand, has been synthesized from a direct reaction of the ligand with Ag^IX, as well as by transmetallation from Ru^{II}/Ru^{IV} chlorides **19.4b** (Scheme 19), but neither its catalytic nor luminescent behavior was reported.[51]

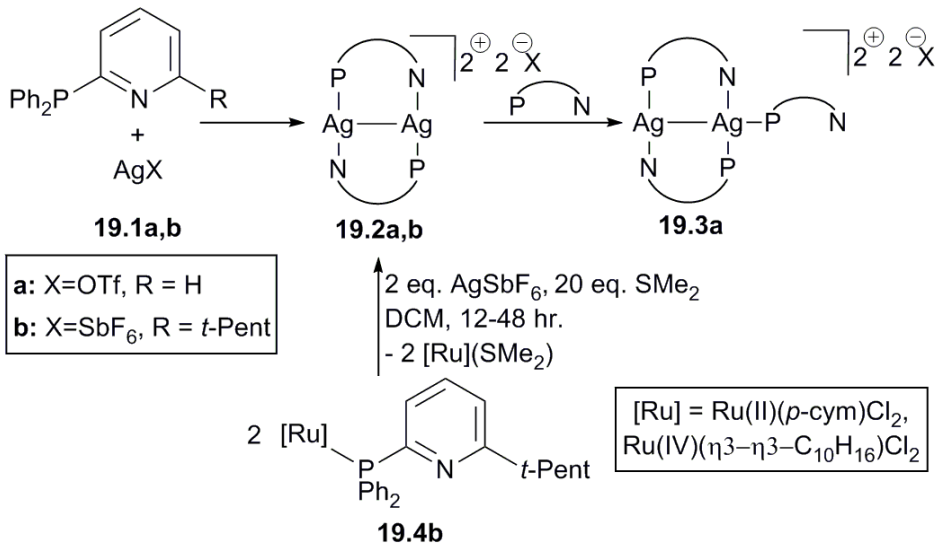

Scheme 19. [Ru]-SMe_2-formation-driven P,N-transmetallation.

Reacting *N*-anionic indolylphosphanes with AgOTf afforded non-emissive head-to-tail complex **20.1**, while their reaction with a 1:1 mixture of AgOTf and $Cu(MeCN)_4PF_6$ gave tetranuclear Ag_2Cu_2 cluster **20.2** with a rare Z-shaped geometry (Scheme 20).[52] Complex **20.2** is moderately emissive in the solid state (λ = 650 nm, τ = 0.76 μs) but only weakly in solution due to suspected Ag-Ag bond cleavage. Similar results were obtained with Au (vide infra).

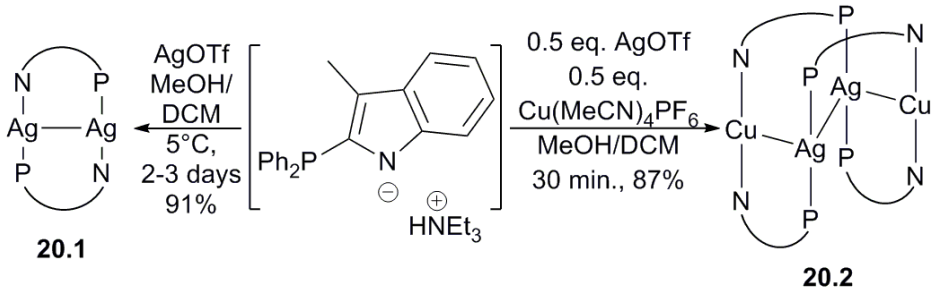

Scheme 20. Formation of P,N-bridged Z-shaped Ag_2Cu_2 cluster.

4.4 Group XI – Gold

Complex **21.2**, the Au_2 analogue of Ag_2 complex **20.1**, has been generated from its Au^I monomer **21.1** (Scheme 21).[52] Upon treatment with Cu^I, both **21.1** and **21.2** provide head-to-head AuCu complex **21.5**, while treatment with Ag^I yields a mixture of complexes **20.1, 21.2**, **21.3**, and **21.4** (Scheme 21). This difference in selectivity may not be surprising. For the 'soft' gold, only the combination with the 'hard' copper results in distinctive coordination preferences, while silver has a similar 'softness' as gold. Like **20.1**, complexes **21.1**-**21.5** do not show any emission. The luminescent behavior of related complexes (sections 4.2, 4.3) suggests the observed lack of emission is ligand-related (e.g. due to its anionicity).

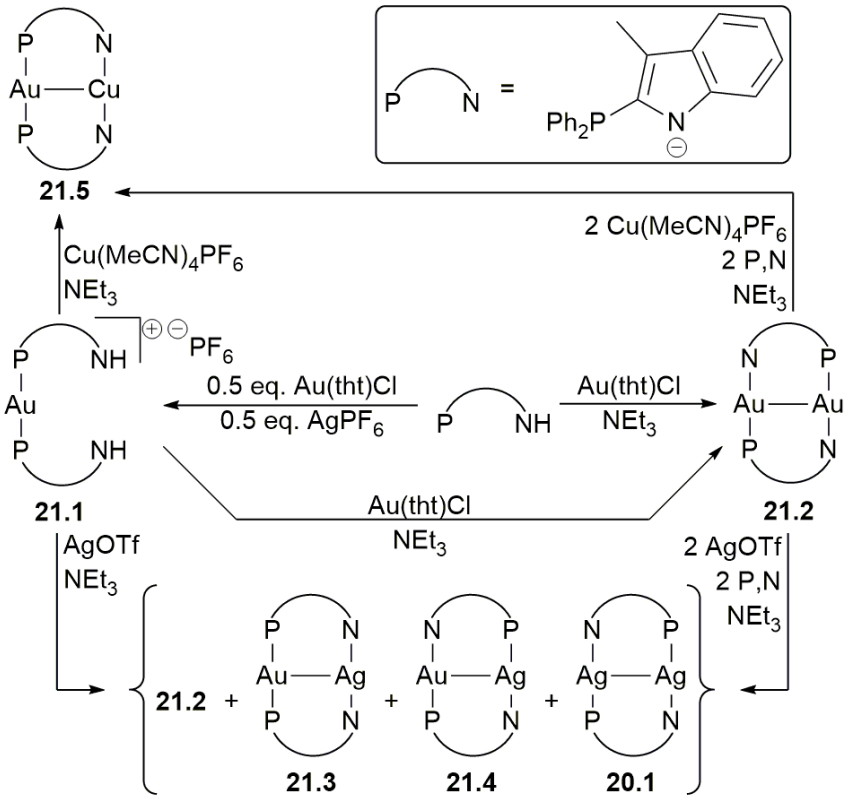

Scheme 21. Interactions of *N*-anionic indolylphosphanes with coinage metals.

Phosphaamidinates **22.1** delocalize charge over both donor atoms (Scheme 22), in contrast to the discussed N-anionic indolyl ligands. Coordination to $Au^{I}Cl$ resulted in an unexpected 1,3-P,N-bonding mode with the phosphorus atoms bridging the gold atoms of the six-membered pseudo-triangular P_3Au_3 core of **22.2**.[53] Each gold atom in this complex has a distorted linear environment without Au-Au interactions, rendering it unsuited for photoluminescence. Further exploitation of the free N-sites has not been reported upon.

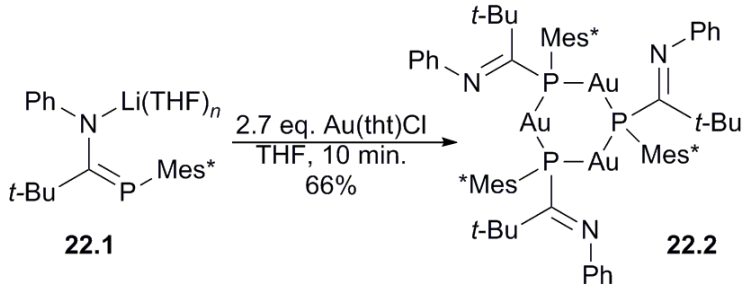

22.1 **22.2**

Scheme 22. Phosphaamidinate Au^{I} coordination.

Established Au^{I} thiolates have served as starting point to explore the photoluminescence properties of multinuclear Au-based complexes.[54] Reacting $[Au(SC_6F_5)(PyPPh_2)]$ (**23.1**) with $Au(PyPPh_2)(OTf)$ has been shown to give Au_2 **23.2** and Au_3 complex **23.3**, depending on the reagent ratio used. Treating **23.1** with Ag^{I} or Cu^{I} salts resulted in the mixed metal complexes **23.4** (Au_2M_2), **23.5** (Au_2M) and **23.6** (Au_4M_2) (M = Cu, Ag; Scheme 23), which all displayed only weak dual phosphorescent emissions. The effect of copper on gold luminescence has been further examined for Au_2Cu complexes **24.1a**[55] and **24.1b**[56] (Scheme 24). The phosphorescent emission of **24.1a** shows a considerably red-shift from its precursor Au-complex in the solid state (λ = 542 nm, τ = 2.82 µs, φ = 0.14), but this disappears in solution where the trinuclear Au_2Cu structure may not be maintained. TD-DFT calculations revealed the HOMO to be located on the aryl ligands and the LUMO mainly on the pyridyl ring of

the μ-$PyPPh_2$ ligands. The observed emissive states of **24.1a** were attributed to mixed intra-ligand- and metal-to-ligand-charge-transfer. Changing the two Au-ligands R_2 from 3,5-Cl_2-2,4,6-F_3-phenyl (**24.1a**) to Cl (**24.1b**) localizes the HOMO on the metallic core, according to DFT analysis, and results in weak phosphorescent emission (λ = 558 nm, τ = 29 μs). Tweaking the ligand by 6-Me substitution on the pyridyl rings of the two μ-$PyPPh_2$ ligands (**24.1c**) enhances the photoluminescence to provide bright white light emission (λ_{max} = 450 nm, τ = 2.2-12 μs, φ = 0.28).[57] This was attributed to emissive triplet states and strong spin-orbit coupling of the metals. A comparison with Rh, Ir and Pt complexes **24.2b** and **24.3b** (Au-Rh/Pt non-emissive; Au-Ir at 77K, λ = 608 nm), emphasizes how specific the effect is of Cu^I on Au^I-luminescence.[56]

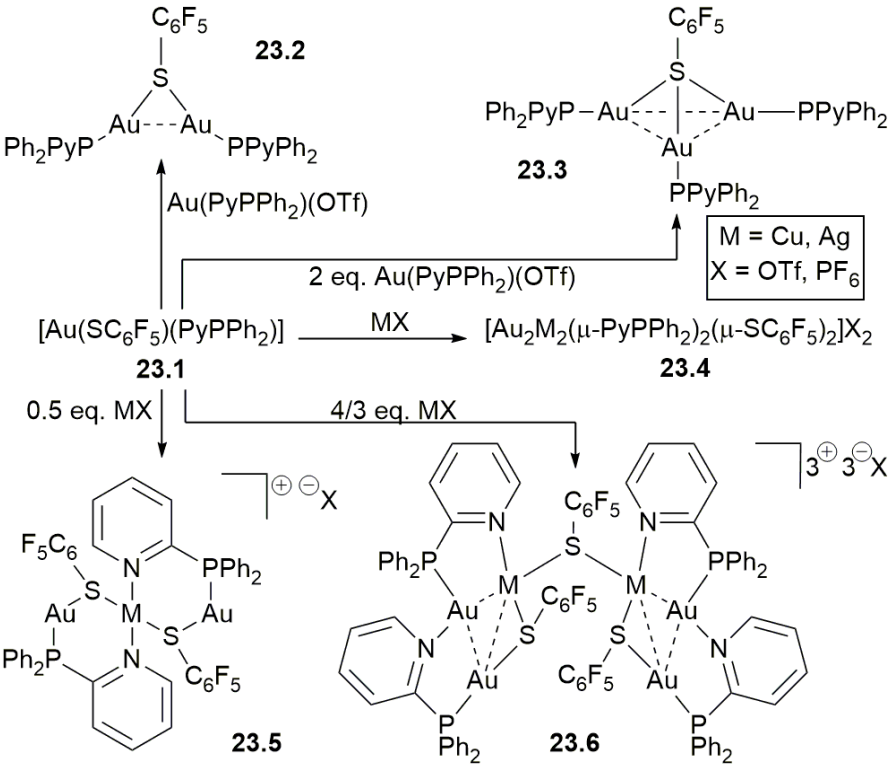

Scheme 23. Thiolato Au^I-coinage metal interactions.

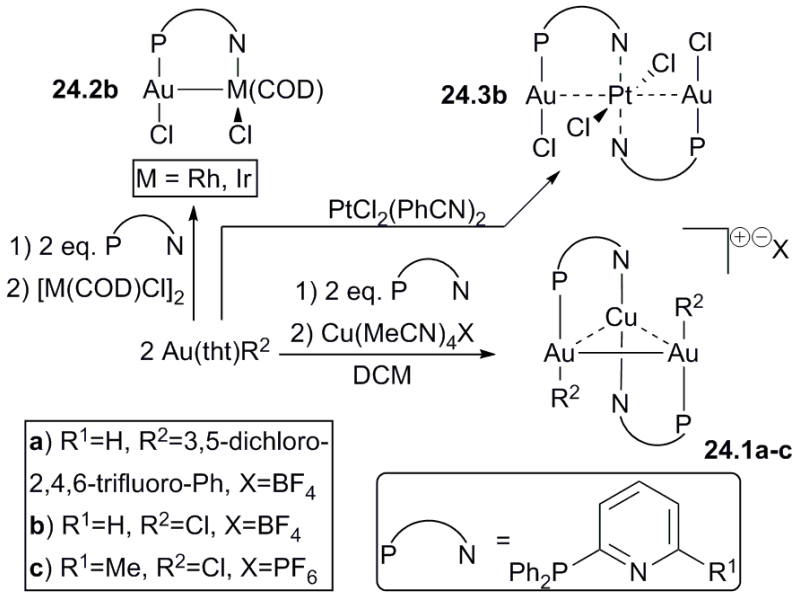

Scheme 24. Au^{I}-heterometal interactions.

When only 1,3-P,N-ligands are present for Au^{I} coordination, the favored product is the trinuclear arrangement as in 1-diphenylphosphino-isoquinoline complex **25.2** (Scheme 25).[58,59] The presence of weakly coordinating tht solvent results in P-monodentate product **25.1**.[58] Trimetallic **25.2** is luminescent in the solid state (λ = 400 nm). Similar trimeric structures have been identified as catalyst deactivation products in gold-catalyzed alkyne hydrations:[59] when the chloride ligand of $[(PyPPh_2)Au^{I}]Cl$ was exchanged for a non-coordinating anion, it provided low catalytic activity due to the formation of the $PyPPh_2$-analogue of **25.2**. Similarly, deactivation of a (4-imidazolylphosphane) Au-based catalyst for alkyne hydration has been attributed to the formation of the $[(\mu\text{-}1,3\text{-}P,N)_2\text{-}Au_3(Cl)_2]Cl$ trimer **26.1** (Scheme 26).[60] This structurally characterized product shows similarity with **24.1**. Trimetallic **26.1** is formed in presence of a coordinating anion, in contrast to the $\mu\text{-}PyPPh_2$-based Au_3 complexes, because of the stronger electron donating ability of imidazolylphosphanes over

pyridylphosphanes. The photoluminescent potential of these Au_3 complexes has unfortunately not yet been addressed.

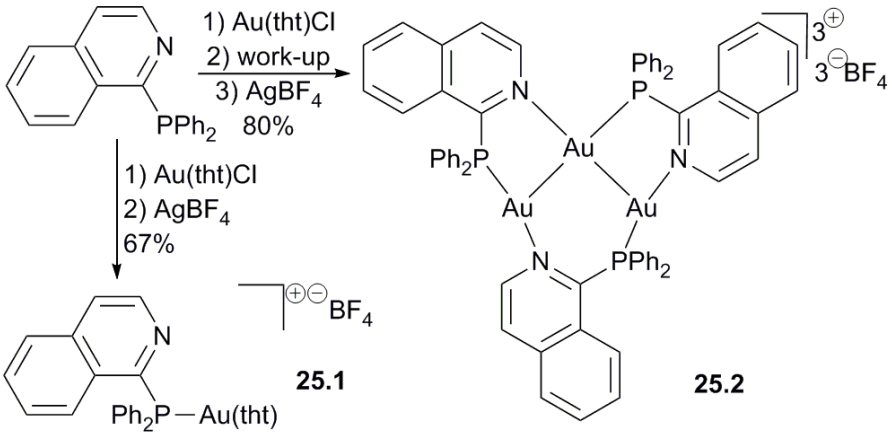

Scheme 25. P,N-Au^I trimerisation.

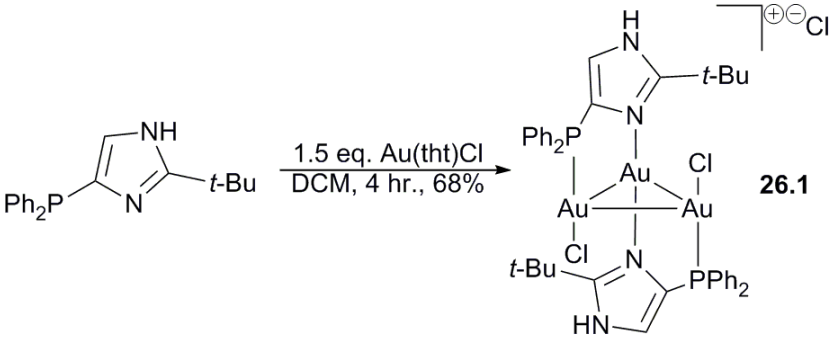

Scheme 26. P,N-Au^I trimerization.

5 Group XI clusters: Photoluminescence and catalysis

1,3-P,N-ligands facilitated metallophilic interactions have attracted much attention of late to access coinage clusters for photoluminescence and catalysis. Discussed here are complexes with more than four metal nuclei, in which especially gold is prominent. Similar to the previously discussed examples (section 4), considerable advances have been made in photophysical investigations. In heterogeneous cluster-based catalysis,

principles from homogeneous mononuclear 1,3-P,N-catalysts proved valuable.

5.1 Photoluminescence

Multinuclear Au^I complexes are typically luminescent in the solid state only, as solvation tends to quench or disassemble the aggregates (section 4.4), but their photoluminescence can still be limited by dynamic behavior. For example, non-emissive relaxation was reported for $(PPh_3)_6Au_6(C)(BF_4)_2$ (**27.1a**, Scheme 27) due to rotation of its terminal Ph_3P-Au bonds, but this could be remedied by introducing rigidity, i.e., by using $PyPPh_2$ ligands in **27.1b**, which then were restrained by Ag^I atoms to form **27.2b**.[61] Cluster **27.2b** is brightly green emissive in the solid state (λ = 625 nm, τ = 5.7 µs, φ = 0.29), probably due to a metal cluster centered excited state. The luminescence is maintained in coordinating solvents, where the P,N-ligand is proposed to protect the cluster from quenchers, the effect of which may be enhanced by adding bulky substituents.

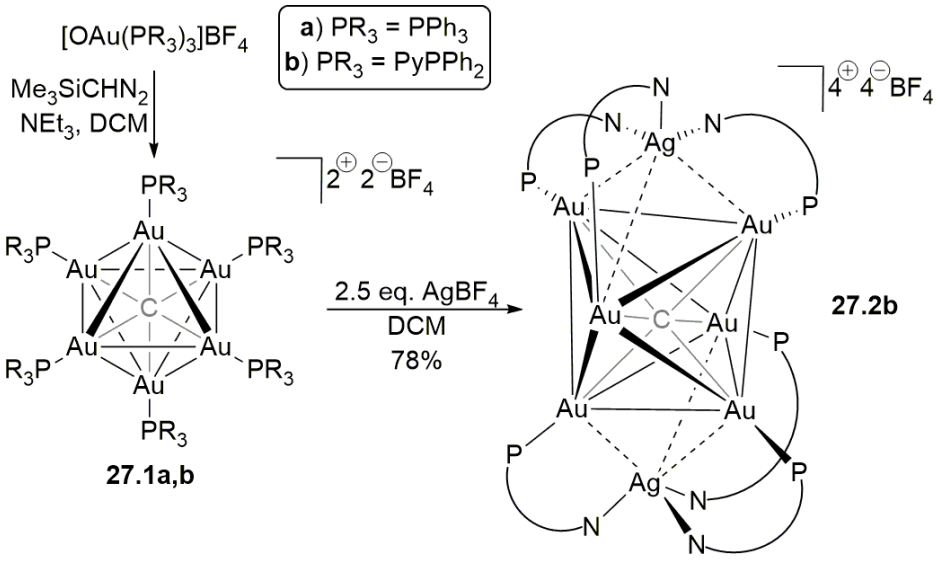

Scheme 27. Enhanced rigidity contributes to the luminescence of **27.2b**.

A similar approach with Cu^{I} and $PyPPh_2$ ligands was shown to yield the unprecedented trigonal prismatic **28.1** instead of the expected octahedral **28.2**, which was, however, obtained on using 5-Me-$PyPPh_2$ ligand (Scheme 28).[62] This latter structure is very similar to **27.2b**. Both complexes display red luminescence (**28.1**: λ = 619 nm, τ = 2.1 μs, φ = 0.043; **28.2**: λ = 615 nm, τ = 7.8 μs, φ = 0.022). On replacing Cu^{I} for Ag^{I} and using 4-CO_2H-$PyPPh_2$ as ligand, the Ag analogues of **28.1** and **28.2** could be obtained.[63] These showed a remarkable interconversion on addition or removal of MeCN and a temperature-dependent ratio in solution. Both complexes were emissive (Ag-**28.1** λ = 600 nm, τ = 1.34-3.23 μs, φ = 0.42; Ag-**28.2** λ = 560 nm, τ = 1.06-3.64 μs, φ = 0.36).

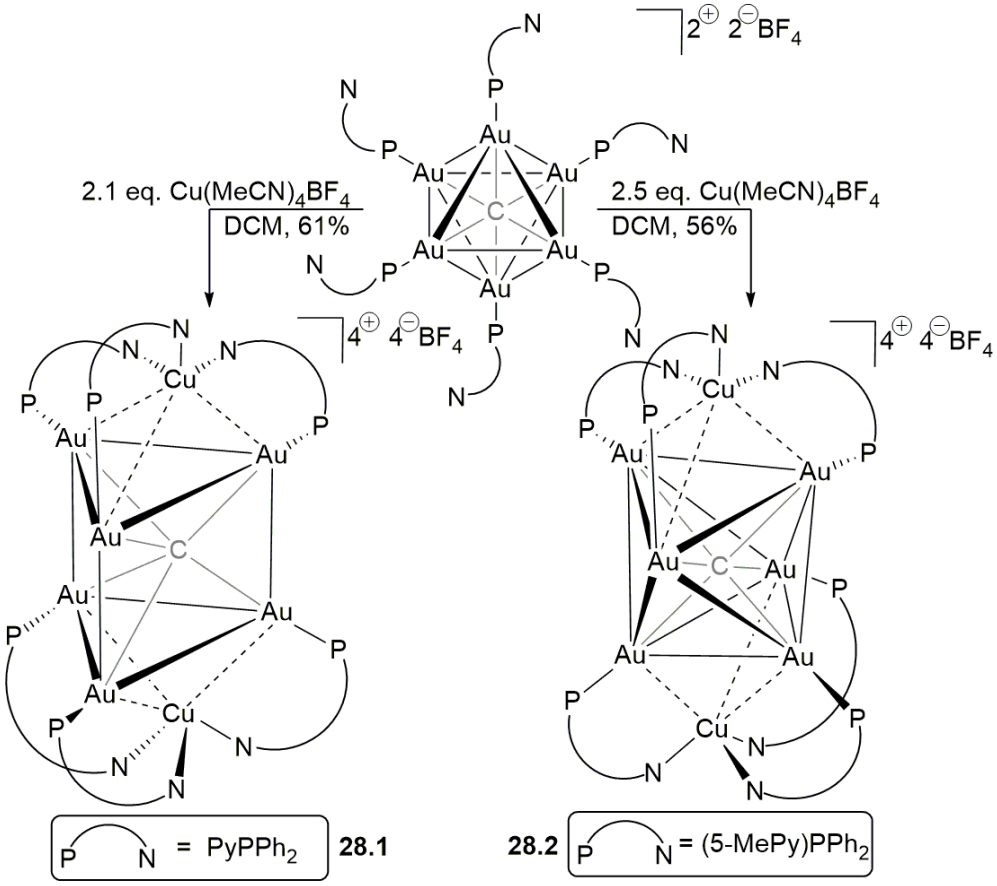

Scheme 28. P,N-facilitated Au_6-Cu_2 interactions.

Enhanced photoluminescence by increased rigidity has also been studied for a rigid Cu-cluster with added Au^0 to improve chemical inertness.[64] Two gold centers cap both sides of a Cu_6-ring, which carries six bridging thiolates on its rim for stabilization (Scheme 29). Surprisingly, the $PyPPh_2$ ligands coordinate in a monodentate fashion to only the Au^0 centers, but they still influence the luminescence of the cluster as the LUMO resides mainly on them (fluorescence, $\lambda = 665$ nm, $\varphi = 0.12$).

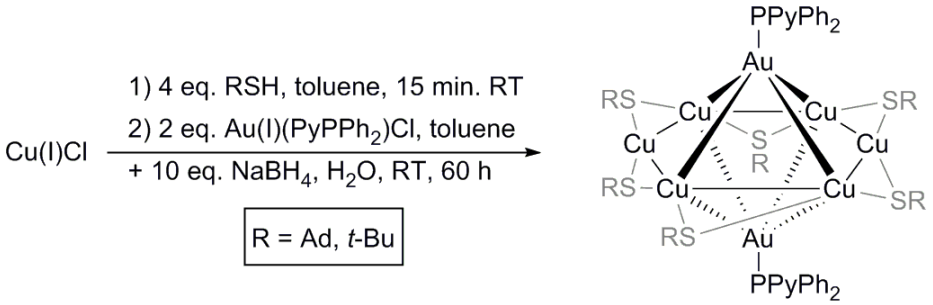

Scheme 29. Increased rigidity in Au_2Cu_6 cluster.

An indirect effect of P,N-ligands was found when $Au^I(PyPPh_2)Cl$ was reduced with $NaBH_4$ and subsequently treated with excess 2-naphtalene-thiol to yield well-defined $Au^0_{25}(SR)_{18}$ and $Au^0_{36}(SR)_{24}$ thiolate clusters.[65] Even though $PyPPh_2$ is not incorporated into these products, it influenced the size of the formed clusters, which may be due to the ligand's ability to stabilize multinuclear intermediates.

C_{3h}-symmetric $Au^I/Au^0/Ag^I$ cluster **30.1** contains two Au_3Ag tetrahedral subunits with stabilizing μ-$PyPPh_2$ ligands, and a central Au_4 triangle with bidentate 2-pyridine-ethynyl ligands (Scheme 30).[66] The cluster shows dual emission in the visible and near-IR of which the former is attributed to the Au_3Ag tetrahedrons and the latter to the central unit (solution: $\lambda = 653$, $\tau = 3.85$ μs, $\varphi = 0.0009$; $\lambda = 971$, $\tau = 0.65$ μs, $\varphi = 0.0489$),

which was confirmed by the emission of complex **30.2** (λ = 651 nm) that contains only the Au_3Ag tetrahedrons.

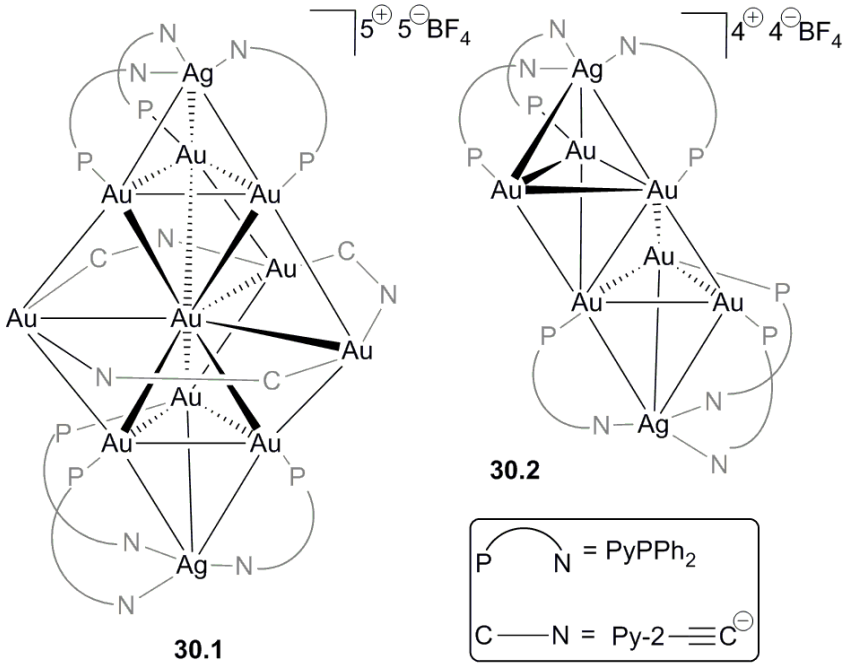

Scheme 30. Combining two emitting cluster cores in **30.1**.

Related $(P,N)_3Au_3Ag$ tetrahedrons, but now carrying S, N, or O ions,[12c] showed similar emissions. Solvents have a strong influence on the intercluster interactions of the (P,N)-SAu_3Ag complexes and thus their luminescence (Scheme 31).[67] Exposure of the green-emissive **31.1** (**a**: λ = 554 nm; **b**: λ = 534 nm) to Et_2O breaks one of the aurophilic interactions to give the blue-emissive **31.2** (**a**: λ = 503 nm; **b**: λ = 474 nm). By replacing the sulfur atoms of **31.2a** for a chiral diamine to connect the two Au_3Ag cores, a chiral cluster could be synthesized, thereby giving access to chiroptical applications.[68] The O-stabilized tetrahedron $[OAu_3Ag(PyPPh_2)_3](BF_4)_2$ **32.1**, has been found to activate all methyl C-H bonds of acetonitrile in the presence of $AgBF_4$ (Scheme 32).[69] The

resulting cluster **32.2** is a dimeric centrosymmetric structure of which its two Ag_2Au_4 units are bound in square pyramidal fashion by two μ_5-bridging C-C≡N units with the terminal carbon coordinating to the Au_4 squares and the C≡N nitrogen to the silver atoms. The oxo anion of **32.1** is suspected to be responsible for the triple deprotonation of MeCN. Cluster **32.2** displays phosphorescent emissions in the solid state (λ = 509 nm, τ = 17.9μs, φ = 0.001) and in solution (λ = 565 nm, τ = 8.5 μs, φ = 0.001).

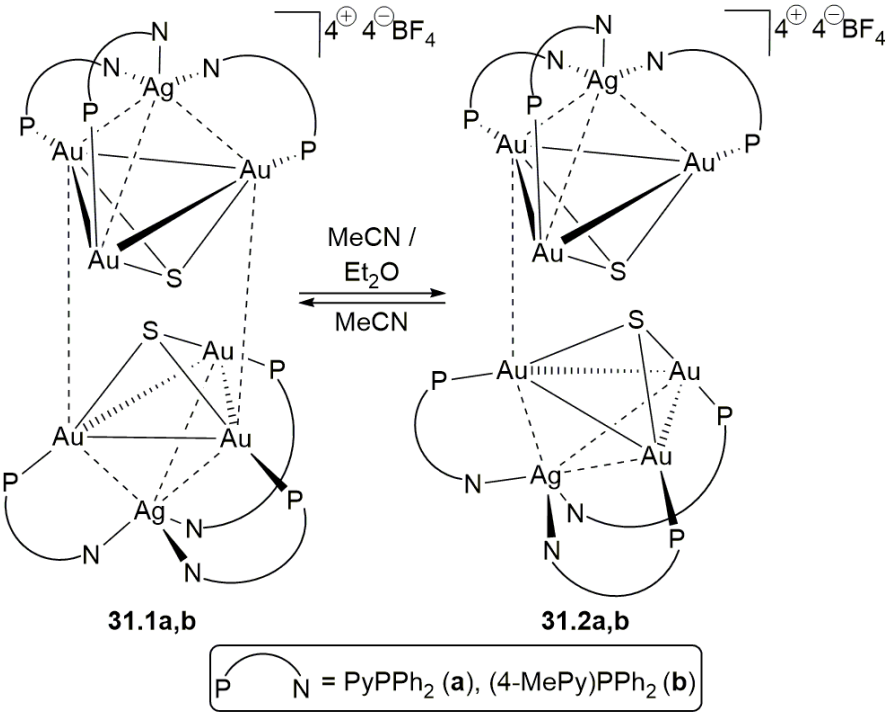

Scheme 31. Et_2O induced intercluster rearrangement.

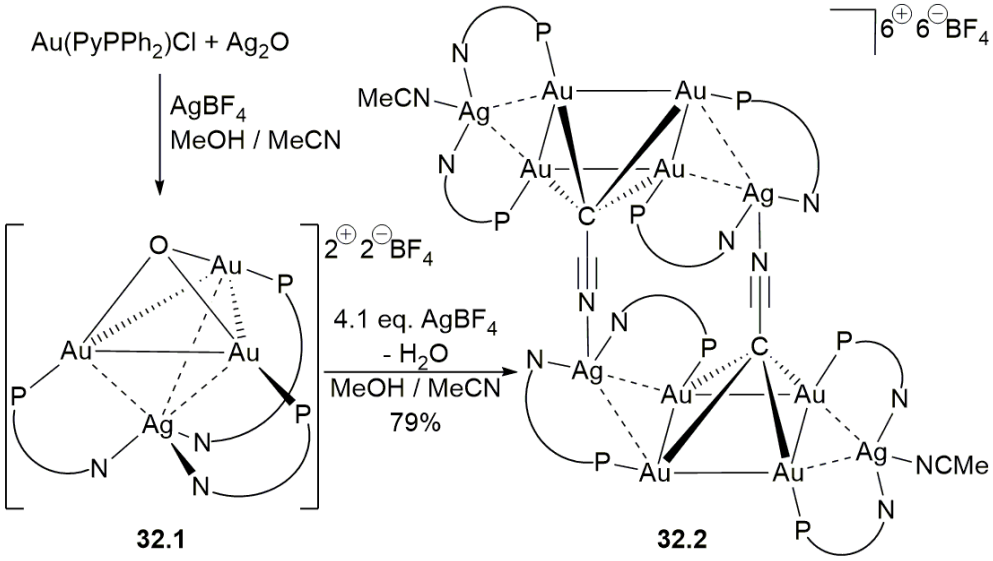

Scheme 32. Triple C-H activation of MeCN provides cluster **32.2**.

5.2 Catalysis

Cluster $[Au_{13}Cu_4(PyPPh_2)_4(SC_6H_4\text{-}t\text{-}Bu)_8]^+$, formed by reduction of Au and Cu with $NaBH_4$ in the presence of thiolates and P,N-ligands, appeared to be inactive for the $NaBH_4$ catalyzed hydrogenation of 4-nitrophenol.[70] The bulky thiolate surface ligands appear to block the metal sites, which was corroborated by the catalytic activity observed for the similar, but less congested $[Au_{13}Cu_8(PyPPh_2)_{12}(S\text{-}Py)]^+$, which provided complete conversion in 10 minutes (2.5 mg cluster, 1.2 mmol $NaBH_4$, 6.8×10^{-3} mmol 4-nitrophenol, water). This cluster also shows some activity in the oxidation of benzylalcohol to benzaldehyde when supported on carbon nanotubes (24% conversion, 42-43.5% selectivity, 100 mg catalyst (1% Au), 0.5 mmol benzyl alcohol, 1.5 mmol K_2CO_3, $P(O_2) = 5$ atm, toluene, 80 °C, 8 h).

Cluster $Au_{11}(PyPPh_2)_7Br_3$ has been shown to hydrogenate 4-nitro-benzaldehyde chemoselectively (90%; TOF = 20 h^{-1}, 1 wt% cluster, 0.05 mmol

4-nitro-benzaldehyde, P(H_2)= 20 bar, 80 °C, 10 h) without the need for external base, which the corresponding PPh_3 complexes did require.[71] The catalytic cycle was proposed to proceed via a mechanism in which cooperative activation of H_2 yields the cluster hydride and protonated ligand. Since the catalyst was supported on CeO_2, it could be isolated and reused after the reaction without loss of activity after four cycles. Considering that 1,3-P,N-ligands are widely used as internal bases in mononuclear transition metal catalysis[2,3] it is rewarding to see such concepts also applicable in cluster catalysis.

6 Conclusions

Recent investigations on multinuclear 1,3-P,N-ligand chemistry have shown a shift in emphasis from catalysis to photophysical studies. The ability of P,N-ligands to facilitate metal-(hetero)metal bonds was especially lucrative in combination with coinage-metals to access photoluminescent complexes, including robust emitters with attractive properties for pragmatic use. Generally, metal-based LUMOs and P,N-ligand-localized HOMOs are found, indicating that a high degree of control of the complexes' emissive behavior is possible by tuning the ligands. In the exploration of coinage-clusters in catalysis, the concepts of ligand-cooperativity (e.g., as internal base / proton shuttle) can be adapted. The decade-long study and experience in mononuclear P,N-catalysis will be helpful for this.

7 References

[1] See for instance: a) S. Liu, A. Motta, A.R. Mouat, M. Delferro, T.J. Marks, J. Am. Chem. Soc., 136 (2014), 10460-10469. b) D.C. Powers, B.L. Anderson, S.J. Hwang, T.M. Powers, L.M. Pérez, M.B. Hall, S.-L. Zheng, Y.-S. Chen, D.G. Nocera, J. Am. Chem. Soc., 136 (2014), 15346-15355.

[2] For a review on multinuclear P,N-ligand complexes, see: S. Maggini, Coord. Chem. Rev., 253 (2009), 1793-1832.

[3] For reviews on 1,3-P,N-ligands, see: a) G.R. Newkome, Chem. Rev., 93 (1993), 2067-2089. b) Z.-Z. Zhang, H. Cheng, Coord. Chem. Rev., 147 (1996), 1-39. c) P. Espinet, K. Soulantica, Coord. Chem. Rev., 193-195 (1999), 499-556. d) M.K. Rong, F. Holtrop, J.C. Slootweg, K. Lammertsma, Coord. Chem. Rev., 380 (2019), 1-16. See also Chapter I.

[4] For a review on hybrid ligands, see: W.-H. Zhang, S.W. Chien, T.S.A. Hor, Coord. Chem. Rev., 255 (2011), 1991-2014.

[5] H. Grützmacher, Angew. Chem. Int. Ed., 47 (2008), 1814-1818.

[6] H.G. Ang, W.E. Kow, K.F. Mok, Inorg. Nucl. Chem. Lett., 8 (1972), 829-832.

[7] a) P. Braunstein, D.G. Kelly, A. Tiripicchio, F. Ugozzoli, Bull. Soc. Chim. Fr., 132 (1995), 1083-1086. b) E.C. Carson, S.J. Lippard, J. Am. Chem. Soc., 126 (2004), 3412-3413.

[8] a) D.B. Grotjahn, C.R. Larsen, J.L. Gustafson, R. Nair, A. Sharma, J. Am. Chem. Soc., 129 (2007), 9592-9593. b) J.J.M. de Pater, C.E.P. Maljaars, E. de Wolf, M. Lutz, A.L. Spek, B.-J. Deelman, C.J. Elsevier, G. van Koten, Organometallics, 24 (2005), 5299-5310.

[9] a) K. Kurtev, D. Ribola, R.A. Jones, D.J. Cole-Hamilton, G. Wilkinson, J. Chem. Soc., Dalton Trans., (1980), 55-58. b) E. Drent, P. Arnoldy, P.H.M. Budzelaar, J. Organomet. Chem., 455 (1993), 247-253. c) E. Drent, P. Arnoldy, P.H.M. Budzelaar, J. Organomet. Chem., 475 (1994), 57-63. d) I. Moldes, E. de la Encarnación, J. Ros, Á. Alvarez-Larena, J.F. Piniella, J. Organomet. Chem., 566 (1998), 165-174. e) A. Caballero, F.A. Jalón, B.R. Manzano, G. Espino, M. Pérez-Manrique, A. Mucientes, F.J. Poblete, M. Maestro, Organometallics, 23 (2004), 5694-5706. f) T. Oshiki, H. Yamashita, K. Sawada, M. Utsunomiya, K. Takahashi, K. Takai, Organometallics, 24 (2005), 6287-6290.

[10] a) S. Harkal, F. Rataboul, A. Zapf, C. Fuhrmann, T. Riermeier, A. Monsees, M. Beller, Adv. Synth. Catal., 346 (2004), 1742-1748. b) R.A. Singer, N.J. Tom, H.N. Frost, W.M. Simon, Tetrahedron Lett., 45 (2004), 4715-4718.

[11] a) F. Shafiq, R. Eisenberg, Inorg. Chem., 32 (1993), 3287-3294. b) H. Ishii, M. Goyal, M. Ueda, K. Takeuchi, M. Asai, J. Mol. Catal. A Chem., 148 (1999), 289-293. c) H. Ishii, M. Goyal, M. Ueda, K. Takeuchi, M. Asai, Macromol. Rapid Commun., 22 (2001), 376-381.

[12] a) V.J. Catalano, S.J. Horner, Inorg. Chem., 42 (2003), 8430-8438. b) D. Drommi, F. Nicolò, C.G. Arena, G. Bruno, F. Faraone, R. Gobetto, Inorg. Chim. Acta, 221 (1994), 109-116. c) Q.-M. Wang, Y.-A. Lee, O. Crespo, J. Deaton, C. Tang, H.J. Gysling, M.C. Gimeno, C. Larraz, M.D. Villacampa, A. Laguna, R. Eisenberg, J. Am. Chem. Soc., 126 (2004), 9488-9489. d) Z.-Z. Zhang, H.-P. Xi, W.-J. Zhao, K.-Y.

Jiang, R.-J. Wang, H.-G. Wang, Y. Wu, J. Organomet. Chem., 454 (1993), 221-228. e) G. Franciò, R. Scopelliti, C.G. Arena, G. Bruno, D. Drommi, F. Faraone, Organometallics, 17 (1998), 338-347.

[13] See for instance: a) Q. Wang, M. Zhu, L. Lu, C. Yuan, S. Xing, X. Fu, Dalton Trans., 40 (2011), 12926-12934. b) Y.-Y. Kuo, M.F. Haddow, A.L. Jamieson, G.R. Owen, Transition Met. Chem., 38 (2013), 641-648. c) H. You, Y. Wang, X. Zhao, S. Chen, Y. Liu, Organometallics, 32 (2013), 2698-2704. d) X. Wang, Y. Wang, J. Zhang, X. Zhao, Y. Liu, J. Organomet. Chem., 762 (2014), 40-47.

[14] See for instance: a) D.M. Zink, T. Baumann, M. Nieger, S. Bräse, Eur. J. Org. Chem., (2011), 1432-1437. b) D.M. Zink, T. Baumann, J. Friedrichs, M. Nieger, S. Bräse, Inorg. Chem., 52 (2013), 13509-13520. c) C.G.J. Tazelaar, E. Nicolas, T. van Dijk, D.L.J. Broere, M. Cardol, M. Lutz, D. Gudat, J.C. Slootweg, K. Lammertsma, Dalton Trans., 45 (2016), 2237-2249. d) S. Hanf, R. García-Rodríguez, S. Feldmann, A.D. Bond, E. Hey-Hawkins, D.S. Wright, Dalton Trans., 46 (2017), 814-824. e) T. Zhang, C. Ji, K. Wang, D. Fortin, P.D. Harvey, Inorg. Chem., 49 (2010), 11069-11076. f) X.-K. Wan, Z.-W. Lin, Q.-M. Wang, J. Am. Chem. Soc., 134 (2012), 14750-14752. g) P.C. Kunz, M.U. Kassack, A. Hamacher, B. Spingler, Dalton Trans., (2009), 7741-7747. h) A. Bakhoda, N. Safari, V. Amani, H.R. Khavasi, M. Gheidi, Polyhedron, 30 (2011), 2950-2956. i) A. Burini, R. Galassi, S. Ricci, F. Bachechi, A.A. Mohamed, J.P. Fackler, Jr., Inorg. Chem., 49 (2010), 513-518.

[15] See for instance: a) K. Mashima, A. Shima, K. Nakao, A. Fukumoto, Y. Kaneda, Y. Kusumi, Inorg. Chem., 48 (2009), 1879-1886. b) K. Pal, K. Nakao, K. Mashima, Eur. J. Inorg. Chem., (2010), 5668-5674. c) N.M. West, J.A. Labinger, J.E. Bercaw, Organometallics, 30 (2011), 2690-2700. d) A.M. Lilio, K.A. Grice, C.P. Kubiak, Eur. J. Inorg. Chem., (2013), 4016-4023. e) P.A. Rudd, S. Liu, L. Gagliardi, V.G. Young, Jr., C.C. Lu, J. Am. Chem. Soc., 133 (2011), 20724-20727. f) L.J. Clouston, R.B. Siedschlag, P.A. Rudd, N. Planas, S. Hu, A.D. Miller, L. Gagliardi, C.C. Lu, J. Am. Chem. Soc., 135 (2013), 13142-13148. g) Q.-L. Ni, X.-F. Jiang, T.-H. Huang, X.-J. Wang, L.-C. Gui, K.-G. Yang, Organometallics, 31 (2012), 2343-2348. h) P.C. Kunz, C. Wetzel, M. Bongartz, A.L. Noffke, B. Spingler, J. Organomet. Chem., 695 (2010), 1891-1897. i) H.-H. Cui, N.-N. Wu, J.-Y. Wang, M.-Q. Hu, H.-M. Wen, C.-N. Chen, J. Organomet. Chem., 767 (2014), 46-53.

[16] See for instance: a) M. Ghalib, C. Schulzke, G.J. Palm, J.W. Heinicke, J. Organomet. Chem., 776 (2015), 60-63. b) J.W. Heinicke, M. Ghalib, C. Schulzke, P.G. Jones, L. Könczöl, L. Nyuászi, Phosphorus, Sulfur, Silicon Rel. Elem., 190 (2015), 806-815. c) A.D. Worthy, C.L. Joe, T.E. Lightburn, K.L. Tan, J. Am. Chem.

Soc., 132 (2010), 14757-14759. d) N. Mager, K. Robeyns, S. Hermans, J. Organomet. Chem., 794 (2015), 48-58.

[17] a) P.L. Dunn, R.K. Carlson, L. Gagliardi, I.A. Tonks, Dalton Trans., 45 (2016), 9892-9901. b) P.L. Dunn, R.K. Carlson, I.A. Tonks, Inorg. Chim. Acta, 460 (2017), 43-48.

[18] P. Li, M. Wang, L. Chen, J. Liu, Z. Zhao, L. Sun, Dalton Trans., (2009), 1919-1926.

[19] Analogous complexes also reported in a) J. He, C.-L. Deng, Y. Li, Y.-L. Li, Y. Wu, L.-K. Zou, C. Mu, Q. Luo, B. Xie, J. Wei, J.-W. Hu, P.-H. Zhao, W. Zheng, Organometallics, 36 (2017), 1322-1330. b) X.-F. Liu, J. Coord. Chem., 70 (2017), 116-126.

[20] P. Das, M. Borah, F. Michaud, F.Y. Pétillon, P. Schollhammer, Inorg. Chim. Acta, 376 (2011), 641-644.

[21] See for instance: C. Kubis, I. Profir, I. Fleischer, W. Baumann, D. Selent, C. Fischer, A. Spannenberg, R. Ludwig, D. Hess, R. Franke, A. Börner, Chem. Eur. J., 22 (2016), 2746-2757.

[22] K. Kartashova, S. Mallet-Ladeira, M.R. Axet, J. Organomet. Chem., 799-800 (2015), 226-231.

[23] Y. Takahashi, N. Murakami, K. Fujita, R. Yamaguchi, Dalton Trans., (2009), 2029-2042.

[24] Bonet, H. Gulyás, I.O. Koshevoy, F. Estevan, M. Sanaú, M.A. Ubeda,, E. Fernández, Chem. Eur. J., 16 (2010), 6382-6390.

[25] M. Gholinejad, H.R. Shahsavari, M. Razeghi, M. Niazi, F. Hamed, J. Organomet. Chem., 796 (2015), 3-10.

[26] Y. Cabon, H. Kleijn, M.A. Siegler, A.L. Spek, R.J.M. Klein Gebbink, B.-J. Deelman, Dalton Trans., 39 (2010), 2423-2427.

[27] a) Y. Cabon, I. Reboule, M. Lutz, R.J.M. Klein Gebbink, B.-J. Deelman, Organometallics, 29 (2010), 5904-5911. b) E.J. Derrah, S. Warsink, J.J.M. de Pater, Y. Cabon, I. Reboule, M. Lutz, R.J.M. Klein Gebbink, B.-J. Deelman, Organometallics, 33 (2014), 2914-2918.

[28] S. Warsink, E.J. Derrah, C.A. Boon, Y. Cabon, J.J.M. de Pater, M. Lutz, R.J.M. Klein Gebbink, B.-J. Deelman, Chem. Eur. J., 21 (2015), 1765-1779.

[29] P.C. Ford, E. Cariati, J. Bourassa, Chem. Rev., 99 (1999), 3625-3647.

[30] S. Jamali, Z. Mazloomi, S.M. Nabavizadeh, D. Milić, R. Kia, M. Rashidi, Inorg. Chem., 49 (2010), 2721-2726.

[31] S. Jamali, R. Ghazfar, E. Lalinde, Z. Jamshidi, H. Samouei, H.R. Shahsavari, M.T. Moreno, E. Escudero-Adán, J. Benet-Buchholz, D. Milic, Dalton Trans., 43 (2014), 1105-1116.

[32] M. Wallesch, D. Volz, D.M. Zink, U. Schepers, M. Nieger, T. Baumann, S. Bräse, Chem. Eur. J., 20 (2014), 6578-6590.

[33] D. Volz, D.M. Zink, T. Bocksrocker, J. Friedrichs, M. Nieger, T. Baumann, U. Lemmer, S. Bräse, Chem. Mater., 25 (2013), 3414-3426.

[34] D. Volz, D.M. Zink, T. Baumann, M. Mydlak, H. Flügge, J. Friedrichs, M. Nieger, S. Bräse, Chem. Mater., 25 (2013), 4471-4486.

[35] D.M. Zink, M. Bächle, T. Baumann, M. Nieger, M. Kühn, C. Wang, W. Klopper, U. Monkowius, T. Hofbeck, H. Yersin, S. Bräse, Inorg. Chem., 52 (2013), 2292-2305.

[36] a) D. Volz, M. Wallesch, S.L. Grage, J. Göttlicher, R. Steininger, D. Batchelor, T. Vitova, A.S. Ulrich, C. Heske, L. Weinhardt, T. Baumann, S. Bräse, Inorg. Chem., 53 (2014), 7837-7847. b) D. Volz, Y. Chen, M. Wallesch, R. Liu, C. Fléchon, D.M. Zink, J. Friedrichs, H. Flügge, R. Steininger, J. Göttlicher, C. Heske, L. Weinhardt, S. Bräse, F. So, T. Baumann, Adv. Mater., 27 (2015), 2538-2543. c) M. Wallesch, A. Verma, C. Fléchon, H. Flügge, D.M. Zink, S.M. Seifermann, J.M. Navarro, T. Vitova, J. Göttlicher, R. Steininger, L. Weinhardt, M. Zimmer, M. Gerhards, C. Heske, S. Bräse, T. Baumann, D. Volz, Chem. Eur. J., 22 (2016), 16400-16405.

[37] D. Volz, A.F. Hirschbiel, D.M. Zink, J. Friedrichs, M. Nieger, T. Baumann, S. Bräse, C. Barner-Kowollik, J. Mater. Chem. C, (2014), 1457-1462.

[38] E.I. Musina, A.V. Shamsieva, I.D. Strelnik, T.P. Gerasimova, D.B. Krivolapov, I.E. Kolesnikov, E.V. Grachova, S.P. Tunik, C. Bannwarth, S. Grimme, S.A. Katsyuba, A.A. Karasik, O.G. Sinyashin, Dalton Trans., 45 (2016), 2250-2260.

[39] T. Hofbeck, U. Monkowius, H. Yersin, J. Am. Chem. Soc., 137 (2015), 399-404.

[40] K. Chen, J. Shearer, V.J. Catalano, Inorg. Chem., 54 (2015), 6245-6256.

[41] X.-L. Chen, R. Yu, X.-Y. Wu, D. Liang, J.-H. Jia, C.-Z. Lu, Chem. Commun., 52 (2016), 6288-6291.

[42] R. Kandel, K. Huynh, L. Dalgliesh, R. Wang, P.G. Jessop, Inorg. Chim. Acta, 445 (2016), 117-123.

[43] Y.-J. Li, Z.-Y. Deng, X.-F. Xu, H.-B. Wu, Z.-X. Cao, Q.-M. Wang, Chem. Commun., 47 (2011), 9179-9181.

[44] J.-J. Cid, J. Mohanraj, M. Mohankumar, M. Holler, G. Accorsi, L. Brelot, I. Nierengarten, O. Moudam, A. Kaeser, B. Delavaux-Nicot, N. Armaroli, J.-F. Nierengarten, Chem. Commun., 49 (2013), 859-861.

[45] Y.-M. Lin, Z. Lei, S.-S. Chang, Q.-M. Wang, CrystEngComm, 15 (2013), 9372-9376.

[46] K. Chen, C.E. Strasser, J.C. Smith, J. Shearer, V.J. Catalano, Inorg. Chem., 51 (2012), 1207-1209.

[47] D.E. Jenkins, Z. Assefa, J. Mol. Struct., 1133 (2017), 374-383.

[48] E. Hobbollahi, M. Himmelsbach, M. List, U. Monkowius, Inorg. Chem. Commun., 71 (2016), 105-108.

[49] O. Crespo, M.C. Gimeno, A. Laguna, C. Larraz, Z. Naturforsch., 64b (2009), 1525-1534.

[50] Also the 2-pyridylphospholane analogue of **12.2a** was reported in: E.I. Musina, A.V. Shamsieva, A.A. Karasik, O.G. Sinyashin, Phosphorus, Sulfur, Silicon Rel. Elem., 190 (2015), 827-830.

[51] E. Tomás-Mendivil, R. García-Álvarez, S.E. Garciá-Garrido, J. Díez, P. Crochet, V. Cadierno, J. Organomet. Chem., 727 (2013), 1-9.

[52] I.O. Koshevoy, J.R. Shakirova, A.S. Melnikov, M. Haukka, S.P. Tunik, T.A. Pakkanen, Dalton Trans., 40 (2011), 7927-7933.

[53] T. van Dijk, S. Burck, M.K. Rong, A.J. Rosenthal, M. Nieger, J.C. Slootweg, K. Lammertsma, Angew. Chem. Int. Ed., 53 (2014), 9068-9071.

[54] O. Crespo, M.C. Gimeno, A. Laguna, F.J. Lahoz, C. Larraz, Inorg. Chem., 50 (2011), 9533-9544.

[55] V.J. Catalano, J.M. López-de-Luzuriaga, M. Monge, M.E. Olmos, D. Pascual, Dalton Trans., 43 (2014), 16486-16497.

[56] M.J. Calhorda, C. Ceamanos, O. Crespo, M.C. Gimeno, A. Laguna, C. Larraz, P.D. Vaz, M.D. Villacampa, Inorg. Chem., 49 (2010), 8255-8269.

[57] E. Hobbollahi, M. List, B. Hupp, F. Mohr, R.J.F. Berger, A. Steffen, U. Monkowius, Dalton Trans., 46 (2017), 3438-3442.

[58] U. Monkowius, M. Zabel, M. Fleck, H. Yersin, Z. Naturforsch., 64b (2009), 1513-1524.

[59] Khin, A.S.K. Hashmi, F. Rominger, Eur. J. Inorg. Chem., 7 (2010), 1063-1069.

[60] Wetzel, P.C. Kunz, I. Thiel, B. Spingler, Inorg. Chem., 50 (2011), 7863-7870.

[61] J.-H. Jia, Q.-M. Wang, J. Am. Chem. Soc., 131 (2009), 16634-16635.

[62] J.-H. Jia, J.-X. Liang, Z. Lei, Z.-X. Cao, Q.-M. Wang, Chem. Commun., 47 (2011), 4739-4741.

[63] X.-Y. Liu, Y. Yang, Z. Lei, Z.-J. Guan, Q.-M. Wang, Chem. Commun., 52 (2016), 8022-8025.

[64] X. Kang, S. Wang, Y. Song, S. Jin, G. Sun, H. Yu, M. Zhu, Angew. Chem. Int. Ed., 55 (2016), 3611-3614.

[65] Y. Zhang, C. Liu, X. Yang, M. Bao, J. Huang, W. Shen, RSC Adv., 6 (2016), 105166-105170.

[66] Z. Lei, Z.-J. Guan, X.-L. Pei, S.-F. Yuan, X.-K. Wan, J.-Y. Zhang,, Q.-M. Wang, Chem. Eur. J., 22 (2016), 11156-11160.

[67] L.-Q. Mo, J.-H. Jia, L.-J. Sun, Q.-M. Wang, Chem. Commun., 48 (2012), 8691-8693.

[68] X. He, Y. Wang, H. Jiang, L. Zhao, J. Am. Chem. Soc., 138 (2016), 5634-5643.

[69] X.-L. Pei, Y. Yang, Z. Lei, Q.-M. Wang, J. Am. Chem. Soc., 135 (2013), 6435-6437.

[70] H. Yang, Y. Wang, J. Lei, L. Shi, X. Wu, V. Mäkinen, S. Lin, Z. Tang, J. He, H. Häkkinen, L. Zheng, N. Zheng, J. Am. Chem. Soc., 135 (2013), 9568-9571.

[71] Liu, H. Abroshan, C. Yan, G. Li, M. Haruta, ACS Catal., 6 (2016), 92-99.

Chapter III

Iminophosphanes: Synthesis, Rhodium Complexes, and Ruthenium(II)-Catalyzed Hydration of Nitriles

Mark K. Rong, Koen van Duin, Tom van Dijk, Jeroen J.M. de Pater, Berth-Jan Deelman, Martin Nieger, Andreas W. Ehlers, J. Chris Slootweg, and Koop Lammertsma

Highly stable iminophosphanes, obtained from alkylating nitriles and reaction of the resulting nitrilium ions with secondary phosphanes, were explored as tunable P-monodentate and 1,3-P,N bidentate ligands in rhodium complexes. X-ray crystal structures are reported for both κ^1 and κ^2 complexes with the counterion in one of them being an unusual anionic coordination polymer of silver triflate. The iminophosphane-based ruthenium(II)-catalyzed hydration of benzonitrile in 1,2-dimethoxyethane (180 °C, 3 h) and water (100 °C, 24 h) and under solvent free conditions (180 °C, 3 h) results in all cases in the selective formation of benzamide with yields of up to 96%, thereby outperforming by far the reactions in which the common 2-pyridyldiphenylphosphane is used as the 1,3-P,N ligand.

Organometallics **2017**, *36*, 1079-1090.

1 Introduction

Hybrid ligands are important in catalysis, as they enable ligand- and metal-based reactivity in bifunctional systems.[1,2] In particular, P,N ligands are of interest because of the presence of both soft phosphorus and hard nitrogen donor sites. [3] Of the various topologies, [4–7] 1,3-P,N ligands have shown ample applicability in transition-metal-based catalysis (Figure 1).

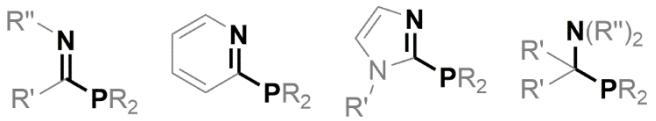

Figure 1. 1,3-P,N ligand systems.

The C_1 spacer provides optimal separation[8] for metal coordination at nitrogen,[9] phosphorus,[10,11] or both atoms,[11] as well as enabling the formation of homo-[12] and hetero-bimetallic[13] complexes for metal activation, photoluminescence, and cooperative metal–metal systems (Figure 2).[13a,14]

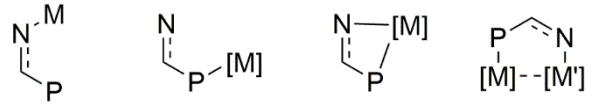

Figure 2. 1,3-P,N coordination modes.

Exemplary reactions that make use of 1,3-P,N ligands are the Ru-catalyzed hydration of nitriles,[10a,11a,h] the Pd-catalyzed carbonylation of alkynes,[10c,11d,e] Pd-catalyzed Buchwald-Hartwig and Suzuki-Miyaura cross-coupling reactions,[15] dinuclear Pd- and [Fe-Rh]-catalyzed carbonylation of alcohols,[12d,e,13c] the Ru- and Au-catalyzed hydration of alkynes,[10d,e] the Ru-catalyzed transfer hydrogenation of ketones and aldehydes,[11b,g] the Ru-catalyzed isomerization of alkenes,[10b] the Ru- catalyzed and dinuclear Rh-catalyzed hydrogenation of alkenes,[11f,12b] the Rh-, Ir-, and

[Ru–Rh]-catalyzed hydroformylation of alkenes,[11c,13a,d] and the Cr-catalyzed tri- and tetramerization of ethylene,[11i] whereas Cu^{I}_2 and [Au^{I}_3-Ag^{I}] complexes have been used in photoluminescence.[12a,c,13b] A popular ligand in the complexes used for these reactions is 2-pyridyldiphenylphosphane ($PyPPh_2$),[3,16] even though it has limited flexibility for steric and electronic tuning of particularly the N-donor site. Replacement of the pyridine group by an imine or amine functionality provides 1,3-P,N ligands with more opportunities to tune the properties of their derived catalysts.

Recently, we reported a simple methodology, based on nitrilium ions, to synthesize iminophosphanes (IUPAC: *C*-phosphanylimines) and anionic phosphaamidinates that carry different substituents at all three C, N, and P sites (Scheme 1).[17] Shortly thereafter Hanton, Dyer, and co-workers reported neutral ligands by condensing silylated phosphanes and imidoyl chlorides, but this method is intrinsically more limited.[11i] These 1,3-P,N ligands coordinate to Au,[17] Rh,[17] Ir,[17b] and Cr[11i] complexes. The iminophosphanes display dynamic κ^1- and κ^2-coordination behavior in the case of Rh^{III}, while 2-pyridylphosphanes generally give exclusively κ^1-Rh-complexes.[18a-c]

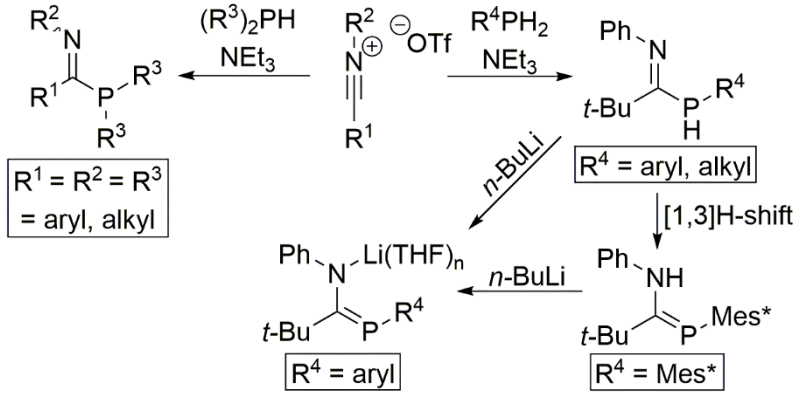

Scheme 1. Synthesis of Iminophosphanes and Phosphaamidinates from Nitrilium Ions.

In the present study we expand on the synthesis of iminophosphanes to display the diversity of the nitrilium ion methodology, report on the chelation to Rh^{III} to further exploit the intricacies of κ^1 versus κ^2 coordination, and examine the performance of the iminophosphane versus the $PyPPh_2$ ligand for the Ru^{II}-catalyzed hydration of nitriles. The last process, first reported in 1986[19] and used for the production of polyacrylates and pharmaceuticals,[19–21] was chosen because of the role of the N-donor site in activating water in the catalytic cycle.

2 Results and Discussion

The synthesis and stability of new iminophosphanes with relatively small substituents is presented first. Next, the coordination to Rh^{III} is examined. This is followed by an assessment of the performance of the ligands in the Ru^{II}-catalyzed hydration of nitriles.

2.1 Ligands

A set of iminophosphanes (**3a–f**) with different electronic properties but similar steric features was prepared from nitrilium triflates **2** (Scheme 2). The procedure is analogous to the protocol we reported recently, the difference being that here nitriles **1** are directly alkylated to provide the ion, whereas previously we obtained the ions from imidoyl chlorides.[17] The choice of synthetic approach depends on the N substituent: with *i*-Pr or larger alkyl groups, imidoyl chlorides are the starting point, sometimes necessitating stabilization of the resulting nitrilium ions with pyridine bases,[17c] but smaller groups are only accessible by nitrile alkylation.[22] Thus, treating **1** with MeOTf gave the corresponding *N*-methyl nitrilium triflates **2** (R = Ph (**a**), 4-CH_3-C_6H_4 (**b**), 4-CF_3-C_6H_4 (**c**)). The reaction with **1b** was carried out in toluene at ambient temperature to provide after 5 days white crystalline **2b** (62%). Methylations of the less nucleophilic **1a,c** were performed without solvent over an 18 h period; in the case of

1c a slightly elevated reaction temperature of 45 °C was used to melt the nitrile. Crystallization of the crude products provided nitrilium salts **2a** (DCM/Et_2O) and **2c** (DCM/pentane) as white solids in 86% and 69% yields, respectively.

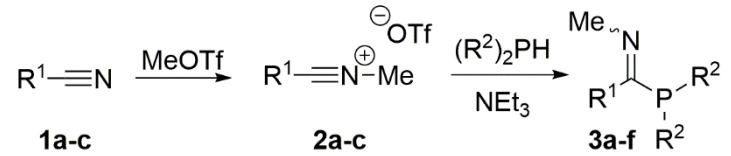

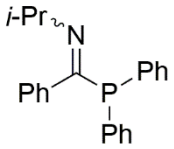

3	R^1	R^2	Yield	E/Z
a	Ph	Ph	91	71/29
b	4-CH_3-C_6H_4	Ph	75	83/17
c	4-CF_3-C_6H_4	Ph	85	45/55
d	Ph	3-CF_3-C_6H_4	46	83/17
e	Ph	3-CH_3-C_6H_4	77	68/32
f	Ph	4-CH_3-C_6H_4	53	76/24

3g

Scheme 2. Synthesis of Iminophosphanes **3**.

Dropwise addition of diphenylphosphane and its 3-methyl, 3-CF_3, and 4-methyl derivatives to a DCM solution of nitrilium triflates **2a-c** at −78 °C, followed by deprotonation with triethylamine at room temperature, resulted in the quantitative formation of iminophosphanes **3a-f** (Scheme 2). Et_2O extraction, filtration over alumina, and crystallization provided the products in 46−91% as *E*/*Z* mixtures, as determined by their ^{31}P NMR chemical shifts (i.e., **3a** 7.8 (*E*), −7.6 (*Z*); **3b** 7.6 (*E*), −8.0 (*Z*); **3c** 8.2 (*E*), −7.7 (*Z*); **3d** 5.9 (*E*), −8.5 (*Z*); **3e** 8.3 (*E*), −7.5 (*Z*); **3f** 6.3 (*E*), −8.8 (*Z*)) with assignments based on related ones reported earlier.[17b] The *E*/*Z* ratios were found to be sensitive to the experimental setup (e.g., concentration), which is in agreement with the calculated very small energy differences (ωB97X-D/6-31+G(d,p); $|\Delta E_{(E\text{-}Z)}| =$ 0.19−0.78 kcal mol^{-1})[23] as well as similar behavior reported for related

systems;[17] **3g** was included for its different *N*-substituent (*i*-Pr versus Me).[17b]

2.2 Ligand Stability

Exploring the applicability of iminophosphanes in transition-metal-catalyzed reactions, such as the hydration of nitriles (vide infra), requires these P,N-ligands to be stable toward water, whereas it is quite conceivable that they are prone to hydrolysis to the corresponding diarylphosphanes and amides. It is then comforting to see, using ^{31}P NMR monitoring, that the stability of *E*-/*Z*-**3a** in acetone toward hydrolysis by degassed water over a period of 211 h showed only slight degradation, which was attributed to oxidation to [**3a**(O)] by air rather than hydrolysis (Figure 3). The oxidation sensitivity of **3a** was confirmed in a separate assessment (see Supporting Information). Similar results were obtained for **3b,c** (see Supporting Information). The presence of 0.10 equiv of triflic acid did not catalyze the hydrolysis of **3a**. Exposure of **3a** to triflic acid at room temperature gave only N-protonated iminophosphane without any degradation over a 46 h period. This indicates that iminophosphanes are reasonably rugged ligands.

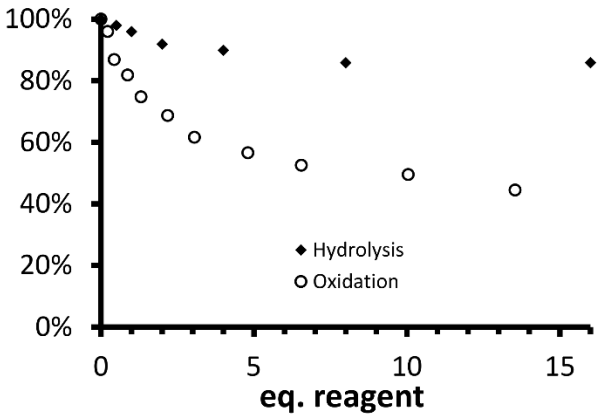

Figure 3. Sensitivity of **3a** (%) toward hydrolysis (reagent H_2O (degassed)) and oxidation (reagent O_2 (in air)).

2.3 Rhodium Coordination

The chelation of the iminophosphanes toward rhodium was explored next. Recently, we found that ligands bulkier than **3a-f** give P-monodentate complexes with Au^{I}, bidentate complexes with Ir^{III}, and both κ^1 and κ^2 complexes with Rh^{III}, of which only bidentate complexes were isolable as the major products.[17b] We wondered whether we could make monodentate Rh complexes the prevalent product, which is of interest for cooperative Rh(III) catalysis,[10,11,13d,24] without relying on steric effects.[25] We also wondered how silver triflate, commonly added in excess in Rh^{III} catalysis,[24b,c] plays a role beyond the formation of bidentate complexes by single Cl abstraction. To address these issues, we focus on the chelation of **3a,c,e**.

Treating *E*-/*Z*-3a in DCM with 1/2 equiv of $[RhCp^*Cl_2]_2$ at room temperature yielded two products in a 96:4 ratio (Scheme 3). The major product ($\delta(^{31}P)$ 34.5 ppm; $^1J_{P,Rh}$ = 145.7 Hz), isolated as an orange solid (89%), is assigned to the *E* isomer of monodentate Rh complex **4a**, in analogy to reported in situ Rh complexes.[17c] The minor product ($\delta(^{31}P)$ −5.1 ppm; $^1J_{P,Rh}$ = 113.4 Hz) is likely bidentate complex **5a** because of its similarity in ^{31}P NMR data to related, bulkier Rh complexes.[17c] Crystallization of **4a** by slow diffusion of pentane into a DCM/Et_2O solution provided crystals suitable for an X- ray structure determination. The molecular structure confirms P-monodentate coordination and the *E* conformation for the imine group (Figure 4), thereby illustrating the ease of *Z* to *E* isomerization of the ligand.[17c] The N1−C1 bond length of 1.2738(17) Å is typical for a C=N bond and the 1.8659(13) Å long P1−C1 bond is normal for a P−alkyl single bond; the Rh1−P1−C1−N1 torsion angle amounts to −56.15(11)°, with H-bonding interactions between Cp*−CH_3 groups and the N lone pair. The 2.3222(4) Å Rh1−P1 bond

length of **4a** is similar to that of the 2-pyridylphosphanyl Rh(III) κ^1 complexes.[18a-c]

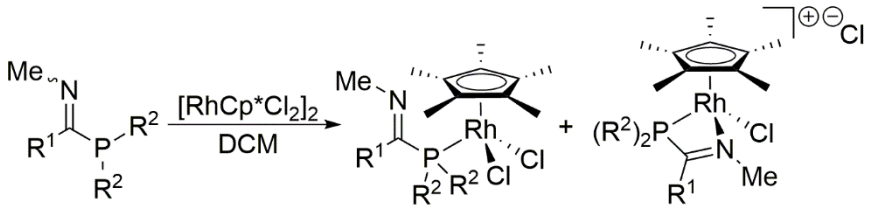

	R^1	R^2	4:5
a	Ph	Ph	96:4
c	4-CF_3-C_6H_4	Ph	100:0
e	Ph	3-CH_3-C_6H_4	94:6

Scheme 3. Synthesis of Mono- and Bidentate Rh(III) Complexes **4** and **5**.

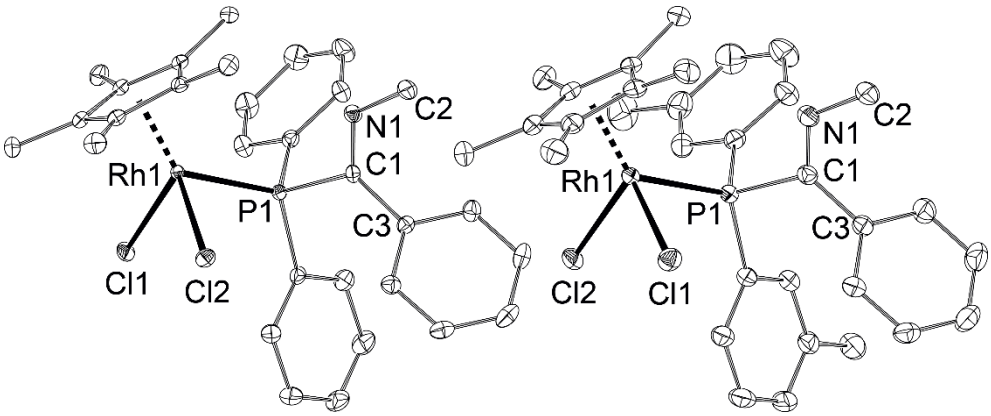

Figure 4. Displacement ellipsoid plots of rhodium complexes **4a** (left) and **4e** (right) at the 50% probability level. Hydrogen atoms and DCM are omitted for clarity. Selected bond lengths (Å) and angles (deg): **4a**, Rh1−P1 = 2.3222(4), Rh1−Cl1 = 2.4056(3), Rh1−Cl2 = 2.4008(4), P1−C1 = 1.8659(13), N1−C1 = 1.2738(17), N1−C2 = 1.4634(17), C1−C3 = 1.4946(17), N1−C1−P1 = 112.72(9), Rh1−P1−C1−N1 = −56.15(11); **4e**, Rh1−P1 = 2.3196(6), Rh1−Cl1 = 2.4013(6), Rh1− Cl2 = 2.4011(6), P1−C1 = 1.870(2), N1−C1 = 1.269(3), N1−C2 = 1.469(3), C1−C3 = 1.493(3), N1−C1−P1 = 113.62(18), Rh1−P1−C1−N1 = −53.92(19).

P-monodentate complexes **4c** ($\delta(^{31}P)$ 35.4 ppm, $^{1}J_{P,Rh}$ = 147.4 Hz) and **4e** ($\delta(^{31}P)$ 34.7 ppm, $^{1}J_{P,Rh}$ = 145.8 Hz) were prepared likewise from **3c,e** and isolated in 69% and 92% yields, respectively (Scheme 3). The molecular structure of **4e**, obtained by a single-crystal X-ray structure determination, reveals structural parameters with bond lengths Rh1–P1 = 2.3196(6) Å, N1–C1 = 1.269(3) Å, and P1–C1 = 1.870(2) Å and a −53.92(19)° Rh1–P1–C1–N1 torsion angle that are comparable to those of **4a** (Figure 4). ^{31}P NMR analysis of the two reactions showed only in the case of **3e** formation of a byproduct (6%) that is assigned to P,N bidentate complex **5e** ($\delta(^{31}P)$ −12.1 ppm, $^{1}J_{P,Rh}$ = 114.7 Hz).

The reproducible ratios of complexes **4**:**5** indicate that the small extent or absence of observed bidentate complexes depends to a degree on the aromatic substituent. In comparison to the *C*- and *P*- phenyl groups, the *m*-tolyl substituent at carbon (**e**) enhances bidentate formation slightly (from 4 to 6%), while the *p*-CF_3- phenyl group at phosphorus (**c**) blocks it (Scheme 3). This trend concurs with the N-donor strength calculated at ωB97X-D/6-31+G(d,p) (Def2-TZVP for Rh) from the energy required to transform cationic complex **5** from a κ^1 to a κ^2 arrangement (Scheme 4);[17b,23] a comparison between neutral **4** and ionic $\mathbf{5}^+$ is not feasible. The Rh–N bond strengths of **5a,c,e** amount to −14.7, −13.4, and −15.2 kcal mol^{-1}, respectively, with corresponding N lone pair orbital energies of −11.2, −11.4, and −11.0 eV. These data support the notion that the selective formation of only P-chelated complexes of 1,3-P,N ligands can be controlled by changing the N-donor strength.

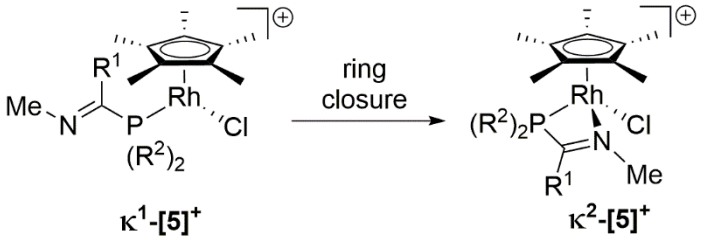

κ^1-[5]$^+$ κ^2-[5]$^+$

	R^1	R^2	$\Delta E_{(ring\ closure)}$ [kcal mol^{-1}]	$\Delta E_{(N\text{-}LP)}$ [eV]
a	Ph	Ph	-14.7	-11.2
c	4-CF_3-C_6H_4	Ph	-13.4	-11.4
e	Ph	3-CH_3-C_6H_4	-15.2	-11.0

Scheme 4. DFT Analysis of the N-Donor Capacity of **3a,c,e**.

Of course, the 1,3-P,N ligands can also undergo clean chelation with rhodium as shown before, but under more forcing conditions. For example, treating **4** with 1 equiv of silver triflate yielded bidentate complex **6** quantitatively (Scheme 5). These ionic complexes, containing a triflate counteranion instead of a chloride anion as in **5**, were isolated as bright orange solids and identified by their ^{31}P NMR characteristics (**6a**, −9.1 ppm, $^1J_{P,Rh}$ = 113.4 Hz; **6c**, −5.0 ppm, $^1J_{P,Rh}$ = 115.0 Hz; **6e**, −8.6 ppm, $^1J_{P,Rh}$ = 113.4 Hz). When **4a** was treated with an excess of 4 equiv of AgOTf,[24b,c] a yellow solid resulted (**7a**, 80%) having a ^{31}P NMR chemical shift (−9.9 ppm; $^1J_{P,Rh}$ = 111.8 Hz) which differs from that of **6a** (Scheme 5). Single-crystal X-ray structure determinations confirm the bidentate nature of both complexes (Figure 5) and reveal that the excess of AgOTf caused the exchange of rhodium's coordinated chloride for an OTf group, without affecting the P,N ligand.

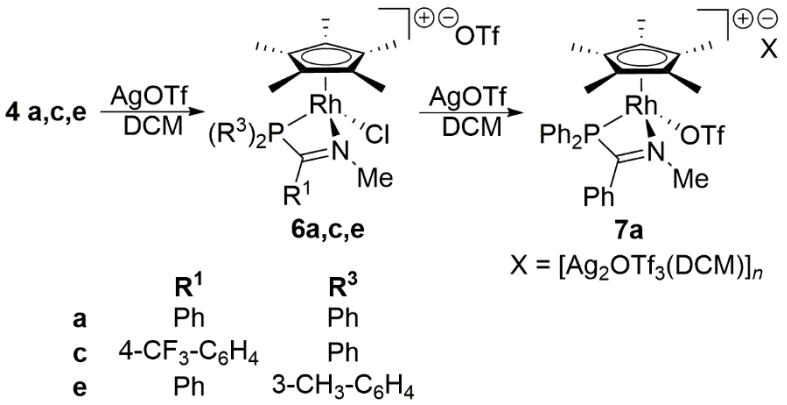

Scheme 5. Bidentate Coordination of **3** to Rh^{III}.

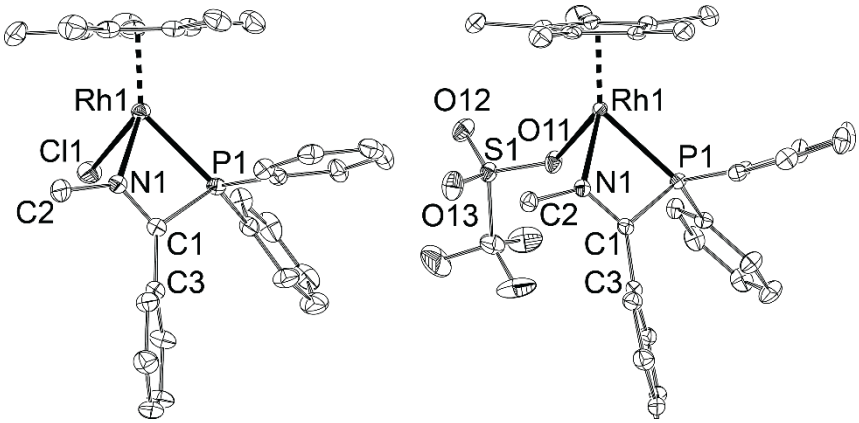

Figure 5. Displacement ellipsoid plots of cationic rhodium complexes **6a** (left) at the 30% probability level and **7a** (right) at the 50% probability level. Hydrogen atoms and counterions (triflate and $[Ag_2OTf_3(DCM)]_n^-$, respectively) are omitted for clarity. Selected bond lengths (Å) and angles (deg): for **6a**, Rh1−P1 = 2.3123(14), Rh1−N1 = 2.106(4), Rh1−Cl1 = 2.3728(13), P1−C1 = 1.842(5), N1−C1 = 1.274(7), N1−C2 = 1.466(7), C1−C3 = 1.461(7), N1−Rh1−P1 = 66.27(12), N1−C1−P1 = 100.4(4); **7a**, Rh1−P1 = 2.3328(7), Rh1−N1 = 2.126(2), Rh1−O11 = 2.1957(18), P1−C1 = 1.844(3), N1−C1 = 1.294(3), N1−C2 = 1.466(3), C1−C3 = 1.471(4), S1−O11 = 1.4711(19), S1−O12 = 1.433(2), S1−O13 = 1.429(2), N1−Rh1−P1 = 67.02(6), N1−C1−P1 = 102.29(18).

The molecular structure of **6a** shows Rh1−P1, Rh1−N1, and Rh1−Cl1 bond lengths of respectively 2.3123(14), 2.106(4), and 2.3728(13) Å and an acute N1−C1−P1 bond angle of 100.4(4)°. The structural features of

7a resemble those of **6a** and other bidentate 1,3-P,N Rh^{III} complexes,[17,18a,b,d] except for its triflate group with an Rh1−O11 bond length of 2.1957(18) Å that is similar to those reported for monodentate Rh^{III}−triflate bonds.[26] Expectedly, the S1−O11 bond is elongated with respect to the S1−O12 and S1−O13 bonds: i.e., 1.4711(19), 1.433(2), and 1.429(2) Å, respectively.

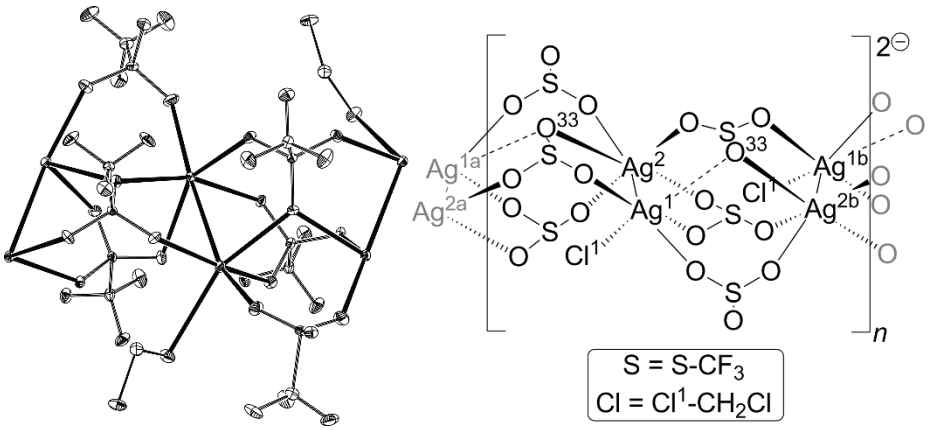

Figure 6. Displacement ellipsoid plot of a dimeric unit of the $[Ag_2OTf_3(DCM)]_n$ counterion of **7a** at the 20% probability level (left) and its simplified numbering scheme (right). Hydrogen atoms and minor disordered part of the solvent DCM are omitted for clarity. Selected bond lengths (Å) and angles (deg): Ag1−Ag2 = 3.0410(3), Ag1- - -Ag2b = 4.0607(3), Ag1- - -Ag2a = 5.9371(3), Ag1−O = 2.345(2)-2.394(2); Ag2−O = 2.321(2)-2.509(2), Ag1- - -O33 = 2.621(2), Ag1−Cl1 = 2.9042(9), Ag1−Ag2−Ag1a = 113.71(1), Ag2−Ag1−Ag2b = 102.17(1), Ag2−Ag1−Ag2b−Ag1b = 6.86(2).

The counterion of **7a** is a coordination polymer of silver triflate (Figure 6). Whereas aggregates of Ag^I sulfonates are known,[27] the present structure is, to the best of our knowledge, the first of its kind in an organometallic complex. The molecular structure shows a linear chain with alternating C_s-symmetric dinuclear Ag^I units (Ag1−Ag2 = 3.0410(3) Å) that are bridged by triflate anions. Each Ag atom has a distorted octahedral geometry with bi-, tri-, and tetradentate coordinating triflate groups labeled as 2, 3, and 4 in Figure 6 (right); the Ag−O bond distances

range from 2.321(2) to 2.509(2) Å.[27] The weak coordination of DCM (Ag1−Cl1 = 2.9042(9) Å) completes the octahedral coordination sphere of Ag1.[28]

2.4 Application in Catalytic Nitrile Hydration

Having established simple synthetic protocols for highly stable iminophosphanes and having demonstrated their ability to function as P monodentate and P,N bidentate ligands, we set out to explore their potential as hydration catalysts for nitriles. This reaction was chosen to compare iminophosphanes to the $PyPPh_2$ ligand for the role of the hard nitrogen donor site to activate water, as is illustrated in Figure 7.[10a,11a,h] We opted for ruthenium catalysts,[29] which are extensively used in homogeneous catalysis[30] and are more robust than those based on rhodium (for comparison and completeness also included in our tests), while their chemistry is comparable. This choice is corroborated by the elevated temperatures needed.

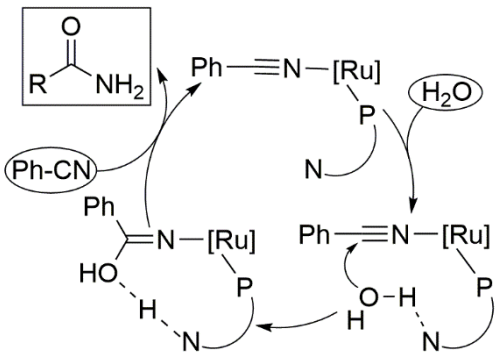

Figure 7. Ru-catalyzed, P,N-assisted hydration of benzonitrile.

To identify a suitable Ru source for benchmarking iminophosphane **3a** against $PyPPh_2$ in the hydration of benzonitrile, we conducted the catalytic reactions in 1,2-dimethoxyethane, in water, and in the absence of a solvent. Table 1 gives the precatalyst, ligand, solvent, and the yield

of benzamide. For the reactions in DME, the procedure of Takai, Oshiki, and co-workers[11h] was followed by premixing 5 mol % of the Ru precursor complex and **3a** for 30 min, upon which the catalyzed hydration of benzonitrile was executed in a closed vessel at 180 °C for 3 h; 2 equiv of water was used to remain consistent with the reported protocol. The results show that precatalyst $[Ru(p\text{-cymene})Cl_2]_2$ (entries 1 and 2) gives better results than $[Ru(C_6Me_6)Cl_2]_2$ (entry 5) and $[Ru(C_6H_5Me)Cl_2]_2$ (entry 6), but even these give reasonable conversions.

Table 1. RuII-catalyzed hydration of benzonitrile.

Entry	Precatalyst (M)	Ligand (L)	Solvent	T [°C]	t [h]	Yield[a] [%]
1[b]	$[Ru(p\text{-cym})Cl_2]_2$	**3a**	DME	180	3	87
2[b]	$[Ru(p\text{-cym})Cl_2]_2$	**3a**[c]	DME	180	3	96
3[b]	$[Ru(p\text{-cym})(Cl)(OTf)]_2$[d]	**3a**[d]	DME	180	3	3
4[b]	$[Ru(p\text{-cym})Cl_2]_2$	Ph_2PPy	DME	180	3	3[11][h]
5[b]	$[Ru(C_6Me_6)Cl_2]_2$	**3a**	DME	180	3	55
6[b]	$[Ru(C_6H_5Me)Cl_2]_2$	**3a**	DME	180	3	84
7[b]	$[RhCp^*Cl_2]_2$	**3a**	DME	180	3	22
8[e]	$[Ru(p\text{-cym})Cl_2]_2$	**3a**	H_2O	100	24	94
9[e]	$[Ru(p\text{-cym})Cl_2]_2$	Ph_2PPy	H_2O	100	24	57[11][a]
10[f]	$[Ru(p\text{-cym})Cl_2]_2$	**3a**	none	180	3	78
11[f]	$[Ru(p\text{-cym})Cl_2]_2$	Ph_2PPy	none	180	3	6
12[f]	$[Ru(p\text{-cym})Cl_2]_2$	None	none	180	3	6

[a] Determined by GC. [b] Ph-C≡N (1 mmol), H_2O (2 mmol), 5 mol% ([M]L); DME (0.5 ml). [c] 2 equiv. [d]Prepared *in situ* from $[Ru(p\text{-cym})Cl_2]_2$ and AgOTf. [e] Ph-C≡N (1 mmol), 5 mol% ([M]L); H_2O (3.0 ml). [f] Ph-C≡N (3.6 mmol), H_2O (7.2 mmol), 1.4 mol% ([M]L).

The presence of 1 equiv. of AgOTf hindered the reaction (Table 1, entry 3), presumably through the formation of inactive bidentate species. Remarkable is the observation that the catalytic hydration using **3a** gave an excellent yield of 87% (entry 1), while the same process with the $PyPPh_2$ ligand performed very poorly with a product yield of a mere

3%[11h] (entry 4). Using 2 equiv. of **3a** further enhanced the yield to 96% (entry 2). In addition, rhodium precatalyst $[RhCp^*Cl_2]_2$ was examined under the same conditions. Even this in situ generated catalyst, presumably **4a**, yields benzamide, albeit in only in 22% yield (entry 7), which is a remarkable observation, as no Rh^{III} catalyst has so far been reported to hydrate nitriles.

Next, we explored the protocol of Cadierno et al. by heating benzonitrile and 5 mol % of precatalyst $[Ru(p\text{-cym})Cl_2]_2$ and the 1,3-P,N ligand in boiling water for 24 h using a closed vessel.[11a,31] Also in this case an outstanding yield of 94% was obtained for the catalytic reaction with **3a** (Table 1, entry 8), which is far better than the 57% that resulted with the $PyPPh_2$ ligand (entry 9).[11a] This performance is in line with that with DME as solvent (entries 1 and 4) by also showing that the catalytic reaction with ligand **3a** outperforms that with Ph_2PPy. Finally, we compared the influence of these ligands in the solvent-free hydration of benzonitrile by heating 1.4 mol % of the catalyst in a 1:2 molar mixture of benzonitrile and water at 180 °C for 3 h in a closed vessel. Again, the reaction of $[Ru(p\text{-cym})Cl_2]_2$ and **3a** (78%, entry 10) gave a far better performance than that with the Ph_2PPy ligand (6%, entry 11), which, in fact, seems to have no effect, as 6% was also obtained when no P,N ligand was present (entry 12). It appears that all three Ru-catalyzed approaches for the hydration of benzonitrile underscore the potential of iminophosphanes as ligands. The observed differences in the activity of **3a** and $PyPPh_2$ were attributed to their difference in N-donor strength. [10a]

Finally, we address briefly the influence of the P,C,N substituents of **3** on the yield of the Ru^{II}-catalyzed hydration using solvent-free conditions. The results are given in Table 2. Whereas the iminophosphanes are only

modestly different from each other, some distinctly affected the benzamide yield. As a reference we used **3a**, which has Ph substituents on the P and C centers and a Me group on the N atom. The catalyzed hydration yield of benzonitrile amounted to 78% (Table 2, entry 1). Changing the N substituent from Me to the bulkier *i*-Pr group (**3g**) decreased the yield by only 3% (entry 5). A similar marginal effect (−2%) was observed on introducing a 4-CF_3 substituent on the *C*-phenyl group (**3c**, entry 2). Slightly larger effects were found on introducing 3-CH_3 and 3-CF_3 substituents on the *P*-phenyl groups, causing modest changes in yield of +4% (entry 3) and −8% (entry 4), respectively. These may possibly be attributed to a difference in electron-donating properties, which affect ruthenium's Lewis acidity via the Ru−P bond.[14d] All of this leads to the observation that the iminophosphanes **3** are all effective ligands enabling the solvent-free Ru^{II}-catalyzed hydration of benzonitrile and that these 1,3-P,N ligands can be modified at the P, C, and N centers to affect the hydration to different degrees.

Table 2. Solvent-Free [(3)Ru(*p*-cym)Cl_2]-Catalyzed Hydration of Benzonitrile[a].

Entry	Ligand (L)	Solvent	T [°C]	t [h]	Yield[b] [%]
1	**3a**	None	180	3	78
2	**3c**	None	180	3	76
3	**3d**	None	180	3	82
4	**3e**	None	180	3	70
5	**3g**	None	180	3	75

[a] Ph-C≡N (3.6 mmol), H_2O (7.2 mmol), 1.4 mol% ([Ru(p-cym)Cl_2]L). [b] Determined by GC.

3 Conclusion

This study shows iminophosphanes to be readily synthesized by simple alkylation of nitriles and reaction of the resulting nitrilium ions with a secondary phosphane. They are very stable in water but do show some sensitivity to oxidation in air. The 1,3-P,N ligands are tunable by

substitution at their P, C, and N centers. Their coordination behavior was explored for rhodium(III) complexes, using $[RhCp^*Cl_2]_2$ as precursor. Both P-monodentate and 1,3-P,N bidentate ligands can be obtained in high yield. Silver triflate is needed to enforce the formation of the κ^2 chelates, and when an excess is used, also the second chloride is exchanged. Several X-ray crystal structures of rhodium complexes are reported, including one with a polymeric aggregate of Ag^I sulfonate with embedded DCM solvent molecules. The ligands were found to be effective in the Ru^{II}-catalyzed hydration of benzonitrile, be it in an organic solvent, in water, or under solvent-free conditions. Its performance appears to be better than that of 2-pyridyldiphenylphosphane, with yields of up to 96% on using the commercial $[Ru(p\text{-cym})Cl_2]_2$ as precatalyst. Modifying the substitution pattern of the iminophosphanes affects the yield of the ruthenium-catalyzed hydration of benzonitrile as well as the coordination to the rhodium complex. Clearly, more extensive studies have to be performed for more catalytic processes, but the easily synthesized iminophosphanes seem to have great prospects as new 1,3-P,N ligands.

4 Experimental Section

4.1 Preparation of Compounds

All experiments were performed under an atmosphere of dry nitrogen using standard Schlenk-line and glovebox techniques, unless stated otherwise. Solvents were distilled under nitrogen over the appropriate drying agent; $CaCl_2$ (DCM), benzophenone/NaK (Et_2O, THF, triethylamine), Na (toluene), $LiAlH_4$ (pentane), P_2O_5 (CD_2Cl_2, $CDCl_3$). C_6D_6 was dried over Na at RT. H_2O was degassed ultrasonically *in vacuo*. Silver salts were handled with minimum light exposure. Diphenylphosphane was purchased from Sigma-Aldrich and tri(3-methylphenyl)phosphane and di(4-methylphenyl)chlorophosphane from STREM Chemicals Inc. Di(3-trifluoromethylphenyl)chlorophosphane was provided by Arkema B.V. Known compounds **2a**,[22b] di(3-trifluoromethylphenyl)phosphane, di(3-methylphenyl)-phosphane and di(4-methylphenyl)phosphane are reported here since their syntheses were revised and/or new analytical data was obtained. All phosphanes and chlorophosphanes were distilled under reduced pressure before use. Solids were predried *in vacuo* for at least 30

minutes. All other reagents were used as received. NMR spectra were recorded on a Bruker Avance 250 (^{1}H: 250.13 MHz, ^{19}F: 235.36 MHz, ^{31}P: 101.25 MHz, room temperature), a Bruker Avance 400 (^{1}H: 400.13 MHz, ^{13}C{^{1}H}: 100.61 MHz, ^{31}P: 161.98 MHz, room temperature) or a Bruker Avance 500 (^{1}H: 500.23 MHz, ^{13}C{^{1}H}: 125.78 MHz; room temperature). ^{1}H-spectra and ^{13}C{^{1}H}-spectra were internally referenced to residual solvent resonances ($CDCl_3$: $\delta^{1}H = 7.26$, $\delta^{13}C\{^{1}H\} = 77.16$; CD_2Cl_2: $\delta^{1}H = 5.32$, $\delta^{13}C\{^{1}H\} = 53.84$; C_6D_6: $\delta^{1}H = 7.16$, $\delta^{13}C\{^{1}H\} = 128.06$) and ^{31}P-spectra were references externally to H_3PO_4. Melting points were measured using a Büchi Melting Point apparatus M-565 (sealed capillaries) and are uncorrected. High resolution electrospray ionization (ESI) mass spectrometry was carried out with a Bruker micrOTOF-Q instrument in positive ion mode (capillary potential of 4500 V). Infrared spectra were recorded on a Shimadzu FT-IR 8400S spectrophotometer.

(N-methyl)(aryl)carbonitrilium trifluoromethyl sulfonates (2a-c).[22b] *Protocol 1:* MeOTf (1.0 eq.) was added dropwise to a solution of arylnitrile (1.0 eq.) in toluene (0.27 mL/mmol arylnitrile). After stirring 18 h at RT, a microcrystalline solid had precipitated. Volatiles were removed *in vacuo*, and after washing with pentane (2 x 0.4 mL/mmol), **2** was obtained as an off-white solid (**2a**: 62%; **2b**: 62%; **2c**: 14%). *Protocol 2:* MeOTf (1.0 eq.) was added dropwise to the arylnitrile (1.2 eq.). The colorless solution was stirred for 18 h (**2a**: RT; **2c**: 45 °C). The resulting white/yellow crystalline solid was washed with pentane (3 x 0.2 mL/mmol) and dried *in vacuo* to provide **2** as a white solid (**2a**: 86%; **2c**: 69%). *Crystallization:* Slow 1:1 diffusion of ether (alternatively pentane) into a saturated DCM solution at 5 °C provides **2** as white crystals. **2a**: Mp: 78.9–79.9 °C. ^{1}H NMR (500.23 MHz, $CDCl_3$): δ 8.31 (d, $^{3}J_{H,H}$ = 8.0 Hz, 2H; *o*-Ph*H*), 7.92 (t, $^{3}J_{H,H}$ = 7.8 Hz, 1H; *p*-Ph*H*), 7.65 (t, $^{3}J_{H,H}$ = 8.0 Hz, 2H; *m*-Ph*H*), 4.20 (s, 3H; NCH_3). ^{13}C{^{1}H} NMR (125.78 MHz, $CDCl_3$): δ 138.6 (s; *p*-Ph*C*), 136.2 (s; *m*-Ph*C*), 130.1 (s; *o*-Ph*C*), 120.9 (q, $^{1}J_{C,F}$ = 319.5 Hz; O_3SCF_3), 106.8 (tm, $^{1}J_{C,14N}$ = 47.2 Hz; *C*N), 103.0 (s; *ipso*-Ph*C*), 32.6 (s; N*C*H$_3$). ^{19}F{^{1}H} NMR (235.36 MHz, $CDCl_3$): δ –78.3 (s; O_3SCF_3). FT-IR: ν = 3277 (w), 3248 (w), 3186 (w), 3026 (w), 2957 (w), 2457 (w), 2366 (s), 1680 (m), 1583 (m), 1528 (m), 1489 (w), 1448 (m), 1402 (m), 1371 (m), 1261 (s), 1223 (s), 1180 (s), 1148 (s), 1024 (s), 987 (s), 943 (m), 843 (w), 762 (s), 704 (s), 679 (s), 633 (s), 573 (s), 538 (s), 515 (s), 484 (w), 467 (m), 426 (w), 413 (w). MS (ESI-Q-TOF): calcd. for C_8H_8N: 118.0651; found: 118.0657. **2b**: Mp: 117.0 °C ≤ decomp; 135.1–135.8 °C. ^{1}H NMR (500.23 MHz, $CDCl_3$): δ 8.18 (d, $^{3}J_{H,H}$ = 8.0 Hz, 2H; *o*-Ar*H*), 7.45 (d, $^{3}J_{H,H}$ = 8.0 Hz, 2H; *m*-Ar*H*), 4.18 (s, 3H; NCH_3), 2.51 (s, 3H; $C_6H_4CH_3$). ^{13}C{^{1}H} NMR (125.78 MHz, $CDCl_3$): δ 151.3 (s; *p*-Ar*C*), 136.1 (s; *o*-Ar*C*), 131.1 (s; *m*-Ar*C*), 120.9 (q, $^{1}J_{C,F}$ = 319.5 Hz; O_3SCF_3), 107.7 (tm, $^{1}J_{C,14N}$ = 50.9 Hz; *C*N), 99.4 (s; *ipso*-Ar*C*), 32.5 (s; NCH_3), 22.9 (s; $C_6H_4CH_3$). ^{19}F NMR (235.36 MHz, $CDCl_3$): δ –78.4 (s, O_3SCF_3). FT-IR: ν = 3051

(w), 2959 (w), 2473 (w), 2424 (w), 2368 (s), 2328 (w), 1670 (w), 1605 (s), 1506 (w), 1418 (m), 1389 (m), 1258 (s), 1225 (s), 1192 (s), 1148 (s), 1128 (s), 1028 (s), 974 (w), 943 (s), 824 (s), 791 (m), 756 (s), 739 (m), 702 (w), 635 (s), 573 (s), 540 (s), 517 (s), 488 (w), 447 (m), 438 (m), 409 (w). MS (ESI-Q-TOF): calcd. for $C_9H_{10}N$: 132.0808; found: 132.0811. **2c:** Mp: 106.9–108.0 °C. ^{1}H NMR (500.23 MHz, $CDCl_3$): δ 8.50 (d, $^3J_{H,H}$ = 8.3 Hz, 2H; *o*-Ar*H*), 7.90 (d, $^3J_{H,H}$ = 8.3 Hz, 2H; *m*-Ar*H*), 4.26 (s, 3H; NC*H*$_3$). ^{13}C{^{1}H} NMR (125.78 MHz, $CDCl_3$): δ 162.5 (d, $^2J_{C,F}$ = 13.8 Hz; *p*-Ar*C*), 139.4 (q, $^1J_{C,F}$ = 34.0 Hz; $C_6H_4CF_3$), 137.1 (s; *o*-Ar*C*), 127.0 (s; *m*-Ar*C*), 122.4 (q, $^1J_{C,F}$ = 274.2 Hz; O_3SCF_3), 107.4 (s; *ipso*-Ar*C*), 105.2 (tm, $^1J_{C,14N}$ = 50.0 Hz; *C*N), 32.9 (s; N*C*H$_3$). ^{19}F NMR (235.36 MHz, $CDCl_3$): δ –64.5 (s; $C_6H_4CF_3$), –78.7 (s; O_3SCF_3). FT-IR: v = 3117 (w), 3067 (w), 3036 (w), 2957 (w), 2366 (s), 1688 (w), 1508 (w), 1412 (m), 1389 (w), 1319 (s), 1252 (s), 1225 (s), 1165 (s), 1130 (s), 1113 (s), 1067 (s), 1030 (s), 1018 (s), 928 (w), 847 (s), 756 (s), 733 (w), 706 (s), 683 (w), 636 (s), 596 (s), 573 (s), 536 (s), 517 (s), 469 (m), 449 (m), 432 (m). MS (ESI-Q-TOF): calcd. for $C_9F_3H_7N$: 186.0525; found: 186.0533.

Di(3-trifluoromethylphenyl)phosphane.[35] A solution of freshly distilled di(3-trifluoromethyl-phenyl)chlorophosphane (5.88 g, 16.50 mmol, 1.00 eq.) in 30 mL Et_2O was added dropwise at –78 °C to a suspension of $LiAlH_4$ (0.25 g, 6.59 mmol, 0.40 eq.) in 50 mL Et_2O, during which gas evolved from the mixture. After addition, the grey suspension was allowed to warm to RT. After stirring for 1.5 h, the mixture was cooled to 0 °C and H_2O (0.95 mL, 52.63 mmol, 3.19 eq.) was added dropwise. After stirring for 0.5 h at RT, volatiles were removed *in vacuo* and the resulting grey/white suspension was extracted into 3 x 10mL pentane. The combined extracts were evaporated to provide di(3-trifluoromethyl-phenyl)phosphane as a colorless liquid (4.94 g, 15.33 mmol, 93%). ^{1}H NMR (500.23 MHz, C_6D_6): δ 7.61 (d, $^3J_{H,P}$ = 6.9 Hz, 2H; PC-C*H*-CCF$_3$), 7.17 (d, $^3J_{H,H}$ = 6.3 Hz, 2H; *p*-Ar*H*), 7.05 (t, $^3J_{H,H}$ = 6.9 Hz, 2H; PC-C*H*-CH), 6.71 (t, $^3J_{H,H}$ = 7.7 Hz, 2H; *m*-Ar*H*), 4.81 (d, $^1J_{H,P}$ = 219.7 Hz, 1H; P*H*). ^{13}C{^{1}H} NMR (125.78 MHz, C_6D_6): δ 137.2 (d, $^2J_{C,P}$ = 17.3 Hz; PC-C*H*-CH), 135.9 (d, $^1J_{C,P}$ = 13.6 Hz; *ipso*-Ar*C*), 131.2 (qd, $^2J_{C,F}$ = 32.7 Hz, $^3J_{C,P}$ = 6.4 Hz; PC-CH-*C*CF$_3$), 130.5 (dq, $^2J_{C,P}$ = 18.2 Hz, $^3J_{C,F}$ = 4.5 Hz; PC-*C*H-CCF$_3$), 129.3 (d, $^3J_{C,P}$ = 5.5 Hz; *m*-Ar*C*), 125.7 (q, $^3J_{C,F}$ = 3.6 Hz; *p*-Ar*C*), 124.6 (q, $^1J_{C,F}$ = 272.5 Hz; *C*F$_3$). ^{19}F NMR (235.36 MHz, C_6D_6): δ –63.3 (s; $C_6H_4CF_3$). ^{31}P NMR (161.98 MHz, C_6D_6): δ –41.1 (dq, $^1J_{P,H}$ = 218.3 Hz, $^3J_{P,H}$ = 6.7 Hz).

Di(3-methylphenyl)phosphane.[36] A colorless solution of tri(3-methylphenyl)phosphane (4.18 g, 13.73 mmol, 1.00 eq.) in 30 mL THF was prepared in a separate vessel and added dropwise at 0 °C to an excess of finely cut Li (0.21 g 30.23 mmol, 2.20 eq.) suspended in 5 mL THF. Afterwards, the vessel was washed with 2 x 10

mL THF, which was also added to the reaction mixture. After addition, the mixture was allowed to warm RT. After stirring for 26 h at RT, a deep red mixture was obtained, which was decanted to remove excess Li. The resulting solution was cooled to 0 °C and H_2O (1.0 mL, 55.40 mmol, 4.04 eq.) was added dropwise to give a white/grey mixture. After 1 h of stirring at RT, volatiles were removed *in vacuo* to provide a white oil, which was extracted sequentially into 50 mL Et_2O for 24 h and 40 mL Et_2O for 20 h. The combined extracts were evaporated to give a light yellow liquid, which was distilled ($3.2x10^{-2}$ mbar, heated with Bunsen-burner) to provide di(3-methylphenyl)phosphane (1.71 g, 7.99 mmol, 58%) as a colorless liquid. ^{1}H NMR (500.23 MHz, C_6D_6): δ 7.30 (t, $^3J_{H,H}$ = 8.2 Hz, 4H; *o*-Ar*H*), 7.00 (t, $^3J_{H,H}$ = 7.4 Hz, 2H; *m*-Ar*H*), 6.87 (d, $^3J_{H,H}$ = 6.6 Hz, 2H; *p*-Ar*H*), 5.27 (d, $^1J_{H,P}$ = 215.0 Hz, 1H; P*H*), 1.99 (s, 6H; CH_3). ^{13}C{^{1}H} NMR (125.78 MHz, C_6D_6): δ 138.3 (d, $^2J_{C,P}$ = 6.4 Hz; *m*-Ar*C*-CH_3), 135.4 (d, $^1J_{C,P}$ = 10.9 Hz; *ipso*-Ar*C*), 135.0 (d, $^2J_{C,P}$ = 18.2 Hz; *o*-Ar*C*), 131.5 (d, $^2J_{C,P}$ = 16.4 Hz; *o*-Ar*C*), 129.5 (s; *p*-Ar*C*), 128.8 (d, $^3J_{C,P}$ = 6.4 Hz; *m*-Ar*C*), 21.2 (s; *C*H_3). ^{31}P NMR (161.98 MHz, C_6D_6): δ –40.3 (dq, $^1J_{P,H}$ = 215.4 Hz, $^3J_{P,H}$ = 7.9 Hz).

Di(4-methylphenyl)phosphane.[35] A solution of di(4-methylphenyl)chlorophosphane (1.81 mL, 8.01 mmol, 1.00 eq.) in 15 mL Et_2O was added dropwise to a suspension of $LiAlH_4$ (0.094 g 2.48 mmol, 0.31 eq) at –78 °C. After addition, the grey suspension was allowed to warm to RT. After stirring for 1.5h at RT, the mixture was cooled to 0 °C and H_2O (0.15 mL, 8.31 mmol, 1.04 eq.) was added dropwise. After stirring for 1h at RT, the grey-white suspension was filtered onto anhydrous Na_2SO_4 (2.71 g), after which it was filtered again. Volatiles were removed *in vacuo* to provide a white suspension, which was extracted into 20 mL pentane. After evaporation of the extract, the obtained white suspension was distilled (2.3×10^{-2} mbar, 100 °C). Di(4-methylphenyl)phosphane (0.81 g, 3.78 mmol, 47%) was obtained as a colorless liquid. ^{1}H NMR (500.23 MHz, C_6D_6): δ 7.38 (t, $^3J_{H,H}$ = 7.8 Hz, 4H; *o*-Ar*H*), 6.89 (d, $^3J_{H,H}$ = 7.5 Hz, 4H; *m*-Ar*H*), 5.28 (d, $^1J_{H,P}$ = 214.1 Hz, 1H; P*H*), 2.02 (s, 6H; CH_3). ^{13}C{^{1}H} NMR (125.78 MHz, $CDCl_3$): δ 138.4 (s; *p*-Ar*C*), 134.5 (d, $^2J_{C,P}$ = 17.3 Hz; *o*-Ar*C*), 132.2 (d, $^2J_{C,P}$ = 9.1 Hz; *ipso*-Ar*C*), 129.7 (d, $^3J_{C,P}$ = 6.4 Hz; *m*-Ar*C*), 21.1 (s; *C*H_3). ^{31}P NMR (161.98 MHz, C_6D_6): δ –42.6 (dq, $^1J_{P,H}$ = 215.4 Hz, $^3J_{P,H}$ = 3.2 Hz).

((N-methyl)arylimidoyl)diarylphosphanes (3a-f). *Protocol **3a-d**:* Diarylphosphane (1.0 eq.) was added dropwise to a solution of **2a** (1.1 eq.) in DCM (4.0 mL/mmol) at –78 °C to give a bright yellow solution, which was allowed to warm to RT and stirred for 15 min. Triethylamine (1.1 eq.) was added to give a yellow solution, which was stirred for 1 h. Volatiles were removed *in vacuo* to give a yellow oil, which was extracted into Et_2O (3 x 4 mL/mmol). The extract was concentrated to saturation and filtered over neutral alumina.

Evaporation provided **3** as an off-white solid (mixture of E/Z isomers; **3a**: 91%; **3b**: 75%; **3c**: 85%; **3d**: 45%*). **Crystallization:* a saturated Et_2O solution was cooled to –80 °C. *Protocol **3e-f**:* Diarylphosphane (1.0 eq.) was added dropwise to a solution of **2a** (1.1 eq.) in DCM (4.0 mL/mmol) at –78 °C to give a bright yellow solution, which was allowed to warm to RT and stirred for 15 min. Triethylamine (1.1 eq.) was added to give a yellow solution, which was stirred for 1 h. Volatiles were removed *in vacuo* to provide a yellow oil, which was extracted into Et_2O overnight (3 x 4 mL/mmol). The extract was concentrated to saturation and filtered over neutral alumina. Evaporation provided an off-white solid, which was extracted into pentane (5 mL/mmol). Evaporation of the extract provided **3e-f** (**3e**: 77%*; **3f**: 53%).**Crystallization:* a saturated pentane solution was cooled to –80 °C. **3a:** Mp: 79.0–79.4 °C. *Since not all ^{1}H- and ^{13}C NMR resonances of the E-**3a** and Z-**3a** can be distinguished, one set of signals is reported (integrals normalized separately for each isomer).* ^{1}H NMR (500.23 MHz, $CDCl_3$): δ 7.45–7.38 (m, 4H; P-Ar*H* (E)), 7.32–7.21 (m, 6H; P-Ar*H* (E) and 10H; Ar*H* (Z)), 7.21–7.13 (m, 3H; C-*m,p*-Ar*H* (E)), 7.09–7.03 (m, 1H; Ar*H* (Z)), 7.03–6.99 (m, 4H; C-Ar*H* (Z)), 6.95 (d, $^3J_{H,H}$ = 6.6 Hz, 2H; C-*o*-Ar*H* (E)), 3.57 (s, 3H; CN-C*H*$_3$ (Z)), 3.25 (d, $^4J_{H,P}$ = 0.9 Hz, 3H; CN-C*H*$_3$ (E)). ^{13}C{^{1}H} NMR (125.78 MHz, $CDCl_3$): δ 179.2 (d, $^1J_{C,P}$ = 8.2 Hz; *C*N-CH_3 (E)), 176.7 (d, $^1J_{C,P}$ = 42.7 Hz; *C*N-CH_3 (Z)), 141.4 (d, $^2J_{C,P}$ = 7.3 Hz, C-*ipso*-Ar*C* (Z)), 137.6 (d, $^2J_{C,P}$ = 24.5 Hz; C-*ipso*-Ar*C* (E)), 134.7 (d, $J_{C,P}$ = 19.1 Hz, P-Ar*C* (E)), 134.6 (d, $^1J_{C,P}$ = 10.0 Hz; P-*ipso*-Ar*C* (Z)), 133.9 (d, $J_{C,P}$ = 20.0 Hz; P-Ar*C* (Z)), 133.9 (s; P-*ipso*-Ar*C* (E)), 129.1 (s; P-Ar*C* (Z)), 129.0 (s; P-Ar*C* (E)), 128.8 (s; P-Ar*C* (Z)), 128.7 (d, $J_{C,P}$ = 7.3 Hz; C-Ar*C* (E)), 128.5 (d, $J_{C,P}$ = 20.9 Hz; P-Ar*C* (E)), 128.3 (d, $^5J_{C,P}$ = 7.3 Hz; C-Ar*C* (Z), 128.2 (s; C-Ar*C* (E)), 128.0 (d, $^4J_{C,P}$ = 20.0 Hz; C-Ar*C* (Z)), 127.6 (d, $^3J_{C,P}$ = 5.4 Hz; C-Ar*C* (Z)), 127.0 (d, $^3J_{C,P}$ = 3.6 Hz; C-*o*-Ar*C* (E)), 43.9 (d, $^3J_{C,P}$ = 33.6 Hz; CN-*C*H$_3$ (Z)), 43.2 (d, $^3J_{C,P}$ = 8.2 Hz; CN-*C*H$_3$ (E)). ^{31}P NMR (161.98 MHz, $CDCl_3$): δ 7.8 (t, $^3J_{P,H}$ = 7.9 Hz; E-isomer, 71%); –7.6 (t, $^3J_{P,H}$ = 7.9 Hz; Z-isomer, 29%). FT-IR: v = 3069 (m), 2901 (m), 2849 (w), 2746 (w), 1599 (s), 1572 (w), 1518 (w), 1479 (s), 1433 (s), 1383 (m), 1367 (w), 1277 (m), 1261 (m), 1242 (m), 1202 (m), 1155 (m), 1090 (m), 1067 (m), 1028 (s), 974 (m), 939 (m), 903 (m), 862 (m), 839 (m), 808 (m), 758 (s), 737 (s), 692 (s), 640 (s), 609 (s), 573 (s), 548 (m), 507 (s), 474 (s), 449 (s), 426 (s). HR-MS (ESI-Q-TOF): calcd. for $C_{20}H_{19}NP$: 304.1250; found: 304.1245. **3b:** Mp: 44.0–46.1 °C. *Since not all ^{1}H- and ^{13}C NMR resonances of the E-**3b** and Z-**3b** can be distinguished, one set of signals is reported (integrals normalized separately for each isomer).* ^{1}H NMR (500.23 MHz, $CDCl_3$): δ 7.46–7.39 (m, 6H; P-Ar*H* (E), P-Ar*H* (Z)), 7.32–7.23 (m, 14H; P-Ar*H* (E), P-Ar*H* (Z)), 7.02 (d, $^3J_{H,H}$ = 7.9 Hz, 2H; C-*o*-Ar*H* (E)), 6.95 (d, $^3J_{H,H}$ = 8.2 Hz, 2H; C-*o*-Ar*H* (Z)), 6.89 (d, $^3J_{H,H}$ = 7.9 Hz, 2H; C-*m*-Ar*H* (E)), 6.84 (d, $^3J_{H,H}$ = 7.9 Hz, 2H; C-*m*-Ar*H* (Z)), 3.56 (s, 3H; CN-C*H*$_3$ (Z), 3.26 (d, $^4J_{H,P}$ = 1.9 Hz, 3H; CN-C*H*$_3$ (E)), 2.26 (s, 3H; C-Ar-C*H*$_3$ (E)), 2.20 (s, 3H; C-Ar-C*H*$_3$ (Z)). ^{13}C{^{1}H} NMR (125.78 MHz, $CDCl_3$): δ 179.1 (d,

$^{1}J_{C,P}$ = 8.2 Hz; *C*N-CH$_3$ (E)), 139.4 (s; C-*ipso*-Ar*C* (Z)), 138.0 (s; C-*ipso*-Ar*C* (E)), 134.8 (d, $J_{C,P}$ = 20.0 Hz; P-Ar*C* (E)), 134.8 (s; P-*ipso*-Ar*C* (Z)), 134.6 (d, $^{1}J_{C,P}$ = 10.9 Hz; P-*ipso*-Ar*C* (E)), 133.9 (d, $J_{C,P}$ = 19.1 Hz; P-Ar*C* (Z)), 129.0 (s; P-Ar*C* (E)), 129.0 (s; P-Ar*C* (Z)), 128.9 (s; P-Ar*C*), 128.8 (d, $J_{C,P}$ = 7.3 Hz; P-Ar*C*), 128.3 (d, $^{4}J_{C,P}$ = 10.3 Hz; C-*m*-Ar*C* (Z)), 127.8 (s; C-*o*-Ar*C* (Z)), 127.1 (d, $^{4}J_{C,P}$ = 4.1 Hz; C-*m*-Ar*C* (E)), 43.6 (d, $^{3}J_{C,P}$ = 36.3 Hz; CN-*C*H$_3$ (Z)), 43.2 (d, $^{3}J_{C,P}$ = 9.1 Hz; CN-*C*H$_3$ (E)), 21.4 (s; C-Ar-*C*H$_3$ (E)), 21.3 (s; C-Ar-*C*H$_3$ (Z)). ^{31}P NMR (161.98 MHz, CDCl$_3$): δ 7.6 (s; E-isomer, 83%), –8.0 (s; Z-isomer, 17%). FT-IR: ν = 3072 (m), 3001 (m), 2943 (m), 2907 (m), 2853 (m), 2756 (m), 1601 (s), 1570 (m), 1506 (s), 1481 (s), 1433 (s), 1404 (m), 1391 (s), 1375 (m), 1310 (m), 1261 (m), 1217 (m), 1182 (s), 1157 (m), 1111 (s), 1095 (s), 1065 (s), 1028 (s), 970 (s), 951 (s), 920 (s), 845 (m), 812 (s), 791 (s), 733 (s), 690 (s), 665 (s), 635 (s), 619 (s), 525 (s), 484 (s), 453 (s), 440 (s), 411 (s). HR-MS (ESI-Q-TOF): calcd. for $C_{21}H_{21}NP$: 318.1406; found: 318.1404. **3c:** Mp: 46.8–47.4 °C. *Since not all ^{1}H- and ^{13}C NMR resonances of the E-**3c** and Z-**3c** can be distinguished, one set of signals is reported (integrals normalized separately for each isomer).* ^{1}H NMR (500.23 MHz, CDCl$_3$): δ 7.47–7.38 (m, 6H; P-Ar*H* (E), P-Ar*H* (Z), C-Ar*H* (E)), 7.33–7.22 (m, 18H; P-Ar*H* (E), P-Ar*H* (Z), C-Ar*H* (Z)), 7.11 (d, $^{3}J_{H,H}$ = 8.2 Hz, 2H; C-Ar*H* (Z)), 7.04 (d, $^{3}J_{H,H}$ = 7.9 Hz, 2H; C-Ar*H* (E)), 3.60 (s; CN-C*H*$_3$ (Z)), 3.24 (d, $^{4}J_{H,P}$ = 1.6 Hz; CN-C*H*$_3$ (E)). ^{13}C{^{1}H} NMR (125.78 MHz, CDCl$_3$): δ 178.0 (d, $^{1}J_{C,P}$ = 9.1 Hz; *C*N-CH$_3$), 144.6 (d, $^{2}J_{C,P}$ = 6.4 Hz; C-*ipso*-Ar*C*), 141.3 (d, $^{2}J_{C,P}$ = 24.5 Hz; C-*ipso*-Ar*C*), 134.7 (d, $J_{C,P}$ = 20.0 Hz, P-Ar*C*), 133.8 (d, $J_{C,P}$ = 19.1 Hz; P-Ar*C*), 133.8 (d, $^{1}J_{C,P}$ = 9.1 Hz; P-*ipso*-Ar*C*), 133.2 (d, $^{1}J_{C,P}$ = 9.1 Hz; P-*ipso*-Ar*C*), 130.2 (q, $^{1}J_{C,F}$ = 31.8 Hz; *C*F$_3$), 129.4 (d, $J_{C,P}$ = 8.2 Hz; P-Ar*C*), 129.0 (d, $J_{C,P}$ = 7.3 Hz; P-Ar*C*), 128.5 (d, $J_{C,P}$ = 7.3 Hz; P-Ar*C*), 128.0 (s; C-Ar*C* (Z)), 127.4 (d, $J_{C,F}$ = 3.6 Hz; C-Ar*C* (E)), 125.2 (q, $J_{C,F}$ = 3.6 Hz; C-Ar*C* (E)), 125.1 (d, $^{2}J_{C,F}$ = 14.5 Hz; C-*p*-Ar*C*), 124.5 (q, $J_{C,F}$ = 7.7 Hz; C-Ar*C* (Z)), 123.0 (d, $^{2}J_{C,F}$ = 14.5 Hz; C-*p*-Ar*C*), 44.1 (d, $^{3}J_{C,P}$ = 32.7 Hz; CN-*C*H$_3$ (Z)), 43.4 (d, $^{3}J_{C,P}$ = 8.2 Hz; CN-*C*H$_3$ (E)). ^{19}F NMR (235.36 MHz, CDCl$_3$): δ –62.7 (s; Z-isomer, 55%), –62.8 (s; E-isomer, 45%). ^{31}P NMR (161.98 MHz, CDCl$_3$): δ 8.2 (t, $^{3}J_{P,H}$ = 6.7 Hz; E-isomer, 45%), –7.7 (s; Z-isomer, 55%). FT-IR: ν = 3074 (w), 3065 (w), 3051 (w), 2962 (w), 2932 (w), 1664 (w), 1610 (w), 1582 (m), 1568 (m), 1483 (m), 1435 (m), 1406 (m), 1385 (m), 1321 (s), 1261 (m), 1236 (w), 1157 (s), 1109 (s), 1065 (s), 1009 (s), 999 (s), 970 (m), 918 (m), 843 (s), 818 (m), 802 (m), 771 (m), 743 (s), 696 (s), 681 (s), 650 (s), 615 (s), 598 (m), 579 (w), 546 (m), 507 (s), 482 (s), 447 (s), 430 (m), 419 (m). HR-MS (ESI-Q-TOF): calcd. for $C_{21}F_3H_{18}NP$: 372.1123; found: 372.1123. **3d:** Mp: 40.6 °C ≤ decomp. *Since not all ^{1}H- and ^{13}C NMR resonances of the E-**3d** and Z-**3d** can be distinguished, one set of signals is reported (integrals normalized separately for each isomer).* ^{1}H NMR (500.23 MHz, CDCl$_3$): δ 7.71 (d, $^{3}J_{H,H}$ = 7.6 Hz, 2H; Ar*H* (E)), 7.68–7.54 (m, 9H; Ar*H* (E), Ar*H* (Z)), 7.49–7.41 (m, 6H; Ar*H* (E), Ar*H* (Z)), 7.31–7.22 (m, 2H; Ar*H* (Z)), 7.14 (t, $^{3}J_{H,H}$ = 7.9 Hz, 1H; Ar*H* (Z)), 7.08 (t, $^{3}J_{H,H}$ = 7.6 Hz, 2H; Ar*H* (Z)), 7.00 (d, $^{3}J_{H,H}$ = 7.3 Hz, 2H; Ar*H* (E)),

6.97 (d, $^{3}J_{H,H}$ = 7.3 Hz, 2H; Ar*H* (Z)), 3.65 (s, 3H; CN-C*H*$_3$ (Z)), 3.34 (s, 3H; CN-C*H*$_3$ (E)). $^{13}C\{^{1}H\}$ NMR (125.78 MHz, $CDCl_3$): δ 177.5 (d, $^{1}J_{C,P}$ = 8.2 Hz; *C*N-CH$_3$ (E)), 171.8 (s; *C*N-CH$_3$ (Z)), 140.3 (d, $^{2}J_{C,P}$ = 8.2 Hz; C-*ipso*-Ar*C*), 137.8 (d, $J_{C,P}$ = 19.1 Hz; Ar*C*), 137.2 (t, $J_{C,P}$ = 10.9 Hz; Ar*C*), 136.8 (d, $J_{C,P}$ = 15.4 Hz; Ar*C*), 136.6 (d, $^{2}J_{C,P}$ = 25.4 Hz, C-*ipso*-Ar*C*), 135.5 (d, $^{1}J_{C,P}$ = 12.3 Hz; P-*ipso*-Ar*C*), 134.9 (d, $^{1}J_{C,P}$ = 12.7 Hz; P-*ipso*-Ar*C*), 131.5 (q, $J_{C,F}$ = 3.6 Hz; P-Ar*C* (E)), 131.3 (q, $J_{C,F}$ = 3.6 Hz; P-Ar*C* (E)), 131.2–130.3 (m; P-Ar*C*-CF$_3$, P-Ar*C*), 129.4 (s; Ar*C*), 129.4 (t, $J_{C,P}$ = 2.7 Hz; Ar*C*), 128.9 (d, $J_{C,P}$ = 7.3 Hz; Ar*C*), 128.7 (s; Ar*C*), 128.6 (s; Ar*C* (Z)), 127.9 (s; Ar*C*), 127.3 (s; Ar*C*), 126.9 (d, $J_{C,P}$ = 4.5 Hz; Ar*C* (E)), 126.5 (q, $J_{C,F}$ = 3.6 Hz; P-Ar*C* (Z)), 126.2 (q, $J_{C,F}$ = 3.6 Hz; P-Ar*C* (E)), 124.0 (q, $^{1}J_{C,F}$ = 272.5 Hz; *C*F$_3$ (E)), 123.8 (qd, $^{1}J_{C,F}$ = 272.5, $^{4}J_{C,P}$ = 5.4 Hz; *C*F$_3$ (Z)), 44.1 (d, $^{3}J_{C,P}$ = 34.5 Hz; CN-*C*H$_3$(Z)), 43.2 (d, $^{3}J_{C,P}$ = 8.2 Hz; CN-*C*H$_3$ (E)). ^{19}F NMR (235.36 MHz, $CDCl_3$): δ –62.8 (s; E-isomer, 62%), –62.9 (s; Z-isomer, 38%). ^{31}P NMR (161.98 MHz, $CDCl_3$): δ 5.9 (t, $^{3}J_{P,H}$ = 6.5 Hz; E-isomer, 83%), –8.5 (s; Z-isomer, 17%). FT-IR: ν = 3065 (w), 2962 (w), 1624 (m), 1603 (m), 1522 (m), 1479 (w), 1443 (m), 1416 (m), 1367 (w), 1321 (s), 1310 (s), 1259 (s), 1225 (m), 1161 (s), 1107 (s), 1088 (s), 1067 (s), 1028 (s), 999 (s), 935 (w), 905 (m), 891 (w), 866 (w), 795 (s), 762 (m), 743 (m), 692 (s), 683 (s), 636 (s), 611 (m), 575 (m), 542 (m), 517 (s), 482 (s), 467 (s), 453 (s). HR-MS (ESI-Q-TOF): calcd. for $C_{22}F_6H_{17}NP$: 440.0997; found: 440.1002. **3e:** Mp: n.a. (≤ –20 °C). *Since not all ^{1}H- and ^{13}C NMR resonances of the E-**3e** and Z-**3e** can be distinguished, one set of signals is reported (integrals normalized separately for each isomer).* ^{1}H NMR (500.23 MHz, $CDCl_3$): δ 7.25–7.12 (m, 13H; Ar*H*), 7.12–7.06 (m, 9H; Ar*H*), 7.06–7.00 (m, 4H; Ar*H*), 6.96 (d, $^{3}J_{H,H}$ = 7.6 Hz, 2H; Ar*H* (E)), 3.58 (s, 3H; CN-C*H*$_3$ (Z)), 3.26 (s, 3H; CN-C*H*$_3$ (E)), 2.26 (s, 6H; P-Ar-C*H*$_3$ (E)), 2.24 (s, 6H; P-Ar-C*H*$_3$ (Z)). $^{13}C\{^{1}H\}$ NMR (125.78 MHz, $CDCl_3$): δ 179.4 (d, $^{1}J_{C,P}$ = 7.3 Hz; *C*N-CH$_3$ (E)), 177.0 (d, $^{1}J_{C,P}$ = 42.7 Hz; *C*N-CH$_3$ (Z)), 141.5 (d, $^{2}J_{C,P}$ = 7.3 Hz; C-*ipso*-Ar*C* (Z)), 138.3 (d, $^{3}J_{C,P}$ = 7.3 Hz; P-Ar*C*-CH$_3$), 137.8 (d, $^{3}J_{C,P}$ = 8.2 Hz; P-Ar*C*-CH$_3$), 137.8 (d, $^{2}J_{C,P}$ = 24.5 Hz; C-*ipso*-Ar*C* (E)), 135.5 (d, $J_{C,P}$ = 20.9 Hz; Ar*C*), 134.6 (d, $J_{C,P}$ = 21.8 Hz; Ar*C*), 134.3 (d, $^{1}J_{C,P}$ = 9.1 Hz; P-*ipso*-Ar*C*), 133.7 (d, $^{1}J_{C,P}$ = 9.1 Hz; P-*ipso*-Ar*C*), 131.7 (d, $J_{C,P}$ = 17.3 Hz; Ar*C*), 130.8 (d, $J_{C,P}$ = 17.3 Hz; Ar*C*), 129.8 (d, $J_{C,P}$ = 20.9 Hz; Ar*C*), 129.0 (d, $J_{C,P}$ = 39.1 Hz; Ar*C*), 128.5 (d, $J_{C,P}$ = 7.3 Hz; Ar*C*), 128.2 (d, $J_{C,P}$ = 7.3 Hz; Ar*C*), 128.0 (d, $J_{C,P}$ = 19.1 Hz; Ar*C*), 127.5 (d, $J_{C,P}$ = 22.7 Hz; Ar*C* (Z)), 127.1 (s; Ar*C* (E)), 127.0 (s; Ar*C* (E)), 43.9 (d, $^{3}J_{C,P}$ = 33.6 Hz; CN-*C*H$_3$ (Z)), 43.3 (d, $^{3}J_{C,P}$ = 9.1 Hz; CN-*C*H$_3$ (E)), 21.6 (s; P-Ar-*C*H$_3$ (E)), 21.5 (s; P-Ar-*C*H$_3$ (Z)). ^{31}P NMR (161.98 MHz, $CDCl_3$): δ 8.3 (s; E-isomer, 68%), –7.5 (s; Z-isomer, 32%). FT-IR: ν = 3050 (w), 2924 (w), 2859 (w), 2359 (w), 2328 (w), 1738 (w), 1591 (m), 1520 (w), 1476 (w), 1443 (w), 1370 (w), 1265 (s), 1229 (w), 1200 (w), 1107 (w), 1074 (w), 1028 (w), 997 (w), 972 (w), 895 (w), 779 (m), 762 (w), 731 (s). HR-MS (ESI-Q-TOF): calcd. for $C_{22}H_{23}NP$: 332.1563; found: 332.1564. **3f:** Mp: 64.3–65.6 °C. *Since not all ^{1}H- and ^{13}C NMR resonances of the E-**3f** and Z-**3f** can be distinguished, one set of signals*

is reported (integrals normalized separately for each isomer). ^{1}H NMR (500.23 MHz, $CDCl_3$): δ 7.32 (t, $^{3}J_{H,P}$ = 7.7 Hz, 4H; P-Ar*H* (E)), 7.24–7.15 (m, 8H; C-*m*-Ar*H* (E), Ar*H* (Z)), 7.12–7.02 (m, 12H; P-Ar*H* (E), C-*p*-Ar*H* (E), Ar*H* (Z)), 7.00 (dd, $^{3}J_{H,H}$ = 7.9 Hz, $^{4}J_{H,P}$ = 1.6 Hz, 2H; C-*o*-Ar*H* (E)), 3.55 (s, 3H; CN-CH_3 (Z)), 3.24 (d, $^{4}J_{H,P}$ = 1.9 Hz, 3H; CN-CH_3 (E)), 2.30 (s, 6H; P-C_6H_4-CH_3 (E,Z)). ^{13}C{^{1}H} NMR (125.78 MHz, $CDCl_3$): δ 179.6 (s; *C*N-CH_3), 139.1 (s; P-Ar*C*-CH_3), 137.8 (d, $J_{C,P}$ = 25.4 Hz; *ipso*-Ar*C*), 134.8 (d, $J_{C,P}$ = 20.0 Hz; P-Ar*C* (E)), 134.0 (d, $J_{C,P}$ = 20.0 Hz; P-Ar*C* (Z)), 131.0 (d, $J_{C,P}$ = 7.3 Hz; *ipso*-Ar*C*), 130.5 (d, $J_{C,P}$ = 7.3 Hz; *ipso*-Ar*C*), 129.6 (s; Ar*C*), 129.5 (s; Ar*C*), 129.2 (s; Ar*C*), 129.1 (s; Ar*C*), 128.2 (s; Ar*C*), 128.1 (s; Ar*C*), 127.9 (d, $J_{C,P}$ = 2.7 Hz; Ar*C*), 127.7 (s; Ar*C*), 127.5 (s; Ar*C*), 127.1 (d, $J_{C,P}$ = 4.5 Hz; C-*o*-Ar*C* (E)), 43.4 (d, $^{3}J_{C,P}$ = 32.7 Hz; CN-*C*H_3 (Z)), 43.2 (d, $^{3}J_{C,P}$ = 8.2 Hz; CN-*C*H_3 (E)), 21.5 (d, $^{5}J_{C,P}$ = 9.1 Hz; P-ArC-*C*H_3 (E,Z)). ^{31}P NMR (161.98 MHz, $CDCl_3$): δ 6.3 (s; E-isomer, 76%), –8.8 (s; Z-isomer, 24%). FT-IR: v = 3063 (w), 3032 (w), 3015 (w), 2961 (m), 2910 (m), 2854 (w), 1653 (w), 1632 (w), 1591 (s), 1560 (w), 1524 (w), 1495 (s), 1439 (s), 1394 (m), 1306 (m), 1259 (s), 1202 (m), 1186 (m), 1099 (s), 1092 (s), 1070 (s), 1018 (s), 972 (m), 935 (m), 897 (m), 866 (w), 843 (m), 797 (s), 762 (s), 700 (s), 673 (m), 652 (s), 642 (s), 629 (s), 615 (s), 552 (w), 536 (s), 503 (s), 492 (s), 451 (s), 420 (m), 401 (s). HR-MS (ESI-Q-TOF): calcd. for $C_{22}H_{23}NP$: 332.1563; found: 332.1562.

Hydrolysis study 3a-c. 3 (0.02 g, 1.00 eq) was dissolved in 0.6 mL acetone in an NMR tube. Next, a solution of H_2O in acetone (10%) was added. The mixture was vigorously shaken and subsequently kept at RT, during which the reaction mixture was monitored using ^{31}P NMR spectroscopy. Using this methodology, systematically H_2O was added to the mixture, which was kept at RT during the described time span.

H_2O added	**3a** : Ph_2PH	Time of measurement
0	100% : 0%	0
0.5 eq.	97% : 0%	21h05m
1.0 eq.	95% : 0%	89h26m
2.0 eq.	91% : 0%	118h13m
4.0 eq.	89% : 0%	144h37m
8.0 eq.	85% : 1%	163h16m
16.0 eq.	85% : 1%	187h39m
500 eq.*	62% : 4%	210h11m
*Precip.	93% : 0%	216h04m

H_2O added	**3b** : Ph_2PH	Time of measurement
0	98% : 0%	0
0.5 eq.	95% : 0%	17h48m
1.0 eq.	91% : 0%	65h24m
4.0 eq.	88% : 1%	91h07m
16.0 eq.	84% : 2%	115h35m
Excess (redissolved)	36% : 6%	524h12m

H_2O added	**3c** : Ph_2PH	Time of measurement
0	100% : 0%	0
0.5 eq.	95% : 0%	41h36m
2.8 eq.	94% : 0%	68h52m
20.0 eq.	92% : 1%	91h26m
Excess	72% : 3%	165h27m

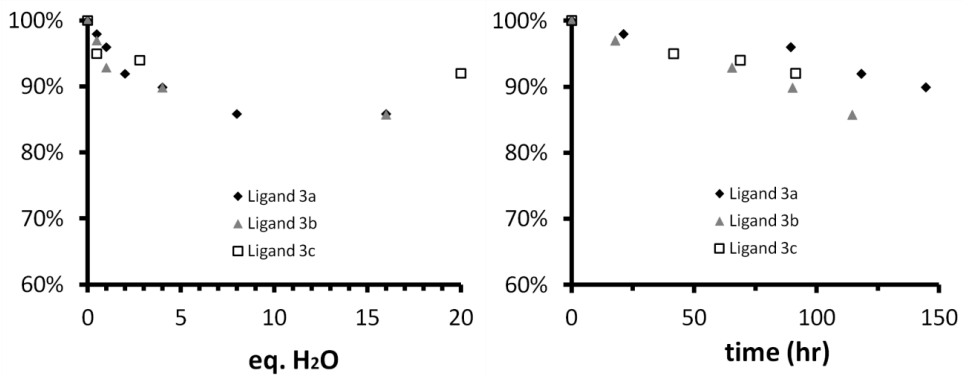

Figure S1. Water sensitivity of ligand **3a-c**.

Acid stability study 3a. 3a (0.0203 g, 0.066 mmol, 1.00 eq.) was dissolved in 0.4 mL DCM to give a yellowish solution. Addition of a solution of TfOH in DCM (0.23 mL of a 0.28 M solution, 0.064 mmol, 0.98 eq.) provided a bright yellow solution, which was vigorously shaken and kept at RT for 20 h, during which the reaction was monitored using ^{31}P NMR spectroscopy. Next, again TfOH in DCM (0.23 mL of a 0.28 M solution, 0.064 mmol, 0.98 eq.) was added. The mixture was vigorously shaken and kept at RT for 24 h, during which the reaction was monitored using ^{31}P NMR spectroscopy. Excess triethylamine (0.20 ml, 1.43 mmol, 21.74 eq.) was added to the mixture at 0 °C, resulting in a light yellow solution of pure **3a**.

Reagents present	Mixture	Time of measurement
-	99% **3a**	0
1.0 eq. TfOH	98% **3a**H^+	18h26m
2.0 eq. TfOH	98% **3a**H^+	40h36m
2.0 eq. TfOH	97% **3a**H^+	66h26m
2.0 eq. TfOH	97% **3a**H^+	110h34m
Excess NEt_3, 2.0 eq. NEt_3•HOTf	100% **3a**	156h59m

Acid catalysed hydrolysis study 3a. 3a (0.0267 mg, 0.088 mmol, 1.00 eq.) was dissolved in 0.6 ml DCM to give a yellowish solution. Addition of a solution of TfOH in DCM (31 µL of a 0.28 M solution, 0.009 mmol, 0.10 eq.) provided a more intensely colored yellow solution, which was vigorously shaken and kept at RT for 1 h. Subsequently, H_2O (0.8 µL, 0.044 mmol, 0.50 eq.) was added to the mixture, which then was vigorously shaken and kept at RT for 2 days, during which the reaction was monitored using ^{31}P NMR spectroscopy. Next, excess H_2O (5.6 µL, 0.310 mmol, 3.52 eq.) was added to the mixture. After vigorous shaking, the mixture was kept at RT for 24 days.

Reagents present	**3a** : Ph_2PH	Time of measurement
0.1 eq. TfOH	100% : 0%	0
0.1 eq. TfOH, 0.5 eq. H_2O	86% : 1%	17h22m
0.1 eq. TfOH, 0.5 eq. H_2O	76% : 3%	60h08m
0.1 eq. TfOH, 4.0 eq. H_2O	74% : 3%	107h38m
0.1 eq. TfOH, 4.0 eq. H_2O	68% : 5%	248h16m
0.1 eq. TfOH, 4.0 eq. H_2O	58% : 9%	603h18m
0.1 eq. TfOH, 4.0 eq. H_2O	49% : 12%	1250h52m

Oxidation study 3a. Under N_2 atmosphere, **3a** (0.012 g, 0.04 mmol, 1.00 eq.) was dissolved in 0.6 mL acetone. Stepwise, O_2 (21% in air) was bubbled manually through the mixture with a rate of approx. 6 bubbles per second using a needle with an inner diameter of 1.194 mm. During additions, the mixture was kept in a water bath at RT to inhibit acetone evaporation. After each addition, the NMR tube was sealed using a screw cap and the reaction mixture was monitored using ^{31}P NMR spectroscopy. Using this methodology, systematically O_2 (21% in air) was added to the mixture at RT over the described intervals. From addition #7 onwards, a white solid started to precipitate. After the additions, the mixture was allowed to fully oxidize by dissolving the mixture in 10 mL acetone (technical grade) and stirring the resulting solution in under closed air atmosphere for 42 h at RT. Subsequently, the reaction vessel was opened to the external

air atmosphere and stirred for an additional 173.5 h. The resulting solution was evaporated to provide a white oil.

Step	Air added	**3a**	Time of measurement
0	0	100%	0
1	1 mL	95%	17m
2	2 mL	86%	24m
3	4 mL	82%	30m
4	6 mL	74%	37m
5	10 mL	68%	46m
6	14 mL	61%	55m
7	22 mL	56%	1h06m
8	30 mL	52%	1h17m
9	46 mL	49%	1h31m
10	62 mL	44%	1h47m
11	Excess (closed atm.)	4%	46h07m
12	Excess (open atm.)	0%	219h38m

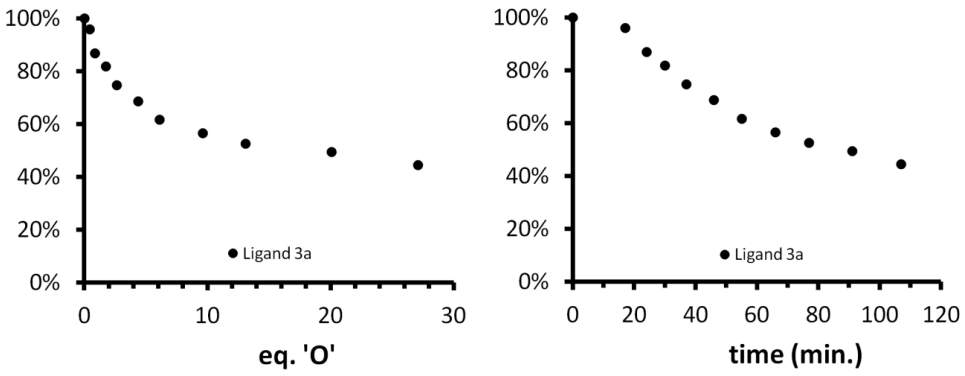

Figure S2. Air sensitivity of ligand **3a**.

(((N-methyl)arylimidoyl)diarylphosphanyl) (pentamethylcyclopentadienyl) rhodium(III) dichlorides (4a,c,e). Under an Argon atmosphere, a solution of **3** (102 mg 0.34 mmol, 2.4 eq.) in 9 mL DCM was added to a red/brown solution of $[RhCp^*Cl_2]_2$ (87 mg 0.14 mmol, 1.0 eq.) in 5 mL DCM. The resulting red/brown solution was stirred for 30 min at RT. Evaporation of the obtained red solution provided a red/orange solid, which was washed with 3 x 5 mL Et_2O to provide **4** as an orange solid (**4a**: 90%; **4c**: 68%; **4e**: 92%). *Crystallization:* Subsequently Et_2O and pentane were diffused into a DCM solution

at RT. Next, the solution was slowly cooled to provide red needles. **4a:** Mp: 164.6 °C. ^{1}H NMR (500.23 MHz, $CDCl_3$): δ 7.71 (s, 5H; P-Ar*H*), 7.18 (s, 5H; P-Ar*H*), 6.99 (s, 3H; C-*o,p*-Ar*H*), 6.92 (s, 2H; C-*m*-Ar*H*), 3.36 (s, 3H; NCH_3), 1.44 (s, 15H; Cp*-CCH_3). ^{13}C{^{1}H} NMR (125.78 MHz, $CDCl_3$): δ 137.0 (d, $^{2}J_{C,P}$ = 11.8 Hz, P-*o*-Ar*C*), 135.4 (d, $^{1}J_{C,P}$ = 22.7 Hz; P-*ipso*-Ar*C*), 130.2 (s; P-*p*-Ar*C*), 127.8 (s; C-*p*-Ar*C*), 127.7 (s; C-*o*-Ar*C*), 127.4 (s; P-*m*-Ar*C*), 127.0 (s; C-*m*-Ar*C*), 99.7 (d, $^{1}J_{C,Rh}$ = 5.5 Hz; Cp*-*C*CH$_3$), 43.1 (d, $^{3}J_{C,P}$ = 21.8 Hz; CN-*C*H$_3$), 9.0 (s; Cp*-C*C*H$_3$), signals for C-*ipso*-Ar*C* and *C*N-CH$_3$ are unresolved. ^{31}P NMR (161.98 MHz, DCM): δ 37.3 (d, $^{1}J_{P,Rh}$ = 146.6 Hz; **4a**, 96%), –2.2 (d, $^{1}J_{P,Rh}$ = 113.0 Hz; **5a**, 4%). FT-IR: v =3055 (w), 2961 (w), 2914 (w), 1609 (m), 1609 (m), 1572 (w), 1489 (m), 1479 (m), 1433 (s), 1383 (m), 1369 (w), 1261 (m), 1209 (m), 1200 (m), 1188 (m), 1157 (m), 1092 (s), 1072 (s), 1022 (s), 970 (m), 951 (m), 860 (w), 800 (s), 764 (s), 743 (s), 690 (s), 648 (m), 611 (m), 550 (s), 511 (s), 494 (s), 469 (s), 451 (s), 430 (m), 401 (s). HR-MS (ESI-Q-TOF): calcd. for $C_{30}H_{34}Cl_2NPRh^+$: 612.0855; found: 612.0873. **4c:** Mp: 200.7 °C ≤ decomp. ^{1}H NMR (400.13 MHz, $CDCl_3$): δ 7.71 (br. s, 4H; P-Ar*H*), 7.42–7.09 (br. m, 8H; C-*o*-Ar*H*, P-Ar*H*), 7.02 (d, $^{3}J_{H,H}$ = 7.1 Hz, 2H; C-*m*-Ar*H*), 3.32 (d, $^{3}J_{H,P}$ = 2.8 Hz, 3H; CN-C*H*$_3$), 1.43 (d, $^{3}J_{H,Rh}$ = 3.5 Hz, 15H; Cp*-CC*H*$_3$). ^{13}C{^{1}H} NMR (125.78 MHz, $CDCl_3$): δ 175.1 (d, $^{1}J_{C,P}$ = 57.2 Hz; *C*N-CH$_3$), 139.1 (d, $^{1}J_{C,P}$ = 20.9 Hz; P-*ipso*-Ar*C*), 135.4 (br. s; P-Ar*C*), 130.6 (s; P-Ar*C*), 129.8 (q, $^{2}J_{C,F}$ = 32.7 Hz; C-*p*-Ar*C*), 127.7 (s; C-*m*-Ar*C*), 124.6 (q, $^{4}J_{C,F}$ = 3.6 Hz; C-*o*-Ar*C*), 124.2 (q, $^{1}J_{C,F}$ = 272.5 Hz; *C*F$_3$), 99.8 (dd, $^{1}J_{C,Rh}$ = 6.4 Hz, $^{2}J_{C,P}$ = 2.7 Hz; Cp*-*C*CH$_3$), 43.2 (d, $^{3}J_{C,P}$ = 20.9 Hz; CN-*C*H$_3$), 9.0 (s; Cp*-C*C*H$_3$), signals for C-*ipso*-Ar*C* and one P-Ar*C* are unresolved. ^{19}F NMR (235.36 MHz, $CDCl_3$): δ –63.3 (s). ^{31}P NMR (161.98 MHz, DCM): δ 35.1 (d, $^{1}J_{P,Rh}$ = 146.9 Hz). FT-IR: v = 3057 (w), 2989 (w), 2953 (w), 2908 (w), 1624 (w), 1614 (w), 1572 (w), 1508 (m), 1479 (m), 1448 (m), 1433 (s), 1406 (m), 1369 (m), 1321 (s), 1263 (w), 1205 (w), 1188 (m), 1165 (s), 1122 (s), 1109 (s), 1090 (m), 1067 (s), 1020 (s), 997 (m), 972 (m), 933 (w), 924 (w), 837 (s), 800 (w), 743 (s), 696 (s), 689 (s), 663 (m), 619 (m), 606 (m), 550 (s), 509 (s), 498 (s), 465 (s), 449 (s), 432 (m). HR-MS (ESI-Q-TOF): calcd. for $C_{31}H_{33}Cl_2F_3NPRh^+$: 680.0705; found: 680.0705. **4e:** Mp: 139.6 °C ≤ decomp. ^{1}H NMR (500.23 MHz, $CDCl_3$): δ 7.66–7.35 (m, 5H; P-Ar*H*), 7.22–6.95 (m, 6H; C-Ar*H*, P-Ar*H*), 6.91 (s, 2H; C-Ar*H*), 3.35 (s, 3H; CN-C*H*$_3$), 2.19 (br. s, 6H; P-ArC*H*$_3$), 1.43 (d, $^{3}J_{H,Rh}$ = 2.8 Hz, 15H; Cp*-CC*H*$_3$). ^{13}C{^{1}H} NMR (125.78 MHz, $CDCl_3$): δ 176.6 (d, $^{3}J_{C,P}$ = 60.9 Hz; *C*N-CH$_3$), 135.6 (d, $^{1}J_{C,P}$ = 20.9 Hz; P-*ipso*-Ar*C*), 134.4 (d, $J_{C,P}$ = 2.7 Hz; P-Ar*C*), 130.9 (s; P-Ar*C*), 129.9 (d, $J_{C,P}$ = 12.7 Hz; P-Ar*C*), 129.1 (d, $J_{C,P}$ = 11.8 Hz; P-Ar*C*), 127.7 (s; C-Ar*C*), 127.5 (s; C-Ar*C*), 126.9 (s; C-Ar*C*), 99.6 (dd, $^{1}J_{C,Rh}$ = 6.4 Hz, $^{2}J_{C,P}$ = 2.7 Hz; Cp*-*C*CH$_3$), 43.1 (d, $^{3}J_{C,P}$ = 21.8 Hz; CN-*C*H$_3$), 21.5 (s; P-Ar*C*H$_3$), 9.0 (d, $^{2}J_{C,Rh}$ = 1.8 Hz; Cp*-C*C*H$_3$), signals for C-*ipso*-Ar*C* and P-Ar *C*-CH$_3$ are unresolved. ^{31}P NMR (161.98 MHz, DCM): δ 34.7 (d, $^{1}J_{P,Rh}$ = 144.6 Hz; **4e**, 94%), –12.1 (d, $^{1}J_{P,Rh}$ = 114.7 Hz; **5e**, 6%). FT-IR: v = 2962 (m), 2907 (w), 1479 (w), 1443 (w), 1400 (w), 1258 (s), 1078 (s), 1011 (s), 864 (m), 789 (s), 690 (s), 662 (m),

611 (w), 557 (m), 542 (m), 480 (m), 465 (s), 465 (s). HR-MS (ESI-Q-TOF): calcd. for $C_{32}H_{38}Cl_2NPRh^+$: 640.1168; found: 640.1163.

Chloro (((N-methyl) arylimidoyl) diarylphosphanyl) (pentamethylcyclopentadienyl) rhodium(III) trifluoromethylsulfonates (6a,c,e). Under an Argon atmosphere, to a solution of **3** (0.31 mmol, 2.1 eq.) in 14 mL DCM, was added $[RhCp^*Cl_2]_2$ (95 mg 0.15 mmol, 1.0 eq.) to provide a red solution, which was stirred for 30 min at RT. Next, AgOTf (79 mg, 0.30 mmol, 2.0 eq.) was added and the resulting suspension was stirred for 60 min at RT in absence of light, during which the mixture turned bright orange. Filtration provided an orange-red solution, which was evaporated to provide a yellow-orange solid. After washing (**6a,e**: 3 x 5 mL Et_2O; **6c**: 3 x 5 mL pentane, **6** was obtained as an orange powder (**6a**: quant.; **6c**: 97%; **6e**: 97%). **6a:** Mp: 138.8 °C. ^{1}H NMR (500.23 MHz, $CDCl_3$): δ 7.66–7.59 (m, 8H; P-Ar*H*), 7.47–7.42 (m, 3H; C-*o*-Ar*H*, P-Ar*H*), 7.36 (t, $^3J_{H,H}$ = 6.9 Hz, 2H; C-*m*-Ar*H*), 7.23 (d, $^3J_{H,H}$ = 7.6 Hz, 2H; C-*o*-Ar*H*), 3.69 (d, $^3J_{H,Rh}$ = 3.8 Hz; N-C*H*$_3$), 1.70 (d, $^3J_{H,Rh}$ = 3.8 Hz; Cp*-CC*H*$_3$). ^{13}C{^{1}H} NMR (125.78 MHz, $CDCl_3$): δ 190.9 (dd, $^1J_{C,P}$ = 50.0 Hz, $^2J_{C,Rh}$ = 2.7 Hz; *C*N-CH$_3$), 136.7 (d, $^2J_{C,P}$ = 11.8 Hz; P-*m*-Ar*C*), 133.8 (d, $^4J_{C,P}$ = 2.7 Hz; P-*p*-Ar*C*), 133.0 (d, $^3J_{C,P}$ = 10.9 Hz; P-*o*-Ar*C*), 132.9 (d, $^4J_{C,P}$ = 2.7 Hz; P-*p*-Ar*C*), 132.3 (dd, $^3J_{C,Rh}$ = 7.3 Hz, $^2J_{C,P}$ = 1.8 Hz; C-*ipso*-ArC), 131.8 (s; C-*p*-Ar*C*), 130.4 (d, $^3J_{C,P}$ = 10.9 Hz; P-*m*-Ar*C*), 129.4 (d, $^2J_{C,P}$ = 11.8 Hz; P-*o*-Ar*C*), 129.2 (s; C-*m*-Ar*C*), 127.5 (d, $^2J_{C,P}$ = 1.8 Hz; C-*o*-Ar*C*), 123.7 (d, $^1J_{C,P}$ = 45.4 Hz; P-*ipso*-Ar*C*), 121.2 (q, $^1J_{C,F}$ = 320.6 Hz; O_3SCF_3), 120.7 (d, $^1J_{C,P}$ = 36.3 Hz; P-*ipso*-Ar*C*), 99.8 (dd, $^1J_{C,Rh}$ = 7.3 Hz, $^2J_{C,P}$ = 2.7 Hz; Cp*-*C*CH$_3$), 44.7 (d, $^2J_{C,Rh}$ = 18.2 Hz; N*C*H$_3$), 9.6 (d, $^2J_{C,Rh}$ = 1.8 Hz; Cp*-C*C*H$_3$). ^{19}F NMR (235.36 MHz, $CDCl_3$): δ –78.2 (s). ^{31}P NMR (161.98 MHz, DCM): δ –9.1 (d, $^1J_{P,Rh}$ = 113.4 Hz). FT-IR: v = 3065 (w), 2978 (w), 2908 (w), 1603 (w), 1479 (w), 1439 (m), 1381 (w), 1265 (s), 1240 (s), 1221 (s), 1188 (w), 1140 (s), 1097 (m), 1078 (m), 1030 (s), 997 (m), 951 (w), 854 (w), 847 (m), 814 (w), 752 (s), 719 (m), 692 (s), 635 (s), 565 (m), 517 (s), 482 (s), 463 (s), 440 (s). HR-MS (ESI-Q-TOF): calcd. for $C_{30}H_{33}ClNPRh^+$: 576.1089; found: 576.1112. **6c:** Mp: 120.9–128.5 °C. ^{1}H NMR (500.23 MHz, $CDCl_3$): δ 7.74–7.66 (m, 6H; P-*o,p*-Ar*H*), 7.66–7.58 (m, 4H; P-*m*-Ar*H*, C-*o*-Ar*H*), 7.53–7.46 (m, 2H; P-*m*-Ar*H*), 7.41 (d, $^3J_{H,H}$ = 7.9 Hz, 2H; C-*m*-Ar*H*), 3.68 (d, $^3J_{H,Rh}$ = 4.1 Hz, 3H; CN-C*H*$_3$), 1.71 (d, $^3J_{H,Rh}$ = 4.7 Hz, 15H; Cp*-CC*H*$_3$). ^{13}C{^{1}H} NMR (125.78 MHz, $CDCl_3$): δ 189.6 (dd, $^1J_{C,P}$ = 50.0 Hz, $^2J_{C,Rh}$ = 4.5 Hz; *C*N-CH$_3$), 136.8 (d, $^2J_{C,P}$ = 11.8 Hz; P-*m*-Ar*C*), 135.1 (d, $^3J_{C,Rh}$ = 7.3 Hz; C-*ipso*-Ar*C*), 134.0 (d, $^4J_{C,P}$ = 2.7 Hz; P-*p*-Ar*C*), 133.1 (t, $^2J_{C,F}$ = 33.6 Hz; C-*p*-Ar*C*), 133.1 (d, $^2J_{C,P}$ = 10.9 Hz; P-*o*-Ar*C*), 130.6 (d, $^2J_{C,P}$ = 10.9 Hz; P-*o*-Ar*C*), 129.5 (d, $^3J_{C,P}$ = 10.9 Hz; P-*m*-Ar*C*), 128.4 (s; C-*m*-Ar*C*), 126.2 (q, $^3J_{C,F}$ = 3.6 Hz; C-*o*-Ar*C*), 123.4 (q, $^1J_{C,F}$ = 272.6 Hz; C-Ar-*C*F$_3$), 123.1 (d, $^1J_{C,P}$ = 44.5 Hz; P-*ipso*-Ar*C*), 121.2 (q, $^1J_{C,F}$ = 320.6 Hz; O_3SCF_3), 120.5 (d, $^1J_{C,P}$ = 34.5 Hz; P-*ipso*-Ar*C*), 99.9 (dd, $^1J_{C,Rh}$ = 7.3 Hz, $^2J_{C,P}$ = 2.7 Hz; Cp*-*C*CH$_3$),

45.1 (d, $^{2}J_{C,Rh}$ = 18.2 Hz; CN-*C*H$_3$), 9.6 (s; Cp*-C*C*H$_3$), signal for one P-*p*-Ar*C* is unresolved. ^{19}F NMR (235.36 MHz, $CDCl_3$): δ –63.2 (s; C*F*$_3$), –78.2 (s; O$_3$SC*F*$_3$). ^{31}P NMR (161.98 MHz, DCM): δ –5.0 (d, $^{1}J_{P,Rh}$ = 114.7 Hz). FT-IR: ν = 3072 (w), 2926 (w), 1616 (w), 1481 (w), 1456 (w), 1437 (w), 1406 (w), 1379 (w), 1323 (s), 1258 (s), 1223 (m), 1128 (m), 1113 (m), 1101 (m), 1067 (m), 1067 (m), 1030 (s), 993 (m), 993 (m), 839 (m), 839 (m), 746 (m), 746 (m), 719 (w), 690 (m), 636 (s), 571 (m), 527 (m), 517 (m), 492 (m), 474 (m), 444 (m). HR-MS (ESI-Q-TOF): calcd. for $C_{31}H_{32}ClF_3NPRh^+$: 644.0963; found: 644.0967. **6e:** Mp: 153.2 °C ≤ decomp. ^{1}H NMR (500.23 MHz, $CDCl_3$): δ 7.59–7.53 (m, 1H; P-Ar*H*), 7.48–7.30 (m, 10H; P-Ar*H*, C-*m*,*p*-Ar*H*), 7.23 (d, $^{3}J_{H,H}$ = 7.6 Hz, 2H; C-*o*-Ar*H*), 3.7 (d, $^{3}J_{H,Rh}$ = 4.1 Hz, 3H; CN-C*H*$_3$), 2.45 (s, 3H; P-Ar-C*H*$_3$), 2.29 (s, 3H; P-Ar-C*H*$_3$), 1.70 (d, $^{3}J_{H,Rh}$ = 4.4 Hz, 15H; Cp*-CC*H*$_3$). ^{13}C{^{1}H} NMR (125.78 MHz, $CDCl_3$): δ 191.0 (dd, $^{1}J_{C,P}$ = 50.0 Hz, $^{2}J_{C,Rh}$ = 3.6 Hz; *C*N-CH$_3$), 140.7 (d, $^{3}J_{C,P}$ = 10.9 Hz; P-Ar*C*-CH$_3$), 139.2 (d, $^{3}J_{C,P}$ = 10.9 Hz; P-Ar *C*-CH$_3$), 137.0 (d, $J_{C,P}$ = 10.9 Hz; P-Ar*C*), 134.5 (d, $J_{C,P}$ = 2.7 Hz; P-Ar*C*), 133.8 (s; P-Ar*C*), 132.9 (d, $J_{C,P}$ = 10.9 Hz; P-Ar*C*), 132.4 (d, $^{3}J_{C,Rh}$ = 7.3 Hz; C-*ipso*-Ar*C*), 131.7 (s; C-*p*-Ar*C*), 130.3 (dd, $^{2}J_{C,P}$ = 11.4 Hz, $^{3}J_{C,Rh}$ = 3.2 Hz; P-*o*-Ar*C*), 129.1 (s; C-*m*-Ar*C*), 127.6 (s; C-*o*-Ar*C*), 123.6 (d, $^{1}J_{C,P}$ = 43.6 Hz; P-*ipso*-Ar*C*), 121.2 (q, $^{1}J_{C,F}$ = 320.6 Hz; O$_3$S*C*F$_3$), 120.4 (d, $^{1}J_{C,P}$ = 36.3 Hz; P-*ipso*-Ar*C*), 99.7 (dd, $^{1}J_{C,Rh}$ = 7.3 Hz, $^{2}J_{C,P}$ = 2.7 Hz; Cp*-*C*CH$_3$), 44.6 (d, $^{2}J_{C,Rh}$ = 19.1 Hz; CN-*C*H$_3$), 21.5 (d, $^{4}J_{C,P}$ = 1.8 Hz; P-Ar-*C*H$_3$), 9.6 (s; Cp*-C*C*H$_3$), signals for three P-*p*-Ar*C* are unresolved. ^{19}F NMR (235.36 MHz, $CDCl_3$): δ –78.6 (s). ^{31}P NMR (161.98 MHz, DCM): δ –8.5 (d, $^{1}J_{P,Rh}$ = 112.4 Hz). FT-IR: ν = 3065 (w), 2962 (w), 2920 (w), 1655 (w), 1593 (w), 1541 (w), 1474 (m), 1447 (m), 1375 (m), 1319 (w), 1259 (s), 1223 (s), 1205 (s), 1146 (s), 1107 (s), 1080 (s), 1030 (s), 995 (s), 864 (w), 789 (s), 762 (s), 690 (s), 636 (s), 569 (s), 548 (s), 517 (s), 496 (w), 474 (m), 446 (s). HR-MS (ESI-Q-TOF): calcd. for $C_{32}H_{37}ClNPRh^+$: 604.1402; found: 604.1409.

[(((N-methyl)phenylimidoyl)diphenylphosphanyl) (pentamethylcyclopentadienyl) Rhodium(III) (trifluoromethylsulfonate)] [poly(disilver(I) tri(trifluoromethanesulfonate)(methylene chloride))] (7a). Under an Argon atmosphere, to a solution of **3a** (92 mg 0.30 mmol, 2.0 eq.) in 15 mL DCM, was added $[RhCp^*Cl_2]_2$ (94 mg 0.15 mmol, 1.0 eq.) to provide a red solution, which was stirred for 30 min at RT. Next, AgOTf (317 mg, 1.23 mmol, 8.2 eq.) was added and the resulting suspension was stirred for 60 min at RT in absence of light, during which the mixture turned yellow. Filtration provided an orange-red solution, which was evaporated to provide an orange-red solid. After washing with 20 mL pentane, **7a** was obtained as a yellow solid (306 mg, 0.21 mmol, 71%). *Crystallization:* Slow diffusion of pentane (55 mL/mmol compound) into a DCM solution (45 mL/mmol compound) at RT provided red blocks. Mp: 178.6 °C. ^{1}H NMR (500.23 MHz, $CDCl_3$): δ 7.76–7.63 (m, 6H; P-*o*,*p*-Ar*H*),

7.49–7.46 (m, 5H; P-*m*-Ar*H,* C-*p*-Ar*H*), 7.40 (t, $^{3}J_{H,H}$ = 7.7 Hz, 2H; C-*m*-Ar*H*), 7.33 (d, $^{3}J_{H,H}$ = 7.6 Hz, 2H; C-*o*-Ar*H*), 4.01 (d, $^{3}J_{H,Rh}$ = 4.4 Hz, 3H; CN-C*H*$_3$), 1.72 (d, $^{3}J_{H,Rh}$ = 5.0 Hz, 15H; Cp*-CC*H*$_3$). $^{13}C\{^{1}H\}$ NMR (125.78 MHz, $CDCl_3$): δ 193.9 (dd, $^{1}J_{C,P}$ = 48.1 Hz, $^{2}J_{C,Rh}$ = 3.6 Hz; *C*N-CH$_3$), 136.2 (dd, $^{3}J_{C,P}$ = 11.8 Hz, $^{4}J_{C,Rh}$ = 3.6 Hz; P-*m*-Ar*C*), 134.4 (d, $^{4}J_{C,P}$ = 8.2 Hz; P-*p*-Ar*C*), 133.6 (d, $^{4}J_{C,P}$ = 7.3 Hz; P-*p*-Ar*C*), 133.3 (d, $^{2}J_{C,P}$ = 10.9 Hz; P-*o*-Ar*C*), 132.3 (s; C-*p*-Ar*C*), 132.1 (d, $^{2}J_{C,P}$ = 6.4 Hz; C-*ipso*-Ar*C*), 130.8 (d, $^{2}J_{C,P}$ = 8.2 Hz; P-*o*-Ar*C*), 129.7 (d, $^{3}J_{C,P}$ = 10.7 Hz; P-*m*-Ar*C*), 129.3 (s; C-*m*-Ar*C*), 127.7 (d, $^{3}J_{C,P}$ = 1.8 Hz; C-*o*-Ar*C*), 100.8 (dd, $^{1}J_{C,Rh}$ = 8.2 Hz, $^{2}J_{C,P}$ = 2.7 Hz; Cp*-*C*CH$_3$), 46.1 (d, $^{2}J_{C,Rh}$ = 17.3 Hz; CN-*C*H$_3$), 9.8 (s; Cp*-C*C*H$_3$), signals for P-*ipso*-Ar*C* are unresolved. ^{19}F NMR (235.36 MHz, $CDCl_3$): δ –78.2 (d, $^{4}J_{F,Rh}$ = 12.1 Hz; Rh-OS(O$_2$)C*F*$_3$). ^{31}P NMR (161.98 MHz, $CDCl_3$): δ –9.9 (d, $^{1}J_{P,Rh}$ = 111.2 Hz). FT-IR: ν = 3065 (w), 2995 (w), 1580 (w), 1483 (w), 1437 (m), 1379 (w), 1304 (s), 1261 (s), 1229 (s), 1202 (s), 1159 (s), 1144 (s), 1099 (m), 1082 (m), 1030 (s), 1005 (s), 951 (m), 926 (w), 771 (m), 754 (m), 733 (m), 689 (s), 635 (s), 573 (m), 557 (m), 536 (w), 515 (s), 476 (s), 463 (m), 442 (m). HR-MS (ESI-Q-TOF): calcd. for $C_{31}H_{33}F_3NO_3PRhS^+$: 690.0920; found: 690.0915.

[(1,3-P,N)Ru(II)]-catalyzed hydrations of benzonitrile. *Protocol 1:* [Ru(Ar)Cl$_2$]$_2$ (Ar = *p*-cym, C$_6$Me$_6$, C$_6$H$_5$Me, Cp*) (0.025 mmol, 5 mol%) and ligand **3a** or Ph$_2$PPy (0.05 mmol, 5 mol%) were dissolved in DME (0.5 mL) under an argon atmosphere and stirred for 30 minutes. Benzonitrile (105 µL, 1.02 mmol, 1.0 eq.) and H$_2$O (36 µL, 1.99 mmol, 2.0 eq.) were added and the sealed vessel was stirred at 180 °C for 3 h. *Protocol 2:* [Ru(*p*-cym)Cl$_2$]$_2$ (16 mg, 0.026 mmol, 5 mol% [Ru]) and ligand **3a** or Ph$_2$PPy (0.052 mmol, 5 mol%) were dissolved in benzonitrile (105 µL, 1.02 mmol, 1.0 eq.) under an argon atmosphere and stirred for 30 minutes. H$_2$O (3.0 mL, 166 mmol, 163 eq.) was added and the sealed vessel was stirred at 100 °C for 24 h. *Protocol 3:* [Ru(*p*-cym)Cl$_2$]$_2$ (15 mg, 0.024 mmol, 1.4 mol% Ru) and ligand (0.050 mmol, 1.4 mol%) were dissolved in benzonitrile (370 µL, 3.58 mmol, 1.0 eq.) under argon atmosphere and stirred for 30 minutes. H$_2$O (130 µL, 7.2 mmol, 2.0 eq.) was added and the sealed vessel was stirred at 180 °C for 3 h. *Analysis:* After cooling to RT, the mixtures were extracted with *i*-PrOH under atmospheric conditions and analyzed by GC (internal standard: naphthalene).

Protocol	Metal source	ligand	Benzamide yield
1	$[Ru(p\text{-cym})Cl_2]_2$	**3a**	86.7
1	$[Ru(C_6Me_6)Cl_2]_2$	**3a**	54.6
1	$[Ru(C_6H_5Me)Cl_2]_2$	**3a**	83.6
1	$[Ru(PPh3)_3Cl_2]_2$	**3a**	0.0
1	$[Ru(p\text{-cym})Cl_2]_2$	**3a** (2 eq.)	96.1
1	$[Ru(p\text{-cym})Cl_2]_2$ / + 2 AgOTf	**3a**	2.9
1	$[RhCp^*Cl_2]_2$	**3a**	22.0
2	$[Ru(p\text{-cym})Cl_2]_2$	**3a**	93.7
2	$[Ru(p\text{-cym})Cl_2]_2$	$PyPPh_2$	1.1
3	$[Ru(p\text{-cym})Cl_2]_2$	**3a**	77.8
3	$[Ru(p\text{-cym})Cl_2]_2$	**3c**	76.0
3	$[Ru(p\text{-cym})Cl_2]_2$	**3d**	82.3
3	$[Ru(p\text{-cym})Cl_2]_2$	**3e**	70.1
3	$[Ru(p\text{-cym})Cl_2]_2$	**3g**	75.2
3	$[Ru(p\text{-cym})Cl_2]_2$	PyPPh2	6.0
3	$[Ru(p\text{-cym})Cl_2]_2$	-	6.1
3	-	**3a**	0.0

4.2 Computational Procedure

Density functional calculations were performed at the ωB97X-D[32] level of theory using Gaussian09, revision A.02.[23] Geometry optimizations were performed using the 6-31+G(d,p)[33] basis set (Def2-TZVP for Rh)[34] and the nature of each stationary point was confirmed by frequency calculations.

Donor capacity 3a,c,e

Complex	E [a.u.]	N-Lonepair orbital	$E_{\text{N-Lonepair orbital}}$ [a.u.]
$[\kappa^1$-**3a**-RhCp*Cl$]^+$	–2129.51071291	HOMO	–0.411209813
$[\kappa^2$-**3a**-RhCp*Cl$]^+$	–2129.53417269	-	-
$[\kappa^1$-**3c**-RhCp*Cl$]^+$	–2466.47571225	HOMO	–0.417133444
$[\kappa^2$-**3c**-RhCp*Cl$]^+$	–2466.49702854	-	-
$[\kappa^1$-**3e**-RhCp*Cl$]^+$	–2208.13175882	HOMO	–0.405049746
$[\kappa^2$-**3e**-RhCp*Cl$]^+$	–2208.1560005	-	-

***E/Z*-Energies 3a-f**

3a	*E*	E = –1168.78866048 a.u.
	Z	E = –1168.78908079 a.u.
3b	*E*	E = –1208.09799401 a.u.
	Z	E = –1208.09829459 a.u.
3c	*E*	E = –1505.75763415 a.u.
	Z	E = –1505.75829593 a.u.
3d	*E*	E = –1842.72766342 a.u.
	Z	E = –1842.72652848 a.u.
3e	*E*	E = –1247.40708378 a.u.
	Z	E = –1247.40791071 a.u.
3f	*E*	E = –1247.40716156 a.u.
	Z	E = –1247.4084032 a.u.

4.3 Crystal structure determinations

The single-crystal X-ray diffraction study were carried out on a Bruker D8 Venture diffractometer with Photon100 detector at 123(2) K using Mo-Kα radiation (**4a**), an Agilent SuperNova Dual diffractometer with Atlas detector at 120(2) K using Cu-Kα radiation (**4e**), Bruker ApexDuo diffractometer with APEXII detector at 120(2) K using Mo-Kα radiation (**6a**), and a Bruker SmartApex diffractometer with APEXII detector at 120(2) K using Mo-Kα radiation (**7a**). Direct Methods (**4e**, **6a**, **7a**) or Patterson (heavy atom) Methods (**4a**) (SHELXS-97)[37] were used for structure solution and refinement was carried out using SHELXL-2013/2014 (full-matrix least-squares on F^2).[38] Hydrogen atoms were localized by difference electron density determination and refined using a riding model. Semi-empirical absorption corrections were applied. For **6a** the absolute structure was determined. In **6a** the triflate anion and in **7a** the solvent CH_2Cl_2 are disordered.

4a (CCDC-1487761): red crystals, $C_{30}H_{33}Cl_2NPRh \cdot CH_2Cl_2$, M_r = 697.28, crystal size 0.18 × 0.10 × 0.04 mm, monoclinic, space group $P2_1/n$ (No. 14), a = 8.8092(7) Å, b = 22.8273(19) Å, c = 15.6744(13) Å, β = 105.690(3)°, V = 3034.5(4) Å^3, Z = 4, ρ = 1.526 Mg/m^{-3}, μ(Mo-K$_\alpha$) = 0.990 mm^{-1}, F(000) = 1424, $2\theta_{max}$ = 60.0°, 109477 reflections, of which 8904 were independent (R_{int} = 0.025), 349 parameters, R_1 = 0.022 (for 8047 I > 2σ(I)), wR_2 = 0.051 (all data), S = 1.08, largest diff. peak / hole = 0.859 / -0.779 e Å^{-3}.

4e (CCDC-1487762): colourless crystals, $C_{32}H_{37}Cl_2NPRh \cdot CH_2Cl_2$, M_r = 725.33, crystal size 0.21 × 0.04 × 0.02 mm, monoclinic, space group $P2_1/n$ (No. 14), a = 8.9362(1) Å, b =

23.6047(3) Å, c = 16.0910(2) Å, β = 104.980(1)°, V = 3278.83(7) Å^3, Z = 4, ρ = 1.469 Mg/m^3, μ(Cu-K$_\alpha$) = 7.845 mm^{-1}, F(000) = 1488, $2\theta_{max}$ = 153.6°, 19225 reflections, of which 6858 were independent (R_{int} = 0.029), 369 parameters, R_1 = 0.034 (for 6296 I > 2σ(I)), wR_2 = 0.084 (all data), S = 1.02, largest diff. peak / hole = 1.447 / -1.838 e Å^{-3}.

6a (CCDC-1487763): orange crystals, $C_{30}H_{33}ClNPRh \cdot CF_3O_3S$, M_r = 725.97, crystal size 0.30 × 0.10 × 0.03 mm, orthorhombic, space group Pna2$_1$ (No. 33), a = 14.4195(3) Å, b = 14.5992(3) Å, c = 15.1828(3) Å, V = 3196.18(11) Å^3, Z = 4, ρ = 1.509 Mg/m^{-3}, μ(Mo-K$_\alpha$) = 0.783 mm^{-1}, F(000) = 1480, $2\theta_{max}$ = 55.4°, 25974 reflections, of which 7166 were independent (R_{int} = 0.045, 370 parameters, 92 restraints, R_1 = 0.036 (for 6737 I > 2σ(I)), wR_2 = 0.097 (all data), S = 1.03, largest diff. peak / hole = 0.427 / -0.319 e Å^{-3}, Parsons' x = -0.037(15).

7a (CCDC-1487764): orange crystals, $C_{31}H_{33}F_3NO_3PRhS \cdot C_3Ag_2F_9O_9S_3 \cdot CH_2Cl_2$, M_r = 1438.40, crystal size 0.20 × 0.12 × 0.08 mm, monoclinic, space group P2$_1$/c (No. 14), a = 11.7349(2) Å, b = 41.0647(6) Å, c = 9.9590(1) Å, β = 91.496(1)°, V = 4797.14(12) Å^3, Z = 4, ρ = 1.992 Mg/m^{-3}, μ(Mo-K$_\alpha$) = 1.572 mm^{-1}, F(000) = 2832, $2\theta_{max}$ = 55.0°, 79507 reflections, of which 11006 were independent (R_{int} = 0.025), 645 parameters, 25 restraints, R_1 = 0.030 (for 10140 I > 2σ(I)), wR_2 = 0.065 (all data), S = 1.17, largest diff. peak / hole = 0.859 / -0.860 e Å^{-3}.

5 Acknowledgments

This work was supported by the Council for Chemical Sciences of The Netherlands Organization for Scientific Research (NWO/CW) and by ARKEMA Vlissingen B.V.

6 References

[1] For a review on hybrid ligands, see Zhang, W.-H.; Chien, S.W.; Hor, T.S.A. *Coord. Chem. Rev.* **2011**, *255*, 1991-2024.

[2] For reviews on cooperativity, see (a) Khusnutdinova, J.R.; Milstein, D. *Angew. Chem. Int. Ed.* **2015**, *54*, 12236-12273. (b) van der Vlugt, J.I. *Eur. J. Inorg. Chem.* **2012**, 363-375.

[3] For reviews on 2-pyridylphosphanes, see: (a) Newkome, G.R. *Chem. Rev.* **1993**, *93*, 2067-2089. (b) Zhang, Z.-Z.; Cheng, H. *Coord. Chem. Rev.* **1996**, *147*, 1-39. (c) Espinet, P; Soulantica, K. *Coord. Chem. Rev.* **1999**, *193-195*, 499-556.

[4] For 1,2-P,N ligands, see (a) Cadierno, V.; Díez, J.; Francos, J.; Gimeno, J. *Chem. Eur. J.* **2010**, *16*, 9808-9817. (b) Díaz-Álvarez, A.E.; Crochet, P.; Zablocka, M.; Duhayon, C.; Cadierno, V.; Majoral, J.-P. *Eur. J. Inorg. Chem.* **2008**, 786-794. (c) García-Álvarez, R.; Díez, J.; Crochet, P.; Cadierno, V. *Organometallics* **2011**, *30*, 5442-5451. (d) García-Álvarez, R.; Díez, J.; Crochet, P.; Cadierno, V.

Organometallics **2012**, *31*, 2941-2944. (e) Knapp, S.M.M.; Sherbow, T.J.; Yelle, R.B.; Zakharov, L.N.; Juliette, J.J.; Tyler, D.R. *Organometallics* **2013**, *32*, 824-834.

[5] For 1,4-P,N ligands, see (a) Lundgren, R.J.; Peters, B.D.; Alsabeh, P.G.; Stradiotto, M. *Angew. Chem. Int. Ed.* **2010**, *49*, 4071-4074. (b) Lundgren, R.J.; Stradiotto, M. *Angew. Chem. Int. Ed.* **2010**, *49*, 8686-8690. (c) Ji, K.; Zheng, Z.; Wang, Z.; Zhang, L. *Angew. Chem. Int. Ed.* **2015**, *54*, 1245-1249. (d) Hesp, K.D.; Stradiotto, M. *J. Am. Chem. Soc.* **2010**, *132*, 18026-18029. (e) Hesp, K.D.; Lundgren, R.J.; Stradiotto, M. *J. Am. Chem. Soc.* **2011**, *133*, 5194-5197.

[6] For 1,5-P,N ligands, see (a) Jiang, C.; Lu, Y.; Hayashi, T. *Angew. Chem. Int. Ed.* **2014**, *53*, 9936-9939. (b) Xu, Z.; McNamara, N.D.; Neumann, G.T.; Schneider, W.F.; Hicks, J.C. *ChemCatChem* **2013**, *5*, 1769-1771. (c) Field, L.D.; Messerle, B.A.; Vuong, K.Q.; Turner, P.; Failes, T.; *Organometallics* **2007**, *26*, 2058-2069. (d) Yang, Y.; Gurnham, J.; Liu, B.; Duchateau, R.; Gambarotta, S.; Korobkov, I. *Organometallics* **2014**, *33*, 5749-5757.

[7] For 1,6-P,N ligands, see Li, Y.-X.; Xuan, Q.-Q.; Liu, L.; Wang, D.; Chen, Y.-J.; Li, C.-J. *J. Am. Chem. Soc.* **2013**, *135*, 12536-12539.

[8] For a review on P,N-ligated multinuclear complexes, see Maggini, S. *Coord. Chem. Rev.* **2009**, *253*, 1793-1832.

[9] (a) Braunstein, P.; Kelly, D.G.; Tiripicchio, A.; Ugozzoli, F. *Bull. Soc. Chim. Fr.* **1995**, *132*, 1083-1086. (b) Carson, E.C.; Lippard, S.J. *J. Am. Chem. Soc.* **2004**, *126*, 3412-3413.

[10] (a) Muranaka, M.; Hyodo, I.; Okumura, W.; Oshiki, T.; *Catal. Today* **2011**, *164*, 552-555. (b) Grotjahn, D.B.; Larsen, C.R.; Gustafson, J.L.; Nair, R.; Sharma, A. *J. Am. Chem. Soc.* **2007**, *129*, 9592-9593. (c) de Pater, J.J.M.; Maljaars, C.E.P.; de Wolf, E.; Lutz, M.; Spek, A.L.; Deelman, B.-J.; Elsevier, C.J.; van Koten, G.; *Organometallics* **2005**, *24*, 5299-5310. (d) Grotjahn, D.B.; Lev, D.A.; *J. Am. Chem. Soc.* **2004**, *126*, 12232-12233. (e) Khin, C.; Hashmi, A. S. K.; Rominger, F. *Eur. J. Inorg. Chem.* **2010**, 1063-1069. (f) Tinnermann, H.; Wille, C.; Alcarazo, M. *Angew. Chem. Int. Ed.* **2014**, *53*, 8732-8736.

[11] (a) García-Álvarez, R.; García-Garrido, S.E.; Díez, J.; Crochet, P.; Cadierno, V. *Eur. J. Inorg. Chem.* **2012**, 4218-4230. (b) Kumar, P.; Kumar Singh, A.; Yadav, M.; Li, P.-Z.; Kumar Singh, S.; Xu, Q.; Shankar Pandey, D. *Inorg. Chim. Acta* **2011**, *368*, 124-131. (c) Kurtev, K.; Ribola, D.; Jones, R.A.; Cole-Hamilton, D.J.; Wilkinson, G. *J. Chem. Soc., Dalton Trans.* **1980**, 55-58. (d) Drent, E.; Arnoldy, P.; Budzelaar, P.H.M. *J. Organomet. Chem.* **1993**, *455*, 247-253. (e) Drent, E.; Arnoldy, P.; Budzelaar, P.H.M. *J. Organomet. Chem.* **1994**, *475*, 57-63. (f) Moldes, I.; de la Encarnación, E.; Ros, J.; Alvarez-Larena, Á.; Piniella, J.F. *J. Organomet. Chem.* **1998**, *566*, 165-174. (g) Kumar, P.; Kumar Singh, A.; Sharma, S.; Shankar Pandey, D. *J. Organomet. Chem.* **2009**, *694*, 3643-3652. (h) Oshiki, T.; Yamashita, H.; Sawada, K.; Utsunomiya, M.; Takahashi, K.; Takai, K. *Organometallics* **2005**, *24*, 6287-6290. (i) Radcliffe, J.E.; Batsanov, A.S.; Smith, D.M.; Scott, J.A.; Dyer, P.W.; Hanton, M.J. *ACS Catal.* **2015**, *5*, 7095-7098.

[12] (a) Wallesch, M.; Volz, D.; Zink, D.M.; Schepers, U.; Nieger, M.; Baumann, T.; Bräse, S. *Chem. Eur. J.* **2014**, *20*, 6578-6590. (b) Shafiq, F.; Eisenberg, R. *Inorg. Chem.* **1993**, *32*, 3287-3294. (c) Volz, D.; Hirschbiel, A.F.; Zink, D.M.; Friedrichs, J.; Nieger, M.; Baumann, T.; Bräse, S.; Barner-Kowollik, C. *J. Mater. Chem. C* **2014**, 1457-1462. (d) Ishii, H.; Goyal, M.; Ueda, M.; Takeuchi, K.; Asai, M. *J. Mol. Cat. A Chem.* **1999**, *148*, 289-293. (e) Ishii, H.; Goyal, M.; Ueda, M.; Takeuchi, K.; Asai, M. *Macromol. Rapid Commun.* **2001**, *22*, 376-381.

[13] (a) Drommi, D.; Nicolò, F.; Arena, C.G.; Bruno, G.; Faraone, F.; Gobetto, R. *Inorg. Chim. Acta* **1994**, *221*, 109-116. (b) Wang, Q.-M.; Lee, Y.-A.; Crespo, O.; Deaton, J.; Tang, C.; Gysling, H.J.; Gimeno, M.C.; Larraz, C.; Villacampa, M.D.; Laguna, A.;

Eisenberg, R. *J. Am. Chem. Soc.* **2004**, *126*, 9488-9489. (c) Zhang, Z.-Z.; Xi, H.-P.; Zhao, W.-J.; Jiang, K.-Y.; Wang, R.-J.; Wang, H.-G.; Wu, Y. *J. Organomet. Chem.* **1993**, *454*, 221-228. (d) Franciò, G.; Scopelliti, R.; Arena, C.G.; Bruno, G.; Drommi, D.; Faraone, F. *Organometallics* **1998**, *17*, 338-347.

[14] (a) Cabon, Y.; Kleijn, H.; Siegler, M.A.; Spek, A.L.; Klein Gebbink, R.J.M.; Deelman, B.-J. *Dalton Trans.* **2010**, *39*, 2423-2427. (b) Derrah, E.J.; Warsink, S.; de Pater, J.J.M.; Cabon, Y.; Reboule, I.; Lutz, M.; Klein Gebbink, R.J.M.; Deelman, B.-J. *Organometallics* **2014**, *33*, 2914-2918. (c) Cabon, Y.; Reboule, I.; Lutz, M.; Klein Gebbink, R.J.M.; Deelman, B.-J. *Organometallics* **2010**, *29*, 5904-5911. (d) Warsink, S.; Derrah, E.J.; Boon, C.A.; Cabon, Y.; de Pater, J.J.M.; Lutz, M.; Klein Gebbink, R.J.M.; Deelman, B.-J. *Chem. Eur. J.* **2015**, *21*, 1765-1779. (e) Powers, D.C., Anderson, B.L.; Hwang, S.J.; Powers, T.M.; Pérez, L.M.; Hall, M.B.; Zheng, S.-L.; Chen, Y.-S.; Nocera, D.G. *J. Am. Chem. Soc.* **2014**, *136*, 15346-15355.

[15] (a) Harkal, S.; Rataboul, F.; Zapf, A.; Fuhrmann, C.; Riermeier, T.; Monsees, A.; Beller, M. *Adv. Synth. Catal.* **2004**, *346*, 1742-1748. (b) Singer, R.A.; Tom, N.J.; Frost, H.N.; Simon, W.M. *Tetrahedron Lett.* **2004**, *45*, 4715-4718.

[16] First, respectively, reported and coordinated in: (a) Mann, F.G.; Watson, J. *J. Org. Chem.* **1948**, *13*, 502-531. (b) Ang, H.G.; Kow, W.E.; Mok, K.F. *Inorg. Nucl. Chem. Lett.* **1972**, *8*, 829-832.

[17] (a) van Dijk, T.; Burck, S.; Rong, M.K.; Rosenthal, A.J.; Nieger, M.; Slootweg, J.C.; Lammertsma, K. *Angew. Chem. Int. Ed.* **2014**, *53*, 9068-9071. (b) van Dijk, T.; Burck, S.; Rosenthal, A.J.; Nieger, M.; Ehlers, A.W.; Slootweg, J.C.; Lammertsma, K. *Chem. Eur. J.* **2015**, *21*, 9328-9331. (c) van Dijk, T.; Bakker, M.S.; Holtrop, F.; Nieger, M.; Slootweg, J.C.; Lammertsma, K. *Org. Lett.* **2015**, *17*, 1461-1464.

[18] (a) Govindaswamy, P.; Carroll, P.J.; Mozharivskyj, Y.A.; Kollipara, M.R. *J. Chem. Sci.* **2006**, *118*, 319-326. (b) Drommi, D.; Arena, C.G.; Nicolò, F.; Bruno, G.; Faraone, F. *J. Organomet. Chem.* **1995**, *485*, 115-121. (c) Wajda-Hermanowicz, K.; Ciunik, Z.; Kochel, A. *Inorg. Chem.* **2006**, *45*, 3369-3377. (d) Clarke, M.L.; Slawin, A.M.Z.; Wheatley, M.V.; Woollins, J.D. *J. Chem. Soc., Dalton Trans.* **2001**, 3421-3429.

[19] (a) Murahashi, S.-I.; Naota, T.; Saito, E. *J. Am. Chem. Soc.* **1986**, *108*, 7846-7847. (b) For reviews on the catalytic hydration of nitriles, see: (a) Ahmed, T.J.; Knapp, S.M.M.; Tyler, D.R.; *Coord. Chem. Rev.* **2011**, *255*, 949-974. (b) García-Álvarez, R.; Francos, J.; Tomás-Mendivil, E.; Crochet, P.; Cadierno, V. *J. Organomet. Chem.* **2014**, *771*, 93-104.

[20] Garciá-Álvarez, R.; Francos, J.; Crochet, P.; Cadierno, V. *Tetrahedron Lett.* **2011**, *52*, 4218-4220.

[21] Li, Z.; Wang, L.; Zhou, X. *Adv. Synth. Catal.* **2012**, *354*, 584-588.

[22] (a) Booth, B.L.; Jibodu, K.O.; Proença, M.F. *J. Chem. Soc., Chem. Commun.* **1980**, 1151-1153. (b) Booth, B.L.; Jibodu, K.O.; Proença, M.F.J.R.P. *J. Chem. Soc., Perkin Trans. 1* **1983**, 1067-1073.

[23] Gaussian 09, Revision A.02, Frisch, M.J.; Trucks, G.W.; Schlegel, H.B.; Scuseria, G.E.; Robb, M.A.; Cheeseman, J.R.; Scalmani, G.; Barone, V.; Mennucci, B.; Petersson, G.A.; Nakatsuji, H.; Caricato, M.; Li, X.; Hratchian, H.P.; Izmaylov, A.F.; Bloino, J.; Zheng, G.; Sonnenberg, J.L.; Hada, M.; Ehara, M.; Toyota, K.; Fukuda, R.; Hasegawa, J.; Ishida, M.; Nakajima, T.; Honda, Y.; Kitao, O.; Nakai, H.; Vreven, T.; Montgomery, J.A., Jr.; Peralta, J.E.; Ogliaro, F.; Bearpark, M.; Heyd, J.J.; Brothers, E.; Kudin, K.N.; Staroverov, V.N.; Kobayashi, R.; Normand, J.; Raghavachari, K.; Rendell, A.; Burant, J.C.; Iyengar, S.S.; Tomasi, J.; Cossi, M.; Rega, N.; Millam, J.M.; Klene, M.; Knox, J.E.; Cross, J.B.; Bakken, V.; Adamo, C.; Jaramillo, J.; Gomperts, R.; Stratmann, R.E.; Yazyev, O.; Austin, A.J.; Cammi, R.; Pomelli, C.; Ochterski, J.W.; Martin, R.L.; Morokuma, K.; Zakrzewski, V.G.; Voth,

G.A.; Salvador, P.; Dannenberg, J.J.; Dapprich, S.; Daniels, A.D.; Farkas, O.; Foresman, J.B.; Ortiz, J.V.; Cioslowski, J.; Fox, D.J. Gaussian, Inc., Wallingford CT, 2009.

[24] For rhodium(III) catalysis, see (a) Zhao, D.; Vásquez-Céspedes, S.; Glorius, F. *Angew. Chem. Int. Ed.* **2015**, *54*, 1657-1661. (b) Ai, W.; Yang, X.; Wu, Y.; Wang, X.; Li, Y.; Yang, Y.; Zhou, B. *Chem. Eur. J.* **2014**, *20*, 17653-17657. (c) Hwang, H.; Kim, J.; Jeong, J.; Chang, S. *J. Am. Chem. Soc.* **2014**, *136*, 10770-10776. (d) Chen, W.-J.; Lin, Z. *Organometallics* **2015**, *34*, 309-318.

[25] (a) Hintermann, L.; Dang, T.T.; Labonne, A.; Kribber, T.; Xiao, L.; Naumov, P. *Chem. Eur. J.* **2009**, *15*, 7167-7179. (b) Boeck, F.; Kribber, T.; Xiao, L.; Hintermann, L. *J. Am. Chem. Soc.* **2011**, *133*, 8138-8141. (c) Labonne, A.; Kribber, T.; Hintermann, L. *Org. Lett.* **2006**, *8*, 5853-5856. (d) Almeida Leñero, K.Q.; Guari, Y.; Kamer, P.C.J.; van Leeuwen, P.W.N.M.; Donnadieu, B.; Sabo-Etienne, S.; Chaudret, B.; Lutz, M.; Spek, A.L. *Dalton Trans.* **2013**, *42*, 6495-6512. (e) Wang, Y.; Zheng, Z.; Zhang, L. *Angew. Chem. Int. Ed.* **2014**, *53*, 9572-9576. (f) Tomás-Mendivil, E.; García-Álvarez, R.; García-Garrido, S.E.; Díez, J.; Crochet, P.; Cadierno, V. *J. Organomet. Chem.* **2013**, *727*, 1-9.

[26] (a) Govindaswamy, P.; Süss-Fink, G.; Therrien, B. *Acta Cryst.* **2007**, *E63*, m2046. (b) Han, W.S.; Lee, S.W. *Inorg. Chim. Acta* **2003**, *348*, 15-24. (c) Schwarz, M.B.; Kurzwernhart, A.; Roller, A.; Kandioller, W.; Keppler, B.K.; Hartinger, C.G. *Z. Anorg. Allg. Chem.* **2013**, 1648-1654.

[27] (a) Côté, A.P.; Ferguson, M.J.; Khan, K.A.; Enright, G.D.; Kulynych, A.D.; Dalrymple, S.A.; Shimizu, G.K.H. *Inorg. Chem.* **2002**, *41*, 287-292. (b) Wang, Q.-M.; Guo, G.-C.; Mak, T.C.W. *J. Organomet. Chem.* **2003**, *670*, 235-242. (c) Zhao, L.; Wan, C.-Q.; Han, J.; Chen, X.-D.; Mak, T.C.W. *Chem. Eur. J.* **2008**, *14*, 10437-10444. (d) Shimizu, G.K.H.; Enright, G.D.; Ratcliffe, C.I.; Preston, K.F.; Reid, J.L.; Ripmeester, J.A. *Chem. Commun.* **1999**, 1485-1486. (e) Wang, Q.-M.; Mak, T.C.W. *Chem. Commun.* **2001**, 807-808. (f) Zhang, T.; Ji, C.; Wang, K.; Fortin, D.; Harvey, P.D. *Inorg. Chem.* **2010**, *49*, 11069-11076. (g) Lu, X.L.; Leong, W.K.; Hor, T.S.A.; Goh, L.Y. *J. Organomet. Chem.* **2004**, *689*, 1746-1756.

[28] DCM rarely acts as coordinating solvent but has been observed for Ag(I) complexes. (a) Krossing, I. *Chem. Eur. J.* **2001**, *7*, 490-502. (b) Decken, A.; Knapp, C.; Nikiforov, G.B.; Passmore, J.; Rautiainen, J.M.; Wang, X.; Zeng, X. *Chem. Eur. J.* **2009**, *15*, 6504-6517. (c) Forniés, J.; Martínez, F; Navarro, R.; Urriolabeitia, E.P. *Organometallics* **1996**, *15*, 1813-1819.

[29] For a review on ruthenium catalyzed nitrile hydration, see: García-Álvarez, R.; Francos, J.; Tomás-Mendivil, E.; Crochet, P.; Cadierno, V. *J. Organomet. Chem.* **2014**, *771*, 93-104.

[30] (a) Kumar, P.; Kumar Gupta, R.; Shankar Pandey, D. *Chem. Soc. Rev.* **2014**, *43*, 707-733. (b) Bruneau, C.; Achard, M. *Coord. Chem. Rev.* **2012**, *256*, 525-536. (c) Naota, T.; Takaya, H.; Murahashi, S.-I. *Chem. Rev.* **1998**, *98*, 2599-2660.

[31] (a) For a review on aqueous catalytic nitrile hydration, see: García-Álvarez, R.; Crochet, P.; Cadierno, V. *Green Chem.* **2013**, *15*, 46-66. (b) For a review on aqueous Ru(II) catalysis, see: Crochet, P.; Cadierno, V. *Dalton Trans.* **2014**, *43*, 12447-12462.

[32] (a) Chai, J.-D.; Head-Gordon, M. *Phys. Chem. Chem. Phys.* **2008**, *10*, 6615–6620. (b) Chai, J.-D.; Head-Gordon, M. *J. Chem. Phys.* **2008**, *128*, 084106.

[33] (a) Ditchfield, R.; Hehre, W.J.; Pople, J.A. *J. Chem. Phys.* **1971**, *54*, 724-728. (b) Hehre, W.J.; Ditchfield, R.; Pople, J.A. *J. Chem. Phys.* **1972**, *56*, 2257-2261. (c) Hariharan, P.C.; Pople, J.A. *Theor. Chem. Acc.* **1973**, *28*, 213-222. (d) Hariharan, P.C.; Pople, J.A. *Mol. Phys.* **1974**, *27*, 209-214. (e) Gordon, M.S. Chem. *Phys. Lett.* **1980**, *76*, 163-168. (f) Francl, M.M.; Pietro, W.J.; Hehre, W.J.; Binkley, J.S.;

DeFrees, D.J.; Pople, J.A.; Gordon, M.S. *J. Chem. Phys.* **1982**, *77*, 3654-3665. (g) Binning, R.C., Jr.; Curtiss, L.A. *J. Comp. Chem.* **1990**, *11*, 1206-1216. (h) Blaudeau, J.-P.; McGrath, M.P.; Curtiss, L.A.; Radom, L. *J. Chem. Phys.* **1997**, *107*, 5016-5021. (i) Rassolov, V.A.; Pople, J.A.; Ratner, M.A.; Windus, T.L. *J. Chem. Phys.* **1998**, *109*, 1223-1229. (j) Rassolov, V.A.; Ratner, M.A.; Pople, J.A.; Redfern, P.C.; Curtiss, L.A. *J. Comp. Chem.* **2001**, *22*, 976-984. (k) Clark, T.; Chandrasekhar, J.; Spitznagel, G.W.; Schleyer, P.V.R. *J. Comp. Chem.* **1983**, *4*, 294-301.

[34] Andrae, D.; Häußermann, U.; Dolg, M.; Stoll, H.; Preuß, H. *Theoret. Chim. Acta* **1990**, *77*, 123-141.

[35] Adapted from: Finch, A.; Gardner, P.J.; Gupta, K.K.S. *J. Chem. Soc. B* **1966**, 1162-1164.

[36] Adapted from: Ciola, R.; Burwell, R.L., Jr. *J. Org. Chem.* **1958**, *23*, 1063-1065.

[37] Sheldrick, G.M. *Acta Crystallogr.* **2008**, *A64*, 112-122.

[38] Sheldrick, G.M. *Acta Crystallogr.* **2015**, *C71*, 3-8.

Chapter IV

Atypical And Asymmetric 1,3-P,N-Ligands: The Synthesis, Coordination and Catalytic Performance of Cycloiminophosphanes

Mark K. Rong, Flip Holtrop, Eduard O. Bobylev, Martin Nieger, Andreas W. Ehlers, J. Chris Slootweg, and Koop Lammertsma

Novel seven-membered cyclic imine-based 1,3-P,N-ligands were obtained by capturing an *in situ* generated Beckmann nitrilium ion intermediate from cyclohexanone with benzotriazole, and then displacing it by a secondary phosphane under triflic acid promotion. These 'cycloiminophosphanes' possess flexible non-isomerizable tetrahydroazepine rings with a high basicity, which sets them apart from previously reported iminophophanes. The donor strength of the ligands was investigated using their P-κ^1- and P,N-κ^2-tungsten(0) carbonyl complexes, by determining the IR frequency of the *trans*-CO ligands. Complexes with $[RhCp^*Cl_2]_2$ demonstrated the hemilability of the ligands, by giving a dynamic equilibrium of κ^1- and κ^2-species; treatment with AgOTf gives full conversion to the κ^2-complex. The potential for catalysis was shown in the Ru^{II}-catalyzed solvent-free hydration of benzonitrile and the Ru^{II}- and Ir^{I}-catalyzed transfer hydrogenation of cyclohexanone in isopropanol. Finally, to enable access to asymmetric catalysts, chiral cycloiminophosphanes were prepared from L-menthone, as well as their P,N-κ^2-Rh^{III}- and a P-κ^1-Ru^{II}-complexes.

Chem. Eur. J. **2021**, *27*, 14007-14016.

1 Introduction

Ligand-based reactivity can enhance the activity of transition metal catalysts,[1] as is the case for hybrid ligands,[2] which combine the properties of different heteroatoms to enable hemilability, redox non-innocence, proton-shuttling, and substrate coordination.[1,2] 1,3-P,N-ligands are particularly subject to diverse binding modes (N-κ^1, P-κ^1, P-$\kappa^1\eta^2$, κ^2, and μ; Figure 1) and their complexes have found application in homo/heterogeneous catalysis, bio-inorganic chemistry, and photoluminescence.[3-7] Most of these 1,3-P,N-complexes are based on pyridyl- and imidazolyl-based ligands **A** and **B**, which have structural limitations that are inherent to their syntheses.[4c,5] Recently we reported on the highly tunable iminophosphanes **C** and their tautomers phosphaamidines **D** that can be independently substituted on the P, C, and N-atoms.[6,7] These 1,3-P,N-ligands are readily accessible from (base-stabilized) nitrilium triflate precursors and even though they are obtained as (dynamic) E/Z isomer mixtures, the equilibrium shifts to the desired Z-conformer on coordination to metals (Figure 2).[6] The hapticity in κ^1/κ^2-[(P,N)RhCp*Cl_2]-complexes and the favorable performance in (κ^1-P,N)-Ru(II)-catalyzed nitrile hydration correlated with the electronic properties of the ligands[6d] and the basicity of the nitrogen-donor (Figure 3).[3,4]

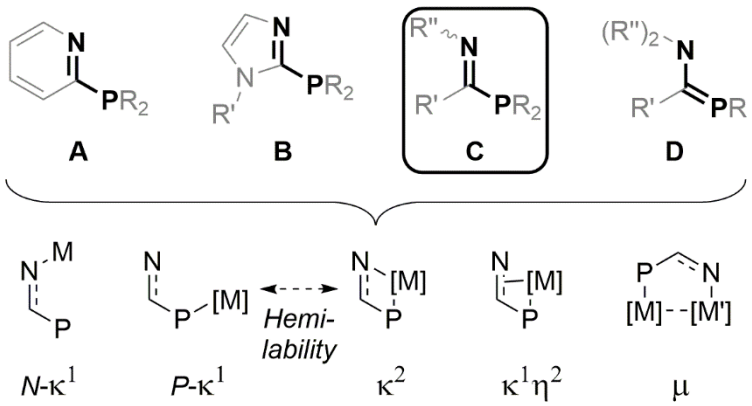

Figure 1. 1,3-P,N ligands and their diverse transition metal complexes.

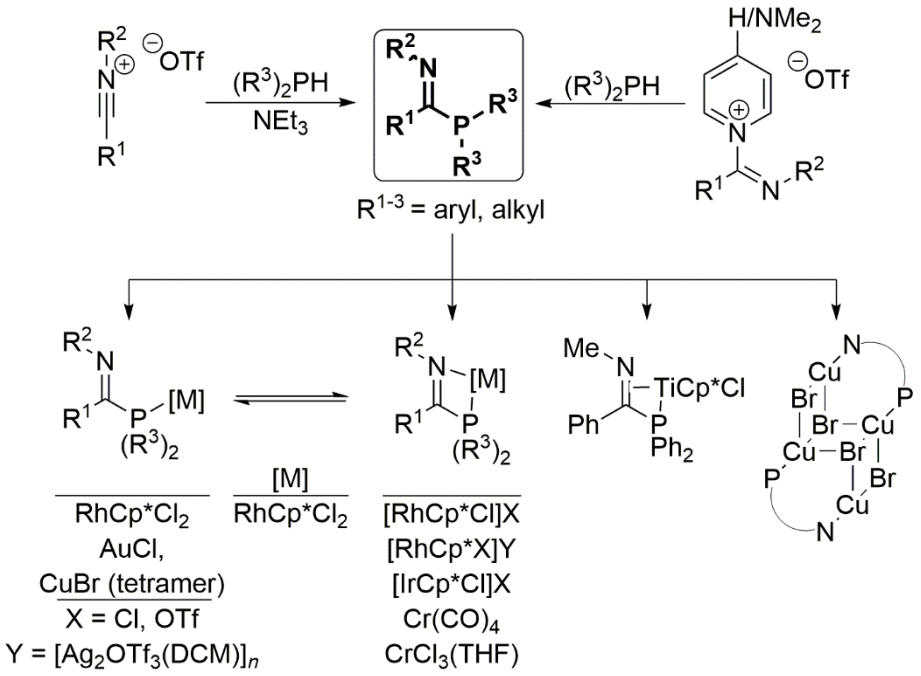

Figure 2. Synthesis of iminophosphanes and hemilabile metal-coordination.

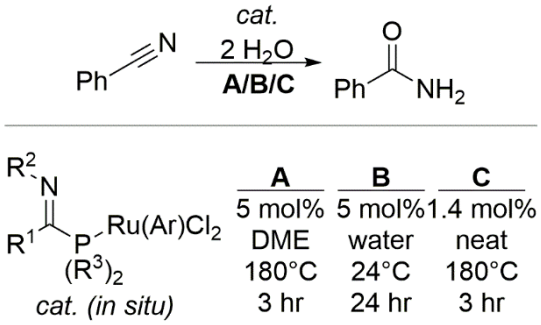

Figure 3. Catalyzed nitrile hydration.

Iminophosphanes **C** are accessed from nitrilium ion precursors, which are known both as reactive synthons and intermediates.[5,8] Illustrative is the Beckmann rearrangement of cyclohexanone oxime to the ring-expanded seven-membered nitrilium intermediate (with an iminium resonance form), which hydrolyzes to the ε-caprolactam that is used as the building block for the commercial production of nylon-6 (Figure 4, top).[9,10] The

intermediate can also be trapped by nucleophiles, for instance by benzotriazole,[11] which under Lewis acid promotion can be displaced by other nucleophiles.[11a] This reactivity mirrors our reported nitrilium triflate approach for the synthesis of **C** and might be suitable to access novel seven-membered cyclic iminophosphanes (Figure 4, **E**). Such 'cycloiminophosphanes' would be conformationally locked, i.e., unable to undergo E/Z-isomerization (Figure 5), may carry chiral groups as the required chiral cyclohexanone precursors are readily available from terpenoids used in, for instance, the flavoring and perfume industry.[12]

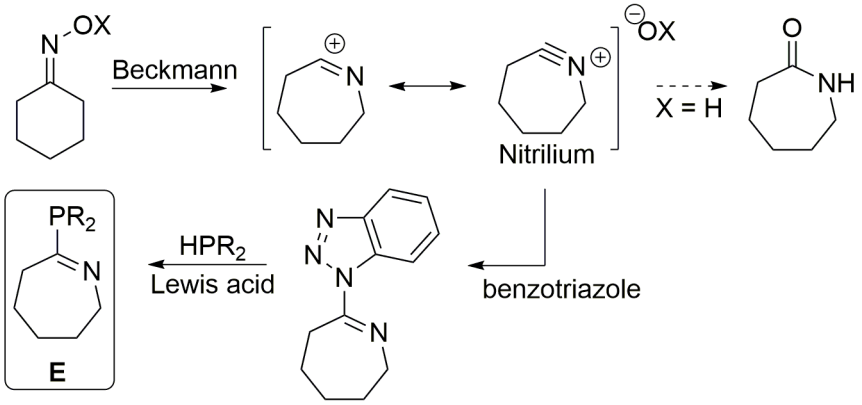

Figure 4. Cycloiminophosphane synthesis from the Beckmann nitrilium intermediate.

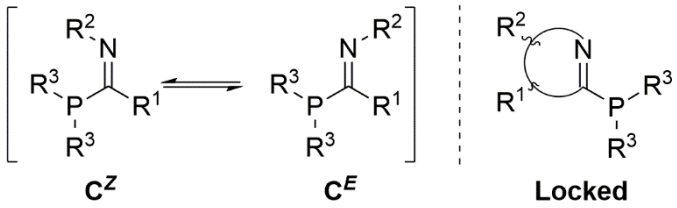

Figure 5. Non-isomerizable cycloiminophosphanes.

In the present study we report on both the synthesis of these novel cyclic 1,3-P,N-ligands and their surprising electronic properties that sets them apart from non-cyclic iminophosphanes. We explore their coordination to early and late transition metals in κ^1/κ^2 complexes and assess their performance in catalytic nitrile hydration and transfer hydrogenation.

Crystal structures are provided for the (a)symmetric tetrahydroazepine synthons, ligands, and a W complex.

2 Results and Discussion

The synthesis of the cyclic ligands is discussed first, followed by an analysis of their donor capacity using IR- and ^{31}P NMR spectroscopy on W^0 carbonyl complexes and dynamic Rh^{III} complexes, respectively. Next, Ru^{II} species are examined to evaluate the ligands' performance in homogeneous catalysis. We also discuss analogous asymmetric ligands with a natural product-derived backbone.

2.1 Precursor synthesis

Our synthetic strategy is based on reacting phosphanes with a seven-membered ring nitrilium ion, i.e., the 3,4,5,6-tetrahydro-azepinium ion.[10] Because this ion could not be accessed by our established methodology in which amides are reacted to imidoyl halides with subsequent halide to triflate exchange,[6] as the activating agents converted ε-caprolactam to thick intractable mixtures of presumably protonated imidoyl chloride, dimers and/or nylon like polymers,[13,14] we decided to generate the desired nitrilium ion in situ using the Beckmann rearrangement and trap it with benzotriazole.[11]

Treating neat cyclohexanone with hydroxylamine·HCl salt by grinding them together in a mortar, while slowly adding NaOH, yielded the corresponding pure oxime conveniently, even on large scale (120 mmol, 82%; Scheme 1).[15] Next, under an atmosphere of nitrogen, the oxime was activated *in situ* as the corresponding methylsulfonate with methylsulfonyl chloride and triethylamine in MeCN at 0 °C.[11c,16] Benzotriazole was added and the mixture was heated to reflux for 2 h to facilitate the ring expansion and trap the nitrilium ion. The reported

work-up[11c] was significantly simplified by adding water to the crude mixture to precipitate pure **4** as a white solid in good yield (60%); alternatively, evaporation, extraction into Et_2O and filtration over neutral alumina also provides **4** (58%). Single crystals suitable for X-ray diffraction analysis were obtained from Et_2O and revealed a remarkably flat conformation [N1-C1-N2-N3 = 179.54(8); C6-C1-N2-N3 = −0.37(12)], presumably due to N1- - -H11 and N3- - -H6A hydrogen bonding (2.50 and 2.29 Å, respectively; Figure 6). The C1-N1 bond length of 1.2643(13) Å is typical for an imine bond and the C1-N2 bond of 1.4334(12) Å is similar to those of other N-heterocycle stabilized imines.[6c]

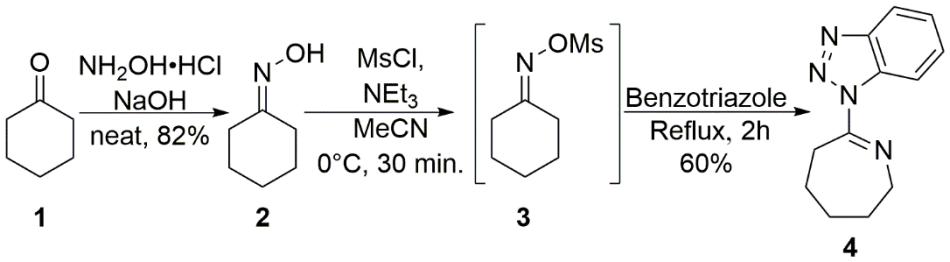

Scheme 1. Benzotriazolyl-tetrahydroazepine synthesis.

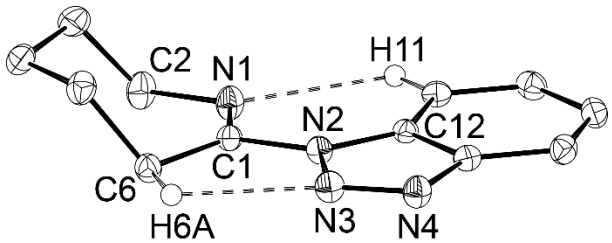

Figure 6. Displacement ellipsoid plot of benzotriazolyl tetrahydroazepine **4** at the 50% probability level. Hydrogen atoms are omitted for clarity, with exception of H6A and H11. Selected bond lengths (Å) and angles (°): C1-N1 =1.2643(13), C1-N2 = 1.4334(12), N1-C2 =1.4693(12), C1-C6 = 1.5046(13), N2-N3 = 1.3746(11), N3-N4 = 1.2947(12), N2-C12 = 1.3780(12), N3 - - -H6A =2.29, N1 - - -H11 = 2.50, N1-C1-N2 = 114.81(9), N1-C1-C6 = 129.01(9), N2-C1-C6 = 116.18(8), C1-N1-C2 = 118.88(9), N1-C1-N2-N3 = 179.54(8), C6-C1-N2-N3 = −0.37(12).

2.2 Phosphane introduction

In analogy to the formation of **4**, we tried to capture the *in situ* generated 3,4,5,6-tetrahydro-azepinium ion directly with a phosphane to obtain the desired cycloiminophosphane ligand **E**, but to no avail. Instead, the benzotriazole group of **4** could be replaced for diphenylphosphane using Lewis acid promotion, which we examined under a variety of conditions (Scheme 2, Table 1). We started with a microwave reaction employed in related displacements by *N*-nucleophiles,[11a] but this reaction using 10 mol% $AlCl_3$ (entry 1) proved to be less effective than regular heating under reflux (entries 2 and 3). The still modest conversion, probably due to Lewis pair interaction with the phosphane,[17] could be enhanced by increasing the amount of $AlCl_3$ (entries 4, 5). Using equimolar amounts, $AlCl_3$ proved to be more selective than $SnCl_2$, $SnCl_4$, and BF_3 (entries 5-10) and resulted in 99% conversion to an Al-adduct of the desired ligand, which on treatment with water gave the protonated ligand and a mixture of oxy aluminum anions. However, the by far most effective and convenient manner to obtain the protonated ligand was found to be the direct activation of **4** through protonation with triflic acid (entry 11).

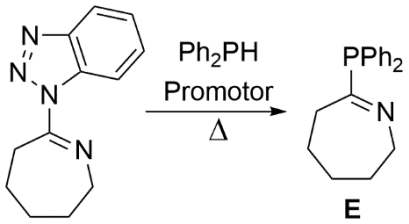

Scheme 2. The activation of **4** for Ph_2PH introduction.

Table 1. Lewis acid induced exchange of the benzotriazolyl group of **4** for PPh_2.[a]

Entry	Promotor	Loading [mol%]	Solvent	t [min.]	Conversion to **E** [%]	Selectivity for **E** [%][b]
1[c]	$AlCl_3$	10%	$CHCl_3$	10	25	100
2	$AlCl_3$	10%	$CHCl_3$	90	40	95
3	$AlCl_3$	10%	$CHCl_3$	300	57	88
4	$AlCl_3$	25%	$CHCl_3$	90	64	93
5	$AlCl_3$	100%	$CHCl_3$	90	99	99[d]
6	$SnCl_2$	100%	$CHCl_3$	90	70	95
7	$SnCl_2$	100%	$CHCl_3$	300	72	97
8	$SnCl_2$	100%	Toluene	300	36	63
9	$SnCl_4$	100%	$CHCl_3$	300	50	50
10	$BF_3{\cdot}OEt_2$	100%	$CHCl_3$	300	76	92
11[e]	HOTf	100%	$CHCl_3$	10	100	100

[a] Conditions: 1 equiv. Ph_2PH, solvent (0.35M), reflux. [b] Determined by ^{31}P NMR spectroscopy. [c] T =80°C, µW conditions, 0.25M. [d] Conversion to the $AlCl_3$ adduct of **6**. [e] RT, 0.5M.

Treatment of **4** with 1 equiv. of triflic acid at 0 °C resulted instantly in a suspension from which its iminium form **5** could be isolated by filtration (Scheme 3). Whereas **5** is subject to decomposition over time, both in solution and as an isolated solid, it reacted cleanly upon immediate resuspension with phosphanes to give **6** within minutes**.** After work-up, diphenyl derivative **6a** was obtained in 77% as an air-stable solid. The aliphatic derivatives **6b**,**c** (conversion 85% (*n*-Bu) and 66% (Cy)) could not be purified satisfactorily until after the subsequent deprotonation-step (vide infra). Bulky substituents may hinder the formation of **6**, as suggested by the lower selectivity found for **6c**. Crystals suitable for X-ray diffraction could be obtained for **6a** and **6c** by slow diffusion of pentane into a THF solution. The molecular structures show a chair conformation for the tetrahydroazepine rings, with the P-lone pair facing away from the imine (Figure 7). Generally, the structures are comparable to those reported for non-cyclic iminophosphane ligands.[6a,b] The imine bond

lengths are in the expected range [**6a**: N1-C1 = 1.2858(16) Å; **6c**: N1-C1 = 1.2892(19) Å], as are the P-C bonds [**6a**: P1-C1 = 1.8269(13) Å; **6c**: P1-C1 = 1.8310(16) Å].[18]

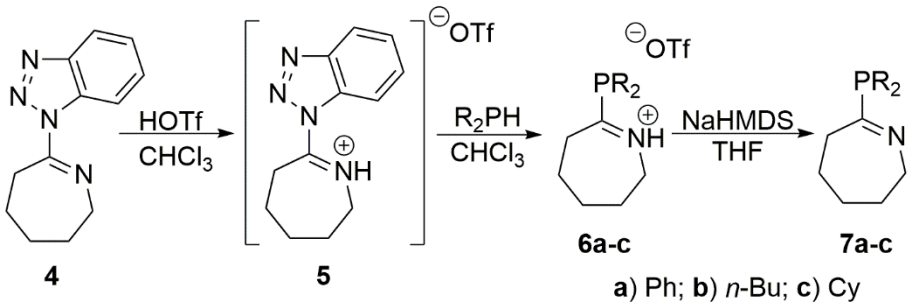

Scheme 3. Acid-facilitated activation of **4** to access ligands **6** and **7**.

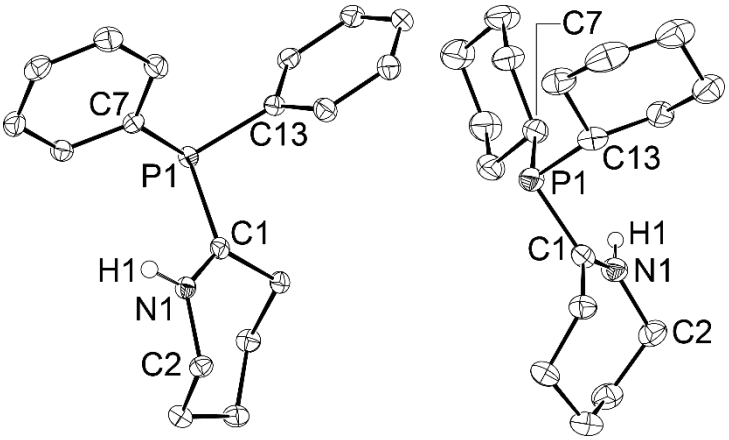

Figure 7. Displacement ellipsoid plot of phosphaazepinium triflates **6a** (left) and **6c** (right) at the 50% probability level. C-H hydrogen atoms and the triflate anions are omitted for clarity. Selected bond lengths (Å) and angles (°) of **6a**: P1-C1 = 1.8269(13), P1-C7 = 1.8249(13), P1-C13 = 1.8223(13), C1-N1 = 1.2858(16), N1-C2 = 1.4839(16), N1-H1 = 0.869(13), N1-C1-P1 = 123.06(10) N1-C1-C6 = 119.70(11), C1-N1-C2 = 125.03(11); Selected bond lengths (Å) and angles (°) of **6c**: P1-C1 = 1.8310(16), P1-C7 = 1.8478(15), P1-C13 = 1.8697(16), C1-N1 = 1.2892(19), N1-C2 = 1.4779(19), N1-C1-P1 = 124.44(12), N1-C1-C6 = 120.25(14), C1-N1-C2 = 125.72(13).

Compounds **6a-c** could be readily deprotonated in THF by using NaHMDS as base at −78 °C and then extracted into pentane to provide

the desired novel ligands (**7a**: 92%; **7b**: 83%; **7c**: 76% yield). Surprisingly, and in contrast to **6**, the products show two distinct sets of signals in the ^{31}P NMR spectra with small differences in chemical shifts [**7a**: δ 6.0 (14%), 5.4 (86%); **7b**: δ −10.7 (95%), −17.5 (5%); **7c**: δ 17.5 (88%), 13.5 (12%)]. Conformational flips of the aliphatic rings, known as flippamers, are known to be observable by NMR spectroscopy,[19] and this may also be the case for the tetrahydroazepine ring in **7** (Figure 8, with the presumed major conformer in the center).

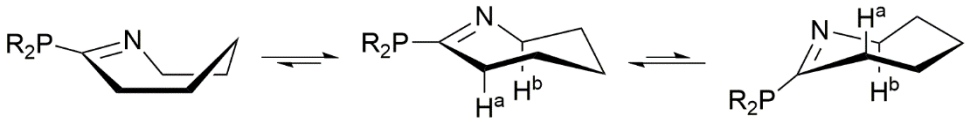

Figure 8. Possible tetrahydroazepine-ring conformations (flippamers) for **7a-c**. Two axial protons are marked for clarity.

A striking property of **7** is its relative basicity. For example, dissolving **7** in $CDCl_3$ led to its instant decomposition, presumably due to protonation (chloroform pK_a > 16). Compared to known iminophosphanes, the seemingly higher basicity of **7** may be attributable to its C- and N-alkyl substituents. For comparison, we synthesized non-cyclic C,N-dimethyl iminophosphane **9** from the nitrilium ion obtained by methylation of acetonitrile (**8**, 91%)[20] and diphenylphosphane (Scheme 4). Also in this case, a strong base (*n*-BuLi) was needed to generate the 1,3-P,N-product (93%; δ(^{31}P) = 6.7 (E), −13.2 (Z)), whereas NEt_3 (pK_a ≈ 11) sufficed for previously reported ligands.[6] The unexpected high basicity of **7** seems akin to that of structurally related 1,3-N,N-bases such as DBU.[21]

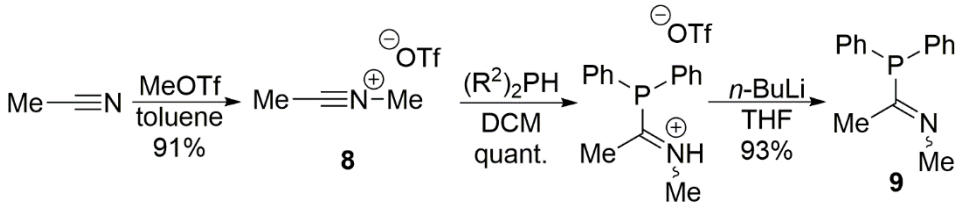

Scheme 4. Synthesis of the non-cyclic **7a**-analogue **8**.

2.3 Coordination Chemistry and Catalysis

The donor strength of P,N-ligands affects their efficiency in cooperative reactions.[3,4,6] To examine the influence of **7** in transition metal complexes, we synthesized the tungsten carbonyl complexes **10, 11** as the IR frequency of their trans-CO ligands reflect the ligand's P,N-donor strength.[22] Reacting ligand **7a** with either $[W(CO)_5(MeCN)]$ or $[(COD)W(CO)_4]$ provided, respectively, κ^1-complex **10** (82%) and κ^2-complex **11** (83%; Scheme 5). IR spectroscopic analysis of the trans-CO ligands indicated increasing electron donation to the metal for **11** (2069, 2008 (*trans*), 1869, 1825 cm^{-1}) with respect to **10** (2069 (*trans*), 1904, 1873 cm^{-1}). Compared to the analogous W-complexes of the widely applied Ph_2PPy ligand (Figure 1, **A**; κ^1: 2050, 1980, 1920 cm^{-1}; κ^2: 2017, 1890, 1870, 1826 cm^{-1})[22a] **7a** appears to be a far stronger *N*-donor. Of note is that the CO-stretches for κ^2-complex **11** are weaker than those of κ^1-complex **10**, which illustrates that the additional coordination of the strong *N*-donor provides a more electron rich metal center with stronger W→(CO) backdonation. Single crystals of **10** were obtained by cooling a toluene solution. The molecular structure (Figure 10) shows a tight bond of the metal center with the trans-CO [W1-C19 = 2.0058(18) Å; $W\text{-}C_{avg.}$ = 2.045525 Å] and a slightly weakened CO triple bond [C19-O1 = 1.142(2) Å; $C\text{-}O_{avg.}$ = 1.1385 Å]. The W1-P1 distance [2.5333(4) Å] is comparable to the one in analogous PPh_3 and Ph_2PPy complexes.[22a,23] Further parameters of the ligand are similar to those for **6a**.

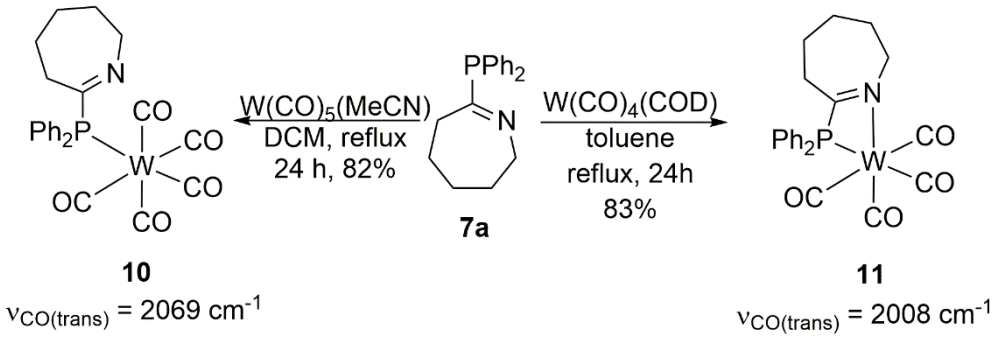

Scheme 5. Analysis donor capacity of **7a** using $W(CO)_n$ complexes.

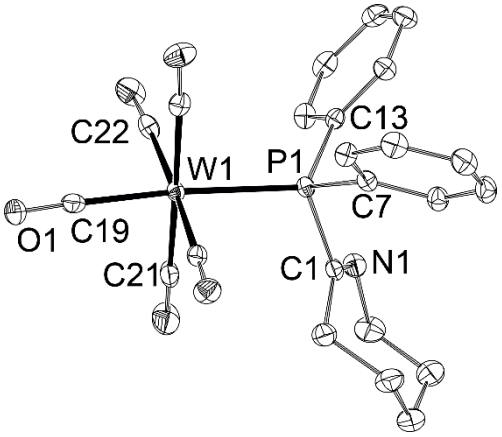

Figure 9. Displacement ellipsoid plot of W carbonyl complex **10** at 50% probability level. Hydrogen atoms are omitted for clarity. Selected bond lengths (Å) and angles (°): W1-P1 = 2.5333(4), W1-C19 = 2.0058(18), C19-O1 = 1.142(2), P1-C13 = 1.8216(15), P1-C7 = 1.8234(16), P1-C1 = 1.8617(16), C1-N1 = 1.265(2), C19-W1-P1 = 175.60(5), O1-C19-W1 = 177.95(15), N1-C1-P1 = 117.22(12), C1-P1-W1-C21 = −15.71(8), C13-P1-W1-C22 = 14.32(7).

The influence of P-substituents[5c] was apparent in [(**7**)Rh^{III}(Cp*)Cl_2] complexes, which can equilibrate between P-κ^1 and P,N-κ^2 forms with characteristic ^{31}P NMR chemical shifts and coupling constants, as has been shown for related iminophosphanes (generally: $^1J_{P,Rh^{\kappa 1}} \approx 146$ Hz; $^1J_{P,Rh^{\kappa 2}} \approx 114$ Hz; e.g. [(Me-NC(Ph)P(3-Me-Ph)$_2$)RhCp*Cl_2] (P-κ^1: δ 34.7 ppm, $^1J_{P,Rh}$ = 144.6 Hz; *P,N*-κ^2: (δ −12.1 ppm, $^1J_{P,Rh}$ = 114.7 Hz); see also Figure 2).[6b,d] To obtain the complexes, **7** was reacted with 0.5 equiv.

[Rh(III)Cp*Cl_2]$_2$ in DCM (Scheme 6) to give exclusively P-κ^1 complexes for the *n*-butyl substituted ligand (**12b**: δ 29.7 ppm, $^1J_{P,Rh}$ = 134.2 Hz, major (98%); 21.3 ppm, $^1J_{P,Rh}$ = 136.2 Hz, minor (2%)) and mainly the P,N-κ^2 complex for the dicyclohexyl ligand (**12c**: δ −1.5 ppm, $^1J_{P,Rh}$ = 104.5 Hz, major (66%); 41.0 ppm, $^1J_{P,Rh}$ = 133.4 Hz, minor (18%); 31.2 ppm, $^1J_{P,Rh}$ = 130.6 Hz, minor (16%)). The observation of two P-κ^1 resonances suggests the presence of flippamers or rotamers; the absence of ^{31}P-^{31}P couplings rules out bridged complexes (μ-coordination).

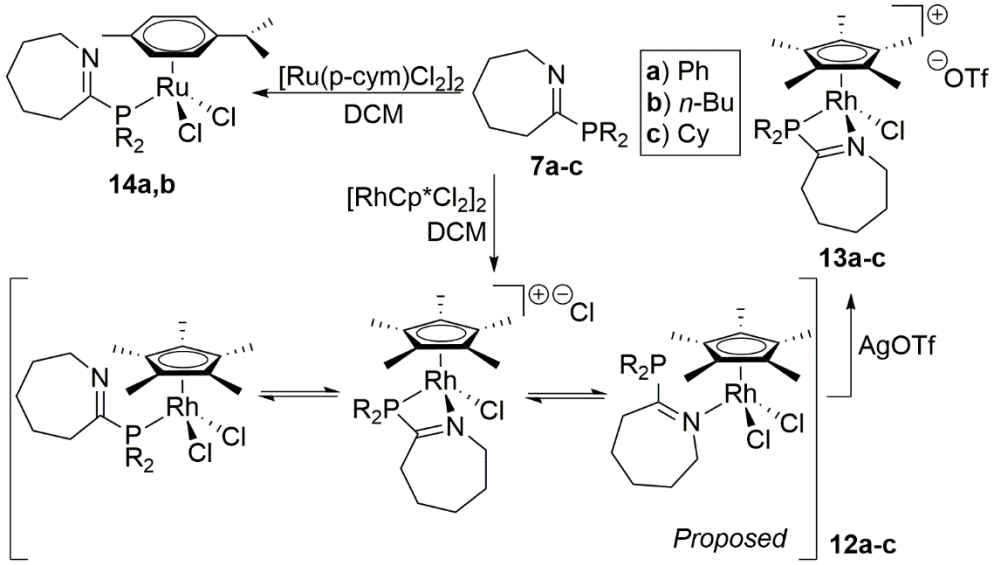

Scheme 6. The coordination of ligands **7** to Rh^{III} and Ru^{II}.

Surprisingly, Rh-complexation of phenyl ligand **7a** did not give a clean P-κ^1/κ^2 mixture. The ^{31}P NMR spectrum of complex **12a** showed a mixture of two broad signals (δ 36.9 ppm, d, $^1J_{P,Rh}$ = 142.5 Hz (42%); δ 30.1 ppm, br. s, (58%)) that resolved into three doublets on lowering the temperature to −94 °C (Figure 10). Their coupling constants suggests a mixture of two P-κ^1 complexes (δ 38.0 ppm, $^1J_{P,Rh}$ = 139.3 Hz (31%); δ 36.5 ppm, $^1J_{P,Rh}$ = 137.7 Hz (54%)) and possibly an N-κ^1 complex, as it has a strikingly different P-Rh coupling and other coordination modes are

unlikely due to the lack of additional P- and/or Rh couplings. (δ 27.5 ppm, $J_{P,Rh}$ = 153.9 Hz, (15%)). The N-monodentate coordination mode of 1,3-P,N-ligands has been reported only for Mn^{II} and Fe^{II},[3,24] and not for rhodium. Apparently, the two P-κ¹ and one N-κ¹ bonding modes interchange rapidly at room temperature.

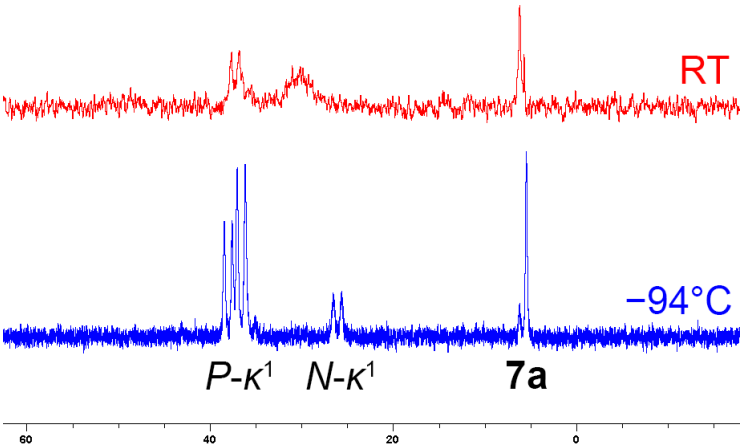

Figure 10. ^{31}P NMR spectra at room temperature and at −94 °C for complex **12a**.

The competing P-κ¹/N-κ¹ coordination modes for **12a** can be attributed to the C,N-dialkyl-P-phenyl substitution pattern of ligand **7a**. Its aryl groups reduce the donating property of the phosphane group as compared to **7b** and **7c**, and the cyclic alkyl chain makes its imine a stronger donor than in reported iminophosphanes.[6] For comparison, we synthesized the Rh-complexes of non-cyclic ligand **9** (Scheme 4), which is similarly substituted as **7a.** The low temperature ^{31}P NMR spectrum showed the P-κ¹ complex (δ 39.1 ppm, $^1J_{P,Rh}$ = 144.2 Hz (55%); δ 27.7 ppm, $^1J_{P,Rh}$ = 132.8 Hz (29%)) together with small amounts of both the N-κ¹ complex (δ 33.9 ppm, $^1J_{P,Rh}$ = 152.3 Hz (4%)) and the P,N-κ² complex (δ −15.0 ppm, $^1J_{P,Rh}$ = 115.0 Hz (6%)) before AgOTf converted it fully to the κ² complex (72% yield, δ(^{31}P) −15.5 (d, $^1J_{P,Rh}$ = 114.6 Hz). Even though the amount of observed N-coordination is lower for **9** than for **7a**, these results highlight

the influence of the C,N,P-substituents of **7** on the P,N-coordination mode.

All Rh-complexes **12a-c** could be fully converted to the bidentate complex **13** upon chloride abstraction with AgOTf (Scheme 6; **13a**: 82% yield, $\delta(^{31}P)$ −16.8 ppm, $^{1}J_{P,Rh}$ = 113.9 Hz; **13b**: 83% yield, $\delta(^{31}P)$ −19.7 ppm, $^{1}J_{P,Rh}$ = 110.0 Hz; **13c**: 76% yield, $\delta(^{31}P)$ −2.6 ppm, $^{1}J_{P,Rh}$ = 106.8 Hz).

Next, we explored the coordination to Ru^{II} (Scheme 6) and the catalytic activity[4a] of the resulting complexes. Reacting **7a,b** with $[Ru(p\text{-cym})Cl_2]_2$ (*p*-cym = *p*-cymene) provided the *P*-κ^1 complex **14b** (66% yield, $\delta(^{31}P)$ 27.3 ppm). Complex **14a** could not be isolated from the reaction mixture that showed the presence of two products ($\delta(^{31}P)$ 31.2 (27%), 23.4 (73%) ppm), which we tentatively assign to the *N*-κ^1 and *P*-κ^1 complexes, respectively, in analogy to Rh^{III} complex **12a** (vide supra).

Next, three Ru^{II} complexes of ligands **7a-c** were preliminary tested for their effectiveness as catalysts in the solvent-free, closed-vessel hydration of benzonitrile[25] at 180 °C for 3 h (Table 2). Surprisingly, in situ generated **14a** with the phenyl substituted ligand **7a** proved to be quite an active catalyst, yielding 79% product. In situ generated **14b** with the *n*-butyl substituted ligand **7b** afforded a somewhat lower yield of 59%, which could be enhanced to 70% by preforming the catalyst (entries 2 and 3, respectively). The least effective catalyst was the Ru^{II} complex of ligand **7c**, giving a hydration yield of only 15% that may have its origin in the more limiting steric factors. Even though the catalytic conditions were not optimized in this brief screen, it is rewarding that a hydration yield as high as 79% was obtained for P-κ^1-Ru^{II}-complex **14a**, which resembles the highest yield of 82% found for the comparable Ru-catalyst with an acyclic iminophosphane.[25] Both perform much better than the analogous

Ru-complex of the established Ph_2PPy ligand, which gives a hydration yield of 6%.[6d]

Table 2. Solvent-free catalyzed hydration of benzonitrile with precatalyst $[Ru(p\text{-}cym)Cl_2]$.[a]

Entry	Ligand (L)	T (°C)	t (h)	Yield[b] (%)
1	**7a**	180	3	79
2	**7b**	180	3	59
3	**7b**[c]	180	3	70
4	**7c**	180	3	15
5	$PyPPh_2$	180	3	6[6d]

[a] Reaction conditions: Ph-C≡N (3.6 mmol), H_2O (7.2 mmol), 1.4 mol% $[Ru(p\text{-cym})Cl_2]$ and ligand **7**. [b] Determined by GC. [c] Preformed catalyst (**14b**).

As complex **14b** performed only modestly in the hydration of benzonitrile, we chose to further screen its potential by preliminarily exploring the transfer hydrogenation of cyclohexanone in *i*-PrOH, under conditions adapted from of Jalón *et al.,* who used the analogous complex of 2-PPh_2-1-methylimidazole to obtain a hydrogenation yield of 21% on using a KOH/catalyst ratio of 333:1 and a substrate/catalyst ratio of 2000:1.[26,27] Table 3 summarizes the effect of changes in catalyst loading, reaction time, and the addition of KOH. After in situ generation of the catalyst, at 3 mol% catalyst loading the conversions were slow (up to 20 h; entries 1-3), but similar to the catalyst of Jalón et al.,[26] the catalyst was substantially more active in presence of KOH (entries 4-5). Even the corresponding κ^2-complex of **14b**, obtained by ion exchange with $NaBF_4$, was active under these conditions (entry 7). With 0.5 mol% catalyst and 2.5 mol% KOH, a reaction time of 2 h still resulted in the quantitative hydrogenation of cyclohexanone (entry 8). Last, as iridium(I) complexes are generally very active hydrogenation catalysts,[28] we also explored the

in situ generation of [(**7b**)Ir(COD)Cl], which showed a similar trend as the Ru^{II} complexes (entries 9-11).

Table 3. Catalytic transfer hydrogenation of cyclohexanone.

Entry	precatalyst (M)	Ligand (L)	Cat. loading (mol%)	t (h)	Yield[a] (%)	Additives
1	$[Ru(p\text{-cym})Cl_2]_2$	**7b**	3	2	3	-
2	$[Ru(p\text{-cym})Cl_2]_2$	**7b**	3	3	20	-
3	$[Ru(p\text{-cym})Cl_2]_2$	**7b**	3	20	quant.	-
4	$[Ru(p\text{-cym})Cl_2]_2$	**7b**	1	20	0	-
5	$[Ru(p\text{-cym})Cl_2]_2$	**7b**	1	4	quant.	5 mol% KOH
6	$[Ru(p\text{-cym})Cl_2]_2$	**7b**	1	4	0	1 mol% $NaBF_4$
7	$[Ru(p\text{-cym})Cl_2]_2$	**7b**	1	4	quant.	5 mol% KOH, 1 mol% $NaBF_4$
8	$[Ru(p\text{-cym})Cl_2]_2$	**7b**	0.5	2	quant.	2.5 mol% KOH
9	$[Ir(COD)Cl]_2$	**7b**	1	4	2	-
10	$[Ir(COD)Cl]_2$	**7b**	1	4	quant.	5 mol% KOH
11	$[Ir(COD)Cl]_2$	**7b**	1	4	84	5 mol% KOH, 1 mol% $NaBF_4$

Reaction conditions: cyclohexanone in *i*-PrOH (2M), reflux. [a] Determined by GC.

These preliminary screenings demonstrate that the conveniently in situ generated κ^1 and κ^2 complexes of Ru^{II} and Ir^{I} with cyclic 1,3-P,N-ligand **7** are active catalysts that warrant further scrutiny.

2.4 Chirality

As, to the best of our knowledge, no asymmetric 1,3-P,N-ligand-based catalysts have been reported,[4] the synthesis of such ligands may be valuable. With a synthetic route toward cyclic iminophosphanes at hand, we pursued substituting the backbone with a chiral group by using an inexpensive terpenoid as asymmetric starting point. The readily available terpenoid L-menthone[12] is well-suited for this purpose, since

its sizeable *2S-i*-Pr group is expected to be favorable for asymmetric induction.[29] Following the synthesis of the chiral ligands, we report their Ru and Rh complexes and briefly reflect on their catalytic potential.

The asymmetric derivatives of **7** were pursued in analogy to the parent compound, albeit that the solventless oxime synthesis was not effective, but reacting L-menthone with the hydroxylamine·HCl salt in an EtOH/H_2O mixture did provide oxime **16** as a colorless liquid after purification via crystallization at 5°C (73%; Scheme 7).[30] Subsequent treatment with MsCl, NEt_3 and benzotriazole induced the Beckmann rearrangement via **17** to the desired benzotriazolyl azepine adduct **19**, which was isolated as an orange liquid (90%).

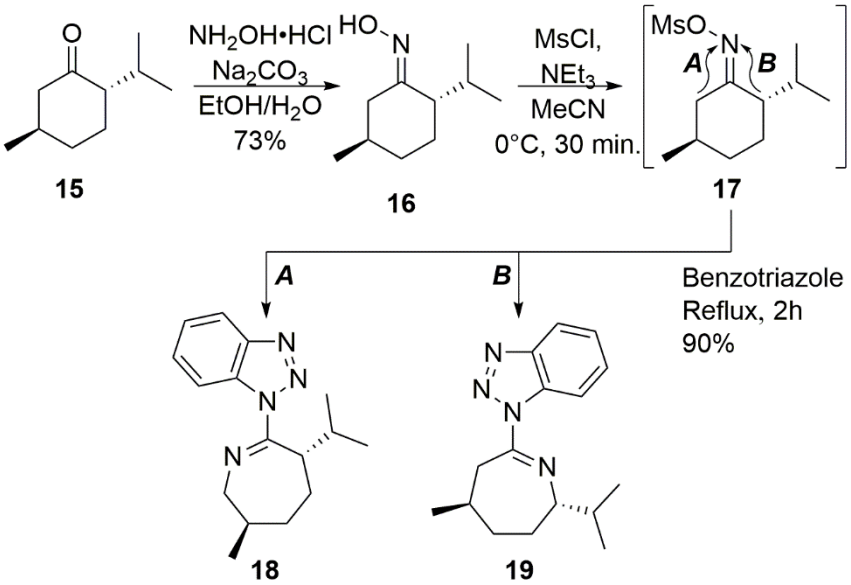

Scheme 7. Chiral benzotriazolyl-tetrahydroazepine synthesis.

Whereas the ring expansion could have generated either or both regioisomers **18** and **19** (Scheme 7, pathways **A** and **B**), the NMR spectra showed only a single set of signals for the Me and *i*-Pr CH_3-groups (δ(^{1}H)

1.11, 1.08, 1.06 ppm; δ(^{13}C) 24.2, 20.1, 17.7 ppm), indicating the formation of a single isomer. Based on the reported selectivity of related asymmetric cyclohexanone substrates In the Beckmann rearrangement,[31] we expected the formation of **19** to be favored. Whereas crystals of **19**, grown in a MeCN solution at −20 °C, were too temperature sensitive to isolate for X-ray crystallography, protonation with HOTf in $CHCl_3$ gave a thermally stable salt (**20**, 79%) in sharp contrast to the highly unstable unsubstituted azepinium triflate **5**. Crystals suitable for X-ray analysis were obtained by slow diffusion of pentane into a DCM solution of **20**. Its molecular structure (Figure 11) concurs with the anticipated (*2S*,*5R*)-2-*i*-Pr-5-Me regioisomer **19** with both alkyl groups in equatorial positions. Compared to the non-protonated **4** (Figure 6), the benzotriazolyl group of **20** is rotated by 155° and tilted with respect to the imine group [**20**: N1-C1-N2-N3 = −25.9(3); **4**: N1-C1-N2-N3 = 179.54(8)]. Clearly, protonation of the imine group prevents the intramolecular H-bonding that facilitated the planar conformation of **4**; the N1-H1 hydrogen interacts only with the triflate anion [H1- - -O1 = 1.97 (2) Å]. The positively charged N1 assumedly causes the slightly tighter benzotriazolyl-bonding [**20**: C1-N2 = 1.384(3), N2-N3 = 1.403(3) Å; **4**: C1-N2 = 1.4334(12), N2-N3 = 1.3746(11) Å]. The parameters of the iminium group [C1-N1 = 1.280(3) Å, N1-C1-C6 = 122.68(19)°, C1-N1-C2 = 125.01(19)°] are comparable to those for **6a** and **6c** (Figure 6).

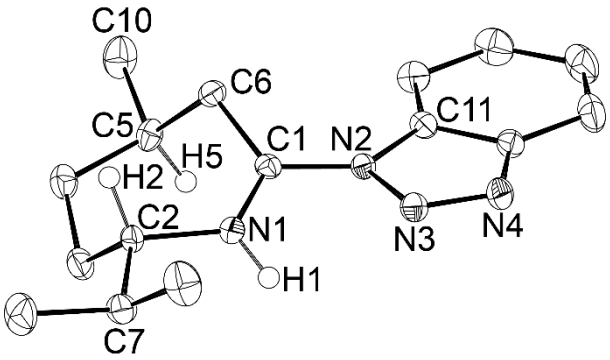

Figure 11. Displacement ellipsoid plot of 1-benzotriazolyl-(*2S*,*5R*)-2-isopropyl-5-methyl tetrahydroazepinium triflate **20** at the 50% probability level. The triflate anion and C-H hydrogen atoms are omitted for clarity, with exception of H2 and H5. Selected bond lengths (Å) and angles (°): C1-N1 = 1.280(3), C1-N2 = 1.384(3), N1-C2 = 1.487(3), N1-H1 = 0.89(2), C1-C6 = 1.490(3), N2-N3 = 1.403(3), N3-N4 = 1.278(3), N2-C11 = 1.390(3), N1-C1-N2 = 117.2(2), N1-C1-C6 = 122.68(19), N2-C1-C6 = 120.1(2), C1-N1-C2 = 125.01(19), N1-C1-N2-N3 = −25.9(3), C6-C1-N2-N3 = 153.6(2).

The introduction of the phosphane group on the chiral ring could not be achieved in analogy with the synthesis of the non-chiral ligands **7** (Scheme 3): surprisingly, treatment of the protonated precursor **20** with diphenylphosphane yielded its dehydrocoupling product tetraphenyldiphosphane.[32-34] Instead, the phosphane group was introduced by treating **19** with lithium phosphides $LiPR_2$ (R = Ph, *n*-Bu) in THF to cleanly give the desired chiral cycloiminophosphane **21** in 53%, after purification via an acid/base work-up involving salt **22** (Scheme 8). The ^{31}P NMR spectrum showed a single resonance at δ 6.6, indicating the absence of flippamers, which was attributed to the reduced flexibility of the ring on which the *i*-Pr and Me substituents favor equatorial positions.

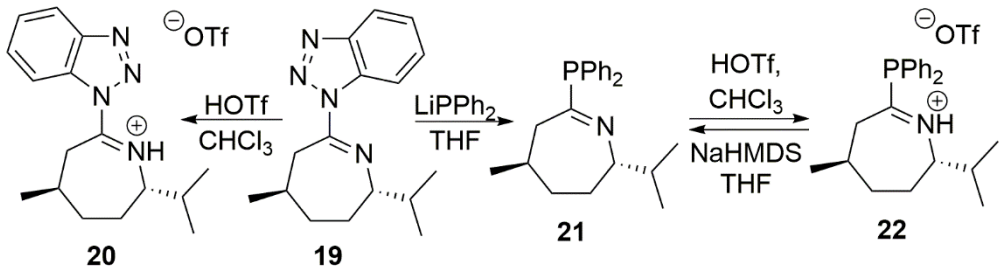

Scheme 8. Access of asymmetric ligands **21** from chiral benzotriazolyltetrahydroazepine **19**.

Single crystals of **22** suitable for an X-ray structure determination were obtained by slow diffusion of pentane into a saturated DCM solution. The molecular structure (Figure 12) shows a tetrahydroazepine chair similar to the one in **20** with the *2S*-*i*-Pr and *5R*-Me indeed in equatorial positions and confirms that the stereochemical information of the L-menthone is retained over the synthesis. The conformation and bonding parameters of **22** compare closely to that of the achiral, non-substituted **6a** (Figure 7) [**22**: C1-N1 = 1.289(2) Å, P1-C1 = 1.8252(18) Å, N1-C1-P1 = 121.79(14)°; **6a**: N1-C1 = 1.2858(16) Å, P1-C1 = 1.8269(13) Å, N1-C1-P1 = 123.06(10)°].

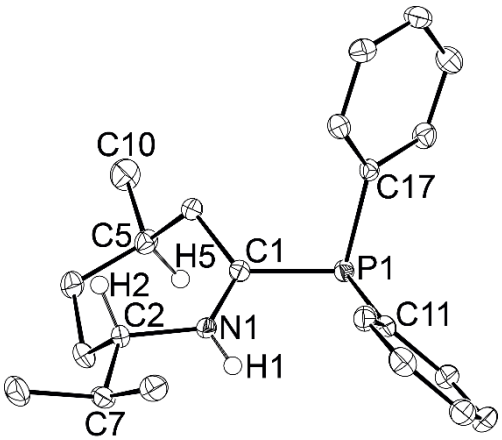

Figure 12. Displacement ellipsoid plot of *2S,5R*-phosphaazepinium triflate **22** at the 50% probability level. The triflate anion and C-H hydrogen atoms are omitted for clarity, with exception of H2 and H5. Selected bond lengths (Å) and angles (°): P1-C1 = 1.8252(18), P1-C11 = 1.8217(19), P1-C17 = 1.8259(18), C1-N1 = 1.289(2), N1-C2 = 1.490(2), N1-C1-P1 = 121.79(14), N1-C1-C6 = 120.82 (16), C1-N1-C2 = 124.57(16).

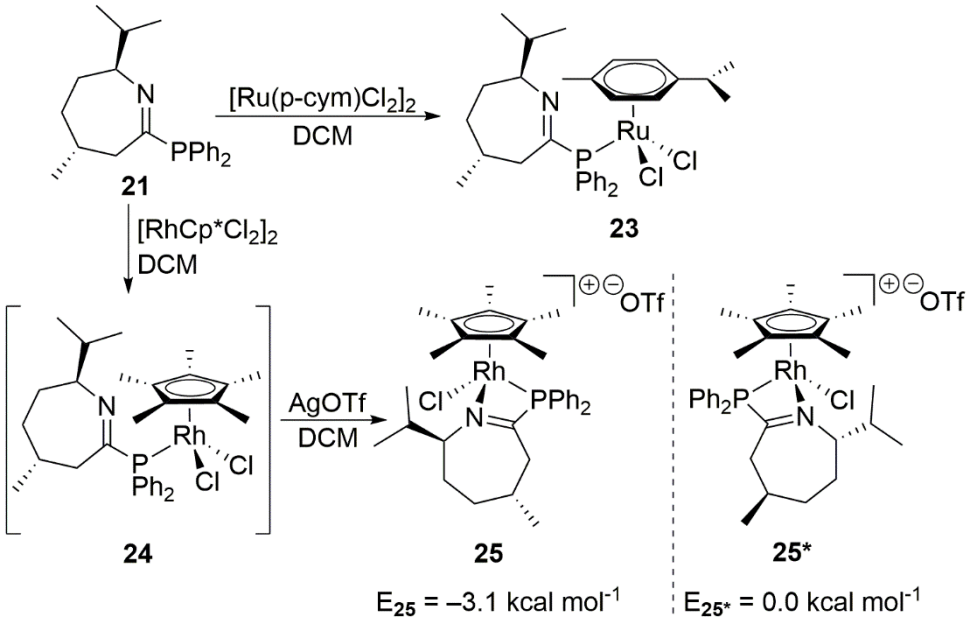

Scheme 9. The coordination of ligands **21** to Ru^{II} and Rh^{III}.

Coordination of chiral ligand **21** to Ru^{II} gave the corresponding P-κ^1 complexes **23** (Scheme 9; 19%, $\delta(^{31}P)$ 24.8 ppm). Likewise, coordination of **21** to Rh^{III} afforded κ^1-Rh^{III} complex **24** that showed, akin to complex **12a** (vide supra), a broad ^{31}P NMR signal at room temperature, which resolved at −90°C into a series of doublets with two major P-κ^1 resonances (δ 34.3 ppm, $^1J_{P,Rh}$ = 140.9 Hz, 38%; δ 22.8 ppm, $^1J_{P,Rh}$ = 142.5 Hz, 42%; Figure 13) and four minor ones with couplings indicative of P-κ^1 and κ^2 bonding (δ 29.9 ppm, $^1J_{P,Rh}$ = 140.9 Hz, 7%; δ 26.5 ppm, $^1J_{P,Rh}$ = 137.7 Hz, 7%; δ 24.7 ppm, $^1J_{P,Rh}$ = 137.7 Hz, 4%; δ 20.7 ppm, $^1J_{P,Rh}$ = 115.0 Hz, 2%). The P-κ^1 signals likely reflect different rotamers, as the absence of ^{31}P-^{31}P couplings rules out μ-complexation. In contrast to **12a**, no N-κ^1 signal was detected for **24**, presumably because the adjacent *i*-Pr group discourages coordination at this site. Chloride abstraction converted **24** and its isomers to κ^2-**25** ($\delta(^{31}P$, DCM) −11.3 ppm, $^1J_{P,Rh}$ = 106.6 Hz), which was calculated to be energetically favored by 3.1 kcal mol^{-1} over its epimer **25*** (ωB97XD/6-31+G(d,p), Def2-TZVP for Rh).[6b,d,35-39] The obtained chiral

transition metal complexes might be useful for asymmetric catalytic reactions, but such investigations were outside the scope of the present study. Based on the performance of ligands **7** (vide supra), asymmetric transfer hydrogenation seems a promising starting point.

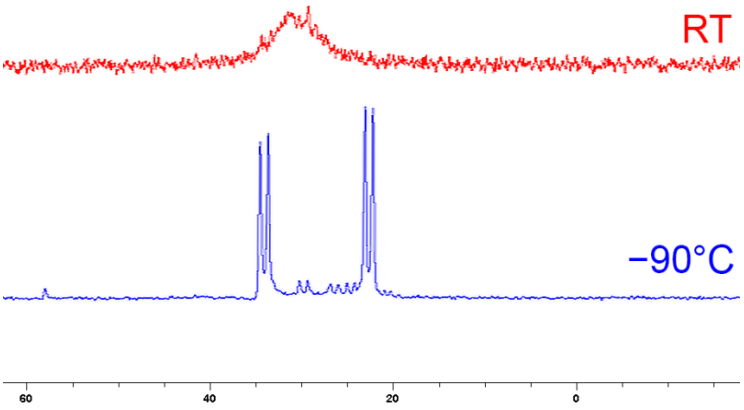

Figure 13. ^{31}P NMR spectra of **24** at room temperature and −90 °C.

3 Conclusion

This study reports the synthesis of cyclic 2-phospha-tetrahydroazepines as novel 1,3-P,N-ligands with the intend to open new opportunities in coordination chemistry and catalysis. This class of cycloiminophosphanes comprises a seven-membered aliphatic imine ring with which it complements other classes of 1,3-P,N-ligands, including the aromatic 2-pyridyl- and 2-imidazolyl-phosphanes, as well as the recently reported acyclic iminophosphanes and phosphaamidines. The ligands were readily obtained in a one pot process, through the Beckmann rearrangement of cyclohexanones to reactive nitrilium ion intermediates, which were then trapped with benzotriazole. The benzotriazole was then quantitatively replaced for a secondary phosphane (R = Ph, *n*-Bu, Cy), facilitated by triflic acid activation. With respect to other 1,3,-P,N ligands, these cycloiminophosphanes distinguish themselves by their high *N*-basicity and their flexible backbone, as ^{31}P NMR spectroscopy of the neutral

ligands reveals the presence of flippamers, indicative of dynamic conformational behavior of the tetrahydroazepine ring. The ligands coordinate both in P-κ^1- and P,N-κ^2-fashion to W(carbonyl) complexes, which were analyzed by IR spectroscopy to quantify the ligands donor strength. Coordination to $[RhCp^*Cl_2]_2$ gave a dynamic mixture of κ^1- and κ^2-complexes, that on treatment with silver triflate culminate in only the κ^2-complexes. The reaction with $[Ru(p\text{-cym})Cl_2]_2$ selectively provides P-κ^1-complexes, which were also effective catalysts for the hydration of benzonitrile (1.4 mol%, 180 °C, 3 h, up to 79%) and the transfer hydrogenation of cyclohexanone (0.5 mol%, 83 °C, 2 h, quant.); for the latter reaction also iridium(I) could be used (1 mol%, 83 °C, 4 h, quant.). Finally, as a preamble to asymmetric catalysis, a chiral cycloiminophosphane could be accessed from the natural precursor l-menthone via a selective Beckmann rearrangement. It was characterized by X-ray crystallography, and used to access Rh^{III}- and Ru^{II}-complexes. These chiral ligands form promising candidates for the study of asymmetric 1,3-P,N-catalysis in the future.

4 Experimental Section

4.1 Preparation of Compounds

All experiments were performed under an atmosphere of dry nitrogen using standard Schlenk-line and glovebox techniques, unless stated otherwise. Solvents were distilled under nitrogen over the appropriate drying agent; $CaCl_2$ (DCM), K_2CO_3 (MeCN), benzophenone/NaK (Et_2O, THF, triethylamine), $LiAlH_4$ (pentane), P_2O_5 (CD_2Cl_2, $CDCl_3$, $CHCl_3$). THF-d_8 was dried over Na at room temperature. H_2O was degassed ultrasonically under reduced pressure. Silver salts were handled with minimum light exposure. Phosphanes were purchased from Sigma-Aldrich and were distilled under reduced pressure before use. Benzotriazole was dried in DCM over Na_2SO_4. Solids were predried *in vacuo* for at least 30 min. All other reagents were used as received. Cyclohexyloxime **2**[15] and L-menthone oxime **16**[30] were prepared according to literature procedures. For compound **4**[11c] a revised synthesis is reported herein. [(**7**)Ru^{II}]-catalyzed nitrile hydrations[6d] and [(**7**)M]-catalyzed transfer hydrogenations[26] were performed according to literature procedures. NMR spectra were recorded on a Bruker Avance 250 (Bruker

Avance 250 (^{1}H: 250.13 MHz, ^{19}F: 235.36 MHz, room temperature), a Bruker Avance 400 (^{1}H: 400.13 MHz, ^{13}C{^{1}H}: 100.61 MHz, ^{31}P: 161.98 MHz, room temperature) or a Bruker Avance 500 (^{1}H: 500.23 MHz, ^{13}C{^{1}H}: 125.78 MHz; room temperature). ^{1}H NMR spectra and ^{13}C{^{1}H} NMR spectra were internally referenced to residual solvent resonances ($CDCl_3$: δ^{1}H = 7.26, δ^{13}C{^{1}H} = 77.16; CD_2Cl_2: δ^{1}H = 5.32, δ^{13}C{^{1}H} = 53.84; C_6D_6: δ^{1}H = 7.16, δ^{13}C{^{1}H} = 128.06; THF-d_8: δ^{1}H = 3.58, 1.72, δ^{13}C{^{1}H} = 67.21, 25.31; DMSO-d_6: 2.50, δ^{13}C{^{1}H} = 39.52) and ^{31}P NMR spectra were references externally to H_3PO_4. Melting points were measured using a Büchi Melting Point M-565 apparatus (sealed capillaries) and are uncorrected. High resolution electrospray ionization (ESI) mass spectrometry was carried out with a Bruker micrOTOF-Q instrument in positive ion mode (capillary potential of 4500 V). Infrared spectra were recorded on a Shimadzu FT-IR 8400S spectrophotometer.

1-Benzotriazolyl-3,4,5,6-tetrahydroazepine (4).[11c] *Protocol 1:* MsCl (2.1 mL, 27.00 mmol, 1.1 equiv.) was added dropwise to a solution of cyclohexanone oxime **2** (2.83 g, 25.01 mmol, 1.0 equiv.) and NEt_3 (7.0 mL, 50.22 mmol, 2.0 equiv.) in MeCN (62 mL) at 0°C. The mixture was stirred for 30 min. to give an orange solution, to which benzotriazole (4.47 g, 37.53 mmol, 1.5 equiv.) was added. The mixture was subsequently refluxed for 2h and the resulting brown solution was cooled to room temperature. Under atmospheric conditions, a solution of K_2CO_3 (100 mL, saturated solution in H_2O)was added, after which water was added until white powder precipitated from the solution. The solid was harvested by repeated addition of water to the reaction mixture and subsequent filtration, until no further precipitate was observed. The combined fractions of solid were washed with ice-water and dried to provide **4** as an off-white solid (3.2 g, 14.93 mmol, 60%). *Protocol 2:* MsCl (3.41 mL, 44 mmol, 1.1 equiv.) was added dropwise to a solution of cyclohexanone oxime (4.53 g, 40 mmol, 1.0 equiv.) and NEt_3 (12.3 mL, 88 mmol, 2.2 equiv.) in MeCN (80 mL) at 0°C. The mixture was stirred for 30 min. to give an orange solution, to which benzotriazole (5.2 g, 44 mmol, 1.1 equiv.) was added. The mixture was subsequently refluxed for 2.5h and the resulting brown solution was cooled to RT. Evaporation provided a brown solid which was extracted into Et_2O (3 x 40 mL) under atmospheric conditions. The combined Et_2O fractions were filtered over a pad of neutral aluminium oxide, after which evaporation provided **4** as a yellow solid (4.98 g, 23 mmol, 58%). *Crystallization:* A saturated hot acetonitrile solution was cooled to 5°C (39%). Single crystals can be obtained by cooling a saturated Et_2O solution to −20 °C to provide colorless blocks. ^{1}H NMR (400.13 MHz, $CDCl_3$): δ 8.45 (d, $^{3}J_{H,H}$ = 8.3 Hz, 1H, CNC-C*H*), 8.08 (d, $^{3}J_{H,H}$ = 8.3 Hz, 1H, CNCC-C*H*), 7.55 (t, $^{3}J_{H,H}$ = 7.8, 1H, CNC-CH-C*H*), 7.43 (t, $^{3}J_{H,H}$ = 7.6 Hz, 1H, CNCC-CH-C*H*),

3.93-3.89 (m, 2H, N-C*H*$_2$), 3.56-3.51 (m, 2H, C-C*H*$_2$), 1.98-1.91 (m, 2H, NCH$_2$CH$_2$-C*H*$_2$), 1.82-1.71 (m, 4H, NCH$_2$C*H*$_2$, CCH$_2$C*H*$_2$).

Screening of (Lewis Acid) catalysts for the synthesis of 7-diphenylphosphanyl-3,4,5,6-tetrahydroazepines. *Method 1*[11a]*:* To a mixture of **4** (105 mg, 0.49 mmol, 1.0 equiv.) and $AlCl_3$ (7 mg, 0.05 mmol, 0.1 equiv.) in 1.6 ml $CHCl_3$, was added diphenylphosphane (0.09 mL, 0.52 mmol, 1.1 equiv.). The resulting mixture was stirred in a closed vial for 10 min. at 80 °C using microwave heating. The resulting mixture was analysed using ^{31}P NMR spectroscopy (25% conversion). *Method 2:* A mixture of **4** (150 mg, 0.70 mmol, 1.0 equiv.) and diphenylphosphane (0.12 mL, 0.69 mmol, 1.0 equiv.) in 2.0 ml $CHCl_3$, was added to the desired Lewis acid. The mixture was refluxed for the indicated time, after which the mixture was analysed using ^{31}P NMR spectroscopy.

7-diphenylphosphanyl-3,4,5,6-tetrahydroazepine aluminium adducts. *Step 1:* A solution of **4** (0.076 g, 0.35 mmol, 1.0 equiv.) in 1.1 ml $CHCl_3$, was added to $AlCl_3$ (0.047 g, 0.35 mmol, 1.0 equiv.), after which a solution of diphenylphosphane (0.06 mL, 0.35 mmol, 1.0 equiv.) in 0.1 ml $CHCl_3$ was added. The mixture was refluxed for 90 min., during which the mixture turned yellow. Evaporation of $CHCl_3$ yielded a yellow solid, which was washed with Et_2O (3 x 10 mL) and provided a yellow solid (100% conversion, yield n.d.). ^{1}H NMR (400.13 MHz, $CDCl_3$): δ 7.67-7.57 (m, 10H, Ar*H*); 4.15-4.11 (m, 2H, C*H*$_2$); 3.50-3.45 (m, 2H, C*H*$_2$); 2.96-2.90 (m, 2H, C*H*$_2$); 1.97-1.92 (m, 2H, C*H*$_2$); 1.85-1.81 (m, 2H, C*H*$_2$); 1.73-1.69 (m, 2H, C*H*$_2$). ^{31}P NMR (161.98 MHz, $CDCl_3$): δ 15.7 (s). *Step 2:* To a solution of the yellow solid (3.00 g) in DCM (20 mL), was added degassed water (0.38 mL, 19.95 mmol) dropwise at 0°C to give a suspension, which then was filtered. The filtrate was evaporated and the obtained solid was extracted into Et_2O (40 mL). Evaporation of the Et_2O fraction yielded a light yellow solid (1.53 g).

1-Benzotriazolyl-3,4,5,6-tetrahydroazepinium triflate (intermediate 5). 1-Benzotriazolyl-3,4,5,6-tetrahydroazepine **4** (0.468 g, 2.18 mmol, 1.0 eq) was dissolved in DCM (6 mL). Triflic acid (2.18 mmol, 1.0 eq, 172 µL) was added dropwise at −78 °C to give a dark suspension, which was stirred for 10 min. and then filtered. The residue was dried *in vacuo* to give **5** as a cream coloured solid (0.68 g, 1.87 mmol, 86%), which due to its unstable nature was used directly without further purification. Mp: 130.2 °C dec. ^{1}H NMR (400.13 MHz, DMSO-d$_6$): δ 14.61 (s, 1H, N*H*), 8.38 (d, $^3J_{HH}$ = 8.2 Hz, 1H, CNC-C*H*), 8.16 (d, $^3J_{HH}$ = 8.2 Hz, 1H, CNCC-C*H*), 7.94- 7.67 (t, $^3J_{HH}$ = 8.2 Hz, CNC-CH-C*H*), 7.53 (t, $^3J_{HH}$ = 7.4 Hz, CNCC-CH-C*H*), 3.91-3.82 (m, 2H , N-C*H*$_2$), 3.52-3.44 (m, 2H, C-C*H*$_2$), 1.93-1.83 (m, 2H, NCH$_2$CH$_2$-C*H*$_2$), 1.74-1.61 (m, 4H, NCH$_2$C*H*$_2$, CCH$_2$C*H*$_2$). ^{13}C{^{1}H} NMR (125.78

MHz, DMSO-d_6): δ 162.3 (s, N*C*N), 146.2 (s, NCN*C*), 130.8 (s, CNC*C*), 129.3 (s, CNCC-CH-*C*H), 125.6 (s, CNC-CH-*C*H), 120.7 (q, $^1J_{C,F}$ = 322 Hz; O_3SCF_3), 119.5 (s, CNCC-*C*H), 115.6 (s, CNC-*C*H), 49.6 (s, N-*C*H_2), 30.3 (s, C-*C*H_2), 29.0 (s, $NCH_2CH_2CH_2$), 25.9 (s, NCH_2CH_2), 22.6 (s, CCH_2CH_2). $^{19}F\{^1H\}$ NMR (235.36 MHz, $CDCl_3$): δ –78.4 (s, O_3SCF_3).

7-phosphanyl-3,4,5,6-tetrahydroazepinium triflates (6a-c). 1-Benzotriazolyl-3,4,5,6-tetrahydroazepine **4** (1.02 equiv.) was dissolved in $CHCl_3$ (2 mL/mmol) and cooled to 0°C. Triflic acid (1.02 equiv.) was added dropwise to give a dark suspension. After stirring for 3 min., the solvent was removed by filtration to give **5** as a cream colored solid (quant.), which was then resuspended in $CHCl_3$ (2 mL/mmol). Dropwise addition of a secondary phosphane (1.00 equiv.) gave a yellow solution which was stirred for 5 min. Evaporation to dryness provided an oil. *Workup for **6a** was as follows:* the oil was washed with Et_2O (2 x 2 mL/mmol) to provide a solid (77%). *Crystallization **6a**:* Single crystals were obtained by slow diffusion of pentane into a THF solution (1:1) at room temperature. Mp: 124.9-130.1°C. ^1H NMR (400.13 MHz, $CDCl_3$): δ 11.04 (s, 1H, N*H*), 7.65-7.51 (m, 10H, P-Ar*H*), 4.10-4.01 (m, 2H, N-CH_2), 2.90-2.81 (m, 2H, C-CH_2), 1.94-1.84 (m, 2H, NCH_2CH_2-CH_2), 1.84-1.74 (m, 2H, CCH_2CH_2), 1.67-1.58 (m, 2H, NCH_2CH_2). $^{13}C\{^1H\}$ NMR (125.78 MHz, $CDCl_3$): δ 207.9 (d, $^1J_{C,P}$ = 45.3 Hz, P*C*N), 136.0 (d, $^2J_{C,P}$ = 22.6 Hz, P-*o*-Ar*C*), 132.6 (P-*p*-Ar*C*), 130.4 (d, $^3J_{C,P}$ = 10.1 Hz, P-*m*-Ar*C*), 121.8 (s, P*C*CH), 120.5 (q, $^1J_{C,F}$ = 319 Hz; O_3SCF_3), 51.7 (s, N-*C*H_2), 35.9 (d, $^2J_{C,P}$ = 18.9 Hz, C-*C*H_2), 29.8 (s, $NCH_2CH_2CH_2$), 25.0 (d, $^4J_{C,P}$ = 3.8 Hz, NCH_2CH_2), 23.5 (d, $^3J_{C,P}$ = 6.3 Hz, CCH_2CH_2). ^{31}P NMR (161.98 MHz, C_6D_6): δ 14.9 (s). FT-IR: v = 3327 (w), 3281 (w), 2934 (w), 2870 (w), 1782 (m). 1655 (m), 1634 (m), 1495 (m), 1468 (m), 1439 (m), 1414 (m), 1285 (s), 1258 (s), 1190 (m), 1144 (s), 1092 (m), 1034 (s), 976 (m), 912 (m), 883 (m), 843 (m), 802 (m), 749 (s), 698 (s), 635 (s), 573 (m), 515 (s), 500 (s), 486 (s), 467 (s), 440 (m). MS (ESI-Q-TOF): calcd. for $C_{18}H_{21}NP$: 282.1407; found: 282.1392. *Workup for **6b** was as follows:* the oil was extracted into Et_2O (4 x 10 mL/mmol) and evaporated to dryness to provide **6b** as an oil, which was used without further purification (^{31}P NMR: 85% pure). ^1H NMR (400.13 MHz, $CDCl_3$): δ 11.69 (s, 1H, *NH*), 4.08-3.98 (m, 2H, N-CH_2), 2.94-2.85 (m, 2H, C-CH_2), 2.09-1.87 (m, 6H, PCH_2 + NCH_2CH_2-CH_2), 1.80-1.65 (m, 4H, CCH_2CH_2 + NCH_2CH_2), 1.55-1.29 (br. m, 8H, $PCH_2CH_2CH_2$, NCH_2-$CH_2CH_2CH_2$), 0.91 (t, $^3J_{HH}$ = 7.2 Hz, 6H, CH_3). Contaminant: benzotriazole (1:1). ^{31}P NMR (161.98 MHz, $CDCl_3$): = 8.8 (s). *Workup for **6c** was as follows:* the oil was washed with Et_2O (3 x 7.5 mL/mmol) to provide a solid, which was used without further purification (66% (crude), contaminant: benzotriazole). *Crystallization **6c**:* A saturated solution in THF:pentane (1:1) was cooled to 5°C (5%). ^1H NMR (500.23 MHz, $CDCl_3$): δ 11.90 (s, 1H, *NH*), 4.07 (br. s, 2H, N-CH_2), 2.97-2.87 (m, 2H, C-CH_2), 2.40-2.29 (m, 2H, P-C*H*), 2.00-1.90 (m, 2H, NCH_2CH_2-CH_2), 1.90-1.68 (m, 14H, Cy-CH_2, NCH_2-

C*H*$_2$C*H*$_2$C*H*$_2$), 1.52-1.39 (m, 4H, Cy-C*H*$_2$), 1.39-1.14 (m, 6H, Cy-C*H*$_2$). ^{13}C{^{1}H} NMR (125.78 MHz, $CDCl_3$): δ 207.5 (d, $^1J_{C,P}$ = 57.9 Hz, P*C*N), 120.6 (q, $^1J_{C,F}$ = 319 Hz; O_3SCF_3), 51.0 (d, $^3J_{C,P}$ = 2.5 Hz, N-*C*H$_2$), 37.7 (d, $^2J_{C,P}$ = 21.4 Hz, C-*C*H$_2$), 31.9 (d, $^1J_{C,P}$ = 16.4 Hz, P-*C*H), 30.1 (s, NCH$_2$CH$_2$*C*H$_2$), 26.8 (s, PCH-*C*H$_2$), 26.7 (s, PCHCH$_2$-*C*H$_2$), 25.9 (s, PCHCH$_2$CH$_2$-*C*H$_2$), 25.2 (d, $^4J_{C,P}$ = 2.5 Hz, NCH$_2$C*H*$_2$), 22.5 (d, $^3J_{C,P}$ = 7.5 Hz, CCH$_2$C*H*$_2$). ^{31}P NMR (161.98 MHz, $CDCl_3$): = 34.4 (s). FT-IR: v = 2922 (m), 2856 (m), 1626 (m), 1452 (w), 1425 (w), 1290 (s), 1261 (s), 1236 (s), 1223 (s), 1157 (s), 1143 (s), 1111 (s), 1090 (m), 1061 (m), 1026 (s), 997 (s), 982 (s), 889 (m), 847 (w), 818 (w), 754 (m), 706 (w), 635 (s), 613 (m), 571 (m), 515 (s). MS (ESI-Q-TOF): calcd. for $C_{18}H_{33}NP$: 294.2346; found: 294.2332.

7-phosphanyl-3,4,5,6-tetrahydroazepines (7a-c). Secondary phosphanyl-3,4,5,6-tetrahydroazepinium triflate **6** (1.0 equiv.) was dissolved in THF (5 mL/mmol) and cooled to −78°C. A solution of NaHMDS (1.0 equiv.) in THF (5 mL/mmol) was added dropwise. The solution was then allowed to warm to room temperature and evaporated. Extraction into pentane (4 x 5 mL/mmol) and subsequent evaporation yielded **7** (**7a**, 92%; **7b**, 83%; **7c**, 76%). *Data for **7a** are as follows:* Mp: 189.6°C dec. *Since not all ^{1}H NMR resonances of the **7a** flippamers can be distinguished, one set of signals is reported (integrals normalized separately for each).* ^{1}H NMR (400.13 MHz, THF-*d*$_8$): δ 7.50-7.14 (m, 10H, Ar*H* + Ar*H* minor), 3.76-3.68 (m, 2H, N-C*H*$_2$), 2.82-2.76 (m, 2H, C*H*$_2$ minor), 2.41-2.32 (m, 2H, C-C*H*$_2$), 2.22-2.15 (m, 2H, C*H*$_2$ minor), 1.79-1.67 (m, 2H, NCH$_2$CH$_2$-C*H*$_2$), 1.61-1.54 (m, 2H, C*H*$_2$ minor), 1.53-1.44 (m, 2H, CCH$_2$C*H*$_2$), 1.33-1.25 (m, 2H, NCH$_2$C*H*$_2$). ^{13}C{^{1}H} NMR (125.78 MHz, THF-d$_8$): δ 181.6 (d, $^1J_{P,C}$ = 6.3 Hz, P*C*N), 136.3 (d, $^1J_{P,C}$ = 10.1 Hz, P-*i*-*pso*-Ar*C*), 135.5 (d, $^2J_{P,C}$ = 17.6 Hz, P-*o*-Ar*C*), 133.7 (d, $J_{P,C}$ = 19.5 Hz, Ar*C* minor), 129.3 (s, P-*p*-Ar*C*), 129.0 (s, Ar*C* minor), 128.9 (d, $J_{P,C}$ = 4.8 Hz, Ar*C* minor), 128.6 (d, $^3J_{P,C}$ = 7.5 Hz, P-*m*-Ar*C*), 54.5 (d, $^3J_{P,C}$ = 10.1 Hz, N-*C*H$_2$), 35.7 (d, $^2J_{P,C}$ = 36.5 Hz , C-*C*H$_2$), 32.6 (s, *C*H$_2$ minor), 32.2 (s, N-CH$_2$CH$_2$*C*H$_2$), 27.7 (s, *C*H$_2$ minor), 27.2 (s, NCH$_2$*C*H$_2$), 24.9 (s, CCH$_2$*C*H$_2$). ^{31}P NMR (161.98 MHz, THF-d$_8$): δ 6.0 (s, minor, 14%), 5.4 (s, major, 86%). FT-IR: *v* 3051 (w), 2921 (m), 2847 (m), 1618 (m), 1479 (m), 1433 (s), 1339 (w), 1259 (w), 1155 (w), 1095 (m), 1068 (w), 1030 (s), 1026 (m), 999 (w), 975 (w), 800 (w), 741 (s), 694 (s), 634 (m), 619 (m), 528 (m), 501 (s), 457 (m), 432 (w), 419 (m). MS (ESI-Q-TOF): calcd. for $C_{18}H_{21}NP$: 282.1407; found: 282.1392. *Data for **7b** are as follows:* ^{1}H NMR (400.13 MHz, THF-*d*$_8$): δ 3.70-3.63 (m, 2H, N-C*H*$_2$), 2.49-2.41 (m, 2H, C-C*H*$_2$), 1.83-1.69 (m, 4H, C*H*$_2$), 1.51-1.25 (m, 14H, NCH$_2$C*H*$_2$C*H*$_2$C*H*$_2$ + PC*H*$_2$C*H*$_2$C*H*$_2$), 0.90 (t, $^3J_{H,H}$ = 7.2 Hz, 6H, C*H*$_3$). ^{13}C{^{1}H} NMR (100.61 MHz, THF-*d*$_8$): δ 184.0 (d, $^1J_{C,P}$ = 13.1 Hz, P*C*N), 54.1 (d, $^3J_{C,P}$ = 7.7 Hz, N-*C*H$_2$), 35.0 (d, $^2J_{C,P}$ = 35.4 Hz, C-*C*H$_2$), 32.6 (s, *C*H$_2$), 29.4 (d, $^2J_{C,P}$ = 12.6 Hz, P-CH$_2$*C*H$_2$), 27.4 (d, $J_{C,P}$ = 2.4 Hz, *C*H$_2$), 25.1 (d, $J_{C,P}$ = 10.6 Hz, *C*H$_2$), 24.7 (d, $^3J_{C,P}$ = 3.1 Hz, *C*H$_2$CH$_3$), 24.2 (d, $^1J_{C,P}$ = 13.0 Hz, P-*C*H$_2$), 14.1 (s, *C*H$_3$). ^{31}P NMR (161.98 MHz, THF-

d$_8$): δ –10.7 (s, major, 95%), –17.5 (s, minor, 5%). FT-IR: could not be determined due to rapid degradation of sample. MS (ESI-Q-TOF): calcd. for $C_{14}H_{29}NP$: 242.2032; found: 242.2029. *Data for* ***7c*** *are as follows:* ^{1}H NMR (400.13 MHz, THF-*d*$_8$): *δ* 3.74-3.65 (m, 2H, N-C*H*$_2$), 2.50-2.42 (m, 2H, C-C*H*$_2$), 1.98-1.56 (m, 14H, C*H*$_2$+ Cy*H*), 1.51-1.37 (m, 4H, C*H*$_2$), 1.37-1.08 (m, 10H, Cy*H*). ^{13}C{^{1}H} NMR (100.61 MHz, THF-*d*$_8$): *δ* 181.6 (d, $^{1}J_{C,P}$ = 18.3 Hz, P*C*N), 54.3 (d, $^{3}J_{C,P}$ = 6.4 Hz, N-*C*H$_2$), 37.9 (d, $^{2}J_{C,P}$ = 40.3 Hz, C-*C*H$_2$), 32.9 (d, $^{1}J_{C,P}$ = 13.4 Hz, P-*C*H), 32.4 (s, *C*H$_2$), 31.3 (d, $J_{C,P}$ = 11.9 Hz, *C*H$_2$), 30.1 (d, $J_{C,P}$ = 10.2 Hz, *C*H$_2$), 28.3 (d, $J_{C,P}$ = 8.8 Hz, *C*H$_2$), 28.0 (d, $J_{C,P}$ = 10.2 Hz, *C*H$_2$), 27.4 (s, *C*H$_2$), 24.2 (d, $J_{C,P}$ = 3.1 Hz, *C*H$_2$). ^{31}P NMR (161.98 MHz, THF-d$_8$): δ 17.5 (s, major, 88%), 13.5 (s, minor, 12%). FT-IR: could not be determined due to rapid degradation of sample. MS (ESI-Q-TOF): calcd. for $C_{18}H_{33}NP$: 294.2346; found: 294.2332.

(*N*-methyl)(methyl)carbonitrilium trifluoromethyl sulfonate (8).[20] Prepared according to literature procedures and used without further purification. ^{1}H NMR (250.13 MHz, CD_2Cl_2): δ 3.89 (sext., $^{5}J_{H,H}$ = 2.7 Hz, N-C*H*$_3$), 2.99 (sext, $^{5}J_{H,H}$ = 2.1 Hz, C-C*H*$_3$). ^{19}F{^{1}H} NMR (235.36 MHz, CD_2Cl_2): *δ* –79.1 (s, O_3SCF_3).

Diphenylphosphanyl(*N*-methyl)acetiminium triflate (intermediate). Diphenylphosphane (1.60 mL, 9.19 mmol, 1.02 equiv.) was added dropwise to a suspension of (*N*-methyl)(methyl)carbonitrilium trifluoromethyl sulfonate **8** (1.844 g, 8.99 mmol, 1.0 equiv.) in DCM (20 mL) at –78 °C to give a yellow solution, which was allowed to warm to RT and stirred for 30 min. Evaporation provided a yellow oil, which was washed with pentane (3 x 20 mL) to provide diphenylphosphanyl(*N*-methyl)acetiminium triflate as a yellow oil that was used without further purification (3.321 g, 8.49 mmol, 94%, mixture of E/Z isomers). *Since not all ^{1}H NMR resonances of the E/Z isomers can be distinguished, one set of signals is reported (integrals normalized separately for each).* ^{1}H NMR (400.13 MHz, $CDCl_3$): *δ* 12.78 (br. s, 1H, N*H* (minor)), 10.60 (br. s, 1H, N*H* (major)), 7.65-7.43 (m, 10H, Ar*H* (major+minor)), 3.52 (t, $J_{H,H}$ = 5.1 Hz, 3H, N-C*H*$_3$ (major)), 3.20 (dt, $J_{H,H}$ = 5.3 Hz, $J_{H,H}$ = 1.6 Hz, N-C*H*$_3$ (minor)), 2.46 (d, $J_{H,H}$ = 10.8 Hz, C-C*H*$_3$ (major)), 2.41 (dt, $J_{H,H}$ = 5.3, $J_{H,H}$ = 1.5 Hz (minor)). ^{31}P NMR (161.98 MHz, $CDCl_3$): δ 15.2 (s, major, 65%), –1.1 (s, minor, 35%). MS (ESI-Q-TOF): calcd. for $C_{15}H_{17}NP$: 242.1093; found: 242.1087.

((*N*-methyl)acetimidoyl)diphenylphosphane (9). *n*-Butyllithium (2.65 mL, 1.6 M, 4.24 mmol, 1.0 equiv.) was added dropwise to a yellow solution of diphenylphosphanyl (*N*-methyl)acetiminium triflate (4.25 mmol, 1.0 equiv.) in THF (15 mL) at –78 °C to give a bright orange solution, which was stirred for 15 min. It was warmed to RT and stirred

for 30 min. to give a yellow solution, which was evaporated and extracted into pentane (3 x 20 mL). The combined extracts were evaporated to dryness to give a yellow oil, which was extracted into DCM (12 mL). Evaporation of the extract provided **9** as yellow oil (0.96 g, 3.97 mmol, 93%, mixture of E/Z isomers). *Since not all ^{1}H NMR resonances of the E-**9** and Z-**9** can be distinguished, one set of signals is reported (integrals normalized separately for each).* ^{1}H NMR (500.23 MHz, CD_2Cl_2): δ 7.48-7.29 (m, 10H, Ar*H* (major+minor)), 3.34-3.30 (m, 3H, N-C*H*$_3$ (minor)), 3.26-3.24 (m, 3H, N-C*H*$_3$ (major)), 1.91-1.86 (m, 3H, C-C*H*$_3$ (major+minor)). ^{13}C{^{1}H} NMR (125.78 MHz, CD_2Cl_2): δ 176.5 (d, $^1J_{P,C}$ = 3.2 Hz, P*C*N (minor)), 174.0 (d, $^1J_{P,C}$ = 38.8 Hz, P*C*N (major)), 135.6 (d, $^1J_{P,C}$ = 8.6 Hz, *ipso*-Ar*C*), 135.0 (d, $^3J_{P,C}$ = 18.2, *m*-Ar*C*), 134.8 (d, $^1J_{P,C}$ = 9.6 Hz, *ipso*-Ar*C*), 134.3 (d, $^3J_{P,C}$ = 19.3, *m*-Ar*C*), 129.4 (s, *p*-Ar*C*), 129.1 (d, $^2J_{P,C}$ = 6.4 Hz, *o*-Ar*C*), 128.7 (d, $^2J_{P,C}$ = 6.4 Hz, *o*-Ar*C*), 43.2 (d, $^3J_{P,C}$ = 35.0 Hz, N-*C*H$_3$ (minor)), 40.6 (d, $^3J_{P,C}$ = 10.6 Hz, N-*C*H$_3$ (major)), 29.7 (d, $^2J_{P,C}$ = 9.7 Hz, C-*C*H$_3$ (major)), 19.4 (d, $^2J_{P,C}$ = 29.2 Hz, C-*C*H$_3$ (minor)). ^{31}P NMR (161.98 MHz, $CDCl_3$): 6.8 (s, *E* isomer, 48%), –13.2 (s, *Z* isomer, 52%). FT-IR: ν = 3075 (w), 3057 (w), 1669 (w), 1605 (w), 1555 (w), 1528 (w), 1482 (w), 1437 (m), 1395 (w), 1360 (w), 1336 (w), 1305 (w), 1277 (w), 1235 (w), 1172 (w), 1102 (w), 1073 (w), 1050 (w), 1030 (w), 1004 (w), 925 (w), 892 (w), 746 (m), 705 (s), 645 (w), 514 (w), 487 (w), 433 (w), 422 (w). MS (ESI-Q-TOF): calcd. for $C_{15}H_{17}NP$: 242.1093; found: 242.1087.

Tungsten (pentacarbonyl) (*P*-κ^1-7-diphenylphosphanyl-3,4,5,6-tetrahydro-azepine) (10). A colorless solution of **7a** (94 mg, 0.33 mmol, 1.0 equiv.) in DCM (10 mL) was added to a yellow solution of $W(CO)_5$(MeCN) (122 mg, 0.33 mmol, 1.0 equiv.) in DCM (10 mL) and heated to reflux for 24h in absence of light. After cooling to RT, it was stirred 18h to give an orange solution. Evaporation to dryness provided an orange oil which was extracted into pentane (6 x 8 mL). The combined extracts were evaporated to provide **10** as a yellow solid (163 mg, 0.27 mmol, 82%). *Crystallization:* Single crystals were obtained by slow evaporation of a pentane solution (130 mL/mmol) to provide colorless needles. Mp: 86.3°C dec. ^{1}H NMR (400.13 MHz, CD_2Cl_2): δ 7.72-7.55 (m, 4H, *m*-Ar*H*), 7.52-7.25 (m, 6H *o,p*-Ar*H*), 4.00-3.86 (m, 2H, N-C*H*$_2$), 2.52-2.39 (m, 2H, C-C*H*$_2$), 1.80-1.66 (m, 2H, N-CH$_2$CH$_2$C*H*$_2$), 1.63-1.47 (m, 2H, N-CH$_2$C*H*$_2$). 1.15-1.03 (m, 2H, C-CH$_2$C*H*$_2$). ^{13}C{^{1}H} NMR (125.78 MHz, CD_2Cl_2): δ 200.3 (d, $^1J_{C,P}$ = 21.7 Hz, *ipso*-ArC), 197.68 (dt, $^1J_{C,W}$ = 63.0 Hz, $^2J_{C,P}$ = 6.8 Hz, *trans*-*C*O), 191.8 (t, $^1J_{C,W}$ = 63.3 Hz, *C*O), 177.4 (d, $^1J_{C,P}$ = 51.7 Hz, P*C*N), 133.8 (d, $^2J_{P,C}$ = 10.7 Hz, *o*-Ar*C*), 130.7 (d, $^4J_{P,C}$ = 1.7 Hz, *p*-Ar*C*), 128.9 (d, $^3J_{P,C}$ = 9.2 Hz, *m*-Ar*C*), 54.6 (d, $^3J_{P,C}$ = 23.9 Hz, N-*C*H$_2$), 34.0 (d, $^2J_{P,C}$ = 28.0 Hz , C-*C*H$_2$), 31.5 (s, N-CH$_2$CH$_2$*C*H$_2$), 26.5 (s, N-CH$_2$*C*H$_2$), 24.5 (d, $^3J_{P,C}$ = 2.7 Hz, C-CH$_2$*C*H$_2$). ^{31}P NMR (161.98 MHz, CD_2Cl_2): δ30.2 (t, $^1J_{P,W}$ = 120.1 Hz). FT-IR: ν = 3065 (s), 2959 (w), 2928 (w), 2854 (w), 2069 (w), 1904 (s), 1873 (s), 1763 (s), 1736 (s), 1720 (m), 1634 (m), 1435 (m), 1421 (s),

1259 (m), 1094 (s), 1072 (s), 1014 (s), 980 (s), 795 (m), 744 (s), 692 (s), 598 (s), 567 (s), 536 (s), 507 (s), 494 (s), 469 (s), 432 (s). MS (ESI-Q-TOF): calcd. for $C_{23}H_{21}NO_5PW$: 606.0661; found 606.0663.

Tungsten (tetracarbonyl) (κ^2-7-diphenylphosphanyl-3,4,5,6-tetrahydroazepine) (11). [$W(CO)_4(COD)$] (190 mg, 0.47 mmol, 1.0 equiv.) was added to a light yellow solution of **7a** (139 mg, 0.49 mmol, 1.04 equiv.) in toluene (14 mL) to give a yellow suspension, which was heated to reflux for 24h in absence of light. After cooling to RT, it was stirred 18h to give a dark mixture, which was evaporated and washed with pentane (4 x 10 mL) to provide **11** as a brown powder (225 mg, 0.39 mmol, 57%). Mp: 64.9°C dec. ^{1}H NMR (400.13 MHz, CD_2Cl_2): 7.63-7.56 (m, 4H, *m*-Ar*H*), 7.56-7.49 (m, 6H, *o,p*-Ar*H*), 3.91-3.84 (m, 2H, N-C*H*$_2$), 2.48-2.40 (m, 2H, C-C*H*$_2$), 1.82-1.73 (m, 2H, N-CH_2CH_2C*H*$_2$), 1.64-1.54 (m, 2H, N-CH_2C*H*$_2$), 1.39-1.29 (m, 2H, C-CH_2C*H*$_2$). ^{13}C{^{1}H} NMR (125.78 MHz, CD_2Cl_2): 212.9 (d, $^2J_{C,P}$ = 6.2 Hz, *C*O), 212.0 (d, $^2J_{C,P}$ = 30.8 Hz, *C*O), 205.4 (td, $^1J_{C,W}$ = 65.3 Hz, $^2J_{C,P}$ = 6.2 Hz, *C*O), 197.7 (d, $^2J_{C,P}$ = 6.8 Hz, *C*O), 195.1 (d, $^1J_{C,P}$ = 35.6 Hz, *ipso*-Ar*C*), 176.9 (d $^1J_{C,P}$ = 50.3 Hz, P*C*N), 133.8 (d, $^2J_{P,C}$ = 14.6, *o*-Ar*C*), 132.0 (d, $^4J_{P,C}$ = 2.2 Hz, *p*-Ar*C*), 129.7 (d, $^3J_{P,C}$ = 10.3 Hz, *m*-Ar*C*), 62.6 (d, $^3J_{P,C}$ = 25.2 Hz, N-*C*H$_2$), 37.8 (d, $^2J_{P,C}$ = 5.1 Hz , C-*C*H$_2$), 30.9 (s, N-CH_2CH_2*C*H$_2$), 25.7 (s, N-CH_2*C*H$_2$), 23.7 (d, $^3J_{P,C}$ = 2.7 Hz, C-CH_2*C*H$_2$). ^{31}P NMR (161.98 MHz, DCM): –11.4 (t, $^1J_{P,W}$ = 92.6 Hz). FT-IR: ν = 3055 (s), 2928 (w), 2854 (w), 2069 (w), 2008 (w), 1869 (m), 1825 (s), 1736 (s), 1720 (m), 1479 (m), 1433 (w), 741 (m), 692 (s), 575 (s), 511 (s), 467 (s), 436 (m), 403 (m). MS (ESI-Q-TOF): calcd. for $C_{22}H_{21}NO_4PW$: 578.0716; found: 578.0713.

(*P*-κ^1-7-phosphanyl-3,4,5,6-tetrahydroazepine) (pentamethylcyclopentadienyl) rhodium(III) dichlorides (intermediates 12a-c). To a solution of *P*-κ^1-7-phosphanyl-3,4,5,6-tetrahydroazepine **7** (2 equiv.) in DCM (5 mL/mmol) was added $[RhCp^*Cl_2]_2$ (1 equiv.). The mixture was stirred for 30 min. and the resulting solution of **12** was used without further purification. *Data for **12a** are as follows:* ^{31}P NMR (161.98 MHz, DCM, RT): δ 36.9 (d, $^1J_{P,Rh}$ = 142.5 Hz, 42%), 30.1 (br. s, 58%). ^{31}P NMR (161.98 MHz, DCM, −94 °C): δ 38.0 (d, $^1J_{P,Rh}$ = 139.3 Hz,31%), 36.5 (d, $^1J_{P,Rh}$ = 137.7 Hz, 54%), 27.5 (d, $^1J_{P,Rh}$ = 153.9 Hz, 15%). *^{31}P NMR data (161.98 MHz, DCM) for **12b** are as follows:* δ 29.7 (d, $^1J_{P,Rh}$ = 134.7 Hz). *^{31}P NMR data (161.98 MHz, DCM) for **12c** are as follows:* δ 41.0 (d, $^1J_{P,Rh}$ = 131.8, 18%), 31.2 (d, $^1J_{P,Rh}$ = 127.7, 16%), −1.5 (d, $^1J_{P,Rh}$ = 105.4 Hz, 67%).

Chloro (κ^2-7-phosphanyl-3,4,5,6-tetrahydroazepine) (pentamethylcyclopentadienyl) rhodium(III) trifluoromethylsulfonates (13a-c). To a solution of **12** (1 equiv.) in DCM (5 mL/mmol) was added AgOTf (1 equiv.). The mixture was stirred for 60 min. at

RT in absence of light, during which the mixture turned bright orange. Filtration provided a red solution, which was evaporated to dryness. Washing with pentane (2 x 25 mL/mmol) provided **13** as a red solid. (**13a**, 82%; **13b**, 83%; **13c**, 75%). *Data for **13a** are as follows:* Mp: 156.8°C dec. ^{1}H NMR (500.23 MHz, CD_2Cl_2): δ 7.87-7.80 (m, 2H, Ar*H*), 7.71-7.61 (m, 4H, Ar*H*), 7.59-7.52 (m, 2H, Ar*H*), 7.45-7.37 (m, 2H, Ar*H*), 4.33-4.16 (m, 1H,C*H*H), 3.97-3.85 (m, 1H, C*H*H), 3.04-2.89 (m 1H, C*H*H), 2.67-2.52 (m 1H, C*H*H), 1.90-1.65 (m 5H, C*H*H), 1.58 (d, $^{3}J_{H,Rh}$ = 4.9 Hz, 15H, C-C*H*$_3$), 1.31-1.18 (m, 1H, C*H*H). ^{13}C{^{1}H} NMR (125.78 MHz, THF-d$_8$): δ 198.5 (dd, $^{1}J_{C,P}$ = 48.6 Hz, $^{2}J_{C,Rh}$ = 3.6 Hz, P*C*N), 136.3 (d, $J_{C,P}$ = 11.7 Hz, Ar*C*), 134.0 (d, $^{4}J_{C,P}$ = 2.6 Hz, *p*-Ar*C*), 133.1 (d, $^{4}J_{C,P}$ = 3.2 Hz, *p*-Ar*C*), 132.9 (d, $J_{C,P}$ = 10.4 Hz, Ar*C*), 130.6 (d, $J_{C,P}$ = 11.1 Hz, Ar*C*), 129.8 (d, $J_{C,P}$ = 11.1 Hz, Ar*C*), 124.0 (d, $^{2}J_{C,P}$ = 43.7 Hz, *ipso*-Ar*C*), 121.7 (d, $^{2}J_{C,P}$ = 33.6 Hz, *ipso*-Ar*C*), 121.3 (q, $^{1}J_{C,F}$ = 321.3 Hz, O_3SCF_3), 99.6 (dd, $^{1}J_{C,Rh}$ = 7.0 Hz, $^{2}J_{C,P}$ = 2.8 Hz, *C*CH$_3$), 59.4 (d, $J_{C,P}$ = 20.9 Hz, *C*H$_2$), 37.2 (d, 6.5 Hz, *C*H$_2$), 30.0 (s, *C*H$_2$), 27.0 (s, *C*H$_2$), 22.9 (d, 2.1 Hz, *C*H$_2$), 9.5 (s, C*C*H$_3$). ^{19}F{^{1}H} NMR (235.36 MHz, CD_2Cl_2): *δ* –78.9 (s, O_3SCF_3). ^{31}P NMR (161.98 MHz, DCM): δ −16.9 (d, $^{1}J_{P,Rh}$ = 114.7 Hz). FT-IR: *ν* 2932 (s), 2860 (w), 1612 (w), 1483 (w), 1437 (w), 1377 (m), 1258 (w), 1225 (s), 1150 (m), 1103 (s), 1028 (m), 922 (s), 802 (w), 748 (w), 694 (m), 636 (m), 571 (s), 555 (w), 515 (m), 471 (s). MS (ESI-Q-TOF): calcd. for $C_{28}H_{35}ClNPRh$: 554.1245; found: 554.1262. *Data for **13b** are as follows:* Mp: 43.2-56.8 °C. ^{1}H NMR (400.13 MHz, $CDCl_3$): *δ* 4.09-3.97 (m, 1H, CH*H*), 3.79-3.68 (m, 1H, CH*H*), 2.98-2.82 (m, 1H, CH*H*), 2.51-2.24 (m, 4H, C*H*$_2$), 2.02-1.23 (m, 30H, CC*H*$_3$, C*H*$_2$, CH*H*), 1.02-0.88 (m, 6H, CH$_2$C*H*$_3$). ^{13}C{^{1}H} NMR (100.61 MHz, $CDCl_3$): δ 199.9 (dd, $^{1}J_{C,P}$ = 45.5 Hz, $^{2}J_{C,Rh}$ = 3.9 Hz, P*C*N), 121.0 (q, $^{1}J_{C,F}$ = 321.1 Hz, O_3SCF_3), 98.6 (dd, $^{1}J_{C,Rh}$ = 7.1 Hz, $^{2}J_{C,P}$ = 2.8 Hz, *C*CH$_3$), 58.6 (d, $J_{C,P}$ = 19.4 Hz, *C*H$_2$), 37.9 (d, $J_{C,P}$ = 4.9 Hz, *C*H$_2$), 30.0 (s, *C*H$_2$), 27.4 (d, $J_{C,P}$ = 8.7 Hz, *C*H$_2$), 25.6 (d, $J_{C,P}$ = 39.0 Hz, *C*H$_2$), 24.4 (d, $J_{C,P}$ = 12.4 Hz, *C*H$_2$), 24.0 (d, $J_{C,P}$ = 15.2 Hz, *C*H$_2$), 22.8 (s, *C*H$_2$), 20.4 (d, $J_{C,P}$ = 15.1 Hz, *C*H$_2$), 17.0 (d, $J_{C,P}$ = 16.6, *C*H$_2$), 13.7 (d, $^{4}J_{C,P}$ = 6.5 Hz, CH$_2$*C*H$_3$), 9.9 (s, C*C*H$_3$). ^{31}P NMR (161.98 MHz, $CDCl_3$): *δ* −19.8 (d, $^{1}J_{PRh}$ = 108.7 Hz). FT-IR: *ν* 2958 (w), 2929 (w), 2866 (w), 1610 (w), 1450 (w), 1379 (w), 1257 (s), 1222 (m), 1143 (s), 1093 (m), 1072 (m), 1029 (s), 981 (w), 966 (w), 925 (w), 910 (w), 894 (w), 860 (w), 800 (m), 752 (w), 721 (w), 715 (w), 653 (w), 636 (s), 588 (w), 570 (m), 543 (m), 516 (s), 489 (w), 459 (m). MS (ESI-Q-TOF): calcd. for $C_{24}H_{43}ClNPRh$: 514.1882; found 514.1881 (100%). *Data for **13c** are as follows:* Mp: 81.1°C dec. ^{1}H NMR (500.23 MHz, $CDCl_3$): *δ* 4.17-4.05 (m, 1H, CH*H*), 3.85-3.76 (m, 1H, CH*H*), 2.94-2.80 (m, 1H, CH*H*), 2.77-2.54 (m, 2H, C*H*), 2.54-2.42 (m, 1H, CH*H*), 2.20-2.09 (m, 1H, CH*H*), 2.01-1.20 (m, 39H, CC*H*$_3$, C*H*$_2$, CH*H*), 0.90-0.76 (m, 1H, CH*H*). ^{13}C{^{1}H} NMR (125.78 MHz, $CDCl_3$): *δ* 199.6 (dd, $^{1}J_{C,P}$ = 38.8 Hz, $^{2}J_{C,Rh}$ = 3.5 Hz, P*C*N), 120.7 (q, $^{1}J_{C,F}$ = 322.0 Hz, O_3SCF_3), 98.6 (dd, $^{1}J_{C,Rh}$ = 7.1 Hz, $^{2}J_{C,P}$ = 2.5 Hz, *C*CH$_3$), 59.3 (d, $J_{C,P}$ = 18.9 Hz, *C*H$_2$), 39.7 (d, $J_{C,P}$ = 5.8 Hz, *C*H$_2$), 35.5 (d, $^{1}J_{C,P}$ = 12.8 Hz, Cy-*C*H), 33.7 (d, $^{1}J_{C,P}$ = 9.3 Hz, Cy-*C*H), 30.3 (d, $J_{C,P}$ = 5.3 Hz, *C*H$_2$),

30.1 (s, *C*H$_2$), 29.7 (d, $J_{C,P}$ = 20.7 Hz, *C*H$_2$), 29.2 (s, *C*H$_2$), 27.3 (d, $J_{C,P}$ = 12.9 Hz, *C*H$_2$), 26.8 (d, $J_{C,P}$ = 11.8 Hz, *C*H$_2$), 26.6 (d $J_{C,P}$ = 13.4 Hz, *C*H$_2$), 26.3 (d, $J_{C,P}$ = 9.7 Hz, *C*H$_2$), 25.6 (d, $J_{C,P}$ = 13.7 Hz, *C*H$_2$), 25.4 (s, *C*H$_2$), 22.4 (s, *C*H$_2$), 10.2 (s, C*C*H$_3$). ^{31}P NMR (161.98 MHz, $CDCl_3$): δ −5.7 (d, $^1J_{PRh}$ = 104.8 Hz). FT-IR: ν 2927 (m), 2854 (w), 1600 (w), 1585 (w), 1448 (m), 1375 (w), 1359 (w), 1257 (s), 1220 (s), 1143 (s), 1103 (m), 1076 (s), 1029 (s), 981 (m), 952 (w), 921 (w), 889 (m), 850 (m), 815 (m), 802 (m), 773 (w), 752 (m), 725 (w), 698 (w), 634 (s), 592 (w), 570 (s), 555 (m), 514 (s), 487 (m), 482 (m), 472 (m), 460 (m). MS (ESI-Q-TOF): calcd. for $C_{28}H_{47}ClNPRh$: 566.2195; found 566.2210.

(*P*-κ^1-((*N*-methyl) acetimidoyl) diphenylphosphanyl) (pentamethylcyclopentadienyl) rhodium(III) dichloride (intermediate). To a solution of ((*N*-methyl)acetimidoyl)diphenylphosphane **9** (47 mg, 0.20 mmol, 2.0 equiv.) in DCM (10 mL) was added $[RhCp^*Cl_2]_2$ (60 mg, 0.10 mmol, 1.0 equiv.). The mixture was stirred for 30 min. and the resulting solution of *P*-κ^1-((*N*-methyl) acetimidoyl) diphenylphosphanyl) (pentamethylcyclopentadienyl) rhodium(III) dichloride was used without further purification. ^{31}P NMR (161.98 MHz, DCM, RT): δ 37.4 (d, $^1J_{P,Rh}$ = 142.0 Hz, 5%), 31.7 (br. s, 89%), −15.1 (d, $^1J_{P,Rh}$ = 114.7 Hz, 4%). ^{31}P NMR (161.98 MHz, DCM, −93 °C): δ 39.1 (d, $^1J_{P,Rh}$ = 144.2 Hz, 55%), 33.9 (d, $^1J_{P,Rh}$ = 152.3 Hz, 4%), 27.7 (d, $^1J_{P,Rh}$ = 132.8 Hz, 29%), 13.3 (d, $^1J_{P,Rh}$ = 142.1 Hz, 5%), −15.0 (d, $^1J_{P,Rh}$ = 115.0 Hz, 6%).

Chloro (κ^2-((*N*-methyl) acetimidoyl) diphenylphosphanyl) (pentamethylcyclopentadienyl) rhodium(III) trifluoromethylsulfonate. To a solution of *P*-κ^1-((*N*-methyl) acetimidoyl) diphenylphosphanyl) (pentamethylcyclopentadienyl) rhodium(III) dichloride (99 mg, 0.18 mmol, 1.0 equiv.) in DCM (9.4 mL) was added AgOTf (47 mg, 0.18 mmol, 1.0 equiv.). The mixture was stirred for 60 min. at RT in absence of light, during which the mixture turned bright orange. Filtration provided a red solution, which was evaporated to dryness. Washing with pentane (3 x 5 mL) provided Chloro (κ^2-((*N*-methyl) acetimidoyl) diphenylphosphanyl) (pentamethylcyclopentadienyl) rhodium(III) trifluoromethylsulfonate as a red solid (86 mg, 0.13 mmol, 72%). ^{1}H NMR (500.23 MHz, $CDCl_3$): δ 7.85-7.79 (m, 2H, Ar*H*), 7.69-7.58 (m, 6H, Ar*H*), 7.56-7.51 (m, 2H, Ar*H*), 3.63 (d, $^3J_{H,Rh}$ = 4.2 Hz, 3H, N-C*H*$_3$), 2.33 (dd, $^3J_{H,P}$ = 7.0 Hz, $^4J_{H,Rh}$ = 0.9 Hz, 3H, NC-C*H*$_3$), 1.63 (d, $^3J_{H,Rh}$ = 4.7 Hz, 15H, Cp*-CC*H*$_3$). $^{13}C\{^1H\}$ NMR (125.78 MHz, $CDCl_3$): δ 192.8 (dd, $^1J_{C,P}$ = 52.4 Hz $^2J_{C,Rh}$ = 3.7 Hz, PC*N*), 136.2 (d, $J_{C,P}$ = 11.5 Hz, Ar*C*), 133.7 (d, $^4J_{C,P}$ = 2.6 Hz, *p*-Ar*C*), 133.1 (d, $J_{C,P}$ = 10.7 Hz, Ar*C*), 132.8 (d, $^4J_{C,P}$ = 2.9 Hz, *p*-Ar*C*), 130.5 (d, $J_{C,P}$ = 11.2 Hz, Ar*C*), 129.6 (d, $J_{C,P}$ = 11.0 Hz, Ar*C*), 123.6 (d, $^1J_{C,P}$ = 44.7 Hz, *ipso*-Ar*C*), 121.6 (d, $^1J_{C,P}$ = 33.5 Hz, *ipso*-Ar*C*), 121.1 (q, $^1J_{C,F}$ = 321.1 Hz, O_3SCF_3), 99.4 (dd, $^1J_{C,Rh}$ = 7.2 Hz, $^2J_{C,P}$ = 2.8 Hz, Cp*-*C*CH$_3$), 43.1 (d, $^2J_{C,Rh}$ =

19.7 Hz, N-*C*CH_3), 21.0 (d, $^3J_{C,Rh}$ = 7.3 Hz, NC-*C*CH_3), 9.5 (s, Cp*-C*C*H_3). $^{19}F\{^1H\}$ NMR (470.61 MHz, CD_2Cl_2): δ –78.2 (s, O_3SCF_3). ^{31}P NMR (161.98 MHz, $CDCl_3$): δ −18.0 ppm, $^1J_{P,Rh}$ = 114.8 Hz). FT-IR: ν 3487 (s), 3061 (w), 2982 (w), 2924 (w), 1618 (w), 1572 (w), 1483 (w), 1437 (w), 1377 (m), 1258 (w), 1223 (s), 1146 (m), 1101 (m), 1028 (m), 916 (s), 800 (w), 746 (w), 692 (m), 636 (m), 509 (s). MS (ESI-Q-TOF): calcd. for $C_{25}H_{31}ClNPRh$: 514.0932; found 514.0939.

(*P*-κ^1-7-phosphanyl-3,4,5,6-tetrahydroazepine) (*p*-cymene) ruthenium(II) dichlorides (14a,b). [Ru(*p*Cym)Cl_2]$_2$ (1.0 equiv) was added to a solution of **7** (2 equiv.) in DCM (50 mL/mmol) and stirred for 30 min. After evaporation to dryness, washing with pentane (4 x 50 mL/mmol) provided **14** (**14a**, n.a.; **14b**, 66%). *Data for **14a** are as follows:* ^{31}P NMR (161.98 MHz, THF): δ 31.2 (s, 27%), 23.4 (s, 73%). *Data for **14b** are as follows:* Mp: 122.9°C dec. ^1H NMR (400.13 MHz, C_6D_6): δ 5.33 (d, $^3J_{HH}$ = 6.0 Hz, 2H, CH_3-CC*H*), 5.26 (d, $^3J_{HH}$ = 6.0 Hz, 2H, C*H*C-CH), 3.74-3.67 (m, 2H, N-CH_2), 2.91 (sept., $^3J_{HH}$ = 7.2 Hz, 1H, C*H*CH_3), 2.66 (q, 2H, N-CH_2), 2.58-2.48 (m, 2H, CCH_2CH_2), 2.38-2.26 (m, 2H, NCH_2CH_2), 1.87-1.72 (m, 5H, C-CH_3 + NCH_2CH_2-CH_2), 1.41-1.18 (m, 12H, $PCH_2CH_2CH_2$), 1.15 (d, $^3J_{HH}$ = 6.8 Hz, 6H, CHCH_3), 0.85 (t, $^3J_{HH}$ = 6.8 Hz, 6H, CH_2CH_3). $^{13}C\{^1H\}$ NMR (100.61 MHz, C_6D_6): δ 182.8 (d, 48.2 Hz, P*C*N), 107.6 (s, *C*-$CHCH_3$), 95.1 (s, CH_3-*C*), 94.4 (s, *C*HC-$CHCH_3$), 89.7 (d $J_{C,P}$ = 3.8 Hz, Ar*C*), 85.0 (d, $J_{C,P}$ = 5.3 Hz, Ar*C*), 53.9 (d, $J_{C,P}$ = 19.5 Hz, N-*C*H_2), 34.1 (d, $J_{C,P}$ = 23.7 Hz, *C*H_2), P-CH_2), 31.6 (s, *C*H_2), 30.9 (s, *C*$H(CH_3)_2$), 27.0 (s, *C*HH), 26.3 (d, $J_{C,P}$ = 4.7 Hz, P-CH_2CH_2*C*H_2), 24.9 (d, $J_{C,P}$ = 12.5 Hz, P-CH_2*C*H_2), 23.8 (d $J_{C,P}$ = 3.2 Hz, *C*H_2), 22.4 (s, $CH(CH_3)_2$), 22.3 (d, $J_{C,P}$ = 28.3 Hz, *C*HH), 18.1 (s, C-*C*H_3 cym), 14.0 (s, CH_2*C*H_3). ^{31}P NMR (161.98 MHz, C_6D_6): δ 29.8 (s). MS (ESI-Q-TOF): calcd. for $C_{24}H_{43}Cl_2NPRu$: 548.1548; found 548.1540.

1-Benzotriazolyl-(2S,5R)-2-isopropyl-5-methyl-3,4,5,6-tetrahydro-2H-azepine (19). MsCl (2.56 mL, 33 mmol, 1.2 equiv.) was added dropwise to a solution of l-menthone oxime (4.68 g, 27.6 mmol, 1.0 equiv.) and NEt_3 (9.2 mL, 66 mmol, 2.2 equiv.) in MeCN (60 mL) at 0 °C. The mixture was stirred for 30 min. to give a yellow solution, to which benzotriazole (3.65 g, 29 mmol, 1.1 equiv.) was added. The mixture was subsequently refluxed for 2.5h and the resulting orange-brown solution was cooled to RT. Evaporation provided a brown solid, which was extracted into Et_2O (3 x 40 mL) under atmospheric conditions. The combined Et_2O fractions were filtered over a pad of neutral aluminium oxide, after which evaporation provided **19** as an orange oil (6.11 g, 22.6 mmol, 90%). *Crystallization:* If desired, crystals (mp <RT) can be obtained by slowly cooling a hot MeCN solution (0.17 mL/mmol compound) to −20°C. ^1H NMR (400.13 MHz, $CDCl_3$): δ 8.52 (d, $^3J_{H,H}$ = 8.5 Hz, 1H, CNC-C*H*), 8.07 (d, $^3J_{H,H}$ = 8.4 Hz, 1H, CNCC-C*H*), 7.57-7.51 (m,

1H, CNC-CH-C*H*), 7.44-7.39 (m, 1H, CNCC-CH-C*H*), 4.00 (d, $^{3}J_{H,H}$ = 14.2 Hz, 1H, NC-C*H*H), 3.47 (dd $^{3}J_{H,H}$ = 9.5 Hz, $^{3}J_{H,H}$ = 4.1 Hz. 1H N-C*H*), 2.74 (dd, $^{3}J_{H,H}$ = 14.2 Hz, $^{3}J_{H,H}$ = 11.4 Hz, 1H, NC-C*H*H), 2.08-2.00 (m, 1H, CH*H*), 1.97-1.85 (m, 1H, CH*H*), 1.80-1.67 (m, 2H, CH*H*+CH*H*), 1.58-1.46 (m, 1H, CH*H*), 1.45-1.33 (m, 1H, CH*H*), 1.11 (d, $^{3}J_{H,H}$ = 6.7 Hz, 3H, C*H*$_3$), 1.08 (d, $^{3}J_{H,H}$ = 6.7 Hz, 3H, C*H*$_3$), 1.06 (d, $^{3}J_{H,H}$ = 6.8 Hz, 3H, C*H*$_3$). ^{13}C{^{1}H} NMR (125.78 MHz, $CDCl_3$): δ 159.0 (s, N*C*N), 147.0 (s, NCN*C*), 131.5 (s, CNC*C*)), 128.8 (s, CNC-CH-*C*H), 125.0 (s, CNCC-CH-*C*H), 119.6 (s, CNCC-*C*H), 116.0 (s, CNC-*C*H), 65.5 (s, N-*C*H), 39.9 (s, NH-CH-CH_2*C*H_2), 36.5 (s, C-*C*H_2), 35.0 (s, CH*C*H-CH_3), 29.8 (s, N-CH-*C*H_2), 29.6 (s, CH_2*C*H-CH_3), 24.2 (s, CH_2CH-*C*H_3), 20.1(s, CHCH-*C*H_3), 17.7 (s, CHCH-*C*H_3). FT-IR: *ν* 2955 (m), 2922 (m), 2870 (w), 2845 (w), 1670 (s), 1637 (m), 1483 (m), 1445 (s), 1389 (s), 1377 (s), 1364 (s), 1352 (m), 1279 (s), 1232 (m), 1198 (m), 1142 (m), 1128 (m), 1094 (m), 1020 (s), 1005 (s), 986 (s), 955 (m), 924 (m), 876 (w), 870 (w), 812 (m), 783 (s), 771 (s), 748 (s), 662 (w), 625 (w), 596 (m), 566 (m), 525 (m), 434 (m). MS (ESI-Q-TOF): calcd. for $C_{10}H_{19}N$: 153.1512, found: 153.1379 ([MH-$C_6H_4N_3$]$^+$); calcd. for $C_{20}H_{37}N_2$: 305.2951, found: 305.2940 ([(M-$C_6H_4N_3$)$_2$H]$^+$). No peak could be observed for [MH]$^+$.

1-Benzotriazolyl-(2S,5R)-2-isopropyl-5-methyl-3,4,5,6-tetrahydro-2H-azepinium trifluoromethanesulfonate (20). To a solution of **19** (500 mg, 1.85 mmol, 1 equiv.) in $CHCl_3$ (4 mL) was added triflic acid (163 µL, 1.85 mmol, 1 equiv.) dropwise at 0°C. The resulting solution was stirred for 30 min., after which it was allowed to heat to RT. Evaporation and washing with pentane (4 x 5 mL) provided **20** as a brown solid yielded (610 mg, 1.45 mmol, 79%). *Crystallization:* Single crystals of **20** were obtained by slow diffusion of pentane into a saturated DCM solution. Mp: 112.4°C dec. ^{1}H NMR (500.23 MHz, DMSO-d$_6$): δ 14.70 (s, 1H, N*H*), 8.45 (d, $^{1}J_{H,H}$ = 8.5 Hz, 1H, CNC-C*H*), 8.15 (d, $^{1}J_{H,H}$ = 8.5 Hz, 1H, CNCC-C*H*), 7.71-7.66 (m, 1H, CNC-CH-C*H*),7.54-7.49 (m, 1H, CNCC-CH-C*H*), 3.74 (d, 1H , $^{2}J_{H,H}$ =14.0 Hz, NH-C-C*H*H), 3.56 (dd, 9.6 3.4 Hz 1H, NH-C*H*), 2.91 (dd, 1H, $^{2}J_{HH}$ = 14.0 Hz, $^{1}J_{HH}$ = 12.0 Hz, NH-C-C*H*H), 1.99-1.82 (m, 2H, C*H*$_2$), 1.76-1.58 (m, 2H, C*H*$_2$), 1.57-1.47 (m, 1H, C*H*), 1.34-1.23 (m, 1H, C*H*), 1.09-0.96 (m, 9H,CH-C*H*$_3$). ^{13}C{^{1}H} NMR (125.78 MHz, DMSO-d$_6$): δ 158.6 (s, N*C*N), 146.2 (s, NCN*C*), 130.8 (s, CNC*C*), 129.2 (s, CNC-CH-*C*H), 125.4 (s, CNCC-CH-*C*H), 120.7 (q, $^{1}J_{CF}$ = 321.1 Hz, O_3SCF_3), 119.6 (s, CNCC-*C*H), 115.3 (s, CNC-*C*H), 64.2 (s, NH-*C*H), 38.8 (s, NH-CH-CH_2*C*H_2), 35.9 (s, C-*C*H_2), 34.4 (s, CH*C*H-CH_3), 29.3 (s, NH-CH-*C*H_2), 29.0 (s, CH_2*C*H-CH_3), 24.0 (s, CH_2CH-*C*H_3), 19.9 (s, CHCH-*C*H_3), 17.4 (s, CHCH-*C*H_3). ^{19}F{^{1}H} NMR (235.36 MHz, $CDCl_3$): *δ* –77.8 (s, O_3SCF_3). FT-IR: *ν* 3097 (w), 2972 (w), 2935 (w), 2880 (w), 1666 (s), 1647 (m), 1593 (w), 1558 (w), 1506 (m), 1481 (m), 1458 (m), 1416 (w), 1332 (w), 1277 (s), 1246 (s), 1223 (s), 1161 (s), 1151 (s), 1128 (s), 1097 (m), 1066 (s), 1026 (s), 993 (m), 957 (m), 947 (m), 935 (m), 906 (m), 887 (m), 824 (m), 808 (m), 773 (s), 754 (s),

633 (s), 611 (s), 573 (s), 513 (s), 417 (m). MS (ESI-Q-TOF): calcd. for $C_{10}H_{19}N$: 153.1512, found: 153.1386 ($[M-C_6H_4N_3]^+$); calcd. for $C_{20}H_{37}N_2$: 305.2951, found: 305.1556 ($[(M-C_6H_4N_3)_2-H]^+$). No peak could be observed for $[M]^+$.

Dehydrocoupling of phosphanes to diphosphanes (attempted synthesis of 7-(diphenylphosphanyl) (2S,5R)-2-isopropyl-5-methyl-3,4,5,6-tetrahydro-2H-azepine (21)). *Protocol 1:* To a solution of **19** (1.12 g, 4.13 mmol, 1.03 equiv.) in $CHCl_3$ (6.5 mL) was added triflic acid (366 µL, 4.13 mmol, 1.03 equiv.) dropwise at 0°C. The resulting brown mixture was stirred for 10 min. and evaporated. Washing with Et_2O (1 x 15 mL) provided a brown oil, which was dissolved in THF (15 mL). Diphenylphosphane (0.7 mL, 4.0 mmol, 1.00 equiv.) was added dropwise, and after 10 min. stirring a red solution was obtained. Analysis by ^{31}P NMR spectroscopy showed 85% conversion to tetraphenyldiphosphane. The solution was evaporated and extracted with Et_2O (1 x 10 mL). Evaporation provided pure tetraphenyldiphosphane (0.21 g, 0.57 mmol, 27%). ^{31}P NMR (161.98 MHz, $CDCl_3$): δ –15.0 (s). *Protocol 2:* To a mixture of **20** (0.020 g, 0.048 mmol, 1.0 equiv.) in THF (0.6 mL) was added 2,4,6-(tri-*tert*-butyl)phenylphosphane (0.027 g, 0.097 mmol, 2.0 equiv.). The resulting mixture was vigorously shaken for several min. Analysis by ^{31}P NMR spectroscopy showed 66% conversion to 1,2-di(2,4,6-(tri-*tert*-butyl)phenyl)diphosphane. ^{31}P NMR (161.98 MHz, THF): δ –63.8 (dm).

Lithium diphenylphosphide. A solution of diphenylphosphane (1 equiv.) in THF (6.25 mL/mmol) was cooled to −78°C, after which *n*-BuLi (1.6 M in hexanes, 1 equiv.) was added dropwise. The mixture was stirred for 15 min. and then allowed to warm to room temperature and used directly without further purification. *^{31}P NMR (161.98 MHz, THF):* δ −23.9 (s).

7-(diphenylphosphanyl) (2S,5R)-2-isopropyl-5-methyl-3,4,5,6-tetrahydro-2H-azepine (21) via 7-(diphenylphosphanyl)-(2S,5R)-2-isopropyl-5-methyl-3,4,5,6-tetrahydro-2H-azepinium trifluoromethylsulfonate (22). *Step 1:* To a solution of **19** (2.11 g, 7.84 mmol, 1.0 equiv.) in THF (40 mL), was added a solution of lithium diphenyl phosphide (9.41 mmol, 1.1 equiv.) in THF (20 mL) dropwise at −78°C over a period of 1h. The resulting solution was allowed to warm to RT and evaporated. The resulting oil was extracted into pentane (5 x 40 mL). The combined extracts were evaporated to provide crude **21** (71% pure; contaminants: Ph_2PLi, Ph_2PH, Ph_2P-PPh_2). *Step 2:* To a solution of crude **21** (5.55 mmol, 1.0 equiv.) in THF (20 mL) was added triflic acid (489 µL, 5.55 mmol, 1.0 equiv.) dropwise at −78°C over a period of 30 min. The resulting mixture was allowed to warm to RT and evaporated. The resulting yellow solid was washed with THF (4 x 10

mL) and pentane (1 x 10 mL) to provide **22** as a white solid (2.1 g, 4.31 mmol, 78%). *Crystallization **22**:* single crystals could be obtained by slow vapor diffusion of pentane into a saturated solution in DCM. *Step 3:* To a suspension of **22** (1.60 g, 3.29 mmol, 1.0 equiv.) in THF (20 mL), was added a solution of NaHMDS (0.78 g, 4.27 mmol, 1.1 equiv.) in THF (5 mL) dropwise at −78°C. The resulting mixture was stirred for 1h and then allowed to warm to RT. Evaporation provided an oil, which was extracted with pentane (4 x 5 mL). The combined extracts were evaporated to give **21** as an orange oil (1.05 g, 3.12 mmol, 95%), which was used without further purification. *Data for **21** are as follows:* ^{1}H NMR (400.13 MHz, THF-d_8): δ 7.56-7.40 (m, 4H, Ar*H*),7.38-7.19 (m, 6H, Ar*H*), 3.25-3.19 (m, 1H, N-C*H*), 2.38-2.26 (m, 1H, C-C*H*H), 2.21-2.13 (m, 1H, C-CH*H*), 1.89-1.82 (m, 1H, CCH_2CH), 1.75-1.64 (m, 1H, N-CH-C*H*H-C*H*H), 1.61-1.53 (m, 1H, N-CH-CHH-C*H*H), 1.39-1.07 (m, 3H, N-CH-C*H*H + N-CH-C*H*), 0.83 (dd, $^{3}J_{H,H}$ = 6.0 Hz, $^{3}J_{H,H}$ = 2.8 Hz, 6H, $CH(CH_3)_2$) , 0.70 (d, $^{3}J_{H,H}$ = 6.0 Hz, 3H, C-CH_2CH-CH_3). Contaminant: $(Me_3Si)_2NH$ (22%). $^{13}C\{^{1}H\}$ NMR (100.61 MHz, THF-d_8): δ 177.9 (d, $^{1}J_{C,P}$ = 7.3 Hz, P*C*N), 136.4 (d, $^{1}J_{C,P}$ = 13.4 Hz, *ipso*-Ar*C*), 136.3 (d, $^{1}J_{C,P}$ = 12.7 Hz, *ipso*-Ar*C*), 135.6 (d, $^{1}J_{C,P}$ = 19.0 Hz, Ar*C*), 135.3 (d, $J_{C,P}$ = 18.8 Hz, Ar*C*), 129.3 (d, $J_{C,P}$ = 5.4 Hz, Ar*C*), 128.7 (d, $J_{C,P}$ = 7.3 Hz, Ar*C*), 128.4 (d, $J_{C,P}$ = 7.3 Hz, Ar*C*), 68.5 (d, $^{3}J_{C,P}$ = 9.5 Hz, N*C*H), 43.3 (d, $^{2}J_{C,P}$ = 36.4 Hz, C-*C*H_2), 40.5 (s, N-CHCH$_2$*C*H_2), 35.8 (s, *C*H(CH_3)$_2$), 30.6 (d, $^{3}J_{C,P}$ = 2.1 Hz, C-CH_2*C*H), 30.5 (d, $^{4}J_{C,P}$ =1.9 Hz, N-CH*C*H_2), 24.1 (s, C-CH_2CH-*C*H_3), 20.1 (s, CH(*C*H_3)$_2$), 17.4 (s, CH(*C*H_3)$_2$). ^{31}P NMR (161.98 MHz, THF-d_8): δ 5.8 (s, 90%). Contaminants: δ 11.2 (s, 3%) δ –15.6 (s, 4%) δ –22.4 (s, 3%). FT-IR: ν 3070 (w), 3053 (w), 2952 (m), 2918 (w), 2869 (w), 2842 (w), 1622 (w), 1585 (w), 1479 (w), 1456 (w), 1434 (m), 1379 (w), 1361 (w), 1303 (w), 1274 (w), 1249 (m), 1178 (m), 1130 (w), 1097 (w), 1068 (w), 1047 (m), 1026 (m), 989 (w), 929 (s), 883 (m), 838 (s), 837 (s), 771 (w), 738 (s), 695 (s), 640 (m), 619 (m), 590 (m), 505 (m), 462 (m). MS (ESI-Q-TOF): calcd. for $C_{22}H_{29}NP$: 338.2032; found 338.2105. *Data for **22** are as follows:* Mp: 190.8-197.7°C. ^{1}H NMR (400.13 MHz, $CDCl_3$): δ 8.85 (br. s, 1H, *NH*), 7.85-7.71 (m, 2H, Ar*H*), 7.71-7.55 (m, 8H, Ar*H*), 4.38-4.28 (m, 1H, NH-C*H*), 3.31-3.16 (m, 1H, C-C*H*H), 2.74 (dd, $^{2}J_{HH}$ = 14.4 Hz, $^{3}J_{HH}$ = 8.0 Hz, 1H, C-CH*H*), 2.05-1.94 (m, 2H, C*H*(CH_3)$_2$ + NH-CH-CHH-C*H*H)), 1.88-1.53 (m, 2H, NH-CHC*H*H, NH-CH-CHH-CH*H*), 1.48-1.33 (m, 1H, NH-CHCH*H*), 0.96 (d, $^{3}J_{HH}$ = 6.0 Hz, 3H, C-CHH-CH-CH_3), 0.88-0.81 (m, 1H, C-CHH-C*H*), 0.79 (d, $^{3}J_{HH}$ = 6.8 Hz, 3H, CH_3-CH-CH_3), 0.73 (d, $^{3}J_{HH}$ = 6.8 Hz, 3H, *C*H_3-CH-CH_3). $^{13}C\{^{1}H\}$ NMR (125.78 MHz, $CDCl_3$): δ 207.5 (d, $J_{C,P}$ = 46.0 Hz, P*C*NH), 136.4 (d, $J_{C,P}$ = 22.4 Hz, Ar*C*), 136.0 (d, $J_{C,P}$ = 21.4 Hz, Ar*C*), 132.8 (d, $J_{C,P}$ = 51.4 Hz, Ar*C*), 130.7 (d, $J_{C,P}$ = 9.7 Hz, Ar*C*), 130.6 (t, $J_{C,P}$ = 10.5 Hz, Ar*C*), 126.1 (d, $^{1}J_{C,P}$ = 7.2 Hz, *ipso*-Ar*C*), 125.7 (d, $^{1}J_{C,P}$ = 1.8 Hz, *ipso*-Ar*C*), 67.6 (d, $^{3}J_{C,P}$ = 2.5 NH-*C*H), 42.8 (d, $^{2}J_{C,P}$ = 16.2 C-*C*H_2), 37.4 (s, NH-CHCH$_2$*C*H_2), 31.4 (s, *C*H(CH_3)$_2$), 30.6 (d, $^{3}J_{C,P}$ = 4.7 Hz, C-CH_2*C*H), 27.7 (d, $^{4}J_{C,P}$ = 3.1 Hz, NH-CH*C*H_2), 23.9 (s, C-CH_2CH-*C*H_3), 17.7 (d, $^{5}J_{C,P}$ = 8.1 Hz, CH(*C*H_3)$_2$). ^{31}P NMR (161.98

MHz, THF): δ 15.8 (s). ^{31}P NMR (161.98 MHz, DMSO-d_6): δ 11.5 (s). FT-IR: ν 3220 (w), 3145 (w), 3050 (w), 2960 (w), 2920 (w), 2890 (w), 1610 (m), 1570 (w), 1470 (w), 1455 (w), 1435 (m), 1390 (w), 1330 (w), 1280 (s), 1250 (s), 1225 (s), 1195 (m), 1185 (m), 1150 (s), 1090 (m), 1075 (m), 1055 (m), 1030 (s), 990 (m), 960 (w), 945 (w), 915 (w), 890 (w), 860 (m), 845 (m), 800 (m), 755 (s), 745 (s), 730 (m), 700 (s), 695 (s), 670 (w), 635 (s), 620 (s), 570 (m), 550 (m), 535 (m), 505 (s), 490 (s).

(*P*-κ^1-7-(diphenylphosphanyl)-(2S,5R)-2-isopropyl-5-methyl-3,4,5,6-tetrahydro-2H-azepine) (*p*-cymene) ruthenium(II) dichloride (23). $[Ru(p\text{-cym})Cl_2]_2$ (53 mg, 0.09 mmol, 1.0 equiv) was added to a solution of **21** (50 mg, 0.17 mmol, 2.0 equiv.) in DCM (1 mL) and stirred for 30 min. The addition of pentane (5 mL) gave a suspension. After filtration, the residue was washed with pentane (3 x 5 mL) to give **23** as a brown solid (22 mg, 0.03 mmol, 19%). Mp: 124.0-126.3 °C. ^{1}H NMR (400.13 MHz, C_6D_6): δ 8.24 (dd, $^3J_{H,P}$ = 15.8 Hz, $^3J_{H,H}$ = 7.5 Hz, 3H, Ar*H*), 7.15-7.00 (m, 7H, Ar*H*), 5.07-4.96 (m, 2H, CH_3-CC*H*), 4.92-4.79 (m, 2H, CH_3-CCHC*H*), 3.23-3.13 (m, 1H, C*H*), 2.91-2.80 (m, 1H, C*H*), 2.09-1.97 (m, 1H, N-C*H*), 1.90-1.77 (m, 1H, CH-C*H*(CH_3)$_2$), 1.65 (s, 3H, CH_3), 1.57-1.48 (m, 1H, C*H*), 1.43-1.14 (m, 3H, C*H*), 1.10-0.96 (m, 12H, CH-CH(CH_3)$_2$ + C-CH(CH_3)$_2$), 0.59 (d, $^3J_{H,H}$ = 6.6 Hz, 3H, CH_3). ^{13}C{^{1}H} NMR (125.78 MHz, C_6D_6): δ 177.4 (d, $^1J_{C,P}$ = 53.0 Hz, P*C*N), 136.7 (d, $^2J_{C,P}$ = 8.1 Hz, P-Ar*C*), 136.2 (d, $^1J_{C,P}$ = 43.1 Hz , P-*ipso*-Ar*C*), 135.0 (d, $^3J_{C,P}$ = 8.5 Hz, P-Ar*C*), 132.5 Hz (d, $J_{C,P}$ = 42.6 Hz, P-*ipso*-Ar*C*), 130.1 (dd, $J_{C,P}$ = 19.0 Hz, $J_{C,P}$ = 2.1 Hz, P-Ar*C*), 127.7 (d, $J_{C,P}$ = 8.9 Hz, P-Ar*C*), 127.5 (d, $J_{C,P}$ = 9.3 Hz, P-Ar*C*), 110.1 (d, $^2J_{C,P}$ = 1.4 Hz, *C*-CH(CH_3)$_2$), 95.0 (s, *cym*-*C*-CH_3), 90.6 (d, $^2J_{C,P}$ = 3.4 Hz, *cym*-Ar*C*H), 90.1 (d, $^2J_{C,P}$ = 3.5 Hz, *cym*-Ar*C*H), 86.6 (d, $^2J_{C,P}$ = 5.7 Hz, *cym*-Ar*C*H), 85.9 (d, $^2J_{C,P}$ = 5.7 Hz, *cym*-Ar*C*H), 81.2 (s, *C*H), 80.5 (s, *C*H), 68.9 (d, $^3J_{C,P}$ = 19.0 Hz, N-*C*H), 43.2 (d, $^4J_{C,P}$ = 28.8 Hz, N-CH*C*H$_2$), 39.9 (s, N-CHCH$_2$*C*H$_2$), 35.6 (s, CH$_2$-*C*H), 30.5 (s, CH$_2$-*C*H), 23.7 (s, C-CH$_2$CH*C*H$_3$), 22.2 (d, $^3J_{C,P}$ = 5.2 Hz, CH-(*C*H$_3$)$_2$), 20.2 (s, CH-(*C*H$_3$)$_2$), 17.8 (d, $J_{C,P}$ = 29.9 Hz, *C*H$_3$). ^{31}P NMR (161.98 MHz, C_6D_6): δ 24.8 (s). FT-IR: ν 3060 (w), 2970 (m), 2867 (m), 1635 (w), 1618 (w), 1541 (w), 1433 (s), 1375 (m), 1257 (m), 1184 (w), 1157 (w), 1093 (s), 1058 (m), 1029 (m), 1004 (m), 864 (w), 800 (m), 746 (s), 694 (s), 634 (w), 516 (s). MS (ESI-Q-TOF): calcd. for $C_{32}H_{43}Cl_2NPRu$: 644.1550; found: 644.1560.

(*P*-κ^1-7-(diphenylphosphanyl)-(2S,5R)-2-isopropyl-5-methyl-3,4,5,6-tetrahydro-2H-azepine) (pentamethylcyclopentadienyl) rhodium(III) dichloride (intermediate 24). To a solution of $[RhCp^*Cl_2]_2$ (45.7 mg, 0.074 mmol, 1 equiv.) in DCM (1 mL) was added **21a** (50 mg, 0.148 mmol, 2 equiv.). The mixture was stirred for 30 min. and the resulting solution of **24** was used without further purification. ^{31}P NMR (161.98 MHz, DCM, RT): δ 31 (br. s). ^{31}P NMR (161.98 MHz, DCM, −90 °C): δ 34.3 (d, $^1J_{P,Rh}$ =

140.9 Hz, 38%), 22.8 (d, $^1J_{P,Rh}$ = 142.5 Hz, 42%), 29.9 (d, $^1J_{P,Rh}$ = 140.9 Hz, 7%), 26.5 (d, $^1J_{P,Rh}$ = 137.7 Hz, 7%), 24.7 (d, $^1J_{P,Rh}$ = 137.7 Hz, 4%), 20.7 (d, $^1J_{P,Rh}$ = 115.0 Hz, 2%).

Chloro (κ^2-7-(diphenylphosphanyl)-(2S,5R)-2-isopropyl-5-methyl-3,4,5,6-tetrahydro-2H-azepine) (pentamethylcyclopentadienyl) rhodium(III) trifluoromethylsulfonate (25). To a solution of **24** (0.148 mmol, 1 equiv.) in DCM (1 mL), was added AgOTf (37.8 mg, 0.148 mmol, 1 equiv.). The mixture was stirred for 60 min. at RT in absence of light. ^{31}P NMR (161.98 MHz, DCM): δ –11.3 (d, $^1J_{P,Rh}$ = 106.9 Hz). MS (ESI-Q-TOF): calcd. for $C_{32}H_{43}ClNPRh$: 610.1871; found: 610.1841.

4.2 Computational Procedure

Density functional calculations were performed at the ωB97X-D[36] level of theory using Gaussian09, revision A.02.[37] Geometry optimizations were performed using the 6-31+G(d,p)[38] basis set (Def2-TZVP for Rh)[39] and the nature of each stationary point was confirmed by frequency calculations.

Epimer **25**: E = -2211.80065800 a.u.; Epimer **25***: E = -2211.79577227 a.u.

4.3 Crystal structure determinations

The single-crystal X-ray diffraction studies of **4**, **6a, 6c, 10, 20** and **22** were carried out out on a Bruker-Nonius KappaCCD diffractometer, a Bruker D8 Venture diffractometer with Photon100 detector or an Agilent SuperNova diffractometer with EOS detector at 173(2) K or 123(2) K using Cu-Kα radiation (λ = 1.54178 Å) or Mo-Kα radiation (λ = 0.71073 Å). Direct Methods or heavy atom methods (SHELXS-97)[40] were used for structure solution and refinement was carried out using SHELXL-2013/2014 (full-matrix least-squares on F^2).[41] Hydrogen atoms were localized by difference electron density determination and refined using a riding model (H(N) free). Semi-empirical absorption corrections were applied. For **6c**, **10**, **20** and **22** an extinction correction were applied. The absolute configuration of **20** and **22** was determined by refinement of Parsons' x-parameter[42] and/or using Bayesian statistics on Bijvoet differences (Hooft's y-parameter).[43]

4 (CCDC-2084404): colourless crystals, $C_{12}H_{14}N_4$, M_r = 214.27, crystal size 0.55 × 0.35 × 0.35 mm, monoclinic, space group $P2_1/n$ (No. 14), a = 9.9574(4) Å, b = 9.9032(4) Å, c = 11.3819(4) Å, β = 106.996(1)°, V = 1073.35(7) Å^3, Z = 4, ρ = 1.326 Mg/m^{-3}, μ(mo-K$_\alpha$) = 0.08 mm^{-1}, F(000) = 456, T = 123 K, $2\theta_{max}$ = 55.0°, 16017 reflections, of which 2463 were

independent (R_{int} = 0.023), 145 parameters, R_1 = 0.036 (for 2255 I > 2σ(I)), wR_2 = 0.093 (all data), S = 1.05, largest diff. peak / hole = 0.30 / -0.24 e Å^{-3}.

6a (CCDC-2084405): colourless crystals, $C_{18}H_{21}NP \cdot CF_3O_3S$, M_r = 431.40, crystal size 0.50 × 0.30 × 0.20 mm, triclinic, space group *P-1* (No. 2), a = 8.746(1) Å, b = 9.967(1) Å, c = 11.335(1) Å, α = 93.91(1)°, β = 91.75(1)°, γ = 91.30(1)°, V = 985.02(17) Å^3, Z = 2, ρ = 1.454 Mg/m^{-3}, μ(Mo-K$_\alpha$) = 0.29 mm^{-1}, F(000) = 448, T = 123 K, $2\theta_{max}$ = 55.0°, 12681 reflections, of which 4503 were independent (R_{int} = 0.033), 256 parameters, 1 restraint, R_1 = 0.030 (for 4085 I > 2σ(I)), wR_2 = 0.082 (all data), S = 1.05, largest diff. peak / hole = 0.36 / -0.46 e Å^{-3}.

6c (CCDC-2084406): colourless crystals, $C_{18}H_{33}NP \cdot CF_3O_3S$, M_r = 443.49, crystal size 0.50 × 0.40 × 0.20 mm, monoclinic, space group $P2_1/c$ (No. 14), a = 11.1693(4) Å, b = 10.4743(3) Å, c = 19.2607(7) Å, β = 104.190(4)°, V = 2184.57(13) Å^3, Z = 4, ρ = 1.348 Mg/m^{-3}, μ(Mo-K$_\alpha$) = 0.27 mm^{-1}, F(000) = 944, T = 173 K, $2\theta_{max}$ = 59.6°, 10149 reflections, of which 5491 were independent (R_{int} = 0.023), 257 parameters, 1 restraint, R_1 = 0.040 (for 4425 I > 2σ(I)), wR_2 = 0.102 (all data), S = 1.02, largest diff. peak / hole = 0.39 / -0.37 e Å^{-3}.

10 (CCDC-2084407): colourless crystals, $C_{23}H_{20}NO_5PW$, M_r = 605.22, crystal size 0.24 × 0.10 × 0.06 mm, triclinic, space group *P-1* (No. 2), a = 9.2114(5) Å, b = 9.7189(6) Å, c = 13.1924(8) Å, α = 72.847(2)°, β = 88.845(2)°, γ = 79.410(2)°, V = 1108.56(11) Å^3, Z = 2, ρ = 1.813 Mg/m^{-3}, μ(Mo-K$_\alpha$) = 5.32 mm^{-1}, F(000) = 588, T = 123 K, $2\theta_{max}$ = 55.0°, 28871 reflections, of which 5075 were independent (R_{int} = 0.024), 281 parameters, R_1 = 0.013 (for 4908 I > 2σ(I)), wR_2 = 0.030 (all data), S = 1.12, largest diff. peak / hole = 0.65 / -0.48 e Å^{-3}.

20 (CCDC-2084408): yellow crystals, $C_{16}H_{23}N_4 \cdot CF_3O_3S$, M_r = 420.45, crystal size 0.60 × 0.40 × 0.30 mm, monoclinic, space group $P2_1$ (No. 4), a = 8.0662(3) Å, b = 14.7811(5) Å, c = 8.7268(3) Å, β = 108.124(1)°, V = 988.85(6) Å^3, Z = 2, ρ = 1.412 Mg/m^{-3}, μ(Cu-K$_\alpha$) = 1.94 mm^{-1}, F(000) = 440, T = 123 K, $2\theta_{max}$ = 144.2°, 13622 reflections, of which 3821 were independent (R_{int} = 0.027), 257 parameters, 2 restraints, R_1 = 0.029 (for 3812 I > 2σ(I)), wR_2 = 0.075 (all data), S = 1.03, largest diff. peak / hole = 0.39 / -0.37 e Å^{-3}, x = 0.010(5).

22 (CCDC-2084409): colourless crystals, $C_{22}H_{29}NP \cdot CF_3O_3S$, M_r = 487.50, crystal size 0.24 × 0.18 × 0.14 mm, orthorhombic, space group $P2_12_12_1$ (No. 19), a = 11.7215)6) Å, b = 14.1210(8) Å, c = 14.2256(7) Å, V = 2354.6(2) Å^3, Z = 4, ρ = 1.375 Mg/m^{-3}, μ(Mo-K$_\alpha$) = 0.25 mm^{-1}, F(000) = 1024, T = 123 K, $2\theta_{max}$ = 55.2°, 48925 reflections, of which 5434 were

independent (R_{int} = 0.035), 294 parameters, 1 restraint, R_1 = 0.024 (for 5147 I > 2σ(I)), wR_2 = 0.058 (all data), S = 1.06, largest diff. peak / hole = 0.26 / -0.21 e Å^{-3}, x = -0.014(15).

5 Acknowledgments

This work was supported by the Council for Chemical Sciences of The Netherlands Organization for Scientific Research (NWO/CW). We thank T. van Dijk for measuring high resolution mass-spectra and for fruitful discussions. M. K. Jongkind and R. Hoogendoorn are acknowledged for contributing to the synthesis of **9**. A. Chirila and M. M. Heeren contributed to screening suitable Beckmann rearrangement substrates.

6 References

[1] For reviews on cooperative ligands, see: (a) Khusnutdinova, J. R.; Milstein, D. *Angew. Chem., Int. Ed.*, **2015**, *54*, 12236−12273. (b) van der Vlugt, J. I. *Eur. J. Inorg. Chem.*, **2012**, 363−375.

[2] For a review on hybrid ligands, see: (a) Zhang, W.-H.; Chien, S. W.; Hor, T. S. A. *Coord. Chem. Rev.* **2011**, *255*, 1991−2024. (b) Grützmacher, H. *Angew. Chem. Int. Ed.*, **2008**, *47*, 1814-1818. (c) Bader, A.; Lindner, E. *Coord. Chem. Rev.*, **1991**, *108*, 27-110.

[3] For reviews on 2-pyridylphosphanes, see: (a) Newkome, G. R. *Chem. Rev.* **1993**, *93*, 2067−2089. (b) Zhang, Z.-Z.; Cheng, H. *Coord. Chem. Rev.* **1996**, *147*, 1−39. (c) Espinet, P.; Soulantica, K. *Coord. Chem. Rev.* **1999**, *193−195*, 499−556.

[4] For reviews on 1,3-P,N-ligated complexes, see: (a) Rong, M.K.; Holtrop, F.; Slootweg, J.C.; Lammertsma, K. *Coord. Chem. Rev.*, **2019**, *380*, 1-16. See also Chapter I. (b) Rong, M.K.; Holtrop, F.; Slootweg, J.C.; Lammertsma, K. *Coord. Chem. Rev.*, **2019**, *382*, 57-68. See also Chapter II. (c) Maggini, S. *Coord. Chem. Rev.* **2009**, *253*, 1793−1832.

[5] 1,3-P,N-ligand substituents affect κ^1/κ^2 coordination, see for instance: (a) L. Hintermann, T.T. Dang, A. Labonne, T. Kribber, L. Xiao, P. Naumov, *Chem. Eur. J.*, **2009**, *15*, 7167-7179 ; (b) P.C. Kunz, I. Thiel, A.L. Noffke, G.J. Reiß, F. Mohr, B. Spingler, *J. Organomet. Chem.*, **2012**, *697*, 33-40; (c) D. B. Grotjahn, Y. Gong, L. Zakharov, J. A. Golen, A. L. Rheingold, *J. Am. Chem. Soc.* **2006**, *128*, 438-453.

[6] (a) van Dijk, T.; Burck, S.; Rong, M. K.; Rosenthal, A. J.; Nieger, M.; Slootweg, J. C.; Lammertsma, K. *Angew. Chem., Int. Ed.* **2014**, *53*, 9068−9071. (b) van Dijk, T.; Burck, S.; Rosenthal, A. J.; Nieger, M.; Ehlers, A. W.; Slootweg, J. C.; Lammertsma, K. *Chem. Eur. J.* **2015**, *21*, 9328−9331. (c) van Dijk, T.; Bakker, M. S.; Holtrop, F.; Nieger, M.; Slootweg, J. C.; Lammertsma, K. *Org. Lett.* **2015**, *17*, 1461−1464. (d) Rong, M.K.; van Duin, K.; van Dijk, T.; de Pater, J.J.M.; Deelman, B.-J.; Nieger, M.; Ehlers, A.W.; Slootweg, J. C.; Lammertsma, K. *Organometallics*, **2017**, *36*, 1079-1090. See also Chapter III. (e) van Dijk, T.; Rong, M. K.; Borger, J. E.; Nieger, M.; Slootweg, J. C.; Lammertsma, K. *Organometallics*, **2016**, *35*, 827-835.

[7] Also, see: (a) Chen, X.-L.; Yu, R.; Wu, X.-Y.; Liang, D.; Jia, J.-H.; Lu, C.-Z. *Chem. Commun.* **2016**, *52* 6288–6291. (b) Radcliffe, J. E.; Batsanov, A. S.; Smith, D. M.;

Scott, J. A.; Dyer, P. W.; Hanton, M. J. *ACS Catal.* **2015**, *5*, 7095−7098. (c) Fischer, M.; Steinert, H.; Schmidtmann, M.; Beckhaus, R. *Dalton Trans.* **2019**, *48*, 1936-1940.

[8] For a review on nitrilium ion synthons, see: van Dijk, T.; Slootweg, J. C.; Lammertsma, K. *Org. Biomol. Chem.* **2017**, *15*, 10134-10144.

[9] "Caprolactam." Tinge J.; Groothaert, M.; op het Veld, H.; Ritz, J.; Fuchs, H.; Kieczka, H.; Moran, W. C.; in *Ullmann's Encyclopedia of Industrial Chemistry*. Wiley-VCH Verlag GmbH & Co. KGaA. **2018**, Weinheim.

[10] See for instance: (a) Beckmann, E., *Ber*. **1886**, *19*, 988. (b) Beckmann, E., *Ber*. **1887**, *20*, 1507. (c) "The Beckmann Reactions: Rearrangements, Elimination–Additions, Fragmentations, and Rearrangement–Cyclizations." Gawley, R.E.; in *Organic Reactions*, **1988**, *35*, 1-61, John Wiley & Sons, Inc. (d) Blatt, A. H., *Chem. Rev.,* **1933**, *12*, 215-260.

[11] (a) Katritzky, A. R.; Cai, C.; Singh, S. K. *J. Org. Chem.* **2006**, *71*, 3375-3380. (b) Katritzky, A. R.; Monteux, D. A.; Tymoshenko, D. O. *Org. Lett.* **1999**, *1*, 577-578. (c) Pi, H.; Liu, L.; Jiang, S.; Du, W.; Deng, W. *Tetrahedron* **2010**, *66*, 6097-6100. (d) Katritzky, A. R.;Lan, X.;Yang, J. Z.;Denisko, O. V.; *Chem. Rev.* **1998**, *98*, 409-548.

[12] "Terpenes: Flavors, Fragrances, Pharmaca, Pheromones." Breitmaier, E. Wiley-VCH Verlag GmbH & Co. KGaA. **2006**, Weinheim.

[13] The success of ε-caprolactam conversion to its imidoyl halide varies between reports. See, for instance: (a) Fodor, G.; Nagubandi, S. *Tetrahedron* **1980**, *36*, 1279-1300. (b) Bonnard, H.; Ferrucio, L.; Senet, J. -P.; Le Roy, P. -Y. *US6699988B2*, **2004**. (c) Nakajima, N.; Ubukata, M. in *Science of Synthesis* **2005**, *22*, 331-343. (d) Jurczak, J.; Koźluk, T.; Kulicki, W.; Pietraszkiewicz, M.; Szymanski, J. *Synthesis* **1983**, 382. (e) Ishida, Y.; Sasatani, S.; Maruoka, K.; Yamamoto, H. *Tetrahedron Lett.* **1983**, *24*, 3255-3258.

[14] Additional activation routes were explored in analogy to: (a) Charette, A.B. ; Mathieu, S. ; Martel, J. *Org. Lett.*, **2005**, *7*, 5401-5404. (b) Heldt, W. Z. *J. Am. Chem. Soc.*, **1958**, *80*, 5880-5885. (c) Matsumura, Y.; Fujiwara, J.; Maruoka, K.; Yamamoto, H. *J. Am. Chem. Soc.* **1983**, *105*, 6312-6314.

[15] Damljanovic, I.; Vukicevic, M.; Vukicevic, R. D. *Monatsh. Chem.* **2006**, *137*, 301-305.

[16] *In situ* generation of the sulfonate was preferable, since isolated batches of the mesylate, as well as its tosylate analogue, were highly reactive and prone to decomposition to thick black oils, suggestive of polymerization. See supporting information and, for instance: Kaneda, A.; Nagatsuka, M.; Sudo, R. *Bull. Chem. Soc. Jap.*, **1967**, *40*, 2705-2706.

[17] See for instance: Bertini, F.; Lyaskovskyy, V.; Timmer, B. J. J.; de Kanter, F. J. J.; Lutz, M.; Ehlers, A. W.; Slootweg, J. C.; Lammertsma, K. *J. Am. Chem. Soc.* **2012**, *134*, 201-204.

[18] Allen, F. H.; Kennard, O.; Watson, D. G. *J. Chem. Soc., Perkin Trans. 2* **1987**, S1-S19.

[19] Chambers, G. M.; Angamuthu, R.; Gray, D. L.; Rauchfuss, T. B. *Organometallics* **2013**, *32*, 6324-6329.

[20] (a) Booth, B.L.; Jibodu, K.O.; Proença, M.F. *J. Chem. Soc., Chem. Commun.* **1980**, 1151-1153. (b) Booth, B.L.; Jibodu, K.O.; Proença, M.F.J.R.P. *J. Chem. Soc., Perkin Trans. 1* **1983**, 1067-1073.

[21] See for instance: (a) Oediger, H.; Möller, F.; Eiter, K. *Synthesis* **1972**, 591–598. (b) Hibbert, F.; Hunte, K. P. P. *J. Chem. Soc., Perkin Trans. 2* **1983**, 1895–1899. (c) Tang, J.; Dopke, J.; Verkade, J. G. *J. Am. Chem. Soc.* **1993**, *115*, 5015–5020. (d) Glasovac, Z.; Eckert-Maksić, M.; Maksić, Z.B. *New J. Chem.* **2009**, *33*, 588-597.

[22] (a) Nishide, K.; Ito, S.; Yoshifuji, M. *J. Organomet. Chem.* **2003**, *682*, 79-84. (b) Baur, J.; Jacobsen,H.; Burger, P.; Artus, G.; Berke, H.; Dahlenburg, L. *Eur. J. Inorg. Chem.* **2000**, 1411-1422.

[23] Orpen, A.G.; Brammer, L.; Allen, F.H.; Kennard, O.; Watson, D.G.; Taylor, R. *J. Chem. Soc. Dalton Trans.* **1989**, S1–S83.

[24] (a) Braunstein, P.; Kelly, D. G.; Tiripicchio, A.; Ugozzoli, F. *Bull. Soc. Chim. Fr.* **1995**, *132*, 1083−1086. (b) Carson, E. C.; Lippard, S. J. *J. Am. Chem. Soc.* **2004**, *126*, 3412−3413. (c) Donovan, E. S.; Barry, B. M.; Larsen, C. A.; Wirtz, M. N.; Geiger, W. E.; Kemp, R. A. *Chem. Commun.* **2016**, *52*, 1685–1688.

[25] (a) García-Álvarez, R.; García-Garrido, S. E.; Díez, J.; Crochet, P.; Cadierno, V. *Eur. J. Inorg. Chem.* **2012**, 4218-4230. (b) Muranaka, M.; Hyodo, I.; Okumura, W.; Oshiki, T. *Catal. Today* **2011**, *164*, 552-555. (c) Oshiki, T.; Yamashita, H.; Sawada, K.; Utsunomiya, M.; Takahashi, K.; Takai, K. *Organometallics* **2005**, *24*, 6287−6290. (d) García-Álvarez, R.; Francos, J.; Tomás-Mendivil, E.; Crochet, P.; Cadierno, V. *J. Organomet. Chem.* **2014**, *771*, 93-104. (e) Ahmed, T. J.; Knapp, S. M. M.; Tyler, D. R. *Coord. Chem. Rev.* **2011**, *255*, 949−974.

[26] Caballero, A.; Jalón, F. A. ; Manzano, B. R.; Espino, G. ; Pérez-Manrique, M. ; Mucientes, A. ; Poblete, F. J. ; Maestro, M. *Organometallics* **2004**, *23*, 5694-5706.

[27] (a) Moldes, I.; de la Encarnación, E.; Ros, J.; Alvarez-Larena, Á.; Piniella, J. F. *J. Organomet. Chem.* **1998**, *566*, 165−174. (b) Kumar, P.; Kumar Singh, A.; Yadav, M.; Li, P.-Z.; Kumar Singh, S.; Xu, Q.; Shankar Pandey, D. *Inorg. Chim. Acta* **2011**, *368*, 124−131. (c) Kumar, P.; Kumar Singh, A.; Sharma, S.; Shankar Pandey, D. *J. Organomet. Chem.* **2009**, *694*, 3643−3652. (d) Yamakawa, M.; Ito, H.; Noyori, R. *J. Am. Chem. Soc.* **2000,** *122,* 1466-1478.

[28] For a review on (asymmetric) Ir(I)-catalyzed transfer hydrogenations, see: Church, T. L.; Andersson, P. G. *Coord. Chem. Rev.* **2008**, *252*, 513–531.

[29] See for instance: Jerphagnon, T.; Renaud, J.-L.; Bruneau, C. *Tetrahedron Asymm.* **2004**, *15*, 2101-2111.

[30] Kulisch, J.; Nieger, M.; Strecker, F.; Fischer, A.; Waldvogel, S. R. *Angew. Chem. Int. Ed.* **2011**, *50*, 5564-5567.

[31] (a) Fleury, L. M., Wilson, E. E.; Vogt, M.; Fan, T. J.; Oliver, A. G.; Ashfeld, B. L. *Angew. Chem. Int. Ed.* **2013**, *52*, 11589-11593. (b) Hattori, K.; Matsumura, Y.; Miyazaki, T.; Maruoka, K.; Yamamoto, H. *J. Am. Chem. Soc.* **1981**, *103*, 7368-7370. (c) Maruoka, K.; Miyazaki, T.; Ando, M.; Matsumura, Y.; Sakane, S.; Hattori, K.; Yamamoto, H. *J. Am. Chem. Soc.* **1983**, *105*, 2831-2843. (d) Komatsu, N.; Simizu, S.; Sugita, T. *Syn. Comm.* **1992**, *22*, 277-279.

[32] See supporting information. The same reactivity was observed when the primary phosphane Mes*-PH_2 was used, which gave Mes*-PH-PH-Mes*. To the best of our knowledge, no similar organocoupling reagents have been reported to facilitate P-P bond formation.

[33] For more information on (main-group) catalyst mediated dehydrocouplings, see for instance: (a) Less, R. J.; Melen, R. L.; Naseri, V; Wright, D. S. *Chem. Commun.*, **2009**, 4929-4937. (b) Melen, R. L. *Chem. Soc. Rev.*, **2016**, *45*, 775-788. (c) Less, R. J.; Melen, R. L.; Wright, D. S. *RSC Adv.*, **2012**, 2191-2199.

[34] For more information on diphosphanes, see for instance: (a) Smit, C. N.; van der Knaap, Th. A.; Bickelhaupt, F. *Tetrahedron Lett.*, **1983**, *24*, 2031-2034. (b) Komen, C. M. D.; de Kanter, F. J. J.; Goede, S. J.; Bickelhaupt, F. *J. Chem. Soc. Perkin. Trans. 2*, **1993**, 807-812.

[35] For similar epimerism in the κ^2-[RuCp*Cl] complexes of chiral 1,4-P,N-ligands, see: Ito, M.; Osaku, A.; Kobayashi, C.; Shiibashi, A.; Ikariya, T. *Organometallics* **2009,** *28,* 390-393.

[36] (a) Chai, J.-D.; Head-Gordon, M. *Phys. Chem. Chem. Phys.* **2008**, *10*, 6615–6620. (b) Chai, J.-D.; Head-Gordon, M. *J. Chem. Phys.* **2008**, *128*, 084106.

[37] Frisch, M. J.; Trucks, G. W.; Schlegel, H. B.; Scuseria, G. E.; Robb, M. A.; Cheeseman, J. R.; Scalmani, G.; Barone, V.; Mennucci, B.; Petersson, G. A.; Nakatsuji, H.; Caricato, M.; Li, X.; Hratchian, H. P.; Izmaylov, A. F.; Bloino, J.; Zheng, G.; Sonnenberg, J. L.; Hada, M.; Ehara, M.; Toyota, K.; Fukuda, R.; Hasegawa, J.; Ishida, M.; Nakajima, T.; Honda, Y.; Kitao, O.; Nakai, H.; Vreven, T.; Montgomery, J. A., Jr.; Peralta, J. E.; Ogliaro, F.; Bearpark, M.; Heyd, J. J.; Brothers, E.; Kudin, K. N.; Staroverov, V. N.; Kobayashi, R.; Normand, J.; Raghavachari, K.; Rendell, A.; Burant, J. C.; Iyengar, S. S.; Tomasi, J.; Cossi, M.; Rega, N.; Millam, J. M.; Klene, M.; Knox, J. E.; Cross, J. B.; Bakken, V.; Adamo, C.; Jaramillo, J.; Gomperts, R.; Stratmann, R. E.; Yazyev, O.; Austin, A. J.; Cammi, R.; Pomelli, C.; Ochterski, J. W.; Martin, R. L.; Morokuma, K.; Zakrzewski, V. G.; Voth, G. A.; Salvador, P.; Dannenberg, J. J.; Dapprich, S.; Daniels, A. D.; Farkas, O.; Foresman, J. B.; Ortiz, J. V.; Cioslowski, J.; Fox, D. J. *Gaussian 09, Revision A.02*; Gaussian, Inc., Wallingford, CT, **2009**.

[38] (a) Ditchfield, R.; Hehre, W.J.; Pople, J.A. *J. Chem. Phys.* **1971**, *54*, 724-728. (b) Hehre, W.J.; Ditchfield, R.; Pople, J.A. *J. Chem. Phys.* **1972**, *56*, 2257-2261. (c) Hariharan, P.C.; Pople, J.A. *Theor. Chem. Acc.* **1973**, *28*, 213-222. (d) Hariharan, P.C.; Pople, J.A. *Mol. Phys.* **1974**, *27*, 209-214. (e) Gordon, M.S. *Chem. Phys. Lett.* **1980**, *76*, 163-168. (f) Francl, M.M.; Pietro, W.J.; Hehre, W.J.; Binkley, J.S.; DeFrees, D.J.; Pople, J.A.; Gordon, M.S. *J. Chem. Phys.* **1982**, *77*, 3654-3665. (g) Binning, R.C., Jr.; Curtiss, L.A. *J. Comp. Chem.* **1990**, *11*, 1206-1216. (h) Blaudeau, J.-P.; McGrath, M.P.; Curtiss, L.A.; Radom, L. *J. Chem. Phys.* **1997**, *107*, 5016-5021. (i) Rassolov, V.A.; Pople, J.A.; Ratner, M.A.; Windus, T.L. *J. Chem. Phys.* **1998**, *109*, 1223-1229. (j) Rassolov, V.A.; Ratner, M.A.; Pople, J.A.; Redfern, P.C.; Curtiss, L.A. *J. Comp. Chem.* **2001**, *22*, 976-984. (k) Clark, T.; Chandrasekhar, J.; Spitznagel, G.W.; Schleyer, P.V.R. *J. Comp. Chem.* **1983**, *4*, 294-301.

[39] Andrae, D.; Häußermann, U.; Dolg, M.; Stoll, H.; Preuß, H. *Theoret. Chim. Acta* **1990**, *77*, 123-141.

[40] Sheldrick, G. M. *Acta Crystallogr.* 2008, **A64**, 112-122.

[41] Sheldrick, G. M. *Acta Crystallogr.* 2015, **C71**, 3-8.

[42] Parson, S.; Flack, H. D.; Wagner, T. *Acta Crystallogr.* 2013, **B69**, 249-259.

[43] Hooft, R.W.W.; Straver, L. H.; Spek, A. L. *J. Appl. Crystallogr.* 2008, **41**, 96-103.

Chapter V

Protic NHC Iridium Complexes with β-H Reactivity: Synthesis, Acetonitrile Insertion, and Oxidative Self-Activation

Mark K. Rong, Andrei Chirila, David Franciolus, Martin Lutz, Martin Nieger, Andreas W. Ehlers, J. Chris Slootweg, and Koop Lammertsma

Protic NHC iridium complexes, obtained from the corresponding azido-phenylene-isocyanide precursor complexes, were investigated for ligand-based reactivity. Under redox-neutral conditions, acetonitrile inserts into the N−H bonds to provide κ^2-NHC-imidoyl ligand-based complexes, while under reductive conditions the complex also expels one N−H proton to provide the corresponding deprotonated analogues. Using zinc as a reductor activates the NHC-iridium complex to form an asymmetric bimetallic iridium hydrido complex, in which two anionic N-deprotonated NHCs bridge the bimetallic core. X-ray crystal structures are reported for the azido-phenylene-isocyanide precursor complex, the protic NHC complex, and the asymmetric bimetallic iridium hydride complex. Density functional computations and a QTAIM analysis of the bimetallic iridium hydrido complex are provided.

Organometallics **2019**, *38*, 4543-4553.

1 Introduction

Since 1968,[1,2] N-heterocyclic carbenes (NHCs) have been prominent ligands of high stability with robust coordination chemistry. Protic NHCs (hereafter NHC^Hs) were first introduced in the 1980s,[3] but only recently has their chemistry become widely accessible through the syntheses of Hahn *et al.*[4] These synthetic routes conveniently mitigate the inherent acidic reactivity of the NHC^H-NH sites, which contrast with the classical nonreactive N-substituted NHCs.[5] This protic character enables hydrogen-bonding interactions, deprotonations, and nucleophilic additions and highlights the ability of NHC^Hs to act as 'cooperative' or 'non-innocent' ligands.[6,7] For instance, H-bonding increases substrate recognition in the competitive Rh^I-catalyzed hydrogenation of esters[8] and assists in the Ru^{II}-catalyzed condensation of allyl alcohols with 2-pyridylbenzimidazole.[9] Deprotonation of the NHC^H provides an N-anionic ligand which can be used to access nonsymmetrical NHCs (Scheme 1) and macromolecular structures[4,10,11] or to bind a second metal center (Figure 1).[12–16] These multimetallic structures generally bear their bridging NHCs in a head-to-tail fashion and are of interest for multinuclear catalysis.[17] Deprotonated NHC-N sites have been used in ruthenium(II) complexes for bifunctional activation of amines, dihydrogen, and alcohols, as demonstrated in the catalytic transfer hydrogenation of acetophenone using *i*-PrOH.[18] Iridium(III) NHC^H complexes have shown bifunctional activation of dihydrogen and acetylene.[19] NHC^H deprotonation has been suggested to be facilitated by intramolecular ligand–metal interactions,[9,20] indicating the importance of the nature of the transition metal. For instance, NHC^Hs can be transformed to the imidazole form by an external base,[13] but in the 2-functionalization of imidazoles by Ru^{II}-[9] and Rh^I-catalysts[20] the tautomerization results from ligand-β-H activation by the metal,

presumably via metal-hydride intermediates (Scheme 2).[20,21] Metal-mediated NHC^{H} reactivity can also be induced by free coordination sites. Illustrative is the chloride displacement on iridium(III) that facilitates a nucleophilic attack of the NHC^{H} on a coordinated MeCN molecule to stoichiometrically provide a formal hydroamination product, which rearranges to a bis(imidazole) complex (Scheme 3).[22–24] Collectively, these examples demonstrate the versatile chemistry of NHC^{H} complexes.

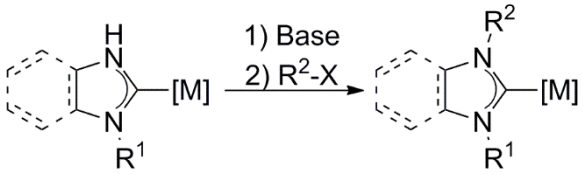

Scheme 1. Ligand-Based NHC Reactivity.

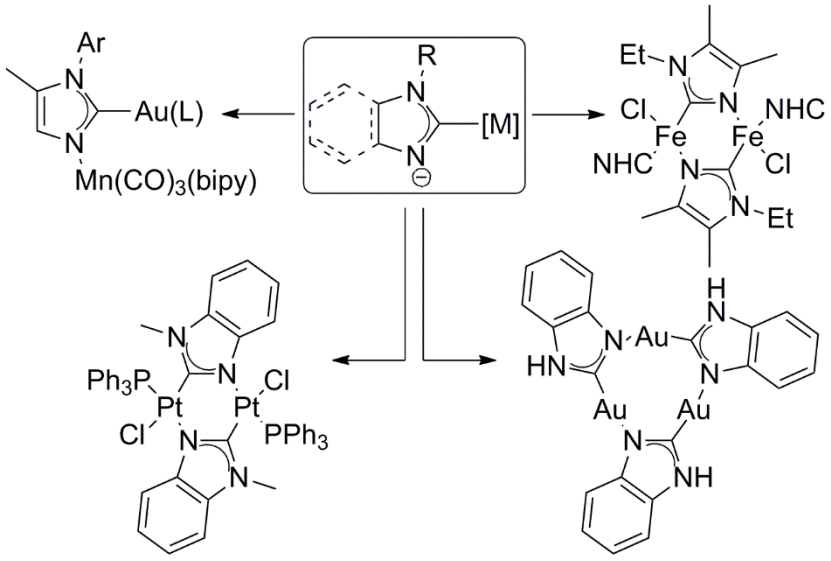

Figure 1. N-anionic protic NHC coordination chemistry.

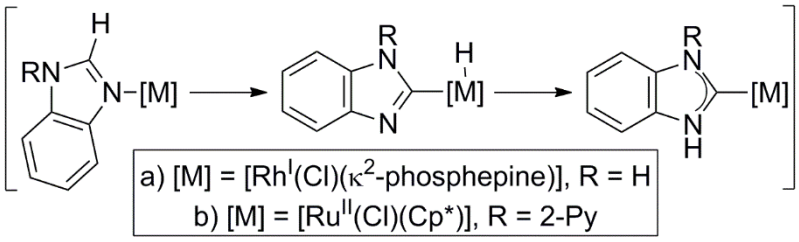

Scheme 2. NHC^{H} Tautomerization Step by Intramolecular Interaction with Catalyst.

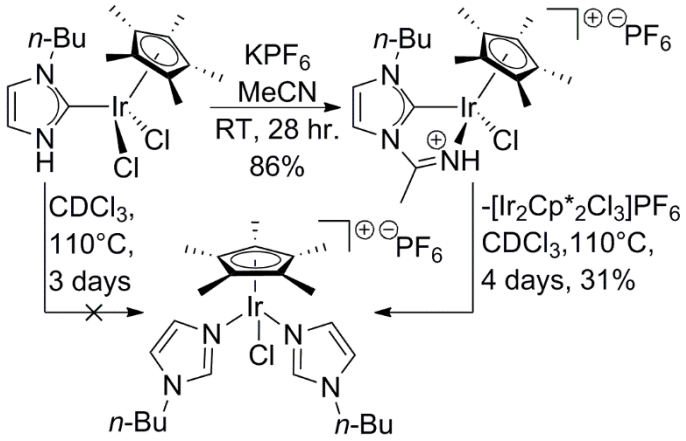

Scheme 3. Capture of MeCN by Protic NHC Followed by Tautomerization.

NHC^{H}s can also differ electronically from their N-substituted analogues. The prominence of NHCs in organometallic catalysis is generally attributed to their strong σ-donation, but NHCs can also be tunable π-acceptors.[25,26] In a computational study on NHC-phosphinidene complexes,[27,28] we found the conformation of the NHC to be crucial for its electronic behavior in the complex. For example, the N-methylated NHC in Ru complex **A** favors the σ-donating orthogonal ⊥ arrangement over the coplanar || arrangement by 12.5 kcal mol^{-1}, but the sterically less encumbered protic NHC in **B** favors instead a coplanar || conformation by 2.5 kcal mol^{-1} (Figure 2),[29] thereby allowing for significant π-acceptor capacity due to increased phosphinidene-NHC orbital overlap. This unique effect of the NHC^{H} ligand is even more

pronounced in benzimidazolidin-2-ylidene iridium complexes as NHC^{Me} complex **C**⊥ is favored by 22.0 kcal mol^{-1}, while NHC^{H} complex **D**|| is favored by 3.4 kcal mol^{-1} (Figure 2).[30–33] These results prompted us to study NHC^{H} iridium complexes and assess the effect of the ligand on the complex's overall reactivity. We address the distinct coordination parameters of NHC^{H} iridium(III) complexes and then explore the reactivity of their *β*-NH groups in stoichiometric hydroamination-type activations, as well as in self-activation under reductive conditions toward a unique bimetallic structure.

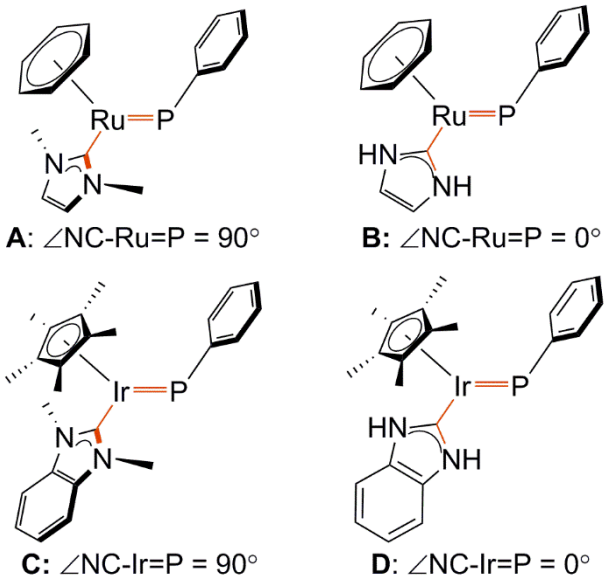

Figure 2. NHC conformations with different electronic effects.

2 Results and Discussion

The syntheses and properties of the NHC^{H} iridium complexes are discussed first. Next, their reactivity toward MeCN is explored under both redox-neutral and reductive conditions. Finally, the NHC^{H} reactivity will be addressed in an oxidative reaction to examine the influence of an N-anionic NHC^{H} on the formation of a dinuclear complex.

Computational methodologies are used to provide background for the observed reactivity.

2.1 Synthesis of NHC^{H} Ir^{III} Complexes

The synthesis of the NHC^{H} iridium(III) complexes was pursued in analogy to that reported for the related ruthenium(II) complexes, in which 2-azido-isonitrile precursors are reduced to amino-isonitrile intermediates that then cyclize.[34] Reacting 2-azidophenylisonitrile (**1**) [35] with 0.5 equiv of $[IrCp^*Cl_2]_2$ in DCM at room temperature provided [(2- azidophenylisonitrile)$IrCp^*Cl_2$] precursor complex **2** in 98% isolated yield as a light-sensitive yellow powder (Scheme 4). Whereas **2** was stable as a solid in darkness for months, it slowly decomposed in solution, even at −80 °C. To allow for full analysis, **2** was treated with NaI in acetone to quantitatively provide the thermally stable diiodo complex **3**. Suitable crystals for an X-ray crystal structure determination were obtained by slow diffusion of pentane into a DCM solution. The molecular structure of **3** shows a linear isocyanide with a C1−N1 triple bond length of 1.159(3) Å (Figure 3). The Ir−C1 bond length of 1.922(2) Å compares well to those of other (aryl)-isocyanide-iridium(III) complexes,[36] as do the iridium−iodide bond lengths (Ir1−I1 = 2.6965(3); Ir1−I2 = 2.6965(3) Å).[36a] The distance of 3.445(3) Å between the C1 and N2 atoms together with the C2−C7−N2−N3 torsion angle of 178.0(2)° illustrate the prearrangement of N2 for nucleophilic attack on C1 in the subsequent reduction step (vide infra). The structural parameters of the isocyanide ligand compare also well with those reported for [**1**-$W(CO)_5$].[35]

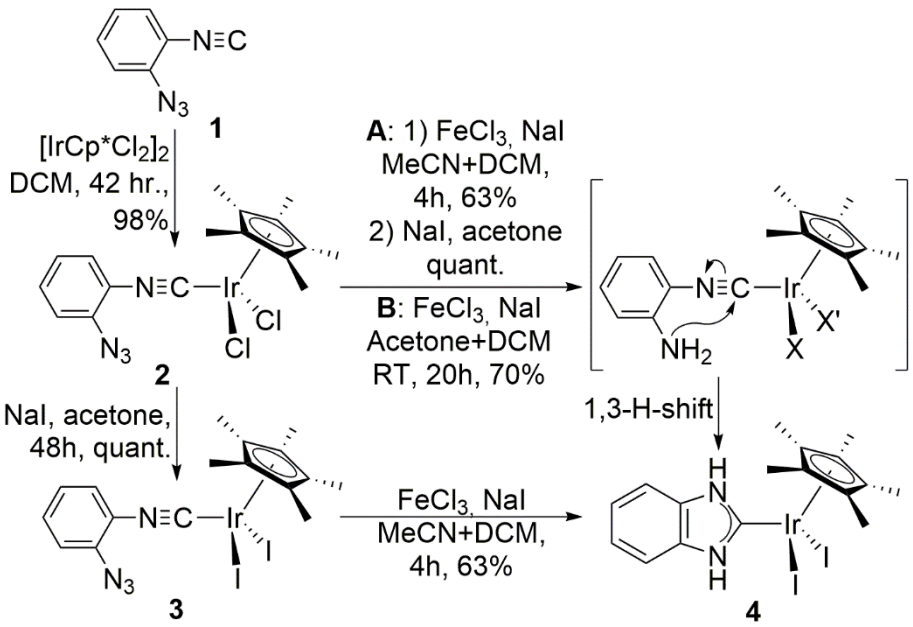

Scheme 4. Synthesis of Protic NHC-Iridium Complex **4**.

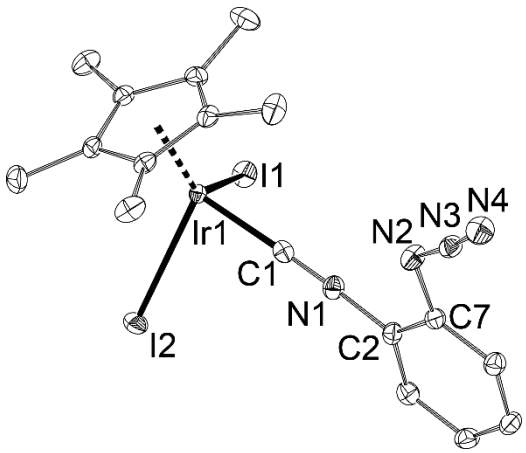

Figure 3. Displacement ellipsoid plot of iridium complex **3** at the 50% probability level. Hydrogen atoms and DCM solvent molecules are omitted for clarity. Selected bond lengths (Å) and angles (deg): Ir1−C1 = 1.922(2), Ir1−I1 = 2.6965(3), Ir1−I2 = 2.6965(3), C1−N1 = 1.159(3), N1−C2 = 1.390(3), C2−C7 = 1.401(3), C7−N2 = 1.416(3), N2−N3 = 1.254(3), N3−N4 = 1.125(3), C1 N2 = 3.445(3), N1−C1−Ir1 = 177.6(2), C1−N1−C2 = 177.2(2), C2− C7−N2 = 115.9(2), N4−N3−N2 = 172.8(3), I1−Ir1−I2 = 90.709(7), C2−C7−N2−N3 = 178.0(2).

Reduction of the azide group of **2** to the corresponding amine induces cyclization to the desired NHC^H complex (Scheme 4).[34,37] This was accomplished by reaction with NaI and $FeCl_3$ in DCM and MeCN for 4 h,[38] after which quenching and purification of the black reaction mixture provided the desired diiodo complex **4** as a yellow solid in 63% yield (δ(^{1}H) 9.88 (N*H*); δ(^{13}C) 161.0 (N*C*N) ppm) (**A** in Scheme 4). The chloride to iodide exchange that occurs on iridium results from the excess of NaI that is required for the azide reduction.[39] This exchange can also be performed prior to the reduction step: i.e., **2** → **3** → **4**. The best results were obtained by performing the azide reduction in a mixture of acetone/DCM over 20 h at room temperature (**B** in Scheme 4) to provide **4** in higher purity and yield (87%).

For completeness, we note that the chloride to iodide exchange on iridium can easily be reversed (Scheme 5); to the best of our knowledge, such a protocol is still undocumented. Thus, reacting **4** with 2 equiv. of AgOTf in THF provides a bright yellow bis(triflate) complex, which on treatment with $NEt_3 \cdot HCl$ as chloride donor turned orange, which indicates the formation of the dichloro complex. Purification and crystallization provided **5** as orange needles (34%; δ(^{1}H) 10.52 (N*H*); δ(^{13}C) 165.7 (N*C*N) ppm).

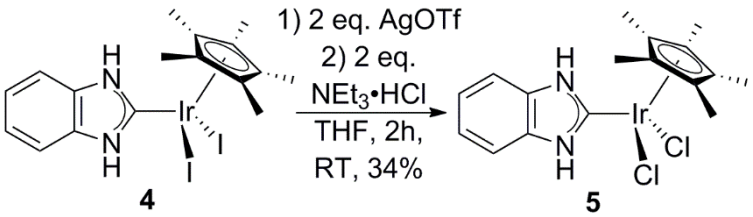

Scheme 5. Iodide to Chloride Ion Exchange.

Next, we compared the properties of NHC^{H} complex **4** with those of NHC^{Me} analogue **6**, which was obtained by coordinating bis(1,3-dimethylbenzimidazolidin-2-ylidene)[40] to $[IrCp^*Cl_2]_2$ (88%) and subsequent Cl → I ion exchange using NaI (quantitative, Scheme 6). The ^{13}C NMR spectra showed an upfield shift for the N*C*N carbene carbon of the NHC^{H} complex (**4**, δ 161.0 ppm; **6**, δ 167.0 ppm), similar to the trend for comparable Pd[10a] complexes, and is suggestive of a stronger C–Ir interaction,[41] which could be confirmed by comparing the molecular structures obtained from X-ray structure determinations (Figure 4). Red crystalline needles of **4** were obtained by slow diffusion of pentane into a DCM solution and those of **6** from DCM/pentane at 5 °C. The molecular structures show a near-C_s symmetry, an identical NHC conformation and parameters comparable to those of related Ir-NHC complexes,[42] with indeed a shorter iridium–carbene bond length for the protic complex (**4**, Ir1–C1 = 2.008(4) Å; **6**, Ir1–C1 = 2.034(4) Å) and a larger I1–Ir1–I2 bond angle (4, 90.381(11)°; 6, 86.008(10)°). These differences may be the result of the sterically smaller N substituents of **4** (see Figure S3 in the Supporting Information) or the observed intermolecular NH- - -I hydrogen bonds (H1- - -I2' = 2.86(3); H2- - -I2" = 2.85(2) Å).[43] ETS-NOCV[44] fragment analysis on BP86-D3(ZORA)/TZ2P[32,33] optimized structures of **4** and **6** revealed tighter orbital interactions for the NHC^{H} ligand (E_{Ir-C}^{4} = −114.1 kcal mol^{-1}; E_{Ir-C}^{6} = −106.2 kcal mol^{-1}), due to significant donation from the carbene to the metal (E_o^{4} = −90.6 kcal mol^{-1}, E_o^{6} = −82.6 kcal mol^{-1}), as well as back- donation to the carbene p-orbital ($E_{\pi 1}^{4}$ = −16.6 kcal mol^{-1}, $E_{\pi 1}^{6}$ = −15.4 kcal mol^{-1}) and the C=N antibonding orbitals ($E_{\pi 2}^{4}$ = −6.9 kcal mol^{-1}, $E_{\pi 2}^{6}$ = −8.2 kcal mol^{-1}). The possibility of a 90° rotation in the NHC conformation and the effect thereof on the electronic parameters was examined as well and appeared to be more accessible for the protic complex **4** (maxima: $\Delta E_{\perp\rightarrow||}^{4}$ = +3.7 kcal mol^{-1}; $\Delta E_{\perp\rightarrow||}^{6}$ = +13.4 kcal mol^{-1}), which weakens the Ir–C bond

(E_{Ir-C} = −110.4 kcal mol^{-1}; E_o = −86.5 kcal mol^{-1}, E_{n1} = −17.2 kcal mol^{-1}, E_{n2} = −6.7 kcal mol^{-1}). Thus, the accessible coplanar conformation and observed hydrogen bonding sets the protic NHC apart from its N-methylated analogue. The stronger Ir−C bond is favorable for anchoring the ligand firmly for followup reactions.

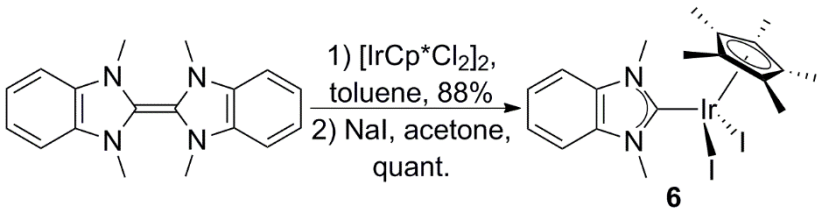

Scheme 6. Synthesis of Me-Substituted NHC-Ir Complex 6.

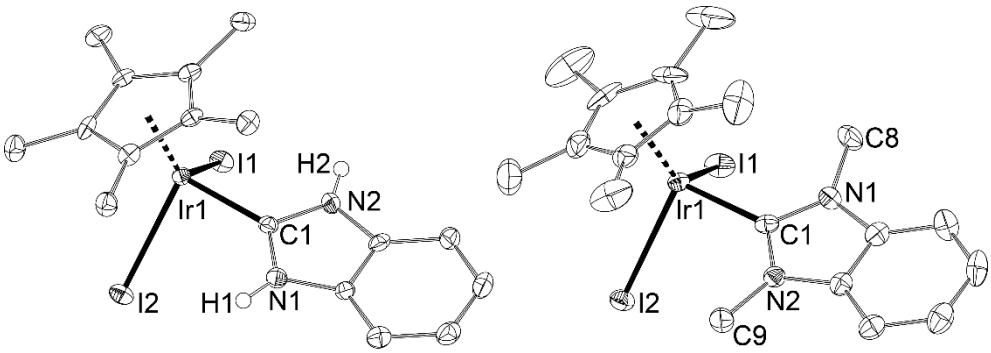

Figure 4. Displacement ellipsoid plots of iridium complexes **4** (left) and **6** (right) at the 50% probability level. C−H hydrogen atoms are omitted for clarity. Selected bond lengths (Å) and angles (deg) of **4**: Ir1−C1 = 2.008(4), Ir1−I1 = 2.6964(4), Ir1−I2 = 2.6982(4), C1− N1 = 1.338(6), C1−N2 = 1.355(6), N1−C1−N2 = 106.2(4), N1− C1−Ir1 = 127.0(3), N2−C1−Ir1 = 126.0(3), I1−Ir1−I2 = 90.381(11). Selected bond lengths (Å) and angles (deg) of **6**: Ir1− C1 = 2.034(4), Ir1−I2 = 2.7254(3), Ir1−I1 = 2.7284(3), C1−N1 = 1.361(5), C1−N2 = 1.370(5), N1−C8 = 1.453(5), N2−C9 = 1.457(5), N1−C1−N2 = 105.0(3), N1−C1−Ir1 = 126.9(3), N2−C1−Ir1 = 127.1(3), I2−Ir1−I1 = 86.008(10).

2.2 NHC^{H} MeCN Activation

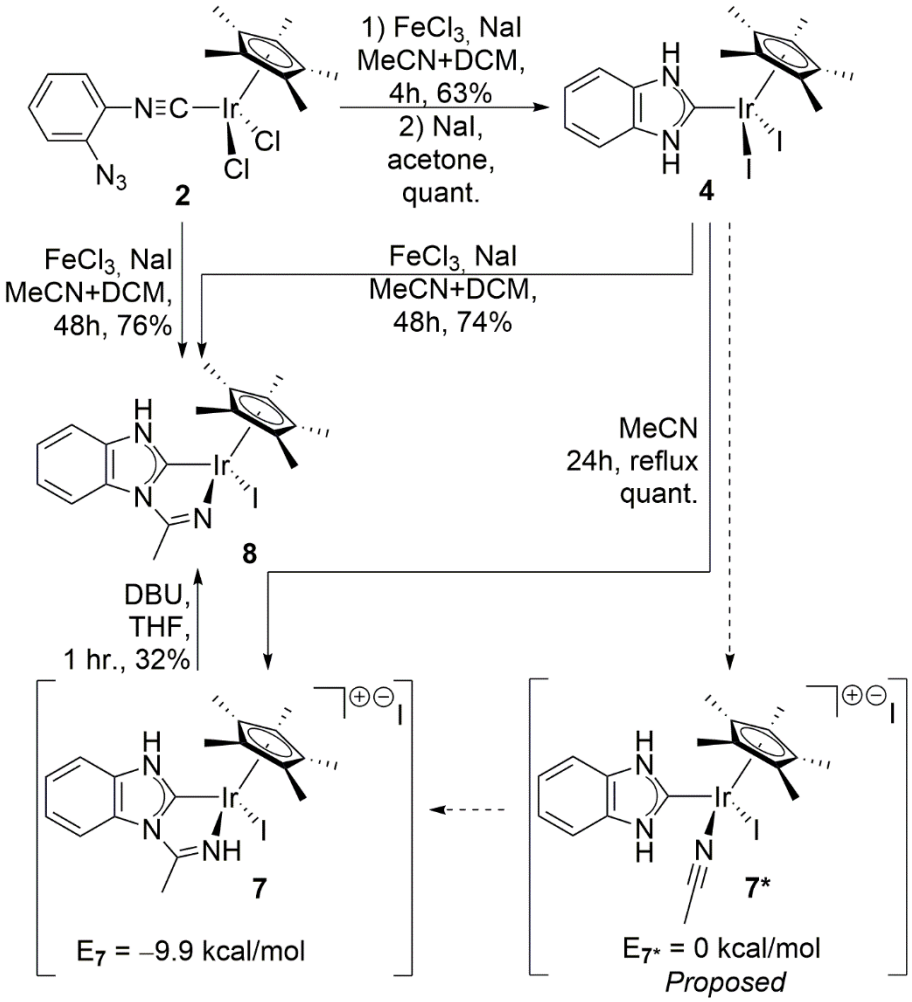

Scheme 7. Protic NHC-NH addition over the MeCN Triple Bond and DFT Analysis of [**7***]$^{+}$ and [**7**]$^{+}$.

Next, stoichiometric hydroamination-type activation by the protic NHC^{H}-Ir complex was assessed.[22] Refluxing **4** for 24 h in MeCN resulted in the nitrile's insertion into one of the ligand's N–H bonds to quantitatively afford **7** as an unstable yellow solid (Scheme 7). The product's asymmetrically substituted benzimidazolin-2-ylidene ligand is

evident from the two different NH groups in the ^{1}H NMR spectrum (δ 13.08, 10.88 ppm). BP86-D3(ZORA)/TZ2P calculations[32,33] indicate that, upon MeCN coordination (**7***), the addition of the NHC^{H}–NH bond to the CN triple bond to give **7** is exothermic by 9.9 kcal mol^{-1} (Scheme 7). No full characterization by ^{13}C NMR or an X-ray structure determination could be performed, as isolated **7** quickly converted into an intractable solid, which we presume to be the (benzimidazolyl)IrCp*I_2 tautomer.[45]

We wondered whether **7** also forms directly from precursor **2** in a one-pot reaction. However, increasing the reaction time for the $FeCl_3$/NaI-facilitated reduction to 48 h provided instead exclusively the deprotonated bidentate [(imidoyl- NHC^{H})IrI] complex **8** (76%, Scheme 7). Its ^{1}H NMR spectrum showed one N–H resonance (δ 7.94 ppm) and an asymmetrically substituted benzimidazolin-2-ylidene with chemical shifts that differ from those of **7** and distinctive carbene and imidoyl ^{13}C NMR resonances (δ 171.6 (N*C*N), 164.6 (*C*NH) ppm). The same product was obtained by deprotonating **7** with DBU in THF (1 h, room temperature, 32%). In contrast to **7**, **8** is stable in air and water. Exposure of intermediate **4** to $FeCl_3$/NaI for 48 h in MeCN yielded the same complex **8** (74%; Scheme 7). This suggests that the reductive reaction medium causes the loss of 1 equiv of HI from **4**, since no deprotonating base is present. The activator could be Fe^{II}, which is generated in situ on mixing $FeCl_3$ and NaI in solution.[38,46]

The observed insertion reactivity in complexes **7** and **8** may have potential in catalysis. Since the products are reminiscent of iminium ions (i.e., nitrogen-stabilized N-protic nitrilium ions), which readily undergo nucleophilic attack,[47] this might be exploited in the (catalytic) functionalization of nitriles or terminal triple bonds.[23,48] Alternatively, **7**

and **8** could serve as, for instance, [(κ^2-imidoyl-aryl)Ir^{III}] transfer hydrogenation catalysts.[49] Overall, it is especially interesting that the reactivity of the NHC^{H} complex changes upon reduction. To better understand the role of the metal center in this, we continued using a well-defined iridium reductor.

2.3 NHC^{H} *β*-Deprotonation to Dinuclear Complex afwdaw

The conversion of **4** to **8** occurred under reductive conditions. Since zinc is a well-known reductor for iridium(III) chlorides[50] and compatible with NHC^{H}s,[51] we decided to explore it for enhanced NH−metal interactions with surprising results. When dichloro complex **5** was refluxed in MeOH for 7 days in the presence of Zn, the μ-hydrido dinuclear complex **9** was obtained as an unexpected product (Scheme 8); no reaction took place in the absence of Zn. Complex **9** also resulted directly from **2** in 75% yield by refluxing in MeOH/H_2O for 7 days in the presence of Zn and NH_4Cl. This method is more efficient than the three-step approach (36%).

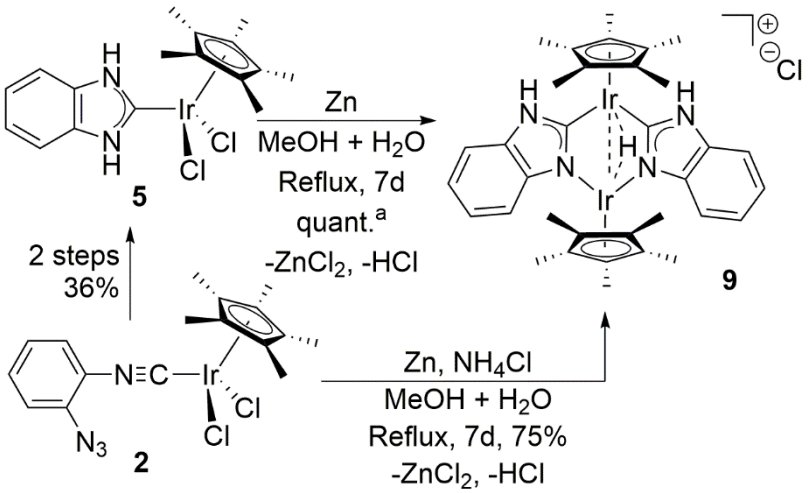

Scheme 8. Formation of dinuclear complex **9**.

Complex **9** has a unique C_s symmetry with two anionic NHC ligands and a hydride bridging its iridium atoms (δ(^{1}H) −20.01 ppm).[52] While bimetallic iridium species with bridging hydride ligands are well-known,[42,53–57] complexes with bridging NHC ligands are rare and tend to have them coordinated in a head-to-tail fashion between identical metal centers.[12–16] In contrast, **9** features a head-to-head arrangement with inequivalent Ir centers. This is supported by two distinct Cp*-CH_3 ^{1}H and ^{13}C NMR chemical shifts (δ(^{1}H) 2.23, 2.15; δ(^{13}C) 11.8, 10.9 ppm). NOESY measurements show coupling of one Cp* ligand with the two NHC N-hydrogens and coupling of the other Cp* ligand with the nearby aromatic N^--CC*H* hydrogens (see Figure S1 in the Supporting Information). The two carbene ^{13}C NMR resonances of **9** are considerably more upfield than that of **5** (**9**: δ 142.2 ppm; **5**, δ 165.7 ppm), which is attributed to the higher shielding in the anionic NHC.

An X-ray crystal structure determination established unequivocally the molecular structure of **9** (Figure 5). Single crystals were obtained by slow diffusion of diethyl ether into a DCM solution in the presence of TPPO.[58,59] The two independent molecules in the asymmetric unit of **9** are located on general positions without crystallographic symmetry. The iridium–carbene distances are similar to those in mononuclear **4** (**9**, Ir11–C11 = 2.016(7) Å, Ir11–C81 = 2.020(7) Å, Ir12– C12 = 2.038(7) Å, Ir12–C82 = 2.014(7) Å; 4, Ir1–C1 = 2.008(4) Å), and the nitrogen–iridium bond lengths (Ir21– N11 = 2.083(6) Å, Ir21–N31 = 2.088(6) Å, Ir22–N12 2.072(6) Å, Ir22–N32 2.078(7)Å) are comparable to those found in structurally similar iridium imidazolate and pyrazolate complexes.[55,60] The location of the μ-hydride could not be determined from difference-Fourier maps, but its calculated position was evident from the geometry of the iridium centers.

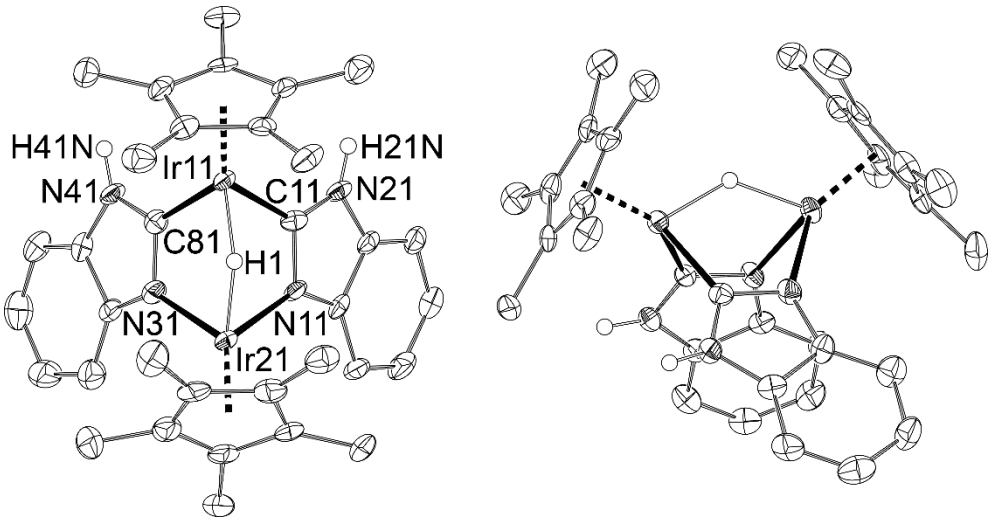

Figure 5. Displacement ellipsoid plots of dinuclear iridium complex **9** at the 50% probability level. Only one of the two independent molecules is shown. C–H hydrogen atoms, the chloride anion, and DCM solvent molecules are omitted for clarity. Selected bond lengths (Å) and angles (deg): Ir11–C11 = 2.016(7), Ir11–C81 = 2.020(7), Ir21–N11 = 2.083(6), Ir21–N31 = 2.088(6), N11–C11 = 1.344(9), N21–C11 = 1.351(9), N31–C81 = 1.341(9), N41–C81 = 1.349(9), Ir11- - -Ir21 = 3.0410(4), C11–Ir11–C81 = 81.0(3), N11–Ir21–N31 = 80.0(2). Atom H1 was introduced in a calculated position.

The intriguing bonding in the metallic core of **9**, with its bridging hydride and delocalized anionicity of the NHC ligands, makes the oxidation states of the metal centers ambiguous[56] (i.e., Ir^{III}- - -Ir^{III}, Ir^{II}- - -Ir^{IV}, or Ir^{II}→Ir^{IV}). Intermetallic interaction between the two Ir centers seems arguable[54–57] because of the rather large separation (Ir11- - -Ir21 = 3.0410(4), Ir12- - -Ir22 = 3.0501(4) Å). Since the low solubility of **9** prevented CV measurements, we used a QTAIM analysis[61] on a BP86-D3(ZORA)/TZ2P[32,33] optimized geometry, which showed near-identical bond paths of the two iridium nuclei to the hydride (critical bond points Ir11–H1 ρ 0.12 au, ε 0.09, Ir21–H1 ρ 0.10 au, ε 0.08; ring critical points Ir11–H1–Ir21–N31–C81: ρ 0.03 au, Ir11–H1–Ir21–N11–C11: ρ 0.03 au) but no intermetallic interactions

(Figure 6 and Figure S2 in the Supporting Information). This indicates true hydride bridging and minimal electronic differences between the Ir nuclei: i.e., a Ir^{III}- - - Ir^{III} complex.[62]

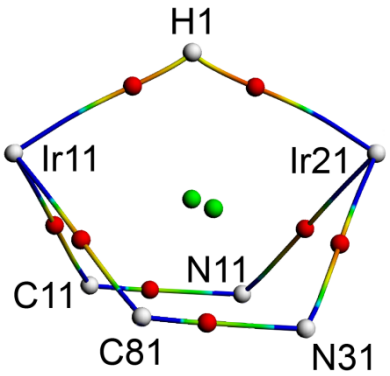

Figure 6. AIM analysis of bond paths in **9**. NHC and Cp* ligands are omitted for clarity. Bond critical points are shown in red and ring critical points in green.

The unique NHCH orientation in **9** was examined computationally, since it contrasts with that of known NHC-bridged complexes.[12–16] The head-to-head coordination of complex **9** is indeed energetically favored at the BP86-D3(ZORA)/TZ2P level[32,33] over head-to-tail complex **10**, but by only 1.9 kcal mol^{-1} (Figure 7). This small energy difference is somewhat surprising, since ^{1}H NMR spectra of the crude reaction mixtures show full selectivity of its formation. For the formation of **9** from the monometallic precursor, one NHC ligand has to undergo an in situ tautomerization, either prior to or after coordination to the second Ir center. Considering that zinc is essential for the conversion, we presume it oxidizes to $ZnCl_2$ to facilitate the $Ir^{III} \rightarrow Ir^{I}$ reduction of one monometallic complex, which then undergoes an auto-oxidative 1,3-H shift to the corresponding hydride complex, as has been reported for alkyl-iridium(III) hydrides.[63] NHC tautomerization is likely for Ir^{I} complexes bearing ligands with a strong trans effect, such as

hydrides.[21,64] Such an oxidative addition–tautomerization sequence has also been suggested for benzimidazole-Ru-hydrides (DFT).[21b] It should be noted that the tautomerization step may also be influenced by the second metal center, as was found for Au/Mn-NHC systems.[13]

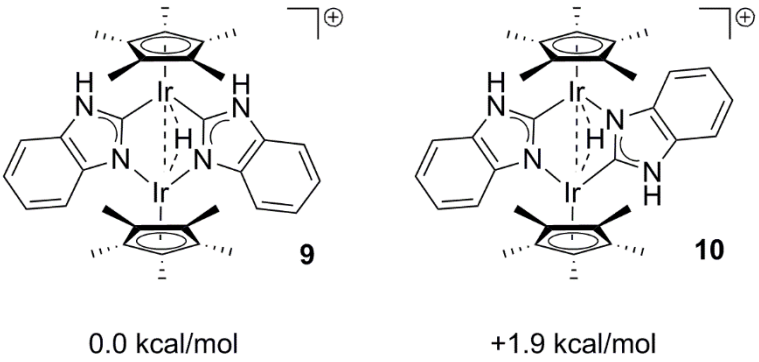

Figure 7. Relative BP86-D3(ZORA)/TZ2P energies of **9** and tautomer **10**.

The observed oxidative activity leading to **9** seems to be specific for iridium; using [Rh^{III}Cp*Cl$_2$] and [Ru^{II}(*p*-cym)Cl$_2$][34] in the same one-pot procedure resulted in a mixture of Rh and Ru analogues of **5** with unidentified side products (see the Supporting Information). The Ir-chloride atoms are essential, as the diiodo complexes **3** and **4** gave no conversion. This halide-specific reactivity may be attributed to the difference in redox potentials or alternatively be related to a difference in H-bonding interactions that can assist 1,3-H shifts in iridium hydrides.[63]

3 Conclusion

Using a robust route from azido-phenylene-isocyanide precursor complexes, we obtained NHC^{H} Ir^{III} complexes. The reactivity of the NHC N–H group in these complexes could be enhanced under reductive conditions, which is suggestive of a metallophilic interaction (*β*-H activation) that distinguishes it from reported base-induced reactions.

The reactivity was used to access various unique complexes. The NHC^H could nucleophilically attack MeCN to provide neutral κ^2-NHC-imidoyl ligands and under reductive conditions their anionic analogues, which both are interesting ligands for catalysis. In the presence of zinc, the NHC^H iridium chloride complex underwent oxidative self-activation, which resulted in the formation of an unprecedented C_s-symmetric dinuclear iridium hydride complex, bearing two head-to-head coordinated bridging N-deprotonated NHCs. Overall, it is exciting to observe that the reactivity of the NHC^Hs changes upon reduction of the complex. It may lead to new applications for these ligands, prove helpful in understanding the mechanistic steps for NHC^H catalysts, and, as such, further the development of NHCs as cooperative ligands.

4 Experimental Section

4.1 Preparation of Compounds

All experiments were performed under an atmosphere of dry nitrogen using standard Schlenk-line and glovebox techniques, unless stated otherwise. Solvents were distilled under nitrogen over the appropriate drying agent; $CaCl_2$ (DCM), benzophenone/NaK (Et_2O, THF), $LiAlH_4$ (pentane), K_2CO_3 (MeCN, acetone), P_2O_5 (CD_2Cl_2, $CDCl_3$). C_6D_6 was dried over Na at RT. Anhydrous MeOH was obtained from Sigma-Aldrich. Water was degassed ultrasonically under reduced pressure. 2-Azido-phenylisonitrile (**1**)[[35]] was kindly provided by C.A. Dumke and F.E. Hahn.[[65]] (1,2,3,4,5-pentamethyl-cyclopentadienyl) iridium(III) dichloride dimer,[[66]] 1,3-dimethyl-benzimidazolium iodide,[[67]] bis(1,3-dimethylbenzimidazolidin-2-ylidene),[[40]] and (2-azido-phenylisonitrile) (1-methyl-4-isopropyl-benzene) ruthenium(II) dichloride[[34]] were prepared according to literature procedures. All other reagents were used as received. Solids were predried *in vacuo* for at least 15 minutes. NMR spectra were recorded on Bruker Avance 400 (^1H: 400.13 MHz, $^{13}C\{^1H\}$: 100.61 MHz, room temperature) or a Bruker Avance 500 (^1H: 500.23 MHz, $^{13}C\{^1H\}$: 125.78 MHz; room temperature). Chemical shifts are reported in ppm downfield from tetramethylsilane. ^1H-spectra were internally referenced to residual solvent resonances: $CDCl_3$ (δ 7.26) and CD_2Cl_2 (δ 5.32). ^{13}C-spectra were internally referenced to residual solvent resonances: $CDCl_3$ (δ 77.16) and CD_2Cl_2 (δ 53.84). Melting

points were measured using a Büchi Melting Point M-565 (sealed capillaries) and are uncorrected. High resolution electrospray ionisation (ESI) mass spectrometry was carried out using a Bruker micrOTOF-Q instrument in positive ion mode (capillary potential of 4500 V). Infrared spectra have been recorded on a Shimadzu FT-IR 8400S spectrophotometer.

(2-azidophenylisonitrile) (1,2,3,4,5-pentamethylcyclopentadienyl) iridium(III) dichloride (2). An orange solution of $[IrCp^*Cl_2]_2$ (626 mg, 0.79 mmol, 1.0 eq.) in DCM (85 mL) was added to 2-azidophenylisonitrile (252 mg, 1.75 mmol, 2.2 eq.) to provide a reddish brown solution which was stirred for 42h at RT, in absence of light. Evaporation provided a yellowish brown powder, which was washed with Et_2O (2 x 15 mL) to provide [(2-azidophenylisonitrile)$IrCp^*Cl_2$] as a yellow powder (835 mg, 1.54 mmol, 98.1%). [(2-azidophenylisonitrile)$IrCp^*Cl_2$] is light-sensitive in solution and was stored as a solid in absence of light at –20 °C. Mp: 160 °C ≤ decomp. ^{1}H NMR (500.23 MHz, $CDCl_3$): δ = 7.46 (dd, $^3J_{H,H}$ = 8.1 Hz, $^4J_{H,H}$ = 1.3 Hz, 1H, *o*-Ar-*H*), 7.43 (td, $^3J_{H,H}$ = 8.0 Hz, $^4J_{H,H}$ = 1.5 Hz, 1H, *m*-Ar-*H*), 7.24 (dd, $^3J_{H,H}$ = 8.3 Hz, $^4J_{H,H}$ = 1.0 Hz, 1H *m*-Ar-*H*), 7.17 (td, $^3J_{H,H}$ = 7.9 Hz, $^4J_{H,H}$ = 1.1 Hz, 1H, *p*-Ar-*H*), 1.90 (s, 15H, Cp-CH_3). $^{13}C\{^1H\}$ NMR (125.78 MHz, $CDCl_3$): δ = 137.5 (s, *m*-Ar-*C*-N_3), 130.7 (s, *o*-Ar-*C*H), 128.7 (s, *m*-Ar-*C*H), 125.5 (s, *m*-Ar-*C*H), 119.0 (s, *p*-Ar-*C*H), 95.3 (s, Cp*-*C*CH_3), 9.3 (s, Cp*-C*C*H_3), signals for Ar-*C*NC and Ar-CN*C* are unresolved. FT-IR: ν = 3086 (w), 3015 (w), 3001 (w), 2966 (w), 2363 (w), 2164 (s), 2129 (s), 2054 (w), 2041 (w), 2015 (w), 2000 (w), 1616 (w), 1578 (w), 1489 (m), 1452 (w), 1441 (w), 1423 (w), 1404 (w), 1377 (w), 1312 (m), 1292 (w), 1283 (w), 1263 (w), 1209 (w), 1148 (w), 1092 (w), 1082 (w), 1024 (w), 962 (w), 831 (w), 798 (w), 779 (m), 756 (w), 733 (w), 704 (w), 687 (w), 650 (w), 619 (w), 577 (m), 544 (w), 530 (w), 517 (w), 474 (w), 449 (m), 420 (w) cm^{-1}. MS (ESI-Q-TOF): calcd. for $C_{17}H_{19}N_4IrCl$: 507.0922; found: 507.0879.

(2-azidophenylisonitrile) (1,2,3,4,5-pentamethylcyclopentadienyl) iridium(III) diiodide (3). [(2-azidophenylisonitrile)$IrCp^*Cl_2$] (298 mg, 0.55 mmol, 1.0 eq.) and NaI (1.5 g, 10 mmol, 18.0 eq.) were dissolved in acetone (20 mL) to provide an orange solution, which was stirred for 48h at RT, in absence of light. The resulting orange suspension was evaporated to provide a red residue, which was repeatedly extracted with DCM until colourless extracts were obtained (approx. 4 x 4 mL). Evaporation of the combined extracts yielded [(2-azidophenylisonitrile)$IrCp^*I_2$] as a dark orange-red solid (335 mg, 0.46mmol, 84%). [(2-azidophenylisonitrile)$IrCp^*I_2$] is light-sensitive in solution and was stored as a solid in absence of light at –20 °C. *Crystallization:* Single crystals could be obtained by slow diffusion of pentane (4.5 mL/mmol compound) into a DCM/pentane

solution (27 mL DCM + 9 mL pentane/mmol compound) at 5 °C. Mp: 145 °C ≤ decomp. ^{1}H NMR (500.23 MHz, $CDCl_3$): δ = 7.40 (dd, $^{3}J_{H,H}$ = 8.0 Hz, $J_{H,H}$ = 1.2 Hz, 1H, *o*-Ar-*H*), 7.36 (td, $^{3}J_{H,H}$ = 7.9 Hz, $J_{H,H}$ = 1.5 Hz, 1H, *m*-Ar-*H*), 7.21 (dd, $^{3}J_{H,H}$ = 8.3 Hz, $J_{H,H}$ = 0.9 Hz, 1H, *m*-Ar-*H*), 7.17 (td, $^{3}J_{H,H}$ = 7.8 Hz, $^{4}J_{H,H}$ = 1.1 Hz , 1H, *p*-Ar-*H*), 2.15 (s, 15H, Cp*-CH_3). ^{13}C{^{1}H} NMR (125.78 MHz, $CDCl_3$): δ = 137.0 (s, *m*-Ar-*C*-N_3), 130.7 (s, *ipso*-Ar-*C*NC), 130.1 (s, *o*-Ar-*C*H), 128.7 (s, *m*-Ar-*C*H), 125.2 (s, *m*-Ar-*C*H), 118.9 (s, *p*-Ar-*C*H), 96.0 (Cp*-*C*CH_3), 10.6 (Cp*-C*C*H_3), the signal for Ar-CN*C* is unresolved. FT-IR: *ν* = 2962 (w), 2916 (w), 2858 (w), 2357 (w), 2349 (w), 2326 (w), 2287 (w), 2118 (s), 2095 (s), 1894 (w), 1578 (w), 1485 (m), 1443 (m), 1423 (w), 1373 (w), 1358 (w), 1312 (s), 1258 (s), 1211 (w), 1080 (m), 1018 (s), 949 (w), 864 (w), 798 (s), 764 (s), 710 (w), 652 (m), 613 (w), 579 (s), 544 (m), 525 (m), 471 (m), 432 (m) cm^{-1}. MS (ESI-Q-TOF): calcd. for $C_{17}H_{19}N_4IrI$: 599.0284; found: 599.0249.

(1H-benzimidazolylidene) (1,2,3,4,5-pentamethylcyclopentadienyl) iridium(III) diiodide (4). NaI (236 mg, 1.58 mmol, 4.1 eq.) was dissolved in acetone (40 mL), after which was added to $FeCl_3$ (113 mg, 0.70 mmol, 1.8 eq.) to provide a black suspension. Immediately afterwards, a solution of [(2-azidophenylisonitrile)IrCp*Cl_2] (207 mg, 0.38 mmol, 1.0 eq.) in DCM (10 mL) was added to the black suspension and the resulting mixture was stirred for 43h at RT, during which the colour turned to dark red. Volatiles (including iodine) were removed *in vacuo* to provide a very dark red residue, which was extracted in DCM (180 mL) under atmospheric conditions. The dark extract was subsequently washed with a solution of $Na_2S_2O_3$ (200 mL, 20% in H_2O), a solution of $NaHCO_3$ (200 mL, saturated solution in H_2O) and brine (200 mL). The resulting orange solution was dried over Na_2SO_4. After evaporation, [(1H-benzimidazolylidene)IrCp*I_2] was obtained as a yellow powder (233 mg, 0.33 mmol, 87%). *Crystallization:* Single crystals could be obtained by slow diffusion of pentane into a DCM solution (pentane/DCM: approx. 1/3). Mp: 330 °C ≤ decomp. ^{1}H NMR (500.23 MHz, CD_2Cl_2): δ = 9.88 (s, 2H, N-*H*), 7.47-7.42 (m, 2H, Ar-*H*), 7.27-7.22 (m, 2H, Ar-*H*), 1.92 (s, 15H, Cp*-CH_3). ^{13}C{^{1}H} NMR (125.78 MHz, CD_2Cl_2): δ = 161.0 (s, N*C*N), 134.2 (s, Ar-*C*), 123.8 (s, Ar-*C*H), 111.3 (s, Ar-*C*H), 91.6 (s, Cp*-*C*CH_3), 10.4 (s, Cp*-C*C*H_3). FT-IR: *ν* = 3275 (w), 2962 (m), 2905 (w), 2380 (w), 1720 (w), 1616 (w), 1489 (w), 1450 (s), 1350 (m), 1304 (w), 1258 (s), 1153 (w), 1076 (s), 1011 (s), 864 (m), 791 (s), 729 (s), 706 (m), 675 (m), 636 (w), 602 (w), 532 (w), 494 (w) cm^{-1}. MS (ESI-Q-TOF): calcd. for $C_{17}H_{21}IN_2Ir$: 573.0373; found: 573.0376. *Alternative protocol 1:* $FeCl_3$ (27 mg, 0.165 mmol, 1.5 eq.) was dissolved in acetonitrile (12 mL), after which NaI (150 mg, 1 mmol, 9.1 eq.) was added to provide a black suspension. Immediately afterwards, a solution of [(2-azidophenylisonitrile)IrCp*Cl_2] (60 mg, 0.11 mmol, 1.0 eq.) in DCM (3 mL) was added to

the black suspension and the resulting mixture was stirred for 4h at RT. Volatiles (including iodine) were removed *in vacuo* to provide a black residue, which was extracted in DCM (40 mL) under atmospheric conditions. The dark extract was subsequently washed with a solution of $Na_2S_2O_3$ (100 mL, 20% in H_2O) and $NaHCO_3$ (100 mL, saturated solution in H_2O). The resulting orange solution was dried over Na_2SO_4. After evaporation, [(1H-benzimidazolylidene)IrCp*I_2] was obtained as a dark yellow powder (48 mg, 0.07 mmol, 63%). *Halogen exchange:* When a mixture of [(1H-benzimidazolylidene)IrCp*I_2] and [(1H-benzimidazolylidene)IrCp*ICl] was obtained, the obtained mixture was dissolved in acetone (66 mL/mmol compound) to which excess NaI (approx. 3.0 eq.) was added. The resulting mixture was stirred for 72h at RT. Volatiles were removed *in vacuo* to yield a yellow residue, which was extracted in DCM (240 mL/mmol compound). Evaporation of the extract yielded [(1H-benzimidazolylidene)IrCp*I_2] as a yellow powder. *Alternative protocol 2:* $FeCl_3$ (49 mg, 0.30 mmol, 1.5 eq.) and NaI (90 mg, 0.60 mmol, 3.0 eq.) were dissolved in acetone (30 mL) to provide a black suspension. Immediately afterwards, a solution of [(2-azidophenylisonitrile)IrCp*I_2] (147 mg, 0.20 mmol, 1.0 eq.) in DCM (6 mL) was added to the black suspension and the resulting mixture was stirred for 20h at RT. Volatiles (including iodine) were removed *in vacuo* to provide a very dark red residue, which was extracted in DCM (80 mL) under atmospheric conditions. The extract was subsequently washed with a solution of $Na_2S_2O_3$ (100 mL, 20% in H_2O), a solution of $NaHCO_3$ (100 mL, saturated solution in H_2O) and brine (100 mL). The resulting orange solution was dried over Na_2SO_4. After evaporation, [(1H-benzimidazolylidene)IrCp*I_2] was obtained as a dark yellow powder (96 mg, 0.14 mmol, 69%).

(1H-benzimidazolylidene) (1,2,3,4,5-pentamethylcyclopentadienyl) iridium(III) dichloride (5). To an orange solution of [(1H-benzimidazolylidene)IrCp*I_2] (69 mg, 0.098 mmol, 1.0 eq.) in THF (14 mL) was added AgOTf (53 mg, 0.206 mmol, 2.1 eq.) to provide a yellow suspension which was stirred for 40 min. at RT, in absence of light. $Et_3N{\cdot}HCl$ (36 mg, 0.262 mmol, 2.7 eq.) was added to provide an orange-yellow solution, which was stirred for 120 min. at RT. Filtration provided a yellow solution, which was evaporated. The resulting yellow solid was redissolved in DCM (40 mL) and washed with H_2O (2 x 40 mL). The yellow organic layer was dried with $MgSO_4$ and evaporated to provide an orange yellow solid. Crystallization by cooling a DCM/pentane solution (20 mL/20 mL) to –80 °C, provided pure [(1H-benzimidazolylidene)IrCp*Cl_2] as an orange solid (17 mg, 0.033 mmol, 34%). Mp: 289 °C ≤ decomp. ^{1}H NMR (500.23 MHz, $CDCl_3$): δ = 10.52 (s, 2H, N-*H*), 7.24-7.19 (m, 2H, Ar-*H*), 7.03-6.98 (m, 2H, Ar-*H*), 1.74 (s, 15H, Cp*-C*H*$_3$). ^{13}C{^{1}H} NMR (125.78 MHz, CD_2Cl_2): δ = 165.7 (s, N*C*N), 133.5 (s, Ar-*C*), 123.4 (s, Ar-*C*H), 111.5 (s,

Ar-*C*H), 90.0 (s, Cp*-*C*CH$_3$), 9.1 (s, Cp*-C*C*H$_3$). FT-IR: ν = 3271 (w), 3204 (w), 2962 (w), 2907 (w), 2853 (w), 1655 (w), 1618 (w), 1618 (w), 1491 (w), 1456 (s), 1400 (w), 1362 (m), 1348 (m), 1259 (s), 1246 (m), 1151 (w), 1080 (s), 1014 (s), 864 (w), 795 (s), 756 (s), 743 (s), 700 (m), 681 (s), 662 (m), 638 (w), 621 (m), 586 (w), 563 (w), 486 (w), 459 (m), 447 (s), 434 (m), 401 (s) cm^{-1}. MS (ESI-Q-TOF): calcd. for $C_{17}H_{21}ClN_2Ir$: 481.1009; found: 481.1013.

(*N*,*N'*-dimethyl-2-benzimidazolylidene) (1,2,3,4,5-pentamethylcyclopentadienyl) iridium(III) dichloride. To an orange solution of [IrCp*Cl$_2$]$_2$ (79.7 mg, 0.10 mmol, 1.0 eq.) in toluene (1 mL) was added a yellow solution of bis(1,3-dimethylbenzimidazolidin-2-ylidene) (29.2 mg, 0.10 mmol, 1.0 eq.) in toluene (1 mL). The reaction mixture was stirred for 4h at 100 °C. The mixture was allowed to cool to RT and stirred for 2d to provide a yellow suspension. Filtration provided a yellow solid, which was washed with diethyl ether (3 x 2 mL) to provide (*N*,*N'*-dimethyl-2-benzimidazolylidene)IrCp*Cl$_2$ as a yellow solid (95 mg, 17.44 mmol, 88%). Mp: 244 °C ≤ decomp. ^{1}H NMR (400.13 MHz, CDCl$_3$): δ= 7.40-7.35 (m, 2H, Ar-*H*), 7.33-7.27 (m, 2H, Ar-*H*), 4.17 (s, 6H, N-C*H$_3$*), 1.68 (s, 15H, Cp*-C*H$_3$*). ^{13}C{^{1}H} NMR (100.61 MHz, CDCl$_3$): δ = 170.6 (s, N*C*N), 135.9 (s, Ar-*C*), 123.5 (s, Ar-*C*H), 110.3 (s, Ar-*C*H), 89.6 (s, Cp*-*C*CH$_3$), 35.6 (s, N-*C*H$_3$), 9.3 (s, Cp*-C*C*H$_3$). FT-IR: v = 3990 (w), 3042 (w), 3028 (w), 2978 (w), 2953 (w), 2912 (w), 2897 (w), 1610 (w), 1508 w), 1489 (w), 1458 (m), 1445 (m), 1400 (w), 1375 (m), 1344 (m), 1250 (w), 1155 (w), 1136 (w), 1094 (m), 1078 (w), 1030 (w), 1013 (w), 955 (w), 808 (w), 795 (w), 768 (s), 696 (w), 681 (w), 613 (w), 567 (w), 532 (w), 469 (w), 447 (w), 434 (w), 417 (w), 401 (w) cm^{-1}. MS (ESI-Q-TOF): calcd. for $C_{19}H_{25}ClN_2Ir$: 509.1330; found: 509.1330.

(*N*,*N'*-dimethyl-2-benzimidazolylidene) (1,2,3,4,5-pentamethylcyclopentadienyl) iridium(III) diiodide (6). To a yellow suspension of (*N*,*N'*-dimethyl-2-benzimidazolylidene)IrCp*Cl$_2$ (71 mg, 0.13 mmol, 1.0 eq.) in acetone (10 mL), was added solution of NaI, (1.0g 6.67 mmol, 51 eq.) in acetone (15 mL) to provide a red-orange suspension which was stirred for 22h at RT. Evaporation provided an orange solid, which was extracted into DCM (3x 10 mL). Evaporation provided an orange red solid, which was washed with pentane (20 mL) to provide (*N*,*N'*-dimethyl-2-benzimidazolylidene)IrCp*I$_2$ as an orange solid (95 mg, 0.13 mmol, quant.). *Crystallization:* Single crystals could be obtained by cooling a saturated solution in DCM/pentane (1/1) to 5 °C. Mp: 270 °C ≤ decomp. ^{1}H NMR (500.23 MHz, CDCl$_3$): δ= 7.37-7.32 (m, 2H, Ar-*H*), 7.31-7.27 (m, 2H, Ar-*H*), 4.16 (s, 6H, N-C*H$_3$*), 1.88 (s, 15H, Cp*-C*H$_3$*). ^{13}C{^{1}H} NMR (125.78 MHz, CDCl$_3$): δ = 167.0 (s, N*C*N), 135.8 (s, Ar-*C*), 123.6 (s, Ar-*C*H), 110.4 (s, Ar-*C*H), 90.8 (s, Cp*-*C*CH$_3$), 40.6 (s, N-*C*H$_3$), 10.7 (s, Cp*-C*C*H$_3$). FT-IR: v = 3989 (w), 3049 (w), 2961 (w), 2934 (w), 2907 (w), 2853 (w),

2841 (w), 1686 (w), 1487 (w), 1456 (m), 1433 (m), 1396 (w), 1366 (m), 1339 (m), 1259 (m), 1242 (m), 1155 (w), 1132 (w), 1082 (s), 1013 (s), 933 (w), 864 (w), 797 (s), 746 (s), 700 (w), 675 (w), 662 (w), 633 (w), 611 (w), 588 (w), 565 (m), 534 (w), 492 (w), 438 (w), 403 (m) cm^{-1}. MS (ESI-Q-TOF): calcd. for $C_{19}H_{25}IN_2Ir$: 601.0686; found: 601.0691.

(κ²-*C,N*-1-(acetimino)-benzimidazolylidene) (1,2,3,4,5-pentamethylcyclopentadienyl) iridium(III) diiodide (7). To [(1H-benzimidazolylidene)IrCp*I$_2$] (0.05 g, 0.07 mmol) was added MeCN (20 mL). The resulting yellow mixture was stirred for 24h at reflux and 70h at RT. Evaporation provided (κ²-*C,N*-1-(acetimino)-benzimidazolylidene) (1,2,3,4,5-pentamethyl-cyclopentadienyl) iridium(III) diiodide as pale yellow solid (quant.), which due to its unstable nature was used directly without further purification. Mp: 194 °C ≤ decomp. ^{1}H NMR (500.23 MHz, CD_2Cl_2): δ = 13.08 (s, 1H, Ir-N(*H*)C-CH$_3$), 10.88 (s, 1H, Ar-N-*H*), 8.25 (d, 9.1 Hz, 1H, Ar-C*H*), 7.70 (d, 8.1 Hz, 1H, Ar-C*H*), 7.40 (t, 7.8 Hz, 1H, Ar-C*H*) 7.34 (t, 7.8 Hz, 1H, Ar-C*H*), 3.35 (s, 3H, Ir-N(H)C-C*H$_3$*), 2.16 (s, 15H, Cp*-C*H$_3$*). FT-IR: ν = 3103 (w), 3053 (w), 2962 (m), 2939 (w), 2907 (w), 1636 (w), 1601 (w), 1501 (w), 1475 (m), 1460 (m), 1445 (m), 1410 (w), 1385 (w), 1296 (w), 1258 (s), 1238 (w), 1190 (w), 1165 (w), 1155 (w), 1082 (s), 1013 (s), 864 (w), 791 (s), 754 (s), 704 (m), 681 (m), 662 (m), 608 (m), 548 (w), 498 (m), 424 (m) cm^{-1}. MS (ESI-Q-TOF): calcd. for $C_{19}H_{24}IN_3Ir$: 614.0639; found: 614.0668.

(κ²-*C,N*-(acetimidoyl)-benzimidazolylidene) (1,2,3,4,5-pentamethylcyclopentadienyl) iridium(III) monoiodide (8). $FeCl_3$ (121 mg, 0.75 mmol, 1.5 eq.) and NaI (750 mg, 5.0 mmol, 10.0 eq.) were dissolved in MeCN (20 mL) to provide a black mixture. Immediately afterwards, a solution of [(2-azidophenylisonitrile)IrCp*Cl$_2$] (270 mg, 0.5 mmol, 1.0 eq.) in DCM (6 mL) was added and the resulting black mixture was stirred for 48h at RT. Volatiles (including iodine) were removed *in vacuo* to provide a black residue, which was extracted with DCM (70 mL) under atmospheric conditions. The extract was subsequently washed with a solution of $Na_2S_2O_3$ (100 mL, 20% in H_2O) and $NaHCO_3$ (100 mL, saturated solution in H_2O). The resulting yellow solution was dried over Na_2SO_4. After evaporation and washing with $CHCl_3$ (10 mL), [(κ²-*C,N*-(acetimidoyl)-benzimidazolylidene)IrCp*I] was obtained as a yellow powder (232 mg, 0.38 mmol, 76%). Mp: 316 °C ≤ decomp. ^{1}H NMR (500.23 MHz, CD_2Cl_2): δ = 7.94 (s, 1H, N*H*), 7.54 (d, $^3J_{H,H}$ = 7.6 Hz, 1H, Ar-*H*), 7.48 (d, $^3J_{H,H}$ = 7.8 Hz, 1H, Ar-*H*), 7.23-7.18 (m, 1H, Ar-*H*), 7.06-7.01 (m, 1H, Ar-*H*), 3.00 (d, $^7J_{H,H}$ = 0.9 Hz, 3H, Ir-NC-C*H$_3$*), 1.94 (s, 15H, Cp*-C*H$_3$*). ^{13}C{^{1}H} NMR (125.78 MHz, $CDCl_3$): δ= 171.8 (s, N*C*N), 164.8 (s, Ir-N*C*-CH$_3$), 123.4 (s, Ar-*C*H), 121.1 (s, Ar-*C*H), 118.4 (s, Ar-*C*H), 110.1 (s, Ar-*C*H), 91.0 (s, Cp*-*C*CH$_3$), 19.8 (s, Ir-NC-

CH_3) 9.58 (s, Cp*-CCH_3), signals for Ar-*C* are unresolved. FT-IR: ν = 3132 (w), 3047 (w), 2974 (w), 2912 (w), 2862 (w), 2812 (w), 1620 (m), 1585 (w), 1493 (s), 1431 (s), 1373 (m), 1327 (w), 1292 (w), 1227 (m), 1184 (w), 1157 (w), 1126 (m), 1088 (m), 1022 (m), 987 (w), 910 (w), 810 (w), 752 (s), 737 (s), 710 (m), 687 (w), 663 (w), 617 (w), 552 (w), 498 (m), 432 (w) cm^{-1}. MS (ESI-Q-TOF): calcd. for $C_{19}H_{24}IN_3Ir$: 614.0639; found: 614.0670. *Alternative protocol 1 / Control reaction 1:* A red solution of $FeCl_3$ (28 mg, 0.17 mmol, 1.9 eq.) in MeCN (6 mL) was added to a colourless solution of NaI (137 mg, 0.91 mmol, 10.1 eq.) in MeCN (6 mL). The resulting black mixture was added to an orange solution of [(1H-benzimidazolylidene)IrCp*I_2] (63 mg, 0.09 mmol, 1.0 eq.) in DCM (3 mL). The resulting black mixture was stirred for 48h at RT. Volatiles (including iodine) were removed *in vacuo* to provide a black residue, which was extracted with DCM (35 mL) under atmospheric conditions. The extract was subsequently washed with a solution of $Na_2S_2O_3$ (50 mL, 20% in H_2O) and $NaHCO_3$ (50 mL, saturated solution in H_2O). The resulting yellow organic layer was dried over Na_2SO_4. After evaporation and washing with $CHCl_3$ (2.5 mL), [(κ^2-*C,N*-(acetimidoyl)-benzimidazolylidene)IrCp*I] was obtained as a yellow powder (41 mg, 0.07 mmol, 74%). *Alternative protocol 2 / Control reaction 2:* [(1H-benzimidazolylidene)IrCp*I_2] (6.5 mg, 0.0093 mmol, 1.2 eq.) was suspended in MeCN (2 mL) and refluxed for 5d. The resulting yellow solution was allowed to cool to RT and evaporated to provide [(κ^2-*C,N*-1-(acetimino)-benzimidazolylidene) IrCp*I_2] as an oily orange-yellow solid, which then was dissolved in THF (3.9 mL) and cooled to –78 °C. A solution of DBU (0.1 mL of a 0.08M solution in THF, 1.0 eq.) in THF (0.1 mL) was added dropwise. The resulting yellow solution was allowed to warm to RT and was stirred for 60 min. Evaporation provided a yellow solid, which was washed with $CHCl_3$ (0.5 mL) to provide [(κ^2-*C,N*-(acetimidoyl)-benzimidazolylidene)IrCp*I] as a light yellow powder (1.5 mg, 0.0026 mmol, 32%). *Control reaction 3:* [(2-azidophenylisonitrile)IrCp*I_2] (90 mg, 0.12 mmol, 1.0 eq.) and NaI (190 mg, 1.27 mmol, 10.6 eq.) were dissolved in MeCN (13 mL) to provide a brown suspension. A red solution of $FeCl_3$ (36 mg, 0.22 mmol, 1.8 eq.) in MeCN (12 mL) was added to provide a very dark brown mixture which was stirred for 49h at RT. Volatiles (including iodine) were removed *in vacuo* to provide a black solid, which was extracted in DCM (2 x 30 mL) under atmospheric conditions. The extract was subsequently washed with a solution of $Na_2S_2O_3$ (60 mL, 20% in H_2O) and $NaHCO_3$ (60 mL, saturated solution in H_2O). The resulting orange solution was dried over Na_2SO_4 and evaporated to provide an orange solid, which was washed with $CHCl_3$ (10 mL), Et_2O (20mL) and pentane (20 mL). ^{1}H NMR analysis of the obtained orange solid (49 mg) revealed a mixture of [(κ^2-*C,N*-(acetimidoyl)-benzimidazolylidene)IrCp*I] and [(1H-benzimidazolylidene)IrCp*I_2].

Bis ((1,2,3,4,5-pentamethylcyclopentadienyl) iridium(III)) (μ-hydrido) di(μ-κ^2-*C,N*-1H-benzimidazolylidene) monochloride (9). [(2-azidophenylisonitrile)IrCp*Cl_2] (299 mg, 0.55 mmol, 1.0 eq.), NH_4Cl (130 mg, 2.43 mmol, 4.4 eq.) and zinc dust (90 mg, 1.38 mmol, 2.5 eq.) were combined in MeOH (60 mL) to give a yellow suspension to which H_2O (0.6 mL) was added. The mixture was stirred at reflux for 166h to provide a red solution, which was allowed to cool to RT and was evaporated to give a red powder, which was washed with pentane (40 mL). Under atmospheric conditions, the powder was dissolved in DCM (120 mL) and washed with H_2O (6 x 50 mL). The organic layer was dried with Na_2SO_4 and the solvent was evaporated, to provide a red powder, which was washed with Et_2O (3 x 30 mL) to yield [(μ-κ^2-*C,N*-1H-benzimidazolylidene)$_2$$Ir_2$Cp*$_2$(μ-H)Cl] as a red solid (198 mg, 0.21 mmol, 75%). *Crystallization:* Crystallization by slow diffusion of Et_2O (5 mL) into a DCM (5 mL) solution at RT, provided [(μ-κ^2-*C,N*-1H-benzimidazolylidene)$_2$ Ir_2Cp*$_2$(μ-H)Cl] as red needles (76 mg, 0.08 mmol, 30%). Single crystals were obtained by slow diffusion of Et_2O (0.6 mL) into a saturated solution of 1 eq. [(μ-κ^2-*C,N*-1H-benzimidazolylidene)$_2$ Ir_2Cp*$_2$(μ-H)Cl] / 2 eq. triphenylphosphaneoxide in DCM (0.5 mL), buffered by a layer of DCM (0.1 mL) in an NMR tube. Mp: 212 °C ≤ decomp. ^{1}H NMR(500.23 MHz, CD_2Cl_2): δ = 12.37 (s, 2H, N*H*), 7.83 (d, $^3J_{HH}$ = 7.9 Hz, 2H, Ar Ir-NC-C*H*), 7.11 (d, $^3J_{HH}$ = 7.9 Hz, 2H, Ar HN-C-C*H*), 6.99 (t, $^3J_{HH}$ = 7.6 Hz, 2H, Ar Ir-NC-CH-C*H*), 6.86 (t, $^3J_{HH}$ = 7.6 Hz, 2H, Ar HN-C-CH-C*H*), 2.23 (s, 15H, C_2-Ir-Cp*-C*H*$_3$), 2.15 (s, 15H, N_2-Ir-Cp*-C*H*$_3$), –20.01 (s, 1H, Ir-*H*-Ir). ^{13}C{^{1}H} NMR (125.78 MHz, CD_2Cl_2): δ = 142.2 (s, N*C*N), 141.5 (s, Ar Ir-N*C*-CH), 137.0 (s, Ar HN-*C*-CH), 120.4 (s, Ar Ir-NC-CH-*C*H), 120.0 (s, Ar N(H)C-CH-*C*H), 112.6 (s, Ar Ir-NC-*C*H), 111.7 (s, Ar N(H)C-*C*H), 94.4 (s, C_2-Ir-Cp*-*C*), 87.4 (s, N_2-Ir-Cp*-*C*), 11.8 (s, N_2-Ir-Cp*-*C*H$_3$), 10.9 (s, C_2-Ir-Cp*-*C*H$_3$). FT-IR: ν = 3313 (w), 3252 (w), 3225 (w), 3117 (w), 3067 (w), 2962 (w), 2920 (w), 2854 (w), 1616 (w), 1450 (m), 1412 (m), 1369 (m), 1346 (w), 1292 (w), 1261 (m), 1219 (w), 1153 (w), 1076 (m), 1026 (s), 980 (w), 868 (w), 798 (m), 744 (s), 698 (w), 617 (w), 575 (w), 536 (w), 498 (w), 436 (w) cm^{-1}. MS (ESI-Q-TOF): calcd. for $C_{34}H_{41}N_4Ir_2$: 889.2561; found: 889.2586. *Alternative protocol 1 / Control reaction 1:* [(1H-benzimidazolylidene)IrCp*Cl_2] (6.5 mg, 0.01 mmol, 1.0 eq.) was suspended in MeOH (1 mL) to provide an orange mixture, to which zinc dust (2 mg, 0.03 mmol, 3 eq.) and H_2O (0.01 mL) were added. The mixture was stirred at reflux for 7d to provide an orange/red solution, which was allowed to cool to RT and was evaporated to provide a red solid. Under atmospheric conditions, the solid was extracted into CD_2Cl_2 (3.0 mL), after which evaporation provided μ-κ^2-*C,N*-1H-benzimidazolylidene)$_2$$Ir_2$Cp*$_2$(μ-H)Cl] as a red solid (quant.). *Control reaction 2:* [(2-azidophenylisonitrile)IrCp*I_2] (65 mg, 0.09 mmol, 1.0 eq.)

was suspended in MeOH (20 mL) to provide an orange mixture, which was added over NH_4Cl (13 mg, 0.24 mmol, 2.7 eq.) and zinc dust (10 mg, 0.15 mmol, 1.7 eq.). H_2O (0.2 mL) was added and the suspension was stirred at reflux for 7d to provide a brown solution, which was allowed to cool to RT and was evaporated. Under atmospheric conditions, the brown solid was extracted in DCM (10 mL + 5 mL) and the combined extracts were evaporated to provide an orange powder, which was washed with Et_2O (15 mL) and pentane (15 mL). The powder was dissolved in DCM (20 mL) and washed with H_2O (20 mL). Evaporation of the organic layer provided a red powder. ^1H NMR analysis showed no [(μ-κ²-*C,N*-1H-benzimidazolylidene)$_2$Ir$_2$Cp*$_2$(μ-H)X] formation. *Control reaction 3:* [(1H-benzimidazolylidene)IrCp*Cl_2] (6.5 mg, 0.01 mmol, 1.0 eq.) was suspended in MeOH (1 mL) to provide an orange mixture, to which H_2O (0.01 mL) was added. The mixture was stirred at reflux for 7d to provide an orange solution, which was allowed to cool to RT and evaporated to yield a red solid. ^1H NMR analysis showed no [(μ-κ²-*C,N*-1H-benzimidazolylidene)$_2$Ir$_2$Cp*$_2$(μ-H)Cl] formation.

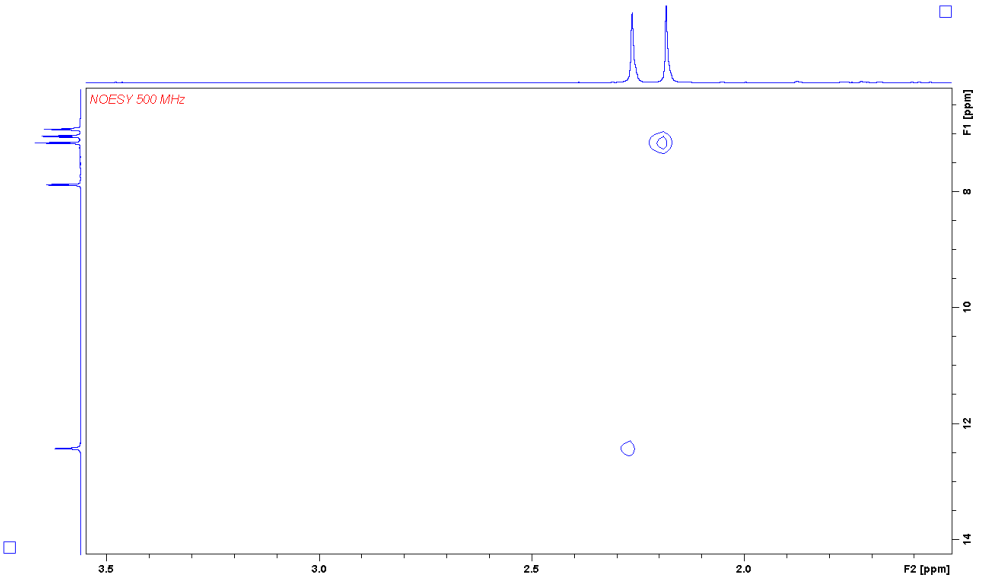

Figure S1. Detail with Cp*-NH correlations in NOESY (500.23 MHz, $CDCl_3$).

2-azidophenylisonitrile) (1,2,3,4,5-pentamethylcyclopentadienyl) rhodium(III) dichloride. [RhCp*Cl_2] (94 mg, 0.15 mmol, 1.0 eq.) in DCM (15 mL) was added to 2-azidophenylisonitrile (49 mg, 0.34 mmol, 2.3 eq.) to provide a red solution, which was stirred for 43.5h at RT, in absence of light. Evaporation provided a red powder, which was

washed with Et_2O (3 x 10 mL) to provide [RhCp*(2-azidophenyl isonitrile)Cl_2] as a red powder (107 mg, 0.24 mmol, 77.7%). [RhCp*(2-azidophenyl isonitrile)Cl_2] was stored as a solid in absence of light at –20 °C. Mp: 324 °C ≤ decomp. ^{1}H NMR (500.23 MHz, CD_2Cl_2): δ = 7.54-7.47 (m, 2H, *o,m*-Ar-*H*), 7.31 (d, $^3J_{H,H}$ = 8.5 Hz, 1H, *m*-Ar-*H*), 7.21 (t, $^3J_{H,H}$ = 7.6 Hz, 1H, *p*-Ar-*H*), 1.81 (s, 15H, Cp*-CH_3). ^{13}C{H} NMR (125.78 MHz, CD_2Cl_2): δ = 138.0 (s, *m*-Ar-*C*-N_3), 131.7 (s, *o*-Ar-*C*H), 128.8 (s, *m*-Ar-*C*H), 125.8 (s, *m*-Ar-*C*H), 119.5 (s, *p*-Ar-*C*H), 101.1 (s, Cp*-*C*CH_3), 9.7 (s, Cp*-C*C*H_3), signals for Ar-*C*NC and Ar-CN*C* are unresolved. FT-IR: ν = 3086 (w), 3013 (w), 3003 (w), 2966 (w), 2947 (w), 2918 (w), 2897 (w), 2353 (w), 2289 (w), 2176 (s), 2141 (s), 2125 (s), 2050 (w), 2029 (w), 1992 (w), 1979 (w), 1967 (w), 1952 (w), 1578 (w), 1560 (w), 1489 (s), 1472 (m), 1445 (m), 1406 (w), 1375 (w), 1358 (w), 1310 (s), 1292 (m), 1263 (w), 1219 (w), 1204 (w), 1148 (m), 1092 (m), 1080 (m), 1040 (m), 1018 (m), 966 (w), 906 (w), 825 (w), 781 (s), 733 (m), 648 (m), 621 (w), 565 (m), 546 (m), 530 (m), 511 (w), 484 (w), 440 (w) cm^{-1}. HRMS (ESI-Q-TOF): calcd for $C_{17}H_{19}ClN_4Rh$: 417.0348; found 417.0366.

Attempted synthesis (3-benzimidazolyl) (1,2,3,4,5-pentamethylcyclopentadienyl) iridium(III) dichloride. To a white suspension of benzimidazole (20 mg, 0.17 mmol, 3.4 eq.) in DCM (5 mL) was added [IrCp*Cl_2]$_2$ (38 mg, 0.05 mmol, 1.0 eq.) to provide a yellow suspension, which was stirred for 2 days at RT. Evaporation yielded a yellow solid, which was washed with Et_2O (3 x 2 mL) to provide a white-yellow solid (22 mg, 0.04 mmol, 44%). The extremely low solubility of the product prevented further identification.

Attempted synthesis bis((1,2,3,4,5-pentamethylcyclopentadienyl) rhodium(III)) (μ-hydrido) di(μ-κ^2-*C,N*-1H-benzimidazolylidene) monochloride. [(2-azidophenyl-isonitrile)RhCp*Cl_2] (56 mg, 0.12 mmol, 1.0 eq.), NH_4Cl (26.2 mg, 0.49 mmol, 4.1 eq.) and zinc dust (20 mg, 0.30 mmol, 2.5 eq.) were combined in MeOH (15 mL) to give a red suspension, to which H_2O (0.12 mL) was added. The resulting mixture was stirred at reflux for 164 hr to provide a red solution, which was allowed to cool to RT and was evaporated. The resulting red powder was washed with pentane (1 x 10 mL, 2 x 6 mL) and Et_2O (2 x 10 mL). Under atmospheric conditions, the residue was dissolved in DCM (60 mL) and washed with H2O (3 x 60 mL, 1 x 40 mL). The organic layer was dried and evaporated to provide a red solid. ^{1}H NMR analysis showed no bis((1,2,3,4,5-pentamethylcyclopentadienyl) rhodium(III)) (μ-hydrido) di(μ-κ^2-*C,N*-1H-benz-imidazolylidene) monochloride) formation but a mixture of [(1H-benzimidazolylidene)RhCp*Cl_2] and unidentified side-products.

Attempted synthesis bis((1-methyl-4-isopropyl-benzene) ruthenium(II)) (μ-hydrido) di(μ-κ²-*C,N*-1H-benzimidazolylidene) monochloride. *Protocol 1:* [Ru(*p*-cymene)(2-azidophenylisonitrile)Cl_2] (74 mg, 0.16 mmol, 1.0 eq.), NH_4Cl (35 mg, 0.64 mmol, 4.0 eq.) and zinc dust (26 mg, 0.40 mmol, 2.5 eq.) were combined in MeOH (16 mL) to provide a yellow/brown suspension to which H_2O (0.17 mL) was added. The mixture was stirred at reflux for 165 hr to provide a black suspension, which was allowed to cool to RT and was evaporated. Washing with Et_2O (3 x 10 mL) provided a black powder (0% bis((1-methyl-4-isopropyl-benzene) ruthenium(II)) (μ-hydrido) di(μ-κ²-*C,N*-1H-benzimidazolylidene) monochloride). ^1H NMR analysis revealed decomposition. *Protocol 2:* [Ru(*p*-cymene)(2-azidophenylisonitrile)Cl_2] (78 mg, 0.17 mmol, 1.0 eq.), NH_4Cl (36 mg, 0.66 mmol, 3.9 eq.) and zinc dust (26 mg, 0.40 mmol, 2.4 eq.) were combined in MeOH (17 mL) to provide a yellow/brown suspension to which H_2O (0.17 mL) was added. The mixture was stirred at RT for 164 hr to provide a black suspension, which was allowed to cool to RT and was evaporated. Washing with Et_2O (3 x 10 mL) provided a black powder (0% bis((1-methyl-4-isopropyl-benzene) ruthenium(II)) (μ-hydrido) di(μ-κ²-*C,N*-1H-benzimidazolylidene) monochloride; partial formation of (1H-benzimidazolylidene) Ru(II)(*p*-cymene)Cl_2;[68] HRMS (ESI-Q-TOF): calcd. for $C_{17}H_{22}ClN_2Ru$: 391.0515; found: 391.0345).

4.2 Computational Procedure

Density functional calculations were performed at the BP86/ZORA/Grimme-D3/TZ2P level of theory[[32]] using Amsterdam Density Functional (ADF)[[33]] 2013.01 (geometry optimizations, QTAIM[[61]]) and ADF2016.102 (ETS-NOCV[[44]]). The nature of each stationary point was confirmed by frequency calculations.

Iridium-carbene bond analysis (ETS-NOCV)

	4	**4||**	**6**
ΔE_{total}	–67.8	–68.2	–62.7
ΔE_{Pauli}	335.2	316.5	317.8
ΔE_{elstat}	–271.7	–256.5	–255.2
ΔE_{orb}	–131.4	–128.1	–125.3
σ	–90.6	–86.5	–82.6
π_1	–16.6	–17.2	–15.4
π_2	–6.9	–6.7	–8.2
polaris.	–9.4	–9.2	–9.0

BP86/ZORA/Grimme-D3/TZ2P; kcal mol^{-1}

Dinuclear complex 9 – QTAIM analysis

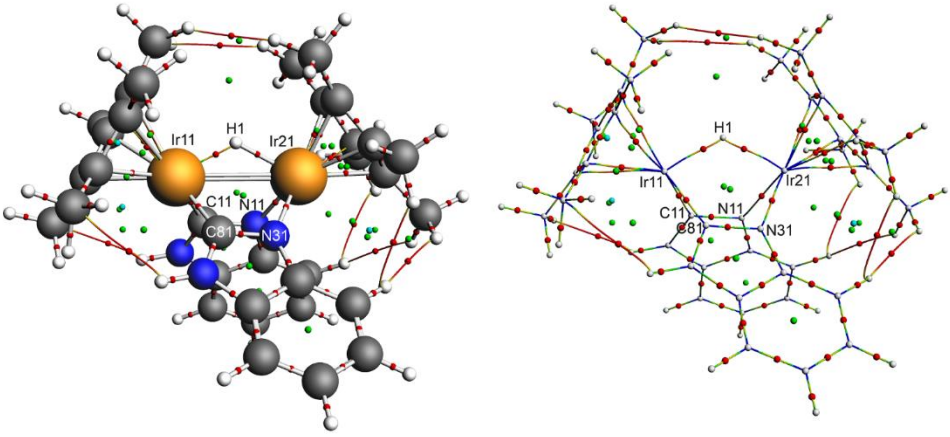

Figure S2. AIM analysis of bond paths in complex **9**. Bond critical points in red, ring critical points in green, cage critical points in blue.

4.3 Crystal structure determinations

The single-crystal X-ray diffraction studies of **3**, **4** and **6** were carried out on a Bruker-Nonius at 123(2) K using Mo-Kα radiation (λ = 0.71073 Å). Direct Methods or heavy atom methods (SHELXS-97)[69] were used for structure solution and refinement was carried out using SHELXL-2013 (full-matrix least-squares on F^2).[70] Hydrogen atoms were localized by difference electron density determination and refined using a riding model (H(N) free). Semi-empirical absorption corrections were applied. For **3** an extinction correction was applied.

3 (CCDC-1915713): red crystals, $C_{17}H_{19}I_2IrN_4 \cdot CH_2Cl_2$, M_r = 810.29, crystal size 0.30 × 0.15 × 0.12 mm, monoclinic, space group $P2_1/n$ (No. 14), a = 9.463(1) Å, b = 11.757(1) Å, c = 20.717(2) Å, β = 95.26(1)°, V = 2295.2(4) Å^3, Z = 4, ρ = 2.345 Mg/m^{-3}, μ(Mo-K$_\alpha$) = 8.75 mm^{-1}, F(000) = 1496, $2\theta_{max}$ = 55.0°, 48478 reflections, of which 5259 were independent (R_{int} = 0.025), 250 parameters, R_1 = 0.015 (for 5061 I > 2σ(I)), wR_2 = 0.032 (all data), S = 1.19, largest diff. peak / hole = 0.52 / -0.59 e Å^{-3}.

4 (CCDC-1915714): orange crystals, $C_{17}H_{21}I_2IrN_2$, M_r = 699.36, crystal size 0.30 × 0.10 × 0.06 mm, monoclinic, space group $P2_1/c$ (No. 14), a = 9.703(1) Å, b = 11.875(1) Å, c = 16.439(2) Å, β = 90.10(1)°, V = 1894.2(3) Å^3, Z = 4, ρ = 2.452 Mg/m^{-3}, μ(Mo-K$_\alpha$) = 10.31 mm^{-1}, F(000) = 1280, $2\theta_{max}$ = 55.0°, 24003 reflections, of which 4339 were independent (R_{int} = 0.052), 210 parameters, 2 restraints, R_1 = 0.025 (for 3812 I > 2σ(I)), wR_2 = 0.062 (all data), S = 1.07, largest diff. peak / hole = 1.47 / -1.77 e Å^{-3}.

6 (CCDC-1915715): red crystals, $C_{19}H_{25}I_2IrN_2$, M_r = 727.41, crystal size 0.40 × 0.20 × 0.03 mm, orthorhombic, space group *Pbca* (No. 61), a = 8.6423(6) Å, b = 17.5203(17) Å, c = 27.4808(18) Å, V = 4161.0(6) Å^3, Z = 8, ρ = 2.322 Mg/m^{-3}, μ(Mo-K$_\alpha$) = 9.39 mm^{-1}, F(000) = 2688, $2\theta_{max}$ = 55.0°, 44349 reflections, of which 4776 were independent (R_{int} = 0.040), 224 parameters, R_1 = 0.023 (for 4295 I > 2σ(I)), wR_2 = 0.054 (all data), S = 1.08, largest diff. peak / hole = 1.98 / -1.16 e Å^{-3}.

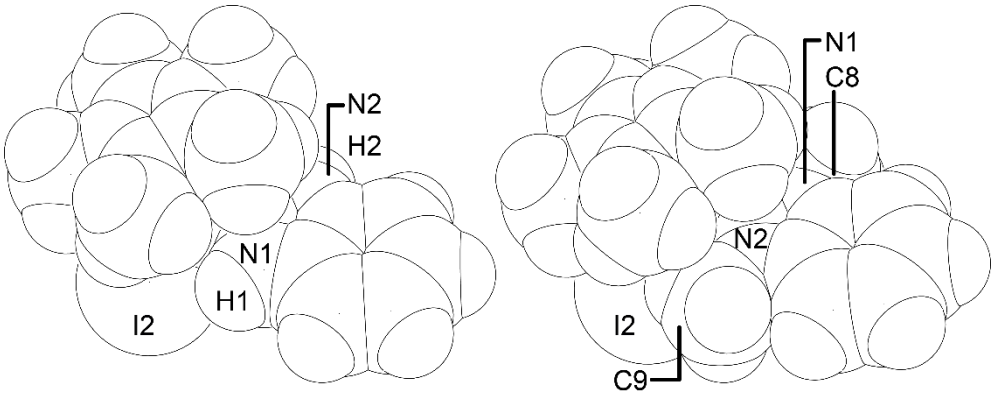

Figure S3. Space-filling (CPK) plots of complexes **4** (left) and **6** (right) in orientations identical to Figure **4**.

The single-crystal X-ray diffraction study of **9** was performed on a Bruker Kappa ApexII diffractometer with sealed tube and Triumph monochromator (λ = 0.71073 Å) at a temperature of 150(2) K up to a resolution of (sin λ/θ)max = 0.61 Å-1. The Eval15 software[71] was used for the intensity integration. For the prediction of reflection profiles a rather large isotropic mosaicity of 1.0 ° was used. A numerical absorption correction and scaling was performed with SADABS[72] (correction range 0.51-0.85). A total of 24638 reflections was measured, 13828 reflections were unique (R_{int} = 0.028) leading to an overall completeness of 94.4%. 10816 reflections were observed [I>2σ(I)]. The structure was solved with Patterson superposition methods using SHELXT.[73] Structure refinement was performed with SHELXL-2018[70] on F^2 of all reflections. Two of the four independent solvent molecules were refined with disorder models. In these disorder components, three C atoms were refined isotropically. All other non-hydrogen atoms were refined freely with anisotropic displacement parameters. The hydrogen atoms were introduced in calculated positions. The Ir-H hydrogen atoms were kept fixed at the calculated position. All other hydrogen atoms were refined with a riding model. 918 Parameters were refined with 202 restraints (concerning distances, angles and displacement parameters in the CH_2Cl_2 solvent). R1/wR2 [I > 2σ(I)]: 0.0370 / 0.0906. R1/wR2 [all refl.]: 0.0549 / 0.0983. S = 1.022. Residual electron density between -2.27 and 1.83 e/Å3. Geometry calculations and checking for higher symmetry was performed with the PLATON program.[74]

9 (CCDC-1921152): $[C_{34}H_{41}Ir_2N_4]Cl \cdot 2\ CH_2Cl_2$, Fw = 1095.41, red needle, 0.58 × 0.11 × 0.04 mm^3, triclinic, $P\overline{1}$ (no. 2), a = 10.0193(6), b = 19.0273(8), c = 21.4413(11) Å, α = 75.059(2), β = 86.963(2), γ = 85.500(3) °, V = 3935.0(3) $Å^3$, Z = 4, D_x = 1.849 g/cm^3, μ = 7.13 mm^{-1}.

5 Acknowledgments

This work was supported by the Council for Chemical Sciences of The Netherlands Organization for Scientific Research (NWO/CW). We thank T. van Dijk for measuring high-resolution mass spectra. 2-Azidophenyl isonitrile was kindly provided by Carolin A. Dumke and F. Ekkehardt Hahn (Institut für Anorganische und Analytische Chemie, WWU Münster, Corrensstr. 28/30, D-48149 Münster, Germany).

6 References

[1] For reviews on N-heterocyclic carbenes, see: a) Herrmann, W.A.; Köcher, C. *Angew. Chem. Int. Ed. Eng.*, **1997**, *36*, 2162–2187. b) Herrmann, W.A. *Angew. Chem. Int. Ed.*, **2002**, *41*, 1290–1309. c) Dröge, T.; Glorius, F. *Angew. Chem. Int. Ed.*, **2010**, *49*, 6940–6952. d) Díez–Gonzáles, S.; Marion, N.; Nolan, S.P. *Chem. Rev.*, **2009**, *109*, 3612–3676. e) Lappert, M.F. *J. Organomet. Chem.*, **2005**, *690*, 5467–5473.

[2] For a review on carbenes (including NHCs), see: de Frémont, P.; Marion, N.; Nolan, S.P. *Coord. Chem. Rev.*, **2009**, *253*, 862–892.

[3] a) Clark, G.R.; Roper, W.R.; Wright, A.H. *J. Organomet. Chem.*, **1982**, *236*, C7–C10. b) Fehlhammer, W.P.; Beck, G. *J. Organomet. Chem.*, **1989**, *369*, 105–116.

[4] For reviews on protic NHCs, see: a) Hahn, F.E. *ChemCatChem*, **2013**, *5*, 419–430. b) Jahnke, M.C.; Hahn, F.E. *Coord. Chem. Rev.*, **2015**, *293–294*, 95–115.

[5] The classical *N*-substituted NHCs only occasionally display *N*-substituent 'wingtip' activations. For more information, see: a) Prinz, M.; Grosche, M.; Herdtweck, E.; Herrmann, W.A. *Organometallics*, **2000**, *19*, 1692–1694. b) Semwal, S.; Ghorai, D.; Choudhury, J. *Organometallics*, **2014**, *33*, 7118–7124. c) Scott, N.M.; Pons, V.; Stevens, E.D.; Heinekey, D.M.; Nolan, S.P. *Angew. Chem. Int. Ed.*, **2005**, *44*, 2512–2515. d) Tang, C.Y.; Smith, W.; Thompson, A.L.; Vidovic, D.; Aldridge, S. *Angew. Chem. Int. Ed.*, **2011**, *50*, 1359–1362. e) Nelson, D.J.; Egbert, J.D.; Nolan, S.P. *Dalton Trans.*, **2013**, *42*, 4105–4109. f) Nelson, D.J.; Truscott, B.J.; Egbert, J.D.; Nolan, S.P. *Organometallics*, **2013**, *32*, 3769–3772. g) Tang, C.Y.; Lednik, J.; Vidovic, D.; Thompson, A.L.; Aldridge, S. *Chem. Commun.*, **2011**, *47*, 2523–2525. h) Fortman, G.C.; Jacobsen, H.; Cavallo, L.; Nolan, S.P. *Chem. Commun.*, **2011**, *47*, 9723–9725.

[6] For reviews on the potential of protic NHC cooperativity, see: a) Kuwata, S.; Ikariya, T. *Chem. Eur. J.*, **2011**, *17*, 3542–3556. b) Kuwata, S.; Ikariya, T. *Chem. Commun.*, **2014**, *50*, 14290–14300.

[7] For a review on cooperative systems, see for instance: Khusnutdinova, J.R.; Milstein, D.; *Angew. Chem. Int. Ed.*, **2015**, *54*, 12236−12273.

[8] a) Meier, N.; Hahn, F.E.; Pape, T.; Siering, C.; Waldvogel, S.R. *Eur. J. Inorg. Chem.*, **2007**, 1210−1214. b) Das, R.; Hepp, A.; Daniliuc, C.G.; Hahn, F.E. *Organometallics*, **2014**, *33*, 6975−6987.

[9] Araki, K.; Kuwata, S.; Ikariya, T. *Organometallics*, **2008**, *27*, 2176−2178.

[10] a) Das, R.; Daniliuc, C.G.; Hahn, F.E. *Angew. Chem. Int. Ed.*, **2014**, *53*, 1163−1166. b) Hahn, F.E.; Langenhahn, V.; Pape, T.; *Chem. Commun.*, **2005**, 5390−5392. c) Hahn, F.E.; García Plumed, C.; Münder, M.; Lügger, T. *Chem. Eur. J.*, **2003**, *10*, 6285−6293. d) Kösterke, T.; Pape, T.; Hahn, F.E.; *J. Am. Chem. Soc.*, **2011**, *133*, 2112−2115.

[11] a) Hahn, F.E.; Langenhahn, V.; Lügger, T.; Pape, T.; Le Van, D. *Angew. Chem. Int. Ed.*, **2005**, *44*, 3759−3763. b) Schmidtendorf, M.; Pape, T.; Hahn, F.E. *Angew. Chem. Int. Ed.*, **2012**, *51*, 2195−2198. c) Flores-Figueroa, A.; Pape, T.; Feldmann, K.-O.; Hahn, F.E. *Chem. Commun.*, **2010**, *46*, 324−326. d) Kaufhold, O.; Stasch, A.; Pape, T.; Hepp, A.; Edwards, P.G.; Newman, P.D.; Hahn, F.E. *J. Am. Chem. Soc.*, **2009**, *131*, 306−317.

[12] Kösterke, T.'; Kösters, J.; Würthwein, E.-U.; Mück-Lichtenfeld, C.; Schulte to Brinke, C.; Lahoz, F.; Hahn, F.E. *Chem. Eur. J.*, **2012**, *18*, 14594−14598.

[13] a) Ruiz, J.; Berros, Á.; Perandones, B.F.; Vivanco, M. *Dalton Trans.*, **2009**, 6999−7007. b) Ruiz, J.; Sol, D.; van der Maelen, J.F.; Vivanco, M. *Organometallics*, **2017**, *36*, 1035−1041.

[14] Fehlhammer, W.P.; Finck, W. *J. Organomet. Chem.*, **1991**, *414*, 261−270.

[15] Xiang, L.; Xiao, J.; Deng, L. *Organometallics*, **2011**, *30*, 2018−2025.

[16] a) Zanotto, L.; Bertani, R.; Michelin, R.A. *Inorg. Chem.*, **1990**, *29*, 3265−3268. b) Bertani, R.; Mozzon, M.; Michelin, R.A.; Benetollo, F.; Bombieri, G.; Castilho, T.J.; Pombeiro, A.J.L. *Inorg. Chim. Acta*, **1991**, *189*, 175−187. c) Poulain, A.; Neels, A.; Albrecht, M. *Eur. J. Inorg. Chem.*, **2009**, 1871−1881.

[17] a) Steinhagen, H.; Helmchen, G. *Angew. Chem. Int. Ed.*, **1996**, *35*, 2339−2342. b) Ma, J.-A.; Cahard, D. *Angew. Chem. Int. Ed.*, **2004**, *43*, 4566−4583. c) Rowlands, G.J. *Tetrahedron*, **2001**, *57*, 1865−1882.

[18] Miranda-Soto, V.; Grotjahn, D.B.; Cooksy, A.L.; Golen, J.A.; Moore, C.E.; Rheingold, A.L. *Angew. Chem. Int. Ed.*, **2011**, *50*, 631−635.

[19] Miranda-Soto, V.; Grotjahn, D.B.; DiPasquale, A.G.; Rheingold, A.L. *J. Am. Chem. Soc.*, **2008**, *130*, 13200−13201.

[20] a) Tan, K.L.; Bergman, R.G.; Ellman, J.A. *J. Am. Chem. Soc.*, **2002**, *124*, 3202−3203. b) Wiedemann, S.H.; Lewis, J.C.; Ellman, J.A.; Bergman, R.G. *J. Am. Chem. Soc.*, **2006**, *128*, 2452−2462. c) Lewis, J.C.; Berman, A.M.; Bergman, R.G.; Ellman, J.A. *J. Am. Chem. Soc.*, **2008**, *130*, 2493−2500.

[21] For more information on NHC^{H}/imidazole tautomerisation, see for instance: a) Burling, S.; Mahon, M.F.; Powell, R.E.; Whittlesey, M.K.; Williams, J.M.J. *J. Am. Chem. Soc.*, **2006**, *128*, 13702−13703. b) Sini, G.; Eisenstein, O.; Crabtree, R.H. *Inorg. Chem.*, **2002**, *41*, 602−604. c) Tonner, R.; Heydenrych, G.; Frenking, G. *Chem. Asian J.*, **2007**, *2*, 1555−1567.

[22] Wang, X.; Chen, H.; Li, X. *Organometallics*, **2007**, *26*, 4684−4687.

[23] For more information on Ir(III) in hydroamination, see for instance: a) Kashiwame, Y.; Kuwata, S.; Ikariya, T. *Chem. Eur. J.*, **2010**, *16*, 766−770. b) Tobisch, S. *Chem. Eur. J.*, **2012**, *18*, 7248−7262. c) Specht, Z.G.; Cortes-Llamas, S.A.; Tran, H.N.; van Niekerk, C.J.; Rancudo, K.T.; Golen, J.A.; Moore, C.E.; Rheingold, A.L.; Dwyer, T.J.; Grotjahn, D.B. *Chem. Eur. J.*, **2011**, *17*, 6606−6609. d) Gray, K.; Page, M.J.; Wagler, J.; Messerle, B.A. *Organometallics*, **2012**, *31*, 6270−6277. e) Kashiwame,

Y.; Kuwata, S.; Ikariya, T. *Organometallics*, **2012**, *31*, 8444−8455. f) Kumaran, E.; How, K.T.S.; Ganguly, R.; Li, Y.; Leong, W.K. *Organometallics*, **2013**, *32*, 4149−4152.

[24] Also rhenium(I)-pyrazolato complexes are known to exhibit similar MeCN hydroaminations. Gómez-Iglesias, P.; Arroyo, M.; Bajo, S.; Strohmann, C.; Miguel, D.; Villafañe, F. *Inorg. Chem.*, **2014**, *53*, 12437−12448.

[25] See for instance: a) Alcarazo, M.; Stork, T.; Anoop, A.; Thiel, W.; Fürstner, A. *Angew. Chem. Int. Ed.*, **2010**, *49*, 2542−2546. b) Collins, M.S.; Rosen, E.L.; Lynch, V.M.; Bielawski, C.W. *Organometallics*, **2010**, *29*, 3047−3053. c) Back, O.; Henry-Ellinger, M.; Martin, C.D.; Martin, D.; Bertrand, G. *Angew. Chem. Int. Ed.*, **2013**, *52*, 2939−2943. d) Mercs, L.; Labat, G.; Neels, A.; Ehlers, A.; Albrecht, M. *Organometallics*, **2006**, *25*, 5648−5656.

[26] Sanford, M.S.; Ulman, M.; Grubbs., R.H. *J. Am. Chem. Soc.*, **2001**, *123*, 749−750.

[27] Aktas, H.; Slootweg, J.C.; Schakel, M.; Ehlers, A.W.; Lutz, M.; Spek, A.L.; Lammertsma, K. *J. Am. Chem. Soc.*, **2009**, *131*, 6666−6667.

[28] For a review on (nucleophilic) phosphinidenes, see: a) Aktas, H.; Slootweg, J.C.; Lammertsma, K. *Angew. Chem. Int. Ed.*, **2010**, *49*, 2102−2113. b) "Phosphinidenes." Lammertsma, K. in *Top. Curr. Chem.*, **2003**, *229*, 95−119.

[29] Method: BP86/ZORA/TZP, using ADF 2005.01b and 2005.01.[27]

[30] Iridium phosphinidene complexes are more stable than their Ru-analogs. Termaten, A.T.; Schakel, M.; Ehlers, A.W.; Lutz, M.; Spek, A.L.; Lammertsma, K. *Chem. Eur. J.*, **2003**, *9*, 3577−3582.

[31] Rong, M.K.; Chirila, A.; Ehlers, A.W.; Slootweg, J.C.; Lammertsma, K. **2011**. Method: BP86/ZORA/TZ2P,[32] using ADF2010.02.[33] See Supporting Information.

[32] a) van Lenthe, E.; Baerends, E.J. *J. Comput. Chem.*, **2003**, *24*, 1142−1156. b) van Lenthe, E.; Baerends, E.J.; Snijders, J.G. *J. Chem. Phys.*, **1993**, *99*, 4597−4610. c) van Lenthe, E.; Baerends, E.J.; Snijders, J.G. *J. Chem. Phys.*, **1994**, *101*, 9783−9792. d) van Lenthe, E.; Ehlers, A.; Baerends, E.J. *J. Chem. Phys.*, **1999**, *110*, 8943−8953.

[33] a) te Velde, G.; Bickelhaupt, F.M.; Baerends, E.J.; Fonseca Guerra, C.; van Gisbergen, S.J.A.; Snijders, J.G.; Ziegler, T. *J. Comput. Chem.*, **2001**, *22*, 931−967. b) Fonseca Guerra, C.; Snijders, J.G.; te Velde, G.; Baerends, E.J. *Theor. Chem. Acc.*, **1998**, *99*, 391−403. c) ADF2010/2013/2016, SCM, Theoretical Chemistry, Vrije Universiteit, Amsterdam, The Netherlands, http://www.scm.com.

[34] Kaufhold, O.; Flores-Figueroa, A.; Pape, T.; Hahn, F.E. *Organometallics*, **2009**, *28*, 896−901.

[35] Hahn, F.E.; Langenhahn, V.; Meier, N.; Lügger, T.; Fehlhammer, W.P. *Chem. Eur. J.*, **2003**, *9*, 704−712.

[36] a) Jones, W.D.; Duttweiler, R.P., Jr.; Feher, F.J. *Inorg. Chem.*, **1990**, *29*, 1505−1511. b) Walsh, A.P.; Brennessel, W.W.; Jones, W.D. *Inorg. Chim. Acta*, **2013**, *407*, 131−138. c) Suzuki, H.; Tajima, N.; Tatsumi, K.; Yamamoto, Y. *Chem. Commun.*, **2000**, 1801−1802. d) Saito, A.; Seino, H.; Kajitani, H.; Takagi, F.; Yashiro, A.; Ohnishi, T.; Mizobe, Y. *J. Organomet. Chem.*, **2006**, *691*, 5746−5752.

[37] Kamal, A.; Ramana, K.V.; Babu Ankati, H.; Ramana, A.V. *Tetrahedron Lett.*, **2002**, *43*, 6861−6863.

[38] No details are reported on the reduction mechanism.[37] We observed *in situ* iodine formation, as evidenced by purple fumes, when $FeCl_3$ and NaI are mixed, indicating the generation of I_2 and $FeCl_2$, which then performs the azide-reduction. Hydrogen-atom donation is assumed to take place during the aqueous work-up.

[39] The same side-reaction had been observed previously for Ru(II).[34] In case of incomplete halogen exchange, the crude product was stirred with excess NaI in acetone at RT (Finkelstein conditions) to reach full conversion to **4**.

[40] Çetinkaya, E.; Hitchcock, P.B.; Küçükbay, H.; Lappert, M.F.; Al-Juaid, S. *J. Organomet. Chem.*, **1994**, *481*, 89−95.

[41] Huynh, H.V.; Han, Y.; Jothibasu, R.;Yang, J.A.; *Organometallics*, **2009**, *28*, 5395–5404.

[42] a) For the molecular structure of (*N*,*N'*-dimethyl-2-benzimidazolylidene)IrCp*Cl_2, see: Meredith, J.M.; Robinson, R., Jr.; Goldberg, K.I.; Kaminsky, W.; Heinekey D.M.; *Organometallics*, **2012**, *31*, 1879-1887. b) For molecular structures of related imidazol-2-ylidene-Ir(III) complexes, see reference 19 and: Hanasaka, F.; Fujita, K.-i.; Yamaguchi, R. *Organometallics*, **2005**, *24*, 3422−3433. c) For the molecular structure of the related (NHC^{H})Ru(II)(p-cym)I_2 complex, see reference 34.

[43] The symmetry operators for the respective I atoms are: (i) −x+1, −y+1, −z+1; (ii) −x+1, y−1/2, −z+3/2. Similar NH---X interactions have been observed previously.[11d,34]

[44] Mitoraj, M.P.; Michalak, A.; Ziegler, T. *J. Chem. Theory Comput.*, **2009**, *5*, 962−975.

[45] The closely related complex (benzimidazolyl)IrCp*Cl_2 was synthetically confirmed to be highly insoluble (see Supporting Information) and complexes akin to **7** are known to rearrange to their imidazolyl tautomers.[22]

[46] Although we are unaware of reports on iron(II)-based Ir(III) reductions, such a transformation might generate Ir(I), which upon oxidative N-H activation could eliminate HI to give the Ir(III) complex. Alternatively, iridium might be activated by Lewis acidic Fe(III) species, which after iodide abstraction generates FeX_4 and a free coordination site. However, this is unlikely to lead to deprotonation, since a synthesis route towards a complex akin to the non-deprotonated **7** was reported by exploiting free coordination sites on iridium(III) (Scheme 3).[22]

[47] Nitriles can be activated for C-functionalization by (catalytic) acid, base or alkylation. Nitrogen bases can stabilize nitrilium intermediates. For instance, see: a) Pinner, A.; Klein, F; *Ber. Dtsch. Chem. Ges.*, **1878**, *11*, 1475–1487. b) Schaefer, F.C.; Peters, G.A.; *J. Org. Chem,* **1961**, *262*, 412-418. c) Rong, M.K.; van Duin, K.; van Dijk, T.; de Pater, J.J.M.; Deelman, B.-J.; Nieger, M.; Ehlers, A.W.; Slootweg, J.C.; Lammertsma, K.; *Organometallics,* **2017**, *365*, 1079-1090. See also Chapter III. d) van Dijk, T.; Bakker, M.S.; Holtrop, F.; Nieger, M.; Slootweg, J.C.; Lammertsma, K. *Org. Lett.,* **2015**, *17*, 1461−1464.

[48] For a review on Group IX hydroamination catalysts, see: Hesp, K.D.; Stradiotto, M. *ChemCatChem*, **2010**, *2*, 1192−1207.

[49] a) Talwar, D.; Wu, X.; Saidi, O.; Salguero, N.P.; Xiao, J. *Chem. Eur. J.*, **2014**, *20*, 12835−12842. b) Talwar, D.; Li, H.Y.; Durham, E.; Xiao, J. *Chem. Eur. J.*, **2015**, *21*, 5370−5379.

[50] a) Randles, M.D.; Simpson, P.V.; Gupta, V.; Fu, J.; Moxey, G.J.; Schwich, T.; Criddle, A.L.; Petrie, S.; MacLellan, J.G.; Batten, S.R.; Stranger, R.; Cifuentes, M.P.; Humphrey, M.G. *Inorg. Chem.*, **2013**, *52*, 11256−11268. b) Tan, X.; Li, B.; Xu, S.; Song, H.; Wang, B. *Organometallics*, **2013**, *32*, 3253−3261. c) Heinekey, D.M.; Millar, J.M.; Koetzle, T.F.; Payne, N.G.; Zilm, K.W. *J. Am. Chem. Soc.*, **1990**, *112*, 909−919. d) Heinekey, D.M.; Fine, D.A.; Harper, T.G.P.; Michel, S.T. *Can. J. Chem.*, **1995**, *73*, 1116−1125. e) Heinekey, D.M.; Hinkle, A.S.; Close, J.D. *J. Am. Chem. Soc.*, **1996**, *118*, 5353−5361. f) Paisner, S.N.; Lavoie, G.G.; Bergman, R.G. *Inorg. Chim. Acta*, **2002**, *334*, 253−275.

[51] Flores-Figueroa, A.; Kaufhold, O.; Feldmann, K.-O.; Hahn, F.E. *Dalton Trans.*, **2009**, 9334–9342.
[52] Based on the Ir-C and Ir-N distances, the ligand is described as an *N*-anionic NHC^H, rather than a *C*-anionic benzimidazole.
[53] See for instance: a) White, C.; Oliver, A.J.; Maitlis, P.M. *J. Chem. Soc., Dalton Trans.*, **1973**, 1901–1907. b) Gill, D.S.; Maitlis, P.M. *J. Organomet. Chem.*, **1975**, *87*, 359–364.
[54] Fujita, K.-i.; Hamada, T.; Yamaguchi, R. *J. Chem. Soc. Dalton Trans.*, **2000**, 1931–1936.
[55] Sola, E.; Bakhmutov, V.I.; Torres, F.; Elduque, A.; López, J.A.; Lahoz, F.J.; Werner, H.; Oro, L.A. *Organometallics*, **1998**, *17*, 683–696.
[56] Padilla-Martínez, I.I.; Cervantes-Vásquez, M.; Leyva-Ramirez, M.A.; Paz-Sandoval, M.A. *Organometallics*, **2014**, *33*, 6305–6318.
[57] Fujita, K.-i.; Takahashi, Y.; Nakaguma, H.; Hamada, T.; Yamaguchi, R. *J. Organomet. Chem.*, **2008**, *693*, 3375–3382.
[58] a) Etter, M.C.; Baures, P.W. *J. Am. Chem. Soc.*, **1988**, *110*, 639–640. b) Hahn, F.E.; Imhof, L. *Organometallics*, **1997**, *16*, 763–769.
[59] Co-crystallization with TPPO was expected to provide beneficial hydrogen-bonding interactions with the *N*-H atoms, but no TPPO was incorporated in the final structure.
[60] Orpen, A.G.; Brammer, L.; Allen, F.H.; Kennard, O.; Watson, D.G.; Taylor, R. *J. Chem. Soc. Dalton Trans.*, **1989**, S1–S83.
[61] a) "Atoms In Molecules." Bader, R.F.W., *Claredon Press*, Oxford, **1994**. b) Rodríguez, J.I.; Bader, R.F.W.; Ayers, P.W.; Michel, C.; Götz, A.W.; Bo, C. *Chem. Phys. Lett.*, **2009**, *472*, 149–152. c) Rodríguez, J.I. *J. Comput. Chem.*, **2013**, *34*, 681–686.
[62] Additionally, Ir(II) and Ir(IV) are paramagnetic species, which should have had a clear effect on the NMR spectroscopic data and no such effects were observed.
[63] Song, G.; Su, Y.; Periana, R.A.; Crabtree, R.H.; Han, K.; Zhang, H.; Li, X. *Angew. Chem. Int. Ed.*, **2010**, *49*, 912–917.
[64] See for instance: a) Su, Y.; Song, G.; Han, K.; Li, X. *J. Organomet. Chem.*, **2011**, *696*, 1640–1646. b) He, F.; Braunstein, P.; Wesolek, M.; Danapoulos, A.A. *Chem. Commun.*, **2015**, *51*, 2814–2817.
[65] Institut für Anorganische und Analytische Chemie, WWU Münster, Corrensstr. 28/30, D-48149 Münster, Germany.
[66] Ball, R.G.; Graham, W.A.G.; Heinekey, D.M.; Hoyano, J.K.; McMaster, A.D.; Mattson, B.M.; Michel, S.T. *Inorg. Chem.*, **1990**, *29*, 2023–2025.
[67] Bostai, B.; Novák, Z.; Bényei, A.C.; Kotschy, A. *Organic Letters*, **2007**, *9*, 3437–3439.
[68] For the corresponding diiodo complex see reference 34.
[69] Sheldrick, G.M. *Acta Crystallogr.* **2008**, *A64*, 112-122.
[70] Sheldrick, G.M. *Acta Crystallogr.* **2015**, *C71*, 3-8.
[71] Schreurs, A. M. M.; Xian, X.; Kroon-Batenburg, L. M. J. *J. Appl. Cryst.*, **2010**, *43*, 70-82.
[72] Sheldrick, G.M. **2014**. SADABS. Universität Göttingen, Germany.
[73] Sheldrick, G.M. *Acta Crystallogr.*, **2015**, *A71*, 3-8.
[74] Spek, A. L. *Acta Crystallogr.*, **2009**, *D65*, 148-155.

Summary

The reactivity and selectivity of transition metal catalysts can be synergistically enhanced by interaction with either a second metal atom or a cooperative ligand. Exemplary are redox non-innocent ligands and hybrid ligands, when its second donor atom is subject to hemilabile coordination, thereby providing, for instance, desirable Lewis or Brønsted basicity. With donor atoms positioned appropriately, such as in a 1,3-position, coordination to a second metal may occur to facilitate metal-metal interactions in multinuclear complexes.

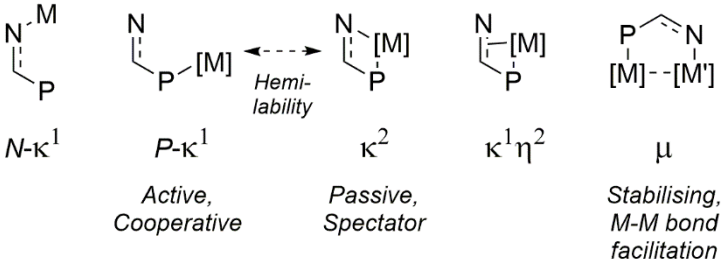

1,3-P,N-ligands are valuable because of their diverse binding modes (N-κ^1, P-κ^1, P-$\kappa^1\eta^2$, κ^2, and μ) by which they can provide cooperative interactions in mononuclear complexes and facilitate metal-metal interactions to access multinuclear species, ranging from bimetallic complexes to clusters. **Chapter 1** reviews their mononuclear transition metal complexes, in which their versatile bonding nature is linked to a number of applications, including coordination chemistry, homo- and heterogeneous catalysis, and bio-inorganic purposes. The contemporary developments are most pronounced in ruthenium and palladium based homogeneous catalysis. The 1,3-P,N-ligands also serve as a favorable template to access multinuclear homo and hetero metallic complexes.

Chapter 2 reviews the interesting coordination chemistry of these complexes and their use in metal-activation and (cooperative) catalysis. Especially photophysical studies of coinage metal complexes are attracting attention because the 1,3-P,N-ligands strongly influence their emissive properties. Several coinage metal 1,3-P,N-clusters were also used as catalysts with cooperative reactivity.

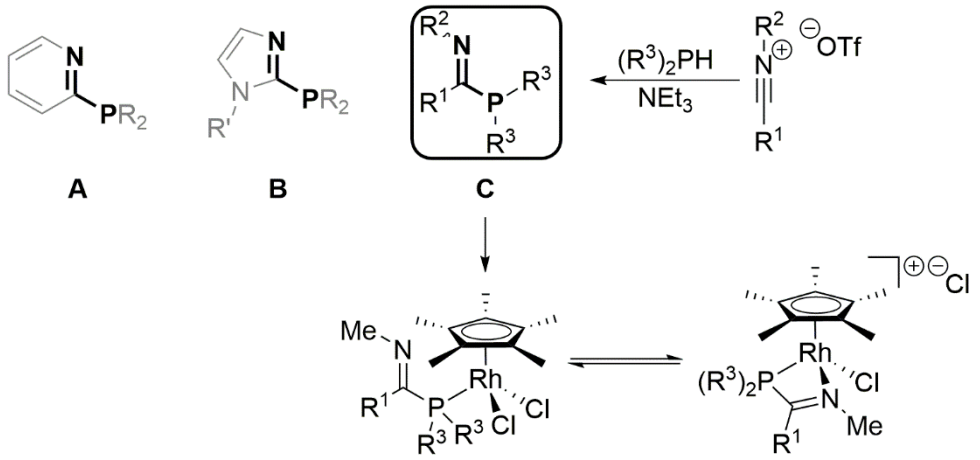

Historically, 2-pyridyl- and 2-imidazolylphosphane ligands **A** and **B** are the most widely applied 1,3-P,N-ligands, but novel synthetic methods based on nitrilium ion synthons provide access to iminophosphanes **C** that can be independently substituted on the phosphorus, carbon, and nitrogen positions to allow electronic and steric variation. **Chapter 3** explores their applicability in coordination chemistry and catalysis. Six novel iminophosphanes were synthesized in two steps by alkylation of nitriles and reacting the resulting nitrilium salts with secondary phosphanes. These water-stable but oxygen-sensitive ligands were obtained as a (dynamic) mixture of E/Z isomers, but coordinate readily in the desired Z-conformation to $[RhCp^*Cl_2]_2$ to provide κ^1/κ^2-complexes, in which the hapticity equilibrium depends on the properties of the ligand. Full conversion to the κ^2 chelates could be enforced with silver triflate.

The potential for catalysis was explored using Ru^{II} complexes for the hydration of benzonitrile in 1,2-dimethoxyethane (5 mol%, 180 °C, 3 h), water (5 mol%, 100 °C, 24 h) and under solvent free conditions (1.4 mol%, 180 °C, 3 h). In all cases benzamide was selectively obtained with yields of up to 96%, thereby outperforming by far catalysts based on the common 2-pyridyldiphenylphosphane **A**. The substitution pattern of the iminophosphanes affected the performance of the catalysts, which was attributed to the electronic properties of the ligands (i.e. the basicity of its nitrogen-donor).

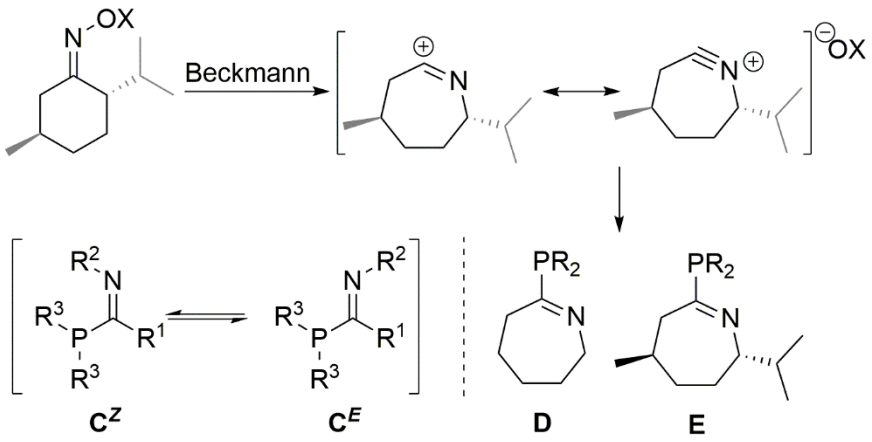

Cyclised iminophosphanes with a 'locked' *C,N*-conformation are explored in **Chapter 4**. These cycloiminophosphanes **D** were obtained from the nitrilium intermediate of the Beckmann rearrangement of cyclohexanone that was captured by benzotriazole. The benzotriazole group could be quantitatively replaced by a secondary phosphane under triflic acid promotion. Whereas the obtained ligands are 'non-isomerizable', their backbone remains flexible, as the observation of flippamers by ^{31}P NMR spectroscopy indicated dynamic conformational behavior of the tetrahydroazepine rings. The ligands have a far higher *N*-basicity than previously reported 1,3-P,N-ligands, which was also demonstrated using their W^0(carbonyl) and hemilabile Rh^{III} complexes. The P-κ^1- and P,N-κ^2-

W(carbonyl) complexes enabled quantification of the ligand's donor strength by analysis of the IR frequency of the *trans*-CO ligands. The analysis confirmed cycloiminophosphanes to be superior N-donors over 2-pyridyldiphenyl-phosphanes **A**. Coordination to $[RhCp^*Cl_2]_2$ gave a dynamic mixture of competing P/N-κ^1- and P,N-κ^2-bonding modes, observable by ^{31}P NMR spectroscopy; treatment with silver triflate allowed full conversion to the κ^2-complexes. Only P-κ^1-complexes were obtained with $[Ru(p\text{-cym})Cl_2]_2$. These were effective catalysts for the hydration of benzonitrile (1.4 mol%, 180 °C, 3h, up to 79%) and for the transfer hydrogenation of cyclohexanone (0.5 mol%, 83 °C, 2h, quant.) that could likewise be conducted with Ir^I catalysts (1 mol%, 83 °C, 4h, quant.). Also the asymmetric ligand **E** could be synthesized from the readily available natural precursor L-menthone. The ligand could be used to access P,N-κ^2-Rh^{III}- and P-κ^1-Ru^{II}-complexes. As no asymmetric 1,3-P,N-ligand-based catalysts have been reported, this is a valuable preamble to asymmetric catalysis.

In contrast to the well-established phosphane derivatives, NHCs are less explored as cooperative ligands. Protic NHCs became synthetically accessible only recently and have reactive NH sites that can be exploited for cooperative interactions. **Chapter 5** describes the reactivity of such NHC^H ligands coordinated to iridium. These complexes were obtained using a metal-templated synthesis in which azido-phenylene-isocyanide ligands were reduced to the corresponding amines, which then cyclized to give the desired NHC^H Ir^{III} complexes. The NHC^H N–H bond was found to be reactive and seemingly interacts with the metal center under reductive conditions. For instance, acetonitrile could be inserted to provide κ^2-NHC-imidoyl ligand-based complexes, but the corresponding deprotonated analogue was obtained under reductive conditions and in the absence of a base. When zinc was used as reductor, the NHC^H-iridium

chloride complex was shown to rearrange to a highly unusual C_s-symmetric dinuclear iridium hydrido complex, in which the bimetallic core is supported by two head-to-head coordinated N-deprotonated NHCs. Reduction of the complexes enhances the reactivity of the NHC^H N−H, which suggests that the observed transformations are facilitated by metallophilic interactions (β-H activation). This non-innocent activation contrasts with more common reactions induced by an external base.

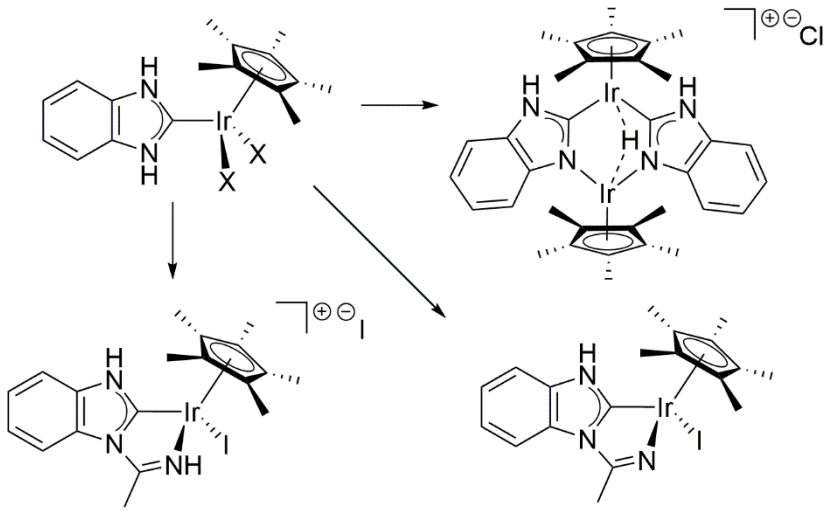

In conclusion, iminophosphanes and protic NHCs are attractive ligands for cooperative catalysts. Compared to the established 2-pyridyl- and 2-imidazolyl-phosphane ligands, the novel iminophosphanes have shown great prospects as new 1,3-P,N ligands. They are easily synthesized and highly tuneable, which affects their coordination to transition metal complexes and thus enables influencing the performance of catalysts. Cycloiminophosphanes further complement the existing classes of 1,3-P,N-ligands; not only structurally, but also electronically with their

high basicity. Moreover, asymmetric derivatives could be obtained with relative ease.

Looking ahead, additional studies will be needed to explore not only more catalytic processes, including asymmetric catalysis, but also catalysts based on first-row transition metals. The highly tunable iminophosphane ligands can also be explored in multinuclear coinage metal complexes for desirable photophysical properties. Finally, the non-innocent properties of protic NHCs ligands may be useful for mechanistic studies of NHC^{H}-based catalysts.

Samenvatting

De reactiviteit en selectiviteit van overgangsmetaalkatalysatoren kan synergistisch worden versterkt door interacties met een tweede metaalcentrum of een coöperatief ligand. Exemplair zijn redox-actieve liganden en hybride liganden wanneer hun tweede donoratoom hemilabiel coördineert, en ze daarmee, bijvoorbeeld, bevorderlijke Lewis of Brønsted basiciteit kunnen voorzien. Wanneer de donoratomen gunstig gepositioneerd zijn, zoals in 1,3-posities, dan kan een tweede metaal gecoördineerd worden om metaal-metaalinteracties te faciliteren in multinucleaire complexen.

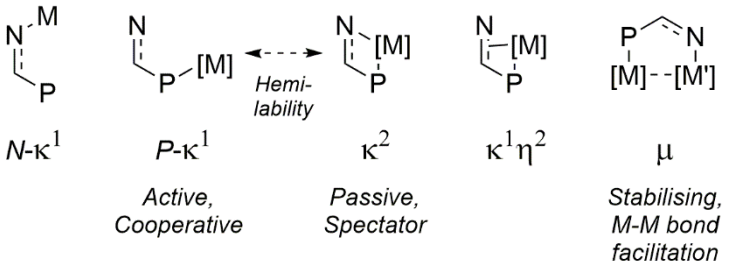

1,3-P,N-liganden zijn waardevol dankzij hun diverse bindingsmodi (N-κ^1, P-κ^1, P-$\kappa^1\eta^2$, κ^2, en μ) waarmee ze zowel coöperatieve interacties in mononucleaire complexen kunnen bieden, als metaal-metaalinteracties kunnen faciliteren om multinucleaire soorten te geven, variërend van bimetallische complexen tot clusters. **Hoofdstuk 1** geeft een overzicht van hun mononucleaire overgangsmetaalcomplexen, waarbij hun veelzijdige bindingsaard bepalend is voor hun toepassingen in coördinatiechemie, homo- en heterogene katalyse, en bio-anorganische doeleinden. De meest prominente actuele ontwikkelingen concentreren zich op homogene katalyse gebaseerd op ruthenium en palladium. De

gunstig opgebouwde 1,3-P,N-liganden verlenen ook toegang tot multinucleaire homo- en heterometaalcomplexen. **Hoofdstuk 2** bespreekt de interessante coördinatiechemie van deze complexen en hun toepasbaarheid in metaalactivatie en (coöperatieve) katalyse. De meeste aandacht gaat echter uit naar fotofysische ontwikkelingen met muntmetalen, omdat de 1,3-P,N-liganden grote invloed hebben op de emissie-eigenschappen. Enkele van zulke muntmetaal 1,3-P,N-clusters waren ook te gebruiken als katalysatoren met coöperatieve reactiviteit.

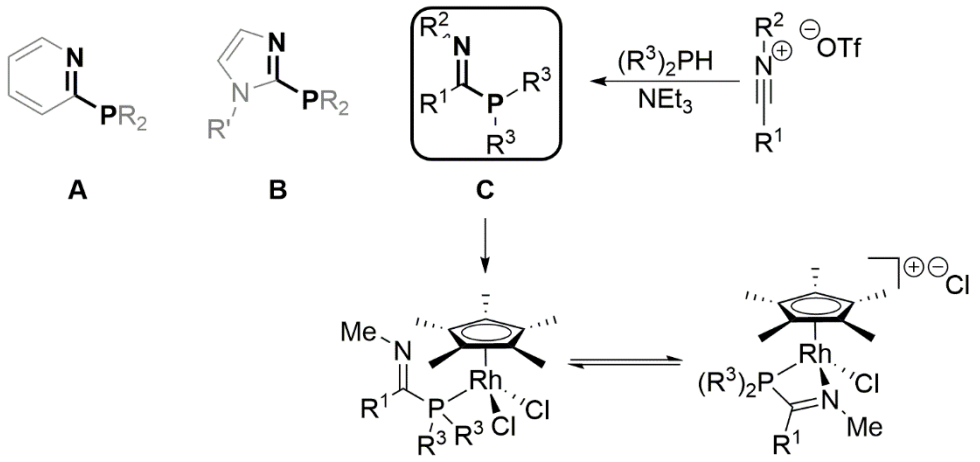

Traditioneel zijn 2-pyridyl- en 2-imidazolylfosfaanliganden **A** en **B** de breedst toegepaste 1,3-P,N-liganden, maar nieuwe synthesemethoden op basis van nitriliumionen verschaffen toegang tot iminofosfanen **C**, die met hun onafhankelijk substitueerbare fosfor-, koolstof- en stikstofposities de optie bieden tot elektronische en sterische variatie. **Hoofdstuk 3** verkent hun toepasbaarheid in coördinatiechemie en katalyse. Zes iminofosfanen werden in twee stappen gemaakt door eerst nitrillen te alkyleren, en de resulterende nitriliumzouten daarna te behandelen met secundaire fosfanen. Deze waterstabiele maar zuurstofgevoelige liganden werden verkregen als (dynamische) mengsels van E/Z isomeren, die onbelemmerd in de gewenste Z-conformatie

coördineren aan $[RhCp^*Cl_2]_2$ om κ^1/κ^2-complexen te geven, waarin het hapticiteitsevenwicht afhangt van de ligandeigenschappen. Volle conversie naar de κ^2 chelaten kon worden afgedwongen met zilvertriflaat. De capaciteit voor katalyse werd verkend met Ru^{II} complexen in de hydratie van benzonitril in 1,2-dimethoxyethaan (5 mol%, 180 °C, 3 h), water (5 mol%, 100 °C, 24 h) en onder oplosmiddelvrije condities (1.4 mol%, 180 °C, 3 h). In alle gevallen werd benzamide selectief verkregen met opbrengsten tot 96%, waarmee het katalysatoren op basis van het ijkligand 2-pyridylfosfaan **A** ver overtreft. Het substitutiepatroon van de iminofosfanen had invloed op de prestatie van de katalysator, wat werd toegekend aan de elektronische eigenschappen van het ligand (d.w.z. de basiciteit van de stikstofdonor).

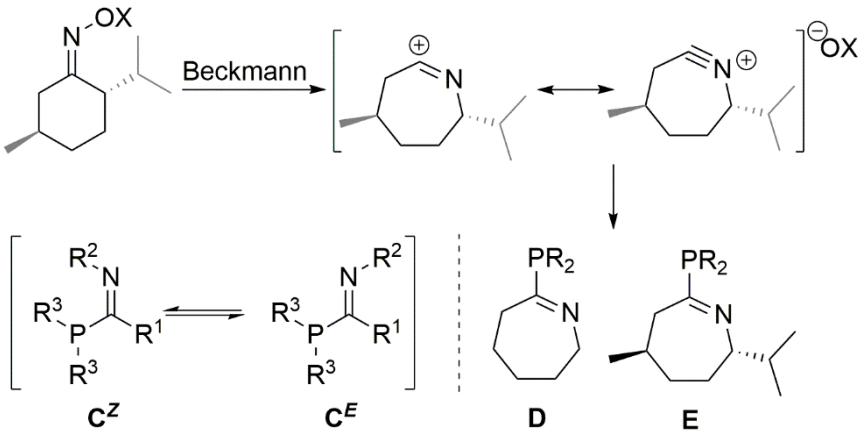

Gecycliseerde iminofosfanen met een 'gesloten' *C,N*-conformatie worden verkend in **Hoofdstuk 4**. Deze cycloiminofosfanen **D** werden verkregen door het nitriliumintermediair van de Beckmann-omlegging van cyclohexanon te onderscheppen met benzotriazool. De benzotriazoolgroep kon daarna kwantitatief worden vervangen door een secundair fosfaan, met triflaatzuur als promotor. Ondanks dat de verkregen liganden niet isomeriseerbaar zijn, blijft hun skelet flexibel, aangezien de waarneming van flippameren met ^{31}P NMR spectroscopie wijst op dynamisch

conformationeel gedrag van de tetrahydroazepine-ringen. De liganden hebben een aanzienlijk hogere N-basiciteit dan eerder gerapporteerde 1,3-P,N-liganden, wat ook gedemonstreerd kon worden met behulp van hun W^0(carbonyl) en hemilabiele Rh^{III} complexen. Met de P-κ^1- en P,N-κ^2-W(carbonyl) complexen kon de donorkracht van de liganden gekwantificeerd worden door de IR frequentie van de *trans*-CO-liganden te analyseren. Deze analyse bevestigde dat de N-donatie van cycloiminofosfanen superieur is aan die van 2-pyridylfosfanen **A**. De coördinatie aan $[RhCp^*Cl_2]_2$ gaf een dynamisch mengsel van concurrerende P/N-κ^1- en P,N-κ^2-bindingsmodi, waarneembaar met ^{31}P NMR spectroscopie; hun behandeling met zilvertriflaat gaf volle conversie naar de κ^2-complexen. Met $[Ru(p\text{-cym})Cl_2]_2$ werden alleen P-κ^1-complexen verkregen. Deze waren effectieve katalysatoren voor de hydratie van benzonitril (1.4 mol%, 180 °C, 3h, tot 79%) en voor de overdrachtshydrogenering van cyclohexanon (0.5 mol%, 83 °C, 2h, kwant.), wat eveneens uitgevoerd kon worden met een Ir^I katalysator (1 mol%, 83 °C, 4h, kwant.). Ook kon het asymmetrische ligand **E** gesynthetiseerd worden uit de ruim beschikbare natuurstof L-menthon, evenals de corresponderende P,N-κ^2-Rh^{III}- en P-κ^1-Ru^{II}-complexen. Aangezien er geen asymmetrische 1,3-P,N-katalysatoren gerapporteerd zijn, is dit een waardevolle stap naar asymmetrische katalyse.

In tegenstelling tot de gangbare fosfaanverbindingen, zijn N-heterocyclische carbenen veel minder verkend als coöperatieve liganden. Protische NHCs werden pas recentelijk synthetisch toegankelijk en hebben reactieve NH-groepen die uitgebuit kunnen worden voor coöperatieve interacties. **Hoofdstuk 5** beschrijft de reactiviteit van zulke NHC^H-liganden gecoördineerd aan iridium. Deze complexen werden verkregen met behulp van een metaalverankerde synthese, waarbij azidofenyleen-isocyanide liganden werden gereduceerd

tot de corresponderende amines, die daarna cycliseerden om de gewenste NHC^{H} Ir^{III} complexen te geven. De NHC^{H} N–H binding bleek reactief en interacteert schijnbaar met het metaalcentrum onder reductieve condities. Zo kon acetonitril bijvoorbeeld geïnserteerd worden om κ^2-NHC-imidoyl ligand-complexen te geven, maar het corresponderende gedeprotoneerde analoog werd verkregen onder reductieve condities in afwezigheid van een base. Wanneer zink werd gebruikt als reductor, legde het NHC^{H}-iridium-chloridecomplex om tot een zeer ongebruikelijk C_s-symmetrisch dinucleair iridium hydrido complex, waarin de bimetallische kern overbrugd wordt door twee kop-aan-kop gecoördineerde N-gedeprotoneerde NHCs. Aangezien de reactiviteit van de NHC^{H} N–H versterkt wordt door het reduceren van de complexen, suggereert dit dat de waargenomen transformaties worden gefaciliteerd door metallofiele interacties (β-H activatie). Deze redox-actieve benadering staat in contrast met de gebruikelijke reacties die geïnduceerd worden door een externe base.

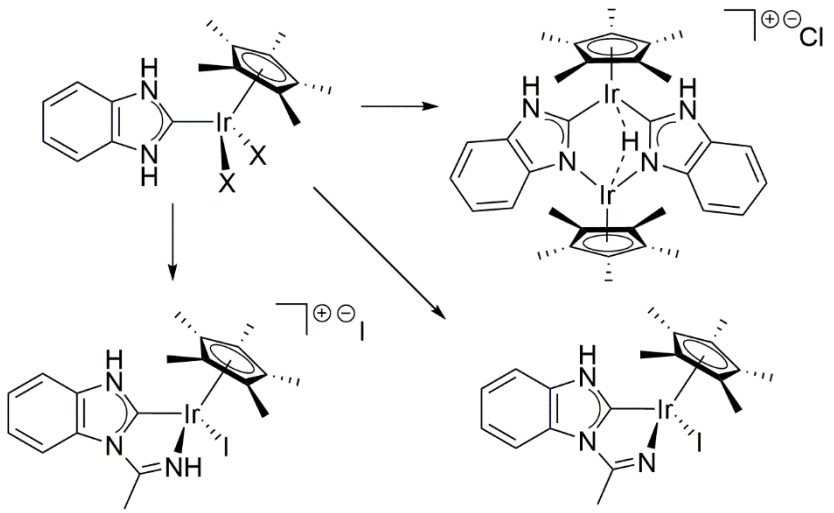

Concluderend, iminofosfanen en protische NHCs zijn aantrekkelijke liganden voor coöperatieve katalysatoren. In vergelijking met de gebruikelijke 2-pyridyl- en 2-imidazolyl-fosfaanliganden, tonen de gepresenteerde iminofosfanen goede vooruitzichten als nieuwe 1,3-P,N-liganden. Ze zijn gemakkelijk te synthetiseren en uitgebreid af te stemmen, wat effect heeft op hun coördinatie aan overgangsmetaalcomplexen, en het daarom mogelijk maken om de prestaties van katalysatoren te beïnvloeden. Cycloiminofosfanen vullen de bestaande klassen van 1,3-P,N-liganden verder aan; zowel structureel als elektronisch met hun hoge basiciteit. Bovendien konden asymmetrische derivaten relatief gemakkelijk verkregen worden.

In de toekomst zijn verdere aanvullende onderzoeken nodig waarin niet alleen meer katalyseprocessen, inclusief asymmetrische katalyse, maar ook katalysatoren op basis van de eerste rij overgangsmetalen verkend worden. De fijn-afstembare iminofosfaanliganden kunnen ook worden gebruikt in multinucleaire muntmetaalcomplexen voor aantrekkelijke fotofysische eigenschappen. Tot slot, de redox-actieve eigenschappen van protische NHCs kunnen verhelderend zijn in mechanistische studies van NHC^{H}-katalysatoren.

Acknowledgements

Soms lijkt de periode 2011-2021 veel langer dan vier jaar. Ik ben dankbaar dat er mensen zijn die me steunden en aanmoedigden, maar ook afleidden en waar nodig een schop onder de kont gaven.

Hoewel ze het me niet gemakkelijk maakten, denk ik dat ik veel geluk heb gehad met mijn team van (co)promotoren. **Koop**, tijdens m'n PhD kwam je regelmatig langs op KB364: eerst om te vragen of de muziek zachter mocht, en vervolgens waar Tom was. Je was zeer betrokken bij mijn schrijfwerk, en na vier jaar van je feedback heb ik eindelijk de kunst van korte verwoordingen leren waarderen. Ik vind het wonderbaarlijk hoe je soms zes maanden aan resultaten, verspreid over twee pagina's, kon reduceren tot drie woorden, zonder daarbij informatie te verliezen. Gecorrigeerde versie: dank. **Chris**. *Hi.* Ik heb jou ontmoet tijdens het tweedejaars BSc synthese practicum. Je viel een half uurtje in tijdens de lunchpauze van onze begeleider Maurice en ik besloot te openen met: "Hallo, ik ben Mark. Vertel het niet aan Maurice, maar ik heb géén idee wat ik aan het doen ben." Vreemd genoeg heb je me later alsnog aangenomen voor een PhD. Ik waardeer het laagdrempelige contact, je aanmoediging, meedenken, en geduld. **Andreas**, na je legendarische vakken en practica was je een grote reden voor mij om in deze groep te willen werken. Ik heb veel geleerd van je: kritisch leren kijken naar berekeningen, onderzoeksvragen terugbrengen tot hun kern, hoe ik mensen het beste oncomfortabel kan maken wanneer ze een domme vraag stellen, en natuurlijk de snelste route binnendoor, via de dienstingang, wat trappen op en af, langs de keuken, tussen het verbijsterde personeel door, om als eerste, een half uur voor de zaal open

gaat, in de rij te staan bij het buffet van het N3C. Ik waardeer je mix van hard en hart: Je vragen waren intimiderend, maar de oprechte complimenten die je kon maken wanneer het onderzoek goed ging waren essentiële motivatie.

Ik wil graag prof.dr. Matthias Bickelhaupt, prof.dr. Iwan de Esch, dr. Tati Fernández Ibáñez, prof.dr. Christian Müller, dr. Edwin Otten, dr. Sonja Pullen en prof.dr. Jarl Ivar van der Vlugt bedanken voor het deelnemen aan mijn lees- en promotiecommissie.

Ik weet niet of dit een goed moment is om het toe te geven, maar ik weet nog steeds de officiële naam van onze (voormalige) onderzoeksgroep niet. …OAC? In ieder geval, ik wil de rest van de 'fosforgroep' bedanken voor de fijne sfeer. Ik waardeerde de diversiteit van het onderzoek en de vrijheid die iedereen had om zijn eigen 'smaak' vreemd te zijn. **Bas**, je was een fantastisch labmaatje: niet alleen had je veel expertise in huis, je had ook 90% van de schlenks van de afdeling. Ik heb erg genoten van je vele destillatiedagen: je bouwde eerst een onmogelijk gecompliceerde opstelling, begon de volgende dag 's ochtends vroeg, gaf me een lezing over schotelgetallen en pomponderhoud, besteedde de hele middag aan het wachten op de goede fractie en eindigde de dag door uit pure frustratie de brander onder je schlenk te gooien (koken, kreng!) en alles binnen 5 minuten over te destilleren. Puur. Je lessen over het lab waren goed, je lessen over het leven waren beter. **Tom**, als mijn masterstage bij jou niet zo goed was geweest, dan was ik gestopt met onderzoek of mogelijk heel scheikunde (I should get into farming). Ook tijdens mijn PhD zorgde je ervoor dat iedere dag een goede dag was. Als de harde kern van de 'KB-bastards', deelden we onderzoeksonderwerpen, humor en muziek. Koop moet dat kunnen bevestigen, aangezien hij een sixth sense heeft om alléén onze kantoren binnen te komen wanneer we tijd namen

voor wat welverdiende onzin. Ik ben heel blij dat je nog even kon blijven hangen als de pirate postdoc (Brostdoc?). Bedankt voor het veelvuldige sparren, de bordspellen en de afleiding. On an unrelated note, stift. **Léon**, bedankt voor het zorgvuldige graven naar pareltjes in de Foutmijn. **Jeroen**, bedankt voor de wazige muziektips (inclusief poweromelet) en de mental image van je krabimitatie. **Jos**, bedankt voor de hulp met het Lisa cluster en de foute truien inspiratie. **Jaap**, je bent de enige persoon die ik ken met een P_4hD. **Tania**, I enjoyed teaching you Dutch. Perhaps some (or all…) of these words did not have the meaning I taught you, but a 'heer' never tells (mind those silent G's!). Also, if you hadn't told me, I would never have guessed that the BBB training at Uilenstede was an acronym for 'belly', 'legs' and 'donkey.' **Emmanuel**, in the middle of a very hot summer you taught me how to change the cat.-bed of the glovebox and it was truly a once in a lifetime experience. At least, I severely hope so. Also thanks to **Tebello**, **Federica** & **Federico** (Italy should be allowed to have more given names), **Yvon** (ik heb nog een goede mop voor je), **Niels**, **Shin-ichi**, **Yu-ichi** (goodnight..), **Maximilian** and, of course, **Volodymir/Vova** (the coolest man in the KGB) and **Basti** (the coolest man who isn't Vova).

The labwork wouldn't have been fun or successful, without my students. **Andrei**, your contributions were invaluable. You are one of the smartest and hardest working people I know: supervising you often felt like restraining a rocket. We never got the phosphinidene thing to work but your enthusiasm and motivation provided the basis for chapter 5 and contributed to the fundament for chapter 4. I enjoyed our morning gym sessions, and starting late at work after, while being unable to lift my arms. Remember: some things burn, even when you feel it really shouldn't. **Martijn**, in de laatste week van je bachelorproject spoelde je per ongeluk je resultaten door het afvalvat. **Koen**, jij hebt een groot deel

van de liganden in hoofdstuk 3 gemaakt, maar de grootste prestatie was dat je me hebt weten over te halen om St. Anger een tweede kans te geven. Bedankt voor alle muziektips! **Michael (Mahatma)**, je hebt je hard ingezet om veel cyclohexanon-derivaten te maken en ik voel me nog steeds schuldig over hoeveel reacties je hebt moeten 'grinden'. **David**, vooral dankzij jouw inspanningen hebben we de kristalstructuur voor het di-iridiumhydride complex in hoofdstuk 5 weten te bemachtigen (scheepsrecht). Ik hoop dat je snel weer een plaat opneemt samen met Nick. Heb je die protonmagneet ooit nog gevonden? **Roelof & Maarten**, jullie waren er maar kort maar het maakte indruk: het lukte jullie om het dimethylligand uit hoofdstuk 4 te maken én we hebben het VUmc bekeken. Jullie eindverslag had vruchtbare omschrijvingen om de kleur van potente productmengsels te beschrijven. **Flip**, met jou had ik de beste balans tussen serieusheid en (vaker) onzinnige, complete chaos. Het heeft geleid tot 3 publicaties (stage en scriptie) en het perfectioneren van je epic troll skills. Ik ben trouwens nog steeds op zoek naar die posterkokerdief! Wanneer gaan we aan je ouders vertellen dat Marissa en ik je geadopteerd hebben? **Nitesh**, in je eerste week op het lab wist je zes maanden aan werk te verzetten. Helaas was het zes maanden van mijn werk, en verplaatste je het naar het afvalvat. Ik weet nog steeds niet wat je bedoelde met het gebruiken van een 'stripperpaard' in het OV. Niet meer snipen in hoekjes. **Eddy**, you were my 'posthumous' student (thanks to Tom, who kept an eye after I left). With your long blonde hair, leather jacket and beard, you were best representative to continue and finish the research of chapter 4. **Kinga**, you were a very welcome whirlwind of cheer when you visited the KB-labs. **Yves:** Je bent een baas.

Ook mijn dank aan de collega's van bio-organische chemie. **Art** en **Tjøstil**: het was fijn om het hele traject Murmellius-(VCS)VU-PhD tegelijk te doorlopen. Mevrouw Weijers is nog steeds boos dat niemand

van ons analytisch wilde doen. Ik kijk trouwens nog wekelijks de DVD met de FlavorWave Turbo reclame. Verdere dank aan **Maurice**, **Sanne** (kies: Herman Finkers of Peer Bink?), en team hoeklab. Ik ben blij dat ik een aantal collega's van toen weer ben tegengekomen tijdens mijn huidige postdoc (technisch gezien tot nu toe slechts een 'post'). **Jurriën**, je had zo in onze groep gekund qua directheid, over the top sarcasme, metaal-fascinatie en vooral trippy youtube-tolerantie. Je spontane dronken filosofie zet me soms 's avonds laat nog steeds aan het denken. Let op those anglicismes, bevoor het too erg wordt. **Jordy**, sorry dat ik teleurstel door te promoveren voor 2030. **John**, wanneer start je een band die the Braun Note heet? **Guido**, succes met je nieuwe carrière als John. **Gydo**, tweede kansen maken me blij. (Hans) **Daniël**, wanneer gaan we die penibele synthese naar PNAS sturen? **Brendan**, tijdens je bachelorpracticum was je al een Pre-hD. **Tom**, poepie. **Matteo**, it's good to see not all Mario brothers are into plumbing. **Elwin**, je humor is fout en je muzieksmaak is goed. Win/win. **Eelco**, het is erg fijn om met je samen te werken. Ik kan je al bijna volgen wanneer je over heterocycli praat. **Romano**, bedankt voor je aanmoediging bij de laatste loodjes.

Roald, **Frans**, **Miep** en **Zanger Rinus**, bedankt voor de ondersteuning. **Anna**, bedankt voor de prettig gestoorde koffiepauzes en al je imitaties.

Martin Nieger, thanks for all the efforts you made to measure even the worst of my crystals. I appreciate the always pleasant contact and of course all those essential crystal structures scattered across this thesis. **Martin Lutz**, when we finally managed to get good quality crystals of the bimetallic compound in chapter 4, there was (of course…) a huge power outage overnight at the Uithof. I'm so happy that you still could determine the structure, thank you.

Wilbert, je gaf me alle vrijheid tijdens mijn nieuwe project om mijn proefschrift nog af te ronden – ik vond dat zo aardig dat ik er uit puur schuldgevoel nooit gebruik van heb durven maken. **Alex**, I never knew I needed a colleague who could sing Britney Spears to me. **Kristina**, nu jij?

Menno, je bent de wijste persoon die ik ken en de belangrijkste reden dat ik nog toerekeningsvatbaar ben. Soort van. Bijna. Je bent meer dan familie. Ik hoop oprecht dat we de verdediging beter door (zijn ge-)komen dan de beruchte colleges met Zaal's balpen of het defecte krijt van Baerends. **Marissa**, je bent het meest roze en blonde wat ooit in mijn kantoor gekomen is. De antipool. Je bent (onuitstaanbaar) vrolijk, aanmoedigend, kleurrijk en aardig. Je gebruikt woorden als 'BFF'. Ik ben blij dat je mij en m'n humeur tolereert. Wanneer leer je Flip om zijn eigen mandarijnen te pellen? **Jim**, jij bent de aardigste persoon die ik ken. De avonden op Uilenstede met whisky en 201 waren belangrijke ontspanning na de werkdagen. Moet je niet met zeepbellen? **Joëlle**, ik geniet van je haat en je vrolijkheid (en hoe vaak die overlappen). **Arien**, ik hoop even hard wel als niet dat je mijn thesis zult gebruiken als tekenmateriaal. Dankjewel voor de whisky, onzin en steun (in die volgorde). Laten we helemaal uit ons orgeltje gaan. Minivans zijn kawaii. **Chewey**, bedankt voor de make-over van mijn bank, kleed en bed. Je was de beste schootwarmer tijdens het schrijven. **Pap** en **mam**, **Martin** en **Annika**, bedankt voor jullie steun en geduld.